2022

Links between electrophilic stress and antifungal resistance in pathogenic Candida species

Amy R. Biermann
Dartmouth College, amy.biermann.gr@dartmouth.edu

Links between carbonyl stress and antifungal resistance in pathogenic *Candida* species

A Thesis
Submitted to the Faculty
in partial fulfillment of the requirements for the
degree of

Doctor of Philosophy

in

Microbiology and Immunology

by Amy Rebecca Biermann

Guarini School of Graduate and Advanced Studies
Dartmouth College
Hanover, New Hampshire

30 Aug 2022

Examining Committee

Chair, Deborah A. Hogan, Ph.D.

Robert A. Cramer, Ph.D.

Lawrence C. Myers, Ph.D.

Robert T. Wheeler, Ph.D.

F. Jon Kull, Ph.D.
Dean of the Guarini School of Graduate and Advanced Studies

Abstract

Collectively, *Candida* species are the most prevalent cause of both superficial and invasive fungal infections worldwide. Invasive *Candida* infections have a high mortality rate and predominantly affect individuals with underlying diseases, such as diabetes, HIV, or cancer. Unfortunately, many invasive *Candida* infections are recalcitrant to antifungal treatment, while intrinsically multidrug-resistant pathogens, like *Candida auris*, are increasing in prevalence. Although the canonical mechanisms of antifungal resistance in *Candida* species are well established, i.e., overexpression of efflux pumps and overexpression of or mutations in genes encoding drug targets, factors affecting the natural evolution and regulation of resistance mechanisms remain poorly understood.

One cause of antifungal resistance in *Candida* species is the acquisition of gain-of-function mutations in the transcription factor Mrr1, resulting in overexpression of the multidrug transporter Mdr1. However, little is known about the functions of other genes regulated by Mrr1 or how Mrr1 activity is modulated *in vivo*. In this work, we demonstrate in *Candida lusitaniae* and in *C. auris* that Mrr1 contributes to resistance against methylglyoxal (MG), a toxic, electrophilic dicarbonyl derived from natural metabolic processes, and that Mrr1-mediated MG resistance is driven in part by expression of the methylglyoxal reductase genes *MGD1* and *MGD2* in *C. lusitaniae* and *MGD1* in *C. auris*. Furthermore, we show that a sublethal concentration of MG induces expression of MDR1 and MG reductase genes in *C. lusitaniae* and *C. auris*, and consequently increases fluconazole (FLZ) resistance in *C. lusitaniae*. Finally, we characterize the complete Mrr1-dependent and independent transcriptional response of *C. auris* to MG and to the known inducer of Mrr1-regulated gene expression, benomyl, and show that both compounds cause

the differential expression of a multitude of genes involved in metabolism and stress response, which could contribute to pathogen survival while colonizing and infecting a mammalian host.

Together, the work presented herein provides valuable insight into a potential mechanism for the regulation of Mrr1-dependent transcription *in vivo* as well as a possible selective pressure for gain-of-function mutations in the *MRR1* gene. This is particularly noteworthy because MG is elevated in many of the same human diseases that are considered risk factors for *Candida* infection, and MG is also produced by activated phagocytes in response to pathogens. Thus, it is conceivable that *Candida* would encounter biologically significant levels of MG in the context of infection. We propose that MG-mediated induction of Mrr1-dependent transcription in *Candida* species is one factor that plays a role in antifungal treatment failure.

Dedication

I dedicate my thesis work to the friends, family, and mentors who have supported and encouraged me throughout the years. I would not be here, writing this, without you.

To every teacher in grade school who fostered my curiosity.

To every college professor who encouraged me to go to graduate school.

To all my friends and colleagues who have given me so many reasons to smile and laugh, in the good times and the bad.

Most of all, to my family, who have all supported me from the beginning. To my parents, Ken and Cherie, who worked tirelessly to give me the opportunity to get here, who nurtured my enthusiasm for science from a young age, who drove me to interviews for jobs, college, and graduate school, and who have always believed in me.

To my sister, brother-in-law, nephew, and niece, whom I don't have the opportunity to visit as often as I'd like.

Thank you, everyone.

Table of contents **Page**

List of Figures **Page**

Chapter 1

Chapter 2

Chapter 4.

List of Tables

Chapter 2

Chapter 3

Chapter 1

Introduction

1.1 Candidemia and candidiasis caused by non-*albicans Candida* species

Together, *Candida* species are the most prevalent etiologic agents of mycosis globally (1). Severity of candidiasis, which refers broadly to infections caused by any *Candida* species, exhibits a wide range from superficial to invasive. Superficial candidiasis includes acute infections of the skin, mucocutaneous membranes, or nails. Invasive candidiasis may be deep or disseminated and usually affects the bloodstream (candidemia) or internal organs. Mortality due to invasive candidiasis is estimated to be between 30 – 60% depending on factors such as geographic location, infecting species and/or strain, and the presence of underlying medical conditions such as diabetes or renal failure (2-10). Historically, *Candida albicans* has been considered the predominant human pathogen among *Candida spp*. and is still generally the most frequently isolated single *Candida* species (2, 5, 6, 8, 11-18). However, the clinical incidence of non-albicans *Candida* (NAC) species has been rising in the past few decades (see references (19-22) for review). Retrospective and cross-sectional epidemiological analyses indicate that NAC collectively account for about 43 – 64% of clinical specimens (5, 8, 15-18, 23, 24).

The increasing clinical prevalence of NAC is concerning because epidemiological evidence indicates that NAC infections lead to increased healthcare burdens such as longer stay in the intensive care unit (16), longer course of antifungal therapy (16, 25), increased duration of symptoms following treatment (25), and increased likelihood of recurrence (26) compared to infection with *C. albicans*. This is likely due, at least in part, to the trend of NAC exhibiting a higher rate of resistance against azoles (2, 6, 23, 27, 28), one of only

three existing classes of antifungal drugs. NAC may be more common in individuals with diseases involving the immune system, such as diabetes mellitus (11, 12, 14) or neutropenia (28, 29). *Candida auris*, which has perhaps become the most notorious NAC species, is a member of the *Metschnikowiaceae* family along with the closely related *Candida haemulonii* complex and *Candida* (*Clavispora*) *lusitaniae*. In contrast, *C. albicans* and most of the clinically predominant NAC belong to the *Debaryomycetaceae* family. Prior to the global emergence of *C. auris*, the *Metschnikowiaceae* family had received little attention as human pathogens. However, it has become clear that multiple members of this group display alarming pathogenic potential.

1.1.1 *Candida auris*

The recently emerged pathogen *C. auris* was first isolated from the external ear canal of an elderly patient in Japan in 2009 and identified as a novel species based on chemotaxonomic qualities and ribosomal DNA sequence (30). A retrospective molecular analysis of banked, previously unidentified fungal isolates traced the earliest known isolate of *C. auris* to 1996 (31), implying that *C. auris* has arisen as a human pathogen quite recently compared to other known pathogenic *Candida* species. Whole-genome sequencing (WGS) of *C. auris* isolates collected from across the globe indicates the simultaneous emergence of four genetically distinct clades on three continents (32, 33); later, a potential fifth clade was reported in Iran (34). *C. auris* is considered an urgent threat worldwide due to its high frequency of multidrug resistance (9, 32, 33, 35-39) and propensity to cause hospital outbreaks (36, 40, 41). Nosocomial transmission of *C. auris* is thought to be facilitated by the organism's remarkable thermo- and osmo-tolerance (42),

resistance to commonly used surface disinfectants (43), and ability to survive on abiotic surfaces for long periods of time (36, 40, 42, 44, 45). Mechanisms of azole resistance in *C. auris* have been well-studied and include overexpression of the ABC transporter Cdr1 (46-49) due to gain-of-function mutations in the transcription factor Tac1b (49-52) and overexpression of or mutations in *ERG11* (33, 38, 49, 52-56), which encodes the target enzyme of azole drugs. Echinocandin resistance in *C. auris* is attributed to mutations in *FKS1* (33, 38, 49), which encodes the target of inhibition by echinocandins. However, there is a dearth of knowledge regarding factors that contribute to the resistance of *C. auris* to abiotic stresses, such as those that may be encountered in a hospital setting.

1.1.2 *Candida haemulonii* species complex

Species belonging to the *C. haemulonii* complex, which include *C. haemulonii*, *Candida duobushaemulonii*, *Candida pseudohaemulonii*, and *Candida vulturna*, are the closest known relatives of *C. auris*. Though members of this complex are clinically uncommon, these species can cause invasive infections of blood or wounds, primarily affecting neonates or adults with existing co-morbidities (57-65). Like *C. auris*, isolates from the *C. haemulonii* complex display high rates of multidrug resistance (57, 63, 66-68), particularly against amphotericin B (AmB) (62, 69, 70) and azoles (58, 60, 64, 71, 72). The multi-azole resistance of *C. haemulonii* complex species appears to be mediated by high efflux pump activity and mutations in *ERG11* (73), while their decreased membrane ergosterol content, fermentative metabolism, and high antioxidant enzyme activity likely contribute to AmB resistance (74). *C. haemulonii* complex species are less virulent than *C. auris* in murine (75, 76), zebrafish (77), and *Galleria melonella* (75) models of infection,

but it should be noted that animals in these studies were immunocompetent and had no underlying disease, in contrast to most humans afflicted by *C. haemulonii* complex species.

1.1.3 *Candida lusitaniae*

Another member of the *Metschnikowiaceae* family that is gaining recognition as an opportunistic pathogen of humans is *C. lusitaniae*, which is known for causing bloodstream infections in cancer patients undergoing chemotherapy (78-85) and can cause opportunistic infections in individuals with other underlying diseases. Although many isolates of *C. lusitaniae* appear susceptible to antifungal drugs *in vitro* (86-89), recalcitrance of *C. lusitaniae* infections to AmB is common (90-92). Furthermore, *C. lusitaniae* exhibits a propensity to develop resistance or tolerance against AmB (81, 84, 85, 93-96), azoles (94, 95, 97), and/or echinocandins (94, 98) during – or, in some cases, even without (97) – treatment, which can make this organism difficult to eradicate once colonization or infection has been established. Mechanisms of drug resistance in *C. lusitaniae* are similar to those reported for other *Candida* species: altered sterol metabolism contributes to resistance against AmB (99, 100), azole resistance is caused overexpression of *ERG11* and/or multidrug transporter genes (94, 97, 101-103), and echinocandin resistance is associated with mutations in *FKS1* (94, 98).

1.1.4 Diabetes as a risk factor for colonization and infection by *Candida* species

Numerous risk factors for colonization and/or infection by *Candida* species have been identified. Perhaps one of the most well-established risk factors for candidiasis is diabetes mellitus, which refers to a group of metabolic diseases characterized by prolonged hyperglycemia. The most common types of diabetes mellitus are Type 1 diabetes –

characterized by insulin insufficiency – and Type 2 diabetes – characterized by insulin resistance – but other types exist, such as gestational diabetes or cystic fibrosis-related diabetes (CFRD). Individuals with diabetes exhibit a higher prevalence and increased risk of oral *Candida* carriage (13, 104-110) and infection (111-113), vulvovaginal candidiasis (VVC) (114-116), and candidemia (6, 35, 39, 117) compared to non-diabetic subjects. The possible causes of increased susceptibility to candidiasis in diabetic patients are manifold and have been reviewed thoroughly in references (118-120). Thus, only a brief overview will be given here.

Undoubtedly, abnormal immune function is one of the factors contributing to the higher prevalence of certain infections, including candidiasis and candidemia, that is observed in diabetic patients. Polymorphonuclear leukocytes (PMNs) from diabetic mammals display defects in chemotaxis (121-123), phagocytosis (122, 124, 125), and killing (123, 126, 127). Likewise, monocytes and macrophages from diabetic subjects exhibit impaired phagocytosis (128-131) and killing (132). Moreover, the adaptive immune response may also be dampened in diabetes; immunoglobulin deficiency has been observed in some children with Type 1 diabetes (133), and Type 1 diabetic patients in a controlled vaccination study displayed a lessened T-cell-mediated antigen response compared to nondiabetic controls (134). However, it should be noted that diabetic patients are not a homogenous group; some studies have failed to find significant differences in the immune functions of diabetics compared to nondiabetics (135-137), and some immune abnormalities seem to correlate with poorer glycemic control (122, 124, 136-140).

In addition to its effects on the immune system, diabetes can also alter the pharmacokinetics and/or pharmacodynamics of medications through delayed gastric

emptying, impaired hepatic function, disruptions in drug distribution, vascular abnormalities, and slower drug absorption (see reference (141) for review). For example, non-enzymatic glycation of albumin by glucose, a process that is rampant in uncontrolled diabetes, changes the topography of albumin and decreases its binding affinity for some drugs (142), including the antifungal itraconazole (143). Additionally, it has been shown *in vitro* that glucose can directly interact with the antifungal drugs voriconazole (VOR) and AmB via stable hydrogen bonds, thus decreasing the antifungal activity of these agents (144). In the same study, VOR and AmB display reduced efficacy in streptozotocin-induced diabetic mice infected with *C. albicans* compared to *Candida*-infected control mice (144). Although data on the absorption and distribution of antifungal drugs in diabetic patients is lacking, it has been shown that diabetic patients with tuberculosis (TB) have significantly lower plasma concentrations of the anti-TB drugs isoniazid and pyrazinamide two hours post-treatment compared to nondiabetic TB patients (145). Additionally, a lower blood accumulation of tenofovir diphosphate, an indicator of cumulative exposure to the antiretroviral drug tenofovir, has also been observed in patients living with diabetes and human immunodeficiency virus (HIV) compared to patients who have only HIV (146).

There is also evidence to suggest that the hyperglycemic environment within a diabetic host may also impact the growth and physiology of microbial denizens, including *Candida* species. For instance, salivary glucose level in diabetics is inversely correlated with salivary pH and positively correlated with oral *Candida* carriage and species diversity (105, 147-149), suggesting that the high glucose and/or acidic pH of diabetic saliva may promote *Candida* growth. Glucose also has been shown to directly affect antifungal resistance; in the presence of 50% human serum, glucose and insulin have species-

dependent effects on the minimum inhibitory concentration (MIC) of different antifungal drugs (150). Furthermore, a transcriptomics analysis revealed that glucose at concentrations ranging from 0.01 to 1.0% (physiological range, 0.06 to 0.1%) induces expression of genes involved in osmotic and oxidative stress response in addition to four genes encoding multidrug transporters in *C. albicans* (151). Consistent transcriptomics data, glucose also increases resistance of *C. albicans* to salt stress, hydrogen peroxide (H_2O_2), and the antifungal miconazole (151). Although this study was not performed in the context of diabetes, it is reasonable to hypothesize that the elevated blood and salivary glucose in diabetic patients may increase the tolerance of resident *Candida* to some stressors, including antifungal drugs. It would be interesting to investigate whether *Candida* species might evolve toward higher baseline expression of certain stress-response genes in diabetic compared to nondiabetic hosts. Intriguingly, some studies have found a higher frequency of antifungal resistance in *Candida* isolates from diabetic patients compared to those from nondiabetic controls (14, 105, 152-154), although others have found no such difference (155). Finally, there have been reports of increased virulence attributes among *Candida* isolates from diabetic versus nondiabetic subjects, such as adherence to fibronectin (156), proteinase activity (157), hemolytic activity (157, 158), esterase activity (158), or biofilm formation (159), but more research is needed to establish a causal link between any of these phenotypes and the diabetic environment.

1.2 The transcription factor Mrr1 contributes to multidrug resistance in *Candida* species

The multidrug resistance regulator Mrr1 is a transcription factor known for its role in regulating expression of the multidrug exporter gene *MDR1*, particularly in *C. albicans*. Mrr1 was first described in *C. albicans* by Morschhäuser et al. (160) and orthologs were later identified in *Candida dubliniensis* (161), *Candida parapsilosis* (162), *Candida tropicalis* (163), *C. lusitaniae* (97, 102), and *C. auris* (50). Morschhäuser et al (160) demonstrated that Mrr1 regulates expression of *MDR1* among other genes and that gain-of-function mutations in the *MRR1* gene confer increased resistance to the antifungal drug fluconazole (FLZ). *MDR1* and several of the other Mrr1-regulated genes and their predicted functions are discussed in the following section. Mrr1 has been most extensively studied *in C. albicans*, although its orthologs have been shown to function similarly in the non-*albicans Candida* species listed above (97, 161-163), though the findings in *C. auris* are less clear (50, 164).

1.2.1 Structure

Mrr1 is a member of the zinc cluster protein family, which are found exclusively in fungi and regulate expression of genes involved in a diverse array of cellular processes, including metabolism of amino acids and sugars, stress or drug response, and ergosterol biosynthesis (see reference (165) for review). In general, zinc cluster proteins share three common functional domains (**Fig. 1.1A**), although with some variations within and across species. The DNA-binding domain is almost always located in the N-terminal end of the protein and consists of the highly conserved $CysX_2CysX_6CysX_{5–12}CysX_2CysX_{6–8}Cys$ zinc-binding motif (Cys_6Zn_2), a coiled-coil dimerization domain, and a linker region thought to contribute to DNA-binding specificity (165). The regulatory domain, also known as the

middle homology region, is thought to be involved in negative autoregulation of the protein's activity, because several characterized zinc cluster proteins display constitutive activity upon deletion of this region (165). Additionally, gain-of-function mutations of certain zinc cluster proteins, such as the drug resistance regulators Pdr1 and Pdr3 of *S. cerevisiae*, have been identified in this regulatory domain (165). Finally, the C-terminal acidic region is the most diverse and consequently, least well-understood domain, but it is thought to play a role in activation of the protein, and in some cases, recruitment of interaction partners for transcriptional activation (165). Gain-of-function mutations in zinc cluster proteins have also been found in the acidic region (165).

C. albicans Mrr1 is a large protein of 1108 amino acids and contains the functional domains characteristic of zinc cluster transcription factors, as determined by Schubert et al (166) (**Fig. 1.1B**). The DNA-binding domain (residues 1 – 106) contains the conserved Cys_6Zn_2 motif and is sufficient to activate the *MDR1* promoter when fused to the activation domain of another transcription factor (166). The region called inhibitory domain 1 (residues 951 – 1050) appears to be involved in autoregulation, as deletion of either residues 951 – 1000 or residues 1001 – 1050 renders Mrr1 constitutively active (166). However, deletion of the entire region eliminates constitutive activity (166). Additionally, deletion of all 175 C-terminal residues ($MRR1^{\Delta C933}$) results in complete loss of Mrr1 activity (166). Activation domain 1 is located at the C-terminus (residues 1051 – 1108) and, when fused to TetR, is sufficient to activate a TetR-dependent reporter promoter in the presence of the Mrr1 inducer benomyl (166). Schubert et al. (166) also found evidence of a second activation domain, slightly upstream of inhibitory domain 1, but were unable to identify the specific residues involved. Like many other zinc cluster proteins, CaMrr1

also contains a middle homology region (residues 560 – 664), although deletions in this region do not cause constitutive activity and in fact, abolish activation by benomyl (166). The mechanisms by which Mrr1 activity is regulated in *Candida* species remain poorly understood, but likely involve complex interactions between activation and inhibitory domains in response to certain signals.

1.2.2 Activation

Gain-of-function mutations

Most gain-of-functions mutations that have been found in *CaMRR1* of clinical isolates as well as *in vitro* evolved *MDR1*-overexpressing strains are located within four "hotspots", three of which are part of the uncharacterized region between the DNA binding domain and the inhibitory domain (specifically, three small regions between residues 335 and 896) and the other is within the inhibitory domain (residues 997 and 998) (167) (**Fig. 1.1B**). It is not known how any of these amino acid substitutions cause constitutive Mrr1 activity, though it is speculated that they may disrupt autoinhibition. Notably, no *MRR1* gain-of-function mutations to date, in any *Candida* species, have been identified in the DNA-binding domain, suggesting that differences in Mrr1 activity are not due to differential binding to target promoters. In *C. albicans*, which is diploid, a single copy of a gain-of-function *MRR1* is sufficient to confer increased FLZ resistance and *MDR1* expression compared to a homozygote without gain-of-function *MRR1* (167). However, strains that are homozygous for gain-of-function *MRR1* display substantially higher FLZ resistance and *MDR1* expression than heterozygotes, and most *MDR1*-overexpressing clinical isolates and *in vitro* evolved strains are homozygous for mutated *MRR1* (167).

Benomyl and H_2O_2

Benomyl is an agricultural fungicide that is known to induce expression of *MDR1* and other Mrr1 target genes in multiple *Candida* species (97, 160, 161, 168-170). Although CaMrr1 is required for induction of *CaMDR1* expression in response to benomyl (160, 171), it is unlikely that benomyl interacts directly with CaMrr1. When targeted to the promoter of *CaCDR2* or *CaERG11* via replacement of its native DNA-binding domain with that of either CaTac1 or CaUpc2 respectively, Mrr1 cannot activate expression of either gene in response to benomyl (172). H_2O_2 can also induce expression of *MDR1* in an Mrr1-dependent manner, though to a lesser extent than benomyl (160, 171). The mechanism by which these chemicals activate expression of Mrr1 target genes in *Candida* species remains unknown, though it is speculated to be mediated by oxidative stress. In *S. cerevisiae*, benomyl induces many genes characteristic of an oxidative stress response, such as the thioredoxin genes *TRX1* and *TRX3*, the glutathione synthase gene *GSH1*, and the glutathione reductase gene *GLR1* (173, 174). Interestingly, benomyl also induces expression of the *MDR1* ortholog *FLR1* (173, 174), and the benomyl response in *S. cerevisiae* is largely dependent on the transcription factors Pdr1 and Yap1 (173, 174), which play comparable roles in *S. cerevisiae* as Mrr1 and Cap1 respectively, in *Candida* species. A similar transcriptional response to benomyl has been observed in *Candida glabrata*, a close relative of *S. cerevisiae*, although with less dependence on the Yap1 ortholog Cgap1 (174).

1.2.3 Interaction partners

In *C. albicans*, there is evidence that other transcription factors and transcriptional machinery interact with Mrr1 to regulate expression of shared target genes. One such example is Cap1, a basic leucine zipper (bZIP) transcription factor of the AP-1 family that plays a major role in the oxidative stress response (175). Cap1 in *C. albicans* shares high identity with, and is a functional homolog of, Yap1 in *S. cerevisiae* (175). Cysteine residues in the N- and C-terminal domains of Yap1 function as redox sensors; oxidation of specific Cys residues disrupts its sequestration by Crm1 and allows Yap1 to accumulate in the nucleus to induce expression of its target genes (176-179). In *C. albicans*, Cap1 shares numerous target genes with Mrr1, including *MDR1* and *GRP2* (160, 171, 180), which will be discussed in more detail in the following section. Although hyperactive Cap1 and hyperactive Mrr1 can activate *MDR1* expression and FLZ resistance independently of one another, homologous expression of both hyperactive transcription factors has an additive effect on FLZ resistance and *MDR1* promoter activity (171). Additionally, Cap1 is required for *MDR1* induction by Mrr1 in response to H_2O_2 and may contribute to *MDR1* induction in the presence of benomyl (171), adding further support for cooperation between Mrr1 and Cap1.

Mcm1 is a member of the MADS box transcription factor family and is essential in yeasts (see reference (181) for review). The *MDR1* promoter in *C. albicans* contains a binding site for Mcm1 (182, 183), and hyperactive Mrr1 cannot activate the *MDR1* promoter in Mcm1-depleted *C. albicans* (184). Additionally, Mcm1 is required for maximal induction of *MDR1* by Mrr1 in response to benomyl but not H_2O_2 (184). Likewise, Mcm1 is dispensable for *MDR1* overexpression by hyperactive Cap1 (184).

Other processes that have been shown to be Mcm1-regulated in *C. albicans* include yeast-hyphae morphogenesis (185), arginine metabolism (183), white-opaque switching (183), and biofilm formation (183). In *S. cerevisiae*, Mcm1 is known to regulate expression of genes involved in mating (186-188), cell cycle progression (189-191), cell wall and membrane maintenance (191), and osmotolerance (192) in addition to arginine metabolism (193). Interestingly, loss-of-function mutations in the genes encoding phosphoglycerate mutase (*PGM1*) or enolase (*ENO2*) lead to increased activity of a loss-of-function Mcm1 in *S. cerevisiae* – and decreased activity of wild-type Mcm1 – suggesting the Mcm1 activity is post-translationally modulated according to the glycolytic flux, although the mechanism is not known (194). Mcm1 activity is also regulated by Sln1 (195, 196), a stress-sensing kinase known for its role in the high-osmolarity glycerol mitogen-activated kinase (HOG-MAPK) signaling cascade in *S. cerevisiae*. Phosphorylated Sln1 activates Mcm1 and represses signaling through the HOG-MAPK pathway (196).

Upc2, another zinc cluster transcription factor, is a master regulator of genes involved in ergosterol biosynthesis and activates their transcription in response to ergosterol depletion (197, 198). In *C. albicans*, Upc2 has also been shown to bind the *MDR1* promoter and can regulate expression of *MDR1* (199), and moderately increased *MDR1* expression has been observed in a clinical *C. albicans* isolate with a gain-of-function mutation in Upc2 (200). Hyperactive Upc2 cannot activate *MDR1* expression in the absence of Mrr1, suggesting that Mrr1 and Upc2 may cooperatively regulate *MDR1* expression (171). However, hyperactive Mrr1 can upregulate *MDR1* expression just as effectively in a *UPC2*-null mutant as in the presence of functional Upc2, indicating that

any interaction between Mrr1 and Upc2 in *C. albicans* plays only a minor role in the regulation of *MDR1* or other target genes (171).

There is also evidence that Mrr1 interacts with the Swi/Snf and Mediator complexes in *C. albicans* (201). Swi/Snf is an ATP-dependent chromatin remodeling complex that aids in transcriptional regulation, and most of its component proteins are conserved throughout eukaryotes (see reference (202) for review). In *C. albicans*, the Swi/Snf complex is essential for hyphal formation (203, 204) but is likely involved in other aspects of *Candida* physiology; for example, deletion of specific components of the Swi/Snf complex in *C. albicans* leads to decreased tolerance to heat stress or cell-wall damaging agents (205, 206). Liu and Myers (201) have demonstrated that the elevated *MDR1* expression and FLZ resistance of *MRR1* gain-of-function mutants depends on Snf2, the catalytic subunit of Swi/Snf (201). Furthermore, Snf2 is required for induction of *MDR1* expression by benomyl and H_2O_2 via histone depletion at the *MDR1* promoter (201). Mrr1 and the Swi/Snf complex display mutual dependence for *MDR1* promoter occupancy, as an *MRR1*-null strain exhibits significantly lower occupancy of Swi/Snf at the *MDR1* promoter (201). Thus, it is hypothesized that Mrr1 recruits the Swi/Snf complex to some of its target promoters, where Swi/Snf displaces the histones and allows for easier access of Mrr1 and other co-activators to bind the DNA (201).

Mediator is another highly conserved, multi-protein complex that cooperates with other aspects of eukaryotic transcriptional machinery. In general, the Mediator complex is comprised of four "modules": the head, middle, tail, and the Cdk8 module (see reference (207) for review). Some individual components of the Mediator modules vary across species, and deletion of specific subunits has different effects on Mediator-dependent

transcriptional regulation (see reference (207) for review). In *C. albicans*, Mediator plays indispensable roles in positive and/or negative regulation of filamentation (208-210), white-opaque switching and mating (211), metabolism (208-210), and virulence (208, 212). A functional Mediator complex is also required for both Mrr1- (201) and Tac1-mediated (213) azole resistance in *C. albicans*. Deletion of the Med3 subunit of Mediator, which abrogates normal assembly of the tail module, leads to decreased induction of *MDR1* expression by either gain-of-function Mrr1 or benomyl without affecting histone displacement or Mrr1 occupancy at the *MDR1* promoter (201). Mediator also demonstrates the ability to negatively regulate expression of Mrr1 target genes. Deletion of *SSN3*, which encodes a kinase subunit of the Cdk8 module, leads to greater induction of *MDR1* and other Mrr1 target genes by benomyl (201). Furthermore, the *ssn3*Δ/Δ mutant exhibits increased histone displacement at the *MDR1* promoter in the presence of benomyl, and increased *MDR1* promoter occupancy by Mrr1 either in strains with a gain-of-function *MRR1* or under benomyl induction (201). Finally, *SSN3* deletion can partially rescue the defects in *MDR1* induction by benomyl or hyperactive Mrr1, histone displacement, and Mrr1 occupancy of the *MDR1* promoter observed in the *snf2*Δ/Δ mutant, suggesting that the Swi/Snf complex and the Mediator Cdk8 module act in opposition to one another at the promoters of *MDR1* and certain other Mrr1 target genes (201). The transcriptional repressor activity of Ssn3 is dependent on its kinase activity, as a strain expressing a kinase-dead *SSN3* allele exhibits many of the same phenotypes as the *SSN3*-null strain (201).

1.2.4 Mrr1 orthologs in *C. lusitaniae* and *C. auris*

C. lusitaniae

The *C. lusitaniae* genome encodes a single *MRR1* ortholog, *CLUG_00542*, which encodes a protein of 1265 amino acids that shares 37% identity with CaMrr1 across 79% of the protein. Naturally occurring gain-of-function mutations in *MRR1* have been reported in clinical isolates of *C. lusitaniae* from cystic fibrosis patients with no prior use of clinical antifungal agents (97), raising questions about other pressures which may have selected for changes in Mrr1 activity. Additionally, a different gain-of-function mutation was found in the *MRR1* locus of a *C. lusitaniae* isolate from a patient who had been treated with multiple types of antifungal drugs (102). Most of the observed gain-of-function mutations in ClMrr1 occur within the regions of the protein homologous to the middle homology region and inhibitory domain of *C. albicans* Mrr1 (102, 166, 214) (**Fig. 1.1C**). Like CaMrr1 with *CaMDR1*, ClMrr1 regulates expression of the *C. lusitaniae MDR1* ortholog *CLUG_01938*/*CLUG_01939*, and Mrr1-mediated induction of *MDR1* expression by benomyl is also observed in *C. lusitaniae* (97, 214). In addition to FLZ, gain-of-function mutations in *ClMRR1* also confer resistance to the human antimicrobial peptide histatin-5 and bacterially produced toxic phenazines (97). However, constitutively active Mrr1 increases susceptibility of *C. lusitaniae* to H_2O_2 for reasons unknown, suggesting the existence of opposing selection for or against Mrr1 activity (214).

C. auris

Three orthologs of CaMrr1 have been identified in *C. auris*: Mrr1a, 1133 amino acids in length with 35% identity to CaMrr1; Mrr1b, 1059 amino acids in length with 29% identity to CaMrr1; and Mrr1c, 851 amino acids in length with 25% identity to CaMrr1 (50). *MRR1b* and *MRR1c* definitively do not contribute to azole resistance in either the

clade III isolate B11221 or the clade IV isolate B11243, as deletion of either gene does not affect the FLZ or VOR MIC of either strain (50). Likewise, the FLZ or VOR MIC of the *mrr1a*Δ mutant in B11243 does not differ from that of the parental isolate, although deletion of *MRR1a* from B11221 results in a twofold decrease in the MIC of FLZ and VOR, suggesting a minor role for Mrr1a in azole resistance in the B11221 background (50). It should be noted, however, that double or triple mutants lacking more than a single *MRR1* ortholog in *C. auris* have not yet been created; it is possible that one or two may compensate for the absence of another. Many isolates of clade III, including B11221, contain a SNP encoding an N647T amino acid substitution in *MRR1a* (33, 215), which is predicted to be gain-of-function due to the resistance of clade III isolates against the novel efflux pump inhibitor azoffluxin (215). Notably, this substitution in *C. auris* occurs in the middle region of Mrr1a, corresponding to the MHR domain where gain-of-function mutations have been identified in Mrr1 of *C. albicans* and *C. lusitaniae* (166, 167, 214). Recently, it has been shown that complementation of the $MRR1a^{N647T}$ allele into a FLZ-susceptible strain of *C. auris* does increase resistance to FLZ and VOR independently of other resistance mechanisms (164). Therefore, the role of Mrr1a in the azole resistance of *C. auris* appears to be strain dependent, and much more remains to be elucidated about its natural functions.

1.3 In addition to *MDR1*, Mrr1 regulates expression of many other genes, including several with homology to aldo-keto reductases

Despite having been discovered over a decade ago (160), the natural function of Mrr1 in *Candida* species remains poorly understood. Though most studies of Mrr1 have

focused on its role in drug resistance via regulating expression of *MDR1*, transcriptional and proteomic analyses have identified numerous other genes that are co-regulated with *MDR1*, many of which encode proteins with known or predicted aldo-keto reductase activity (160, 169, 171, 216-221). It has been hypothesized that some of these other Mrr1-regulated genes contribute to multidrug resistance by mitigating oxidative or osmotic stress that may be induced by toxic xenobiotics such as azoles (160, 219, 220). However, azole antifungal agents are a fairly recent invention; the first report of antifungal activity of an azole compound – benzimidazole – occurred in 1944 (222), and the first clinically available topical azole drug – chlormidazole – was introduced in 1958 (223). FLZ, which one may regard as a canonical substrate of Mdr1, was developed by Pfizer in 1989 (224). Therefore, the evolutionary pressures which had shaped Mrr1 and its regulon in *Candida* species prior to the introduction of commercial azoles remain unknown.

1.3.1 *MDR1*

It is undeniable that *MDR1* is the most extensively studied Mrr1-regulated gene in *C. albicans*. *MDR1*, formerly known as *BEN*^{r}, encodes an efflux protein of the major facilitator superfamily (MFS) and was first identified in a screen of the *C. albicans* genome for genes that confer resistance to benomyl and the dihydrofolate reductase inhibitor methotrexate (**Fig. 1.2A**) when expressed in *S. cerevisiae* (225). It was later shown that expression of *CaMDR1* in *S. cerevisiae* also confers resistance to cycloheximide, benzotriazoles, 4-nitroquinoline-N-oxide (4-NQO), and sulfometuron methyl (226) (**Fig. 1.2A**). All six of the aforementioned compounds are structurally and functionally unrelated, leading to the authors to hypothesize that Mdr1 is a multidrug efflux pump (226).

In *C. albicans*, disruption of *MDR1* causes increased susceptibility to methotrexate, 4-NQO, and cycloheximide, but does not affect benomyl resistance (227). Following the initial cloning and identification of *MDR1*, numerous groups have observed overexpression of *MDR1* in FLZ^R *C. albicans* isolates (228-232), and it has been demonstrated that homozygous deletion of *MDR1* from FLZ^R clinical isolates leads to a significant reduction in FLZ MIC (233). Although overexpression of *CaMDR1* in *S. cerevisiae* increases FLZ resistance (228), overexpression of *MDR1* from the *ADH1* promoter in laboratory strains or clinical isolates of *C. albicans* reduces susceptibility to cerulenin and brefeldin A but not FLZ (234). The lack of an increase in FLZ MIC may be explained by the observation that *MDR1* overexpression from the *ADH1* promoter does not lead to Mdr1 protein levels as high as in the clinical isolates that naturally overexpress *MDR1* (234).

In *C. albicans* strains without gain-of-function mutations in *MRR1*, baseline expression of *MDR1* is low to nondetectable under standard laboratory conditions (228, 229, 231, 232). Nonetheless, as described in the previous section, *MDR1* expression is highly induced by benomyl in *C. albicans* as well as in other *Candida* species (97, 160, 161, 168-170, 235). Moreover, several other chemicals have been shown to induce *CaMDR1* expression: methotrexate (235); the oxidizing agents diethyl maleate (DEM) (170), diamide (170), H_2O_2 (170), and tert-butyl hydrogen peroxide (T-BHP) (170); the alkylating agent methyl methane sulfonate (170); the mutagen 4-NQO (170, 235); the acetolactate synthase inhibitor sulfometuron methyl (235); and the metal chelator *o*-phenanthroline (235) (**Fig. 1.2B**). More recently, it has been demonstrated that expression of *CaMDR1* is upregulated in response to the antibiotic rifampicin (236), and during growth with fructose as a carbon source (237); induction of *MDR1* under either condition

is accompanied by an increase in FLZ resistance (236, 237). Elevated expression of *MDR1* has also been observed during *C. albicans* biofilm formation *in vivo* (238) and *in vitro* (239), which may in part account for the increased azole resistance of *Candida* biofilms relative to planktonic cells.

Orthologs of *CaMDR1* also contribute to FLZ resistance in *C. dubliniensis* (240, 241), *C. parapsilosis* (162, 242-245), *C. tropicalis* (163, 246-248), and *C. lusitaniae* (97, 101, 214). In *C. auris*, *MDR1* is overexpressed in some azole-resistant isolates, but deletion of *MDR1* from these isolates does not substantially affect their azole resistance (47). However, introduction of the predicted gain-of-function $MRR1a^{N647T}$ allele increases the FLZ and VOR resistance of an azole-susceptible *C. auris* strain via upregulation of *MDR1* expression (164). Due to its ability to transport multiple chemicals with structural and functional diversity, the natural function of Mdr1 in *Candida* species is not well understood. Curiously, Kohli et al. (249) demonstrated that methotrexate is a better substrate than FLZ for CaMdr1. In addition to FLZ, Mdr1 has been shown to confer resistance to the human antimicrobial peptide histatin-5 in *C. albicans* (250) and *C. lusitaniae* (97). Furthermore, in *C. lusitaniae*, Mdr1 confers resistance to toxic phenazines produced by the Gram-negative bacterium *Pseudomonas aeruginosa* (97). Thus, it is possible that the *MDR1* gene may have evolved to aid in colonization of mammalian hosts and/or competition with other microbes. Importantly, *Candida* species are frequently co-isolated with bacteria, including *P. aeruginosa*, from human infections (see reference (251) for review), and it would be interesting to investigate the potential importance of Mdr1 for the interactions between *Candida* and their bacterial neighbors.

1.3.2 *GRP2*/*MGD1*

In *C. albicans*, high expression of *GRP2*, also referred to as *MGD1* (252), has been correlated with *MDR1*-mediated azole resistance in numerous independent studies (160, 169, 171, 216-219), and was shown via transcriptional profiling (160) and chromatin immunoprecipitation (ChIP) (171) to be regulated by Mrr1. Like *MDR1*, expression of *GRP2*/*MGD1* is also regulated by Cap1 (180) and is induced by H_2O_2 in a Cap1-dependent manner (175). *GRP2*/*MGD1* expression is also upregulated in response to benomyl (169), salt stress (253, 254), cadmium (253, 254), hypoxia (255), and during biofilm formation (256) or colonization of the murine cecum (257). The closest homolog of *GRP2*/*MGD1* in *S. cerevisiae* is *GRE2*, which was first identified as a gene induced by osmotic, ionic, oxidative, and heat stresses along with *GRE1* and *GRE3* (258). Upregulation of *ScGRE2* in response to cadmium has also been reported, although genetic deletion of *ScGRE2* does not appear to affect cadmium resistance in the *S. cerevisiae* strain YPH98 (259). Like *GRP2/MGD1* in *C. albicans*, overexpression of *GRE2* is correlated with FLZ resistance in *S. cerevisiae* (260).

In 2003, Chen et al. (261) demonstrated that *ScGRE2*, which had previously been uncharacterized, encodes a protein with NADPH-dependent methylglyoxal reductase activity. Methylglyoxal (MG) is a metabolically produced keto-aldehyde compound which will be discussed in further detail in the following section. In addition to MG, Gre2 has also been shown to accept a variety of other biological aldehyde substrates in *S. cerevisiae*. For example, ScGre2 can reduce isovaleraldehyde, a metabolic derivative of leucine, to isoamyl alcohol (262), and overexpression of *GRE2* confers resistance against glycolaldehyde, a toxic intermediate in the production of biofuels (263, 264). Furthermore,

crude cell extracts from *S. cerevisiae* strains overexpressing *GRE2* exhibit the ability to reduce a multitude of aldehyde compounds, including furfural, acetaldehyde, propanal, and butanal, with varying degrees of activity (265). It is not yet known whether this apparent substrate promiscuity extends to *Candida* Grp2/Mgd1.

Aldehyde reductase enzymes like ScGre2 and CaGrp2 may play important roles in yeast metabolism and physiology, particularly under certain types of cellular stress. *S. cerevisiae gre2*Δ mutants do not display a growth defect in favorable conditions but are substantially more sensitive to agents which cause membrane stress, such as NaCl, EGTA, SDS, and brefeldin A (266). Additionally, several proteins involved in the ergosterol biosynthesis pathway are highly induced in *gre2*Δ mutants grown in the presence of the calcium chelator EGTA, and *gre2*Δ mutants exhibit increased susceptibility to inhibitors of ergosterol biosynthesis but not inhibitors of synthesis of other lipids (266). Thus, *GRE2* appears to play a role in ergosterol biosynthesis during stress in *S. cerevisia*e, although it is not known whether this function is related to its aldehyde reductase activity. It has also been reported that *S. cerevisiae gre2*Δ mutants display a hyper-filamentous phenotype; this is speculated to be a consequence of the isovaleraldehyde reductase activity of Gre2 (262).

In *C. albicans*, Grp2/Mgd1 protein (henceforth referred to as Mgd1) is overexpressed in Δ*gcs1* mutants, which are auxotrophic for reduced glutathione (GSH) (252). Purified CaMgd1 exhibits the ability to reduce MG as well as pyruvate in the presence of NADH, with a K_{cat} of 1.15×10^4 and 9.55×10^3 min^{-1}, respectively (252). Genetic deletion of *MGD1* in *C. albicans* leads to increased intracellular MG, pyruvate, and reactive oxygen species, decreased vacuolar pH, and decreased intracellular NADPH (252). Interestingly, both *MGD1*-deficient and *MGD1*-overexpressing *C. albicans* mutants

display a severe virulence defect in mice (252), suggesting that expression of *MGD1* must be finely controlled during infection, likely due to its effects on cellular metabolism and redox balance. Alternatively, an *MGD1*-overexpressing strain may instigate a strong immune response in an animal model, as the protein it encodes appears to be antigenic in humans (267).

1.3.3 *IFD* gene family

Multiple members of the *IFD* gene family have repeatedly exhibited overexpression coordinately with *MDR1* in azole-resistant isolates of *C. albicans* (160, 169, 171, 216-221) and show evidence for regulation by Mrr1 (160, 171). The *IFD* genes share homology to *S. cerevisiae YPL088w*, an uncharacterized member of the aldo-keto reductase (AKR) superfamily which is predicted to encode a protein with aryl alcohol dehydrogenase (AAD) activity. Purified AAD protein from the ligninolytic fungus *Phanerochaete chrysosporium* can reduce a wide array of aromatic benzaldehyde compounds to their cognate alcohols using NADPH as a co-factor (268, 269). The *S. cerevisiae* genome encodes seven other genes which encode proteins with high sequence similarity to the AAD characterized in *P. chrysosporium*; *YPL088w* appears to be more distantly related to these seven genes and to the AAD from *P. chrysosporium* (270). In an individual and combinatorial knockout analysis, deletion of neither *YPL088w* nor the other seven putative AAD genes in *S. cerevisiae* influences general growth, lipid metabolism, or reduction of veratraldehyde (270), the natural substrate of *P. chrysosporium* AAD (268, 269). *YPL088w* is one of 581 genes with increased expression in an *in-vitro* evolved coniferyl aldehyde-resistant *S. cerevisiae* strain relative to the parental strain, though its

potential contribution to coniferyl aldehyde resistance is not known (271). The function of *YPL088w* remains poorly understood, although its expression is known to be reciprocally regulated by the transcription factors Yrm1 and Yrr1 which are associated with multidrug resistance in *S. cerevisiae* (272). Thus, it appears that increased expression of at least one putative AAD may be beneficial to drug-resistant strains of *Saccharomyces* and *Candida*, although a specific mechanism linking drug resistance to AAD activity has not yet been described.

Like *YPL088W*, most *IFD* genes in *Candida* remain uncharacterized. An exception is *IFD4*, now known as *CSH1*. The Csh1 protein was first characterized as the antigen of the monoclonal antibody 6C5-H4CA (273), which partially blocks hydrophobic attachment of *C. albicans* to surfaces. *CSH1*-null mutants in *C. albicans* have lower cell surface hydrophobicity scores and a defect in adhesion to fibronectin-coated wells (273), implicating a role for *CSH1* in maintaining cell surface hydrophobicity. However, the mechanism by which Csh1 modulates cell surface hydrophobicity is not known. Expression of *CaCSH1* is induced by hypoxic growth (274), treatment with ketoconazole (275) or benomyl (169), and in co-culture with J774A murine macrophage-like cells (276). Interestingly, *CSH1* expression in *C. albicans* may be linked to the biosynthesis of sulfur-containing amino acids, as *ECM17*-null mutants, which are deficient in methionine and cysteine biosynthesis, exhibit decreased expression of *CSH1* and other genes involved in adhesion or filamentation (277).

1.3.4 *IPF5987*/*YPR127*

Another gene that appears to be co-regulated with *MDR1* by Mrr1 in *C. albicans* is *IPF5987* (160, 169, 217, 219, 220), also known as *YPR127* due to its homology to the *S. cerevisiae* gene *YPR127w*. Like the *IFD* genes described above, *IPF5987*/*YPR127* is an uncharacterized member of the AKR superfamily. The protein encoded by *S. cerevisiae YPR127w* is also uncharacterized, though shows sequence similarity to the pyridoxal reductase of the fission yeast *Schizosaccharomyces pombe* (278), which catalyzes NADPH-dependent reduction of pyridoxal to pyridoxine (279) and may be important for the biosynthesis of pyridoxal 5-phosphate, a coenzyme form of vitamin B_6. In *S. cerevisiae*, expression of *YPR127w* is regulated by the transcription factor Yrm1 (272) and induced under nitrogen starvation (280), upon entry into stationary phase (280), and during wine fermentation (278, 281). In *C. albicans*, deletion or overexpression of *IPF5987*/*YPR127* does not affect susceptibility to FLZ, 4-NQO, cerulenin, brefeldin A, H_2O_2, menadione, or diamide (220).

1.3.5 *ADH4*

Expression of *ADH4* is also associated with *MDR1*-mediated azole resistance in *C. albicans* (169, 171, 217, 219) and the *ADH4* promoter has been found to be bound by Mrr1 in a ChIP assay (171). *CaADH4* is predicted to encode a protein with 3-hydroxyacyl-CoA dehydrogenase activity, though it remains uncharacterized. Its closest ortholog in *S. cerevisiae* is *YMR226C*, which encodes a short-chain dehydrogenase that can catalyze $NADP^+$-dependent oxidation of L- and D-serine, D-threonine, L-*allo*-threonine, and several other 3-hydroxy acids (282). The protein encoded by *YMR226C* has also

demonstrated activity as a diacetyl reductase and an acetoin reductase; both reactions are dependent on NADPH (283). Thus, it appears that *YMR226C* encodes a broad-specificity oxidoreductase that can catalyze the oxidation or reduction of its substrates depending on factors such as pH and $NADP^+$/NADPH ratio. The role of *ADH4* in *C. albicans* has not been investigated, but its gene product may share similar activities with that of *YMR226C*.

1.3.6 Mrr1-regulated genes in other *Candida* species

Thus far, the Mrr1 regulon has only been described for *C. albicans* (160), *C. parapsilosis* (162), and *C. lusitaniae* (97, 102, 214). Across all three species, the genes which appear most strongly regulated by Mrr1 are *MDR1*, a putative pyridoxal reductase, and at least one putative methylglyoxal reductase, all of which have been described above. Interestingly, two genes encoding putative methylglyoxal reductases are overexpressed along with *MDR1* in azole-resistant *C. parapsilosis* strains (162), and *C. lusitaniae* has three such genes whose expression is regulated by Mrr1 (97, 214). The Mrr1 regulons of *C. parapsilosis* and *C. lusitaniae* also contain several other predicted AKRs, oxidoreductases, and alcohol dehydrogenases, but not the IFD gene family (97, 162, 214). Many of the genes regulated by Mrr1 in these species remain uncharacterized (97, 162, 214). The biological significance of the conserved co-regulation of *MDR1* with the aforementioned genes remains to be understood but will likely shed new light on drivers of *MDR1* expression, and perhaps drug resistance as a whole, in fungal pathogens.

1.4 Methylglyoxal and other reactive carbonyl compounds

Methylglyoxal (MG), also known as pyruvaldehyde or 2-oxopropanal, is a small, electrophilic dicarbonyl molecule that is endogenously formed in all living cells as a byproduct of several metabolic processes. Due to its reactivity toward biomolecules, MG at high concentrations is toxic, but at nonlethal concentrations has been shown to have a signaling effect on both prokaryotic and eukaryotic cells.

1.4.1 Formation from endogenous metabolism

Glycolytic intermediates: dihydroxyacetone phosphate and glyceraldehyde-3-phosphate

It is widely accepted that glycolysis is the predominant source of MG formation in most organisms. Under physiological pH and temperature *in vitro*, MG is spontaneously formed from the triose phosphates glyceraldehyde-3-phosphate (GA3P) and dihydroxyacetone phosphate (DHAP) in a first-order reaction (284) (**Fig. 1.3**). Under these conditions, spontaneous MG formation occurs more rapidly from GA3P, but addition of the enzyme triose phosphate isomerase increases the rate of conversion from DHAP to MG (284). Thus, it is hypothesized that MG formation is the consequence of spontaneous phosphate elimination of the 3-phospho-2,3-enediol intermediate that is formed during the isomerization of DHAP to GA3P (and vice-versa) by triose phosphate isomerase (TPI) (284). Indeed, directed deletion of just four amino acid residues from the highly conserved flexible loop of TPI drastically impedes the enzyme's ability to interact with the phosphate group of the enediol intermediate and results in an increased rate of phosphate release and MG formation *in vitro* (285). Although the phosphate elimination catalyzed by

triosephosphate isomerase is several orders of magnitude slower than the isomerization reaction *in vitro* (286), TPI is highly abundant in mammalian cells (287), and thus MG generation from triose phosphates may have significant consequences for the cell.

The enzyme MG synthase specifically acts upon DHAP to produce MG (288) (**Fig. 1.3**) and has been identified primarily in bacteria, namely *Escherichia coli* (288), *Pseudomonas saccharophilia* (289), *Proteus vulgaris* (290), *Clostridium acetobutylicum* (291), *Bacillus subtilis* (292), and a strain of the thermophilic genus *Thermus* isolated from a hot spring (293). One study from 1971 reported the isolation of MG synthase activity from homogenized goat liver (294), but there have currently been no other published observations of MG synthase activity in animal tissue. Purified MG synthase from *E. coli* is specific for DHAP, exhibits optimal activity at pH 7.5, and is strongly inhibited to varying degrees by phosphoenolpyruvate, 3-phosphoglycerate, pyrophosphate (PP_i), and inorganic phosphate (P_i) (288). The concentration at which P_i inhibits MG synthase is similar to the K_m of the enzyme glyceraldehyde 3-phosphate dehydrogenase (GAPDH) for P_i as a substrate, leading researchers to postulate that MG synthesis by MG synthase is regulated by intracellular P_i (288).

Other compounds capable of being metabolized to glycolytic intermediates may also lead to spontaneous and/or enzymatic MG generation, including hexose phosphates (295), gluconate (296), and five-carbon sugars like xylose and ribose (296, 297) (**Fig. 1.3**). In *E. coli*, overexpression of transporters and/or catabolic pathways for any of these substrates leads to inhibitory or lethal endogenous MG production (295-297), and thus, their intracellular content must be tightly regulated. Glycerol is well-characterized as a precursor to MG through DHAP (**Fig. 1.3**). In *E. coli*, loss of feedback inhibition of

glycerol kinase leads to fatal accumulation of MG via uncontrolled dissimilation of glycerol into GA3P and DHAP (298), and mutants in *S. cerevisiae* (299) and *C. albicans* (300) with defects in MG detoxification cannot utilize glycerol as a carbon source due to increased accumulation of intracellular MG. Glycerol has also been associated with MG formation in *Mycobacterium bovis* (301), *Mycobacterium tuberculosis* (302), and the cyanobacterium *Synechococcus* (303). Another potential source of MG is fructose, which can be metabolized to fructose-6-phosphate and subsequently to fructose-1,6-bisphosphate, a direct triosephosphate precursor (**Fig. 1.3**). Elevated serum or tissue MG has been observed in mice or rats fed a high-fructose diet (304-306) and can be prevented by knockdown of aldolase B (304, 306), the enzyme which converts fructose-1,6-bisphosphate to GA3P and DHAP. Furthermore, *S. cerevisiae* accumulates higher levels of intracellular dicarbonyls – like MG – and glycated proteins when grown in fructose compared to glucose (307). Sorbitol can also be metabolized to MG through this pathway after its oxidation to fructose by sorbitol dehydrogenase (**Fig. 1.3**).

Aminoacetone

MG may also arise as a byproduct of threonine catabolism through oxidation of aminoacetone (**Fig. 1.3**). Suspensions of *Staphylococcus aureus* cells incubated with threonine produce aminoacetone in the presence of oxygen, which was the first indication of aminoacetone as a metabolite of threonine (308, 309). Aminoacetone was also detected in *S. aureus* cell suspensions incubated aerobically with glycine and glucose, although its rate of formation under these conditions was approximately 30 times slower than with threonine (308, 309). When grown with L-threonine as a sole nitrogen source, cultures of

S. cerevisiae accumulate aminoacetone concomitantly with the disappearance of L-threonine from the medium, accompanied by increased activities of MG detoxification enzymes compared to yeast grown with ammonium sulfate as a nitrogen source (310).

Studies in mammalian tissues have demonstrated enzymatic oxidation of aminoacetone of MG via amine oxidase (311-313). There is also evidence to suggest that MG acts as a feedback inhibitor of its own formation from aminoacetone, as it has been shown to inhibit activity of L-threonine dehydrogenase, an enzyme which catalyzes the oxidation of L-threonine to aminoacetone (314). Homogenates of human umbilical artery have been reported to oxidize aminoacetone to MG via semicarbazide-sensitive amine oxidase (SSAO) activity (315, 316). SSAO-mediated deamination of aminoacetone to MG has also been demonstrated in rats via HPLC analysis of urine from rats administered aminoacetone (317). More recently, it has been shown *in vitro* that purified ferricytochrome C, a hemeprotein component of the electron transport chain, can also catalyze oxidation of aminoacetone to MG and H_2O_2 (318).

Acetone

Acetone, a metabolite of fatty acids that becomes elevated in mammalian plasma and urine during ketogenic conditions such as fasting or uncontrolled diabetes (see reference (319) for review), can also be metabolized to MG via acetol (**Fig. 1.3**). Microsomes from the homogenized livers of acetone-fed rats display NADPH- and O_2-dependent enzymatic conversion of acetone to acetol (acetone monooxygenase activity) and acetol to MG (acetol monooxygenase activity) (320). Subsequently, both enzymatic activities were attributed to cytochrome P-450 isozyme 3a in hepatic microsomes from

rabbits treated with either ethanol or acetone (321). Ethanol induces acetone monooxygenase activity of rabbit hepatic microsomes by about 6-fold and acetol monooxygenase activity by about 3-fold relative to untreated rabbits (321). Likewise, acetone induces these enzyme activities by 11-fold and 3-fold respectively (321). There is evidence that ketosis leads to increased serum levels of acetone and MG in humans (322) and dairy cattle (323), suggesting that acetone is a significant source of MG formation in mammals, including humans, during ketogenic conditions.

Catabolism of acetone with the potential to generate MG has also been observed in microbes. In particular, acetone response and catabolism have been studied in the *Mycobacterium* genus (324-326). In *M. smegmatis* and *Mycobacterium goodii*, acetone induces expression of the *mimABCD* gene cluster, which encodes a multicomponent binuclear iron monooxygenase that involved in the catabolism of acetone, propane, and phenol (327). Subsequently, it was confirmed via gas chromatography analysis of recombinant *E. coli* expressing *mimABCD* that the product of this gene cluster directly oxidizes acetone to acetol (328). Additionally, four strains of Gram-positive bacteria, likely all belonging to the genus *Corynebacterium*, isolated from soil in different locations demonstrate the ability to oxidize acetone to acetol and acetol to MG in an NAD^+-dependent manner (329). Recently, isolates of the methanotroph *Methylacidiphilum* have been observed to oxidize acetone to acetol via a particulate methane monooxygenase enzyme; it is hypothesized that this organism subsequently oxidizes acetol to MG and MG to pyruvate, when can then enter the citric acid cycle or gluconeogenesis (330).

Degradation of glucose and glycated proteins

In addition to the metabolic pathways outlined above, glucose can undergo spontaneous degradation to MG, glyoxal, and 3-deoxyglucosone *in vitro* at physiological temperature and pH, albeit at a slow rate (331). Formation of all three compounds occurs at a much faster rate in the presence of either Nα-t- butoxycarbonyl-lysine or human serum albumin, suggesting that glucose glycates amino acids to form a Schiff base which then spontaneously degrades to MG, glyoxal, and 3-deoxyglucosone (331).

1.4.2 Mechanisms of MG-mediated cytotoxicity

Glycation of amino acids

Regarding proteins, MG reacts preferentially with arginine, lysine, and cysteine residues. Studies indicate that arginine is the predominant target of glycation by MG (332-336), the most common products of which are methylglyoxal hydroimidazolone (MG-H1) (335) and argpyrimidine (333) (**Fig. 1.4**). Quantitative studies of MG-derived AGEs in human tissues indicate that from 0.1 to 2% of total cellular arginine is modified by MG (337, 338). This is particularly damaging due to the prevalence of arginine residues in the active sites of many enzymes (339, 340). In fact, arginine residues are present in the catalytic sites of all enzymes involved in glycolysis, with the exception of triosephosphate isomerase (341). The most common products of lysine modification by MG are Ne-carboxyethyl lysine (CEL) and lysine-derived 4-methylimidazolium crosslink (MOLD) (334-336) (**Fig. 1.4**). Additionally, MG can form cross-links between lysine and arginine residues, forming 2-ammonio-6-((2-[(4-ammonio-5-oxido-5-oxopentyl) amino]-4-methyl-4,5-dihydro-1H-imidazol-5-ylidene) amino) hexanoate (MODIC) (342) (**Fig. 1.4**). Human

proteins that have been found to be glycated by MG at arginine and/or lysine residues (see references (343) and (344) for review) include hemoglobin, albumin, lens crystallin, histones, and collagen. Finally, MG can react reversibly with cysteine residues to form hemithioacetal products (345), which may undergo rearrangement to more stable adducts such as S-(2-carboxyethyl) cysteine (CEC) (346). In *S. cerevisiae*, the most prominent targets of glycation by MG are the glycolytic enzymes enolase, aldolase, and phosphoglycerate mutase in addition to the heat shock proteins Hsp71/72 and Hsp26 (347). Remarkably, glycation of these three enzymes in *S. cerevisiae* does not affect the glycolytic flux despite a demonstrated loss of enzymatic activity; mathematical modeling predicts a significant decrease in glycolytic flux only if enolase loses 95% of its native activity (347). MG-induced glycation of glycolytic enzymes has also been reported in several mammalian cell lines (348).

Although protein modification by MG occurs spontaneously, numerous studies indicate that it is a nonrandom process in which specific residues within specific proteins have a higher propensity than others to react with MG under physiological conditions (349-355). For example, an LC-MS/MS-based analysis of lysine or arginine glycation sites on proteins following *in vitro* incubation of human plasma with MG revealed only 14 potential hotspots for MG glycation across five different proteins, including albumin which contains nine of the identified hotspots (351). Interestingly, human serum albumin contains a total of 27 arginine residues and thus it is clear that MG exhibits site-specific reactivity (351). Similarly, another study found via mass spectrometry that when myoglobin is incubated with MG *in vitro*, only two specific lysine residues are modified regardless of the length of incubation time (352). The determinants of site-specific glycation are poorly understood

but are likely based on one or more chemical properties of a given residue within its unique microenvironment. Some studies have reported an association between the pK_a of an arginine or lysine residue and nucleophilic reactivity; that is, a lower pK_a leads to decreased protonation thereby promoting reaction with electrophiles (355-357). In contrast, Sjoblom et al. (350) reported no correlation between MG-dependent glycation of arginine or lysine and either pK_a or content of surface-accessible nucleophilic residues, but that glycation is promoted by proximal tyrosine and hindered by proximal acidic residues (350). Nucleophilic reactivity of thiols such as cysteine may depend on hydrophobicity of the thiol's microenvironment (358, 359).

Glycation of nucleic acids and nucleotides

In addition to amino acid residues, MG and other 2-oxoaldehydes can irreversibly modify nucleic acids in both DNA and RNA. MG predominantly reacts with deoxyguanine (dG), forming the nucleotide AGE N2-(1-carboxyethyl)-deoxyguanosine (CEdG) (360, 361). The abundance of CEdG in human tissue is estimated to range from 0.1 to 1.0 CEdG molecules per 10^6 nucleotides (362, 363). Modification of DNA by MG may lead to DNA-DNA crosslinks (364), DNA-protein crosslinks (365, 366), and DNA strand breaks (363, 367), which likely account for the observed mutagenicity of MG (368-372). Interestingly, MG can also inhibit synthesis of DNA, RNA, and proteins by reacting with free GTP (373). In mammals, MG-modified DNA instigates an autoimmune response, which is likely another mechanism of MG toxicity at the organismal level (374-376).

Oxidative stress

Aside from its direct effects on proteins and nucleic acids, MG can also induce oxidative stress by promoting ROS and RNS formation or depletion of the cellular antioxidant glutathione (see reference (377) for review). Exposure to MG leads to increased fluorescence of the oxidative stress indicator DCFH-DA in the macrophage-derived cell line U937 (378), rat vascular smooth muscle cells (379), rat fetal cortical neurons (380), the rat thoracic aorta cell line A10, and human red blood cells (381). The mechanism(s) of MG-driven ROS and RNS production are not well understood and are likely multifactorial. One possible mechanism is that MG can inhibit the activities of several antioxidant enzymes, such as superoxide dismutase (SOD) (382, 383), glutathione-S-transferase (382), catalase (382), and numerous peroxiredoxins (PRX) (384). Inhibition of Prx activity by MG is hypothesized to be the result of irreversible modification of catalytically important cysteine residues (384), and the inhibition of Sod1 activity appears to be caused by misfolding of the immature form of the enzyme following glycation by MG (383).

Several studies in mammalian cells have indicated that treatment with MG may also lead to depletion of reduced glutathione (GSH), a vital component of the defense machinery against oxidative stress in most organisms (see reference (385) for review). For example, murine hepatocytes incubated in the absence of glucose, pyruvate, or amino acids displayed a significant and lasting decrease in GSH content upon treatment with 20 mM MG (386). However, for hepatocytes treated with MG in medium containing glucose, pyruvate, or amino acids, only a transient loss of cellular GSH was observed (386). Additionally, MG-treated cells are unable to restore their GSH levels in the presence of buthionine sulfoximine, which inhibits GSH biosynthesis (386), suggesting that in

hepatocytes, GSH is newly synthesized in response to high levels of MG. GSH depletion following addition of MG has been observed, to varying degrees, in serval other mammalian cell types, including human platelets (387), rat colonocytes (388), rat lense cells (389), and human umbilical vein endothelial cells (390). Decreased GSH content resulting from MG treatment has also been reported *in vivo*; namely, in the liver (391, 392), spleen (391), and blood (393) of mice either injected with MG or supplemented with it in their drinking water. Furthermore, MG has been observed *in vitro* to inhibit activity of glutathione reductase (394, 395) and glutathione peroxidase enzymes (395), both of which play an essential role in the normal redox cycling of glutathione.

1.4.3 Detoxification and catabolism of MG

GSH-dependent glyoxalase system

The major mechanism for MG detoxification and catabolism in most organisms is the GSH-dependent glyoxalase system, which consists of two enzymes, glyoxalase I and glyoxalase II, and yields D-lactate as a final product (**Fig. 1.5**). The earliest discovery of the glyoxalase system dates as far back as 1913, when Neuberg (396) described the enzymatic conversion of MG to lactic acid in animal tissues. In 1951, Racker (397) demonstrated in *S. cerevisiae* that production of lactic acid from MG was a two-step, GSH-dependent process catalyzed sequentially by two enzymes, which he named glyoxalase I (Glo1) and glyoxalase II (Glo2). Glyoxalase I is a lactoylglutathione lyase that catalyzes the formation of S-D-lactoylglutathione from the product of spontaneous condensation between MG and GSH (**Fig. 1.5**). Glyoxalase I enzymes have been identified across a wide array of mammals, plants, protozoa, fungi, and bacteria (see reference (398) for review),

although a *GLO1* gene appears to be absent from the genomes of the protozoan organisms *Trypanosoma brucei*, *Giardia lamblia*, and *Entamoeba histolytica* (see reference (399) for review). In most species that do express glyoxalase I, enzyme activity requires a catalytic amount of GSH; however, many protozoan parasites of the *Kinetoplastida* class, such as *Trypanosoma cruzi* and *Leishmania major*, preferentially use trypanothione (TSH), a conjugate of two glutathione molecules with spermidine (399). In addition to GSH or TSH, catalytic activity of glyoxalase I is dependent on a divalent metal cation, generally zinc (Zn^{2+}) or nickel (Ni^{2+}) depending on the organism. The glyoxalase I enzymes thus far studied from most eukaryotes are Zn^{2+}-dependent (400-402) and most prokaryotic glyoxalase I enzymes are Ni^{2+}-dependent (403), although some exceptions have been noted (404-408).

Glyoxalase II, a hydroxyacylglutathione hydrolase, catalyzes the hydrolysis of S-D-lactoylglutathione (or, in the case of trypanosomatids, S-lactoyltrypanothione) to D-lactate and GSH (**Fig. 1.5**). Like glyoxalase I, glyoxalase II has been identified in mammals, plants, yeasts, protozoans, and bacteria and is thought to be nearly ubiquitous (see reference (398) for review). In some organisms, such as *S. cerevisiae* (409), *P. falciparum* (410), and *T. brucei* (411, 412), two glyoxalase II enzymes have been characterized. The case of *T. brucei* is particularly interesting because, as stated above, this organism lacks a glyoxalase I. Only one of the glyoxalase II enzymes in *T. brucei* demonstrates S-lactoyltrypanothione hydrolase activity (411). In contrast, both glyoxalase II enzymes in *P. falciparum* are functional; one localizes to the cytosol and the other to the apicoplast (410). Likewise, the two glyoxalase enzymes of *S. cerevisiae*, Glo2 and Glo4, are also differentially localized: Glo2 is cytosolic and Glo4 is mitochondrial (409). Yeast

mitochondria do not contain Glo1, but it has been hypothesized that Glo4 is involved in salvaging GSH from S-D-lactoylglutathione, which can enter the mitochondria (413). Similarly, the single functional glyoxalase II of *T. brucei* is postulated to act as a general trypanothione thioesterase, as it can catalyze the hydrolysis of spontaneously formed thioesters such as S-propionyl- and S-acetyltrypanothione (411).

GSH-independent glyoxalase

Enzymes which catalyze GSH-independent conversion of MG to D-lactate have also been characterized in numerous organisms (**Fig. 1.5**). *E. coli* was the first organism in which GSH-independent glyoxalase activity, termed glyoxalase III (Glo3), was discovered (414). In *E. coli*, expression of the glyoxalase III gene is regulated by RNA polymerase sigma factor (rpoS) and is enriched during the stationary phase of growth (415). Glo3 of *E. coli* appears highly specific for MG; of the other carbonyl compounds tested, only phenylglyoxal could also serve as a substrate for Glo3, and with just 15% of the enzymatic activity compared with MG as a substrate (414). In one study, Glo3 exhibited significantly higher activity than Glo1 or Glo2, suggesting that it may be the predominant mechanism of MG detoxification, although its activity is not induced by MG (416). *In vitro*, Glo3 is sensitive to inactivation by H_2O_2, which can be rescued by addition of purified catalase enzyme (416). *E. coli* Glo3 is encoded by the *hchA* gene (417), the product of which had previously been known as the heat-inducible molecular chaperone Hsp31 (418-420). Prior to its identification as glyoxalase III, Hsp31 was found to contribute to the resistance of *E. coli* against heat shock (420, 421), starvation (420, 421), and acid stress (422); it is

unknown whether the protective effects of Hsp31/Glo3 against these stressors are dependent on its glyoxalase III activity.

GSH-independent glyoxalase III has also been reported in the Gram-positive bacteria *Staphylococcus aureus* (423) and *Bacillus subtilis* (424); the fungi *S. cerevisiae* (425), *S. pombe* (426), and *C. albicans* (300); in humans, mice, and the nematode *Caenorhabditis elegans* (427); and in numerous plant species (428-431). All glyoxalase III enzymes characterized thus far belong to the ThiJ/DJ-1/PfpI protein family, a large group of structurally similar proteins with diverse functions, many of which are involved in cellular stress response (see reference (432) for review). Human glyoxalase III, known as DJ-1 or Park7, has been extensively studied for its role in oncogenesis and early-onset Parkinson's disease (see reference (433) for review) long before its glyoxalase activity became apparent. Human DJ-1 is likely a multifunctional protein, as it also exhibits important roles in ROS signaling, metabolism, serine biosynthesis, glutathione redox cycling, mitochondrial function, and as a molecular chaperone (see reference (433) for review).

The first confirmed glyoxalase III in any species of fungus was *C. albicans* Glx3, identified in 2014 by Hasim et al (300). Relative to the wild-type *C. albicans* strain SC5314, a *glx3*-null mutant exhibits increased intracellular concentrations of MG, increased susceptibility to exogenously added MG, and a growth defect when glycerol is provided as the sole carbon source (300). Like *E. coli* Hsp31, *C. albicans* Glx3 is enriched in stationary phase cultures (434). Expression of the *GLX3* gene in *C. albicans* is regulated by Mrr1 (160, 169, 219), induced by oxidative stress via Cap1 (175) and induced in low iron via Hap43 (435). Two proteins from *S. pombe*, Hsp3101 and Hsp3102, demonstrate

glyoxalase III activity *in vitro*, and overexpression of either one increases resistance against exogenous MG and glyoxal, even in a *glo1*-null mutant (426). Hsp31 in *S. cerevisiae* plays an important role in resistance to oxidative and carbonyl stress and in the maintenance of cellular redox status (425). Additionally, *S. cerevisiae* Hsp31 along with three other DJ-1-like proteins, Hsp32, Hsp33, and Hsp34, are seemingly involved in cytoplasmic protein quality control during stationary phase (436). Expression of *S. cerevisiae HSP31* is strongly induced by MG, ethanol, glycerol, acetic acid, oxidative stress, heat stress, and osmotic stress (437). The *HSP31* promoter contains binding motifs for the stress-responsive transcription factors Yap1, Cad1, Gis1, Haa1, Msn2, Msn4, and Hsf1, and experimental evidence supports a role for each of them in the upregulation of *HSP31* expression in response to specific types of stress (437). Genetic deletion of *HSP31* sensitizes *S. cerevisiae* to many of the stresses which induce its expression, indicating that Hsp31 is a multi-stress response protein (437).

Oxidoreductases and dehydrogenases

The AKR superfamily proteins are a large group of structurally similar enzymes which catalyze the NADPH- or NADH-dependent reduction of carbonyl substrates to their corresponding alcohols and have been identified in prokaryotes, protozoa, fungi, plants, and animals (438). Substrate specificity of these enzymes is determined by variable loops in the C-terminal region of the protein (438); however, many AKRs demonstrate some degree of substrate promiscuity *in vitro* (see reference (439) for review). Many AKR enzymes have been shown to act upon MG as a substrate, even if they are not specific for MG. For example, four AKRs from *E. coli*, YafB, YqhE, YeaE, and YghZ, can reduce MG

to acetol (**Fig. 1.5**) *in vitro* and genetic deletion of any of these proteins increases MG susceptibility in a glyoxalase-deficient mutant (440). In addition to MG, YghZ can reduce 4-nitrobenzaldehyde and Isatin with relatively high specific activities, as well as phenylglyoxal, diacetyl, and several other carbonyl compounds with much lower specific activities (441). In the cyanobacterium *Synechococcus*, the AKR SakR1 reduces MG and several nitrobenzaldehyde derivatives with high specific activities and can act upon many other aldehyde substrates with a fraction of the specific activity shown with MG (303). Moreover, a *sakR1*-deficient mutant accumulates higher levels of MG in the presence of glycerol and is more susceptible to exogenous MG compared to a wild-type strain (303).

In *S. cerevisiae*, the AKR known as aldose reductase, encoded by *GRE3*, contributes to MG detoxification (**Fig. 1.5**). Like *GRE2* described in the previous section, expression of *GRE3* is upregulated in response to a variety of stresses, including heat, osmotic, oxidative, and carbon limitation (258, 442). Induction of *GRE3* in response to these stresses is dependent on the high osmolarity glycerol (HOG) mitogen-activated protein kinase (MAPK) cascade, as deletion of the kinase Hog1 abolishes salt-induced *GRE3* expression and deletion of the downstream transcription factors Msn2 and Msn4 abolishes *GRE3* induction by carbon starvation (442). No induction of *GRE3* expression is observed in a *hog1*Δ/*msn2*Δ/*msn4*Δ triple mutant (442). The thermal-responsive transcription factor Hsf1 is also partially required for *GRE3* induction in response to heat stress. Neither overexpression nor deletion of *GRE3* influences tolerance to the stressors which induce its expression, but *GRE3* overexpression enhances MG tolerance and can even rescue the MG sensitivity of a *glo1*Δ mutant (442). Conversely, deletion of *GRE3* from either a wild-type or a *glo1*Δ background does not increase MG sensitivity (442).

Interestingly, the stresses which induce *GRE3* expression in *S. cerevisiae* also lead to transient elevation of intracellular MG (442), suggesting that MG detoxification may be particularly important under such conditions.

Specific AKR genes have also been implicated in MG detoxification in plants (443-448), mammals (449-451); the yeast *Kluyveromyces marxianus* (452, 453), trypanosomatid parasites (454), and the tapeworm *Moniezia expansa* (455). Notably, the genomes of most organisms encode multiple AKR proteins, some of which may have overlapping substrate specificity (see reference (439) for review). This in combination with the relatively broad substrate specificity of many AKRs makes studying their physiological roles difficult. It has been postulated that the AKR superfamily is the result of evolutionary divergence from an ancestral enzyme that catalyzed NAD(P)H-dependent reduction of a diverse array of carbonyl substrates (438).

Like the AKR superfamily, the short-chain dehydrogenase/reductase (SDR) superfamily consists of NAD(P)H-dependent oxidoreductases, many of which play important roles in metabolic processes. SDRs are more biochemically and functionally diverse than AKRs; types of reactions catalyzed by SDRs include carbonyl-alcohol oxidoreduction, steroid isomerization, enoyl-CoA reduction, decarboxylation, dehalogenation, and dehydrogenation (see reference (456) for review). MG reductases, like Gre2 and Mgd1 described in previous sections, are members of the SDR superfamily that catalyze the irreversible NADPH- or NADH- dependent reduction of MG to lactaldehyde, which is subsequently oxidized to L-lactate by lactaldehyde dehydrogenase (**Fig. 1.5**). This distinguishes MG reductases from the AKRs described above, which yield alcohols as a product of 2-oxoaldehyde reduction. Like the AKRs, MG reductase enzymes are

ubiquitous throughout the tree of life and have been reported in mammals (457, 458), plants (459, 460), fungi (261, 461, 462), protists (463-465), bacteria (466-468), and archaea (469). In general, MG is the preferred substrate of the MG reductases characterized thus far, but many of these enzymes can reduce other aldehyde compounds, albeit with less activity than that observed for MG (457, 458, 461, 462).

Alcohol dehydrogenase (ADH) enzymes are also members of the SDR superfamily that have been shown to contribute to detoxification of MG and other reactive carbonyls in certain species (**Fig. 1.5**). For example, an ADH purified from *E. coli* can catalyze the reversible reduction of MG, acetaldehyde, formaldehyde, and benzaldehyde to their corresponding alcohols in an NADH-dependent manner (470). NADH-dependent reduction of MG to acetol by ADH enzymes has also been observed in horse liver (471), the hyperthermophilic archaeon *Pyrococcus furiosus* (472), the enterobacterium *Dickeya zeae* (473), *S. cerevisiae* (261), and *C. albicans* (474). In *C. albicans*, disruption of the *ADH1* locus leads to increased intracellular accumulation of MG and ROS, increased susceptibility to exogenous MG, and cell cycle arrest in the G2 phase, suggesting that Adh1 is important for maintaining cellular redox balance and regulating cell cycle progression in *C. albicans* (474). Moreover, there is evidence that Adh1 and the MG reductase Mgd1, discussed in the prior section, cooperatively modulate cellular MG and ROS in *C. albicans*. Disruption of *ADH1* and/or *MGD1* leads to increased intracellular MG and ROS, decreased GSH content, and decreased activity of the glutathione reductase Glr1 (474).

Finally, some organisms possess MG dehydrogenase enzymes, which oxidize MG directly to pyruvate in an $NAD(P)^+$ manner (**Fig. 1.5**). This activity has been reported in mammalian livers (475-477) and in the bacterium *Psuedomonas putida* (478).

1.4.4 Methylglyoxal is elevated in many human diseases, including diabetes

MG and other reactive carbonyl compounds have been linked to a myriad of human diseases, including cancer, obesity, neurodegenerative diseases, and diabetes in addition to normal aging (see reference (479) for review). There exists a vast body of literature regarding the role of MG in human disease, and numerous reviews have been published on the topic. Thus, only a brief summary of the sources and effects of MG in the context of diabetes will be given here, linking this section to the summary of fungal infections in relation to diabetes presented in the first section of this chapter.

Despite the variability of MG concentrations measured in human samples – which is likely due to differences in sample preparation and heterogeneity among individuals – concentrations of MG in the blood or urine are consistently observed to be higher in diabetic patients compared to nondiabetic controls (see reference (480) for review). For example, reported plasma concentrations of free MG range from 123 nM to 3.3 μM and from 189 nM to 5.9 μM in nondiabetic and diabetic humans, respectively (reference (480) and the references therein). More recently, elevated MG has also been measured in the saliva of Type 2 diabetic patients compared to healthy controls (481). Additionally, while most studies have focused on the role of MG and AGEs in patients with either Type 1 or Type 2 diabetes, a recent study reported higher levels of MG and pro-inflammatory cytokines in individuals with gestational diabetes compared to nondiabetic, nonpregnant controls (482).

The specific sources of extracellular MG in mammals remain unclear, as most enzymes involved in MG production are intracellular except for SSAO circulating in the

plasma (483), but a few possibilities exist. As described previously, MG can form spontaneously from the degradation of glucose, and this process is accelerated in the presence of protein (331). Therefore, it is plausible that hyperglycemia promotes spontaneous MG generation, especially in the presence of abundant blood proteins like hemoglobin and albumin. Indeed, even transient hyperglycemia leads to elevated plasma MG (484, 485). There is also evidence to support a role for plasma SSAO in extracellular MG production; namely, individuals with Type 1 or Type 2 diabetes exhibit increased plasma SSAO activity compared to nondiabetic controls (486, 487). To date, there are no published studies comparing plasma aminoacetone levels in humans with and without diabetes. However, in vascular smooth muscle cells *in vitro*, aminoacetone is the most potent precursor of MG formation (488), suggesting that if the concentration of aminoacetone is indeed elevated in diabetes, it could be a significant source of plasma MG.

Inevitably, a rise in MG formation that outweighs an organism's detoxification capacity will have biochemical and physiological consequences due to the nature of MG as a reactive electrophile. In fact, MG is thought to be one of the predominant molecular causes of diabetic complications, particularly retinopathy, nephropathy, neuropathy, and cardiovascular disease. Measurements of MG and MG-derived AGEs may be predictive of certain clinical outcomes, even before the presentation of symptoms. For example, plasma concentrations of the MG-derived AGEs MG-H1 and CEL are significantly higher in patients with fast-progressing diabetic nephropathy compared to those with slow-progressing or absent nephropathy (489). Additionally, in Type 1 (490) and Type 2 (491) diabetic patients, plasma MG concentration is associated with both fatal and non-fatal cardiovascular disease. Another study found an association between plasma MG or CEL

and more adverse outcomes and increased risk of amputations in diabetic patients with severe limb ischemia (492). Thus, in general, it appears that higher levels of MG and some of its adducts are correlated with worse clinical outcomes and a greater risk for diabetic complications. But why might that be the case? As it turns out, MG and several MG-derived AGEs have a detrimental effect on the immune system, capable of both triggering inflammatory responses and dampening some aspects of cell-mediated immunity, which likely contribute to the aberrant immune function often seen in diabetic patients.

The effects of MG and its AGEs on the immune system are manifold. One way in which MG modulates immune function is through activation of the p38 MAPK, nuclear factor-κB (NF-κB), and c-Jun N-terminal kinase (JNK) pathways of mammalian cells, promoting secretion of pro-inflammatory cytokines (493-497), ROS (495, 497, 498), and expression of the pro-inflammatory gene *COX-2* which encodes a prostaglandin-endoperoxide synthase (499, 500). Furthermore, glycation by MG creates immunogenic neoepitopes on extracellular proteins such as fibrinogen (501, 502), low-density lipoprotein (LDL) (503, 504), and albumin (505, 506), resulting in an autoimmune reaction. Additionally, MG-derived AGEs such as MG-H1, CEL, and MOLD can act as ligands for the receptor for advanced glycation end products (RAGE) (497, 507-510) to initiate an inflammatory response via the MAPK/extracellular signal-regulated kinase (MAPK/ERK), transforming growth factor-β (TGF-β), JNK, and NF-κB signaling pathways (see reference (511) for review).

In apparent contrast to the induction of inflammation, MG also has an inhibitory effect on monocyte and PMN phagocytic capabilities and on migration of immune cells. Guerra et al. (495) demonstrated that MG and high glucose diminish the phagocytic

capacity of neutrophils while simultaneously increasing myeloperoxidase activity and ROS production. These effects can be synergistically mitigated *in vitro* by administration of the antioxidants astaxanthin and vitamin C (495). MG also impairs phagocytosis of microbes and cellular debris by macrophages (494, 512), which may contribute to the compromised wound healing and microbial clearance that is common among diabetic patients. *In vitro*, addition of the antioxidant pyridoxamine can rescue the phagocytic defect of M1 macrophages (512), which, along with the observation that astaxanthin and vitamin C can restore MG-disrupted neutrophil function (495), suggests that supplementation with specific antioxidants may help ameliorate some of the immune dysregulation in diabetes. MG can also impede the ability of immune cells to localize to the site of an infection by altering the extracellular landscape. For instance, glycation of fibronectin and collagen, components of the extracellular matrix, impairs the migration and attachment of Jurkat T-cells *in vitro* (513). Finally, it is worth noting that activated macrophages (514-516) and neutrophils (517-522) produce MG and other reactive aldehydes in response to microbial antigens, which could, under hyperglycemic conditions with impaired microbial killing, lead to a progressive cycle of inflammation, MG production, and failure to clear the pathogenic targets, resulting in host tissue damage and an unresolved infection.

1.4.5 MG as a stress signal

There is substantial evidence that MG and other physiologically generated reactive electrophiles function as signaling molecules in eukaryotes and prokaryotes alike. Mechanisms of MG-mediated signaling have been well studied in *S. cerevisiae* as well as in numerous human-derived cell lines. This section will overview the signaling pathways

modulated by MG in *S. cerevisiae*, followed by examples of parallels in other organisms in addition to several signaling pathways that have not been identified in yeast.

In *S. cerevisiae*

In *S. cerevisiae*, MG has been shown to interact with multiple independent signaling pathways, including the HOG MAPK cascade (523, 524), the target of rapamycin complex 2 (TORC2)/protein kinase C (Pkc1) kinase cascade (525, 526), the stress-responsive kinase Gcn2 (527, 528), and the redox-sensing transcription factor Yap1 (529). The earliest indication of MG acting as a specific stress signal in yeast was the finding that exposure to MG in the millimolar range induces expression of both *GRE3* and *GLO1*, but not of the general stress response genes *HSP26*, *HSP104*, or *CTT1* (530). In addition, MG also induces expression of the glycerol synthesis gene *GPD1* and consequently, enhanced glycerol production (530).

Because expression of *GRE3*, *GLO1*, and *GPD1* is induced by osmotic stress via the HOG pathway in yeast (442, 531-533), it was hypothesized that this pathway is also involved in the response to MG. Indeed, two independent groups have demonstrated that MG activates the HOG pathway through the Sln1 branch (**Fig. 1.6**) and that the Sln1-mediated HOG kinase cascade is necessary for resistance and adaptation to MG (523, 524). Mutants lacking *HOG1*, the upstream factors *PBS2* or *SSK1*, or the downstream factor *MSN1*, display substantial defects in MG-induced expression of *GPD1*, and are hypersensitive to MG compared to the parental strain (524). In contrast, deletion of the osmosensor *SHO1* or the Hog1-dependent transcription factor *HOT1* has no effect on MG

resistance or on *GPD1* induction, although an *ssk1*Δ/*sho1*Δ double mutant is more susceptible to MG compared to the *ssk1*Δ single mutant (524).

In addition to activation of the HOG-MAPK cascade by MG, Maeta et al. (523) also reported that MG causes an influx of calcium ions (Ca^{2+}), thereby activating calcineurin to dephosphorylate the transcription factor Crz1, resulting in increased nuclear localization of Crz1 and increased expression of the Crz1 target gene *FKS2* (**Fig. 1.6**). The mechanism of MG-induced Ca^{2+} influx has yet to be elucidated, although it is blocked by the Ca^{2+} chelator EGTA and does not appear to depend on the known Ca^{2+} channels Mid1 or Cch1 (523).

The TORC2-Pkc1 kinase cascade is another signaling pathway activated by MG in yeast (525) (**Fig. 1-6**). In brief, the yeast TORC2 complex is known to regulate plasma membrane tension homeostasis, actin polarization, actin-mediated endocytosis, and cell growth via phosphorylation of its protein kinase targets, which initiates a kinase cascade (see reference (534) for review). In *S. cerevisiae*, treatment with MG leads to a Pkc1-dependent increase in phosphorylation of the MAP kinase Mpk1 (also known as Slt2), and mutants defective in the Pkc1-Mpk1 cascade (*pkc1*Δ, *bck1*Δ, *mkk1*Δ/*mkk2*Δ, and *mpk1*Δ) display increased sensitivity to MG compared to the parental strain (525). The increased kinase activity of Pkc1 in response to MG is due to phosphorylation of Pkc1 by TORC2 (525). Activation of the Pkc1-Mpk1 cascade by MG proceeds differently from activation by heat stress, as the former occurs independently of the heat shock responsive proteins Wsc1 and Mid2 (525), which are required for the latter. A more recent study implicates both TORC1 and TORC1 in the adaptive response of *S. cerevisiae* to MG, and genetic deletion of TOR1 and/or TOR2 renders cells more sensitive to MG and glyoxal (535).

The redox-sensing transcription factor Yap1 is yet another target for MG activation in *S. cerevisiae* (529) (**Fig. 1-6**). Though Yap1 is well-known for its role in the yeast oxidative stress response, it has also been implicated in the response to cadmium (259), arsenate (536), carbon limitation (537), ionizing radiation (538), nitrosative stress (539), and a variety of thiol-reactive electrophiles such as vanillin (540), furfural (541), and malondialdehyde (542). Maeta et al. (529) observed that Yap1 is constitutively localized to the nucleus in a *glo1*Δ mutant deficient for MG detoxification, and that this mutant overexpresses a number of Yap1 target genes, including the MG reductase gene *GRE2*. Because the steady-state intracellular concentration of MG is elevated in the absence of *GLO1*, the authors hypothesized that MG itself can activate Yap1 (529). Indeed, exogenous MG also leads to nuclear accumulation of Yap1, which can be reversed by washing the cells and removing the MG-containing medium (529). Any one of the three C-terminal cysteine residues is sufficient for activation by MG, which rules out disulfide bond formation as part of the mechanism (529). Unlike H_2O_2, MG does not affect the redox state of Yap1 on a non-reducing SDS-PAGE, and overexpression of thioredoxin genes *TRX1* and *TRX2* does not reverse the nuclear localization in response to MG (529). Thus, it is hypothesized that MG directly forms adducts with any of the C-terminal cysteine residues of Yap1, thereby blocking the binding site of the exportin Crm1 (529).

Another target of activation by MG in yeast is the protein kinase Gcn2 (**Fig. 1-6**), which either activates or represses its targets via phosphorylation in response to a variety of stresses including starvation, oxidative stress, and UV irradiation (543). Activated Gcn2 can phosphorylate the alpha subunit of eukaryotic translation initiation factor 2 (eIF2a), resulting in attenuation of protein synthesis. Active Gcn2 also positively regulates the

protein level of the bZIP transcription factor Gcn4, which regulates expression of amino acid biosynthetic genes. Nomura et al. (527, 528) have demonstrated that millimolar concentrations of MG lead to overall inhibition of translation by activating Gcn2 to phosphorylate eIF2a. However, Gcn2-mediated translation of *GCN4* mRNA contributes to MG adaptation, as deletion of *GCN4* abolishes the ability of *S. cerevisiae* to acquire tolerance to lethal concentrations of MG following exposure to lower concentrations (527, 528). Therefore, it is apparent that the response of *S. cerevisiae* to MG includes attenuation of overall protein synthesis and redirection of cellular resources into translating only proteins that are beneficial in that condition. The mechanism of Gcn2 activation by MG is not known, but contrary to most other activators of Gcn2, MG does not increase the cellular content of uncharged tRNA (527, 528).

MG can also directly influence yeast metabolism by inhibiting glucose uptake. Specifically, treatment with MG leads to Rsp5-dependent ubiquitination and subsequent endocytosis and vacuolar degradation of hexose transporters (Hxts) (544). Endocytosis of ubiquitinated Hxts is delayed in a mutant lacking protein kinase C (Pkc1) but occurs independently of the downstream Pck1 target Mpk1 (544). Moreover, MG exposure causes the ubiquitination and endocytosis of the low- and high-affinity glucose sensors Rgt2 and Snf3 respectively, resulting in decreased expression of HXT genes (545).

In other eukaryotes

Many signaling pathways that have been characterized in *S. cerevisiae* are conserved across the domain *Eukaryota*. Therefore, it is unsurprising that MG has also been demonstrated to activate some of the same pathways in other eukaryotes that it

activates in *S. cerevisiae*. In *S. pombe*, MG treatment leads to phosphorylation and nuclear accumulation of the stress-response MAPKs Sty1 (546) and Spc1 (547, 548), both of which are orthologous to *S. cerevisiae* Hog1. Phosphorylation of Spc1 persists longer in a *glo1*Δ mutant (547, 548). MG-induced phosphorylation of Spc1 is dependent on the upstream factors Wis1 (a MAPKK) and Mcs4 (a response regulator), but not on the histidine kinases Phk1/Phk2/Phk3 or the phosphorelay protein Spy1 (547). The mechanism by which MG increases phosphorylation of Spc1 appears to be via interaction with the conserved cysteine residue of the protein tyrosine phosphatases Pyp1 and Pyp2, thereby inhibiting their ability to dephosphorylate Spc1 (548). In the same study, inhibition of human protein tyrosine phosphatase 1B by MG was demonstrated *in vitro* (548), suggesting that this mechanism of MG signaling is conserved throughout *Eukaryota*. Numerous studies (493, 499, 500, 506, 549-563) have reported that MG enhances phosphorylation and activation of p38, the mammalian ortholog of Hog1, in human-derived cell lines and in animal models. Depending on the cell type, activation of p38 by MG can lead to apoptosis (552, 555, 558, 560) or secretion of proinflammatory cytokines (506, 549, 557).

As observed in *S. cerevisiae* (523), MG can disrupt Ca^{2+} homeostasis in eukaryotic cells, which can have profound effects on signaling via Ca^{2+}-responsive proteins. In murine neurons, for example, MG has a dose-dependent, biphasic effect on Ca^{2+} influx: a low dose of MG (150 μM) increases Ca^{2+} influx in the presence of KCl, while higher doses decrease Ca^{2+} influx. MG also leads to increased intracellular Ca^{2+} in renal tubular cells (564), murine endothelial and mesangial cells (565), human platelets (566), and in plants (567, 568). In mammals, dysregulation of endothelial Ca^{2+} channel activity by MG causes increased vasoconstriction (569), leading to hypertension (570) and other vascular

complications. In plants, MG-mediated Ca^{2+} signaling regulates stomatal closing (567) and may play a role in thermotolerance (568).

The TOR pathway appears to be another conserved target of MG modulation in eukaryotes. *In vitro*, MG activates mammalian TORC2 (mTORC2), resulting in phosphorylation and activation of the multifunctional regulator Akt (525). MG also stimulates Akt phosphorylation in the adipocytes of obese rats, accelerating cell cycle progression and proliferation (571). Conversely, MG suppresses Akt-dependent hypoxia-inducible factor 1 alpha (HIF-1α) signaling in brain endothelial cells, leading to mitochondrial dysfunction and mitophagy (572). In colorectal cancer cells, MG activates mTORC2 through phosphatidylinositol 3-kinase (PI3K), which enhances resistance against the anticancer drug cetuximab (573). Low level MG produced by *E. coli* extends the lifespan of *C. elegans*, dependent on TORC2 and its downstream target Sgk1 (574). Counter to the lifespan extension observed in *C. elegans*, the same study reported that MG-stimulated hyperphosphorylation of Sgk1 in human dermal fibroblasts results in accelerated senescence (574).

In addition to the pathways outlined above, which are conserved between yeast and mammals, MG also activates several pathways that are thus far only known to exist in higher eukaryotes. As touched upon above, activation of the JNK, ERK, and NF-kB pathways are a crucial aspect of MG-mediated inflammation and immune dysfunction in diabetes and other chronic diseases (493-500). Moreover, MG modulates these and other signaling pathways in a multitude of other cell types in mammals, generally with negative effects for the organism. For instance, activation of JNK by MG in beige adipocytes inhibits thermogenesis via repression of the gene encoding uncoupling protein 1 (*UCP1*),

a phenotype that is associated with obesity and Type 2 diabetes (575). In breast cancer cells, endogenous MG activates MEK/ERK/SMAD1 cascade by repressing expression of phosphatases, thereby promoting metastasis *in vitro* (576). Conversely, MG can also stimulate the stress-responsive transcription factor Nrf2 by reacting with cysteine residues on its inhibitor, Kelch-like ECH-associated protein 1 (KEAP1) (577). When Nrf2 accumulates in the nucleus, it initiates transcription of cytoprotective genes such as those involved in glutathione synthesis and reduction (577-580). There is experimental evidence that activation of Nrf2 prior to MG exposure suppresses MG toxicity and AGE formation *in vitro* (578, 580, 581) and *in vivo* (582, 583); thus, chemical inducers of Nrf2 activity are of interest as potential therapeutic agents in diseases associated with oxidative and carbonyl stress.

In prokaryotes

MG-mediated signaling is not yet as well understood in prokaryotes as in eukaryotes, but some studies have investigated the effects of MG on bacterial transcription and physiology. Ozyamak et al. (584) published a transcriptional analysis of *E. coli* exposed to either a subinhibitory, lethal, or progressively increasing concentrations of MG. Subinhibitory MG leads to upregulated expression of genes involved in DNA repair, such as *recA*, and of the aldehyde detoxification genes *frmAB* and *yqhD* (584). Exposure to a lethal concentration of MG also leads to increased expression of DNA repair genes, in addition to upregulation of many genes regulated by the oxidative stress-responsive transcription factor OxyR (584). Finally, after two to four hours of progressively higher concentrations of MG (0 to 0.7 mM), similar genes described in the first two experiments

are induced, as well as expression of the NemR-repressed genes *gloA* (glyoxalase I) and *nemA* (N-ethylmaleimide reductase) (584). NemR is a member of the TetR family of transcriptional repressors; modification of its conserved cysteine residues by electrophiles (585) or by bleach (586) disrupts its DNA binding affinity resulting in derepression of its target genes. Like *E. coli* NemR, MG modifies one of two conserved cysteine residues in the *Staphylococcus aureus* TetR-family repressor GbaA, thereby derepressing genes involved in biofilm formation (587). In *Pseudomonas aeruginosa*, MG and other toxic electrophiles activate the AraC-like transcription factor CmrA, indirectly leading to upregulation of the multidrug efflux system MexEF-OprN (588). Interestingly, three of the direct targets of CmrA encode a putative oxidoreductase, aldehyde dehydrogenase, and alcohol dehydrogenase (588).

1.4.6 Overview of other reactive electrophiles

In addition to MG, a number of other reactive electrophiles have been implicated in disease and/or cellular signaling. As a thorough description of MG formation, toxicity, and detoxification has been given at the beginning of this section, such details about other compounds will not be discussed here. Rather, the goal of this subsection is to briefly introduce the reader to a few additional physiologically relevant molecules that may have similar effects to MG on gene transcription and cellular physiology due to their propensity to form adducts with biomolecules. The chemical structures of several physiologically relevant aldehydes are presented in **Fig. 1-7**.

Formaldehyde

Formaldehyde (FA) can be endogenously generated through several metabolic processes and is prevalent in cigarette smoke, motor vehicle exhaust, and emissions from coal-burning power plants. Acute exposure to exogenous FA is known to cause dermal allergies and irritation of the mucus membranes (589), while chronic exposure is linked to neurological and pulmonary damage, decreased white blood cell counts, nasopharyngeal cancer, and leukemia (589). The primary source of endogenous FA in mammals is thought to be the oxidative deamination of methylamine by SSAO enzymes (590), which are also implicated in MG formation as previously discussed. The role of endogenous FA production in human disease has not been as well-studied as that of MG. Nonetheless, one recent study of patients with Alzheimer's disease or post-stroke dementia demonstrated a strong correlation between blood SSAO levels, urinary FA levels, and cognitive decline in these patients (591). Additionally, patients with type 2 diabetes and mutations in the gene encoding the FA-detoxifying enzyme aldehyde dehydrogenase 2 (*ALDH2*) exhibit increased levels of FA in the blood and urine and more severe dementia compared to age-matched healthy controls (592). Thus, FA reaches physiologically significant levels in humans under certain conditions. The transcriptional response of *S. cerevisiae* to FA includes downregulation of genes involved in protein synthesis and upregulation of genes involved in methionine metabolism, DNA repair, and stress response (593). Interestingly, FA also induces expression of *FLR1*, the *S. cerevisiae* ortholog of *MDR1* (593), which raises the possibility that it may induce *MDR1* expression in *Candida* species.

Acetaldehyde

Acetaldehyde (ACA), like FA, is a metabolite and a component of air pollution with genotoxic effects. The primary metabolic source of ACA in humans is the oxidation of dietary ethanol by alcohol dehydrogenase enzymes. Levels of ACA in human blood (594), breath (595), and saliva (596) rise significantly after consuming alcoholic beverages; this effect is exacerbated in individuals with alcohol addiction (594, 597) or loss-of-function mutations in the *ALDH2* gene (598-601). Microbial ethanol metabolism in the oral cavity and gastrointestinal tract is another significant source of ACA in the human body (602-610). In particular, *Candida* species are known to produce carcinogenic amounts of ACA in the presence of ethanol or glucose (602, 611-615), and patients with oral cancer exhibit higher frequency and larger burdens of *Candida* colonization compared to healthy controls or patients with non-oral cancer (602, 611, 616). The effects of ACA on *Candida* species are not well characterized, but it has been shown that ACA inhibits the formation of hyphae in *C. albicans* (617) and thus may facilitate dissemination within the host. In contrast, the response of *S. cerevisiae* to ACA has been well-studied, particularly in the context of fermentation and biological aging of wines. After 1 hour of growth in ACA, *S. cerevisiae* exhibits Met4-dependent induction of genes involved in sulfur metabolism (e.g., *STR3*, *MUP3*, multiple *MET* genes, etc.) and Haa1-dependent induction of polyamine transporter genes (e.g., *TPO2* and *TPO3*) among others (618). Several genes encoding heat shock proteins (618, 619) and aldehyde dehydrogenases (620) are also upregulated by ACA in *S. cerevisiae*. Mechanisms of ACA tolerance in *S. cerevisiae* include Stb5-dependent induction of pentose phosphate pathway genes (621, 622) and repression of the glycolysis

enzyme glucose-6-phosphate isomerase (622), as well as nonenzymatic scavenging of AA by GSH (623).

Acrolein

Acrolein originates from a variety of sources, including thermal degradation of glucose or glycerol, cigarette smoke, lipid peroxidation, and polyamine metabolism. Acrolein has been implicated in the pathology of diabetic retinopathy (624) and nephropathy (625), atherosclerosis (626), pulmonary inflammation (627), rheumatoid arthritis (628), and neurodegenerative diseases such as Alzheimer's disease (629) and multiple sclerosis (630). In *S. cerevisiae*, exposure to allyl alcohol, which is intracellularly oxidized to acrolein via ADH enzymes, leads to depletion of GSH and activation of Yap1 (631). Like other thiol-reactive electrophiles (529, 632), activation of Yap1 by this compound occurs independently of the Gpx3-dependent H_2O_2 response (631). The Yap1-dependent transcriptional response of *S. cerevisiae* to acrolein includes upregulation of ribosome biogenesis, RNA processing, and nitrogen- or sulfur-containing compound metabolism (632). Allyl alcohol also causes GSH depletion in *C. albicans* (633), but the possible activation of Cap1 by allyl alcohol or acrolein in *C. albicans* has not been investigated.

Malondialdehyde

Malondialdehyde (MDA) arises primarily from the spontaneous peroxidation of polyunsaturated fatty acids and has gained interest as a biomarker of oxidative stress in human disease. Elevated serum levels of MDA have been observed in patients with a

variety of disease ranging from neurological disorders such as obsessive-compulsive disorder (634) and attention deficit hyperactivity disorder (635); autoinflammatory diseases like psoriasis (636) and rheumatoid arthritis (637); and diseases involving organ function including coronary heart disease (638), chronic obstructive pulmonary disease (639), and diabetic nephropathy (640). MDA is also increased in murine corneas and human corneal epithelial cells infected with *C. albicans* due to fungal stimulation of the mammalian p38 MAPK pathway, resulting in upregulation of mammalian heme oxygenase-1 and cyclooxygenase-2 with concomitant downregulation of the mammalian antioxidant enzymes superoxide dismutase-1, glutathione peroxidase-1, and peroxiredoxin-4 (556). Additionally, alveolar macrophages produce MDA in response to *C. albicans*, *Cryptococcus neoformans*, or *Aspergillus fumigatus in vitro* (641), indicating that these fungi would likely encounter MDA in the context of inflammation *in vivo*. Studies regarding the effects of MDA on any fungal species are lacking, but it has been shown that in *S. cerevisiae*, Yap1 is required for adaption to MDA independently of the H_2O_2 response (542), suggesting that MDA stimulates Yap1 activity in a similar manner as MG (529) and acrolein (632).

1.5 Summary of thesis work

The origins of the work presented herein can be drawn from the detection of remarkably high burdens of *C. lusitaniae* in the bronchoalveolar lavage (BAL) fluid and sputum from three cystic fibrosis (CF) patients receiving care at Dartmouth-Hitchcock Medical Center in New Hampshire, USA. All three patients had a previous history of *Staphylococcus*-positive culture from BAL fluid and sputum, which had become

undetectable at the time *C. lusitaniae* was isolated from these patients. One of the patients has Type 2 diabetes and another has CFRD. Isolates from all three patients displayed phenotypic heterogeneity *in vitro*, and whole genome sequencing (WGS) revealed remarkable genotypic heterogeneity of the *MRR1* locus among isolates from one patient (97). Other genetic differences between isolates from within single patients and across the three patients were also observed but are beyond the scope of this work.

In total, twelve different alleles of *MRR1* were identified among the twenty sequenced isolates from one patient (97). It was shown that different *MRR1* alleles confer differing levels of FLZ resistance and *MDR1* expression in these isolates, and some of these mutations are gain-of-function (97). Interestingly, none of the three CF patients had prior history of clinical antifungal use, which prompted the question of which other pressures might have led to selection for gain-of-function in *MRR1*. Initial RNA sequencing of isolates with different *MRR1* alleles revealed a set of genes putatively regulated by Mrr1 in *C. lusitaniae*, including multiple genes orthologous to *C. albicans MGD1* (97). As previously discussed, expression of *MGD1* is regulated by Mrr1 in *C. albicans* and expression of two genes orthologous to *MGD1* is regulated by Mrr1 in *C. parapsilosis* (162). Thus, we hypothesized that Mrr1 plays a role in resistance against the toxic electrophile MG in multiple *Candida* species, either partially or wholly dependent on its regulation of genes encoding MG reductases.

The work presented in **Chapter 2** confirms that in *C. lusitaniae*, Mrr1 regulates expression of *MGD1* (*CLUG_01281*) and *MGD2* (*CLUG_04991*) which contribute to MG resistance. Mrr1 itself is also involved in MG resistance, as a strain complimented with a gain-of-function *MRR1* allele exhibits more robust growth in MG compared to an isogenic

strain complimented with an *MRR1* allele encoding a premature stop codon. Additionally, we show that a nonlethal concentration of MG induces expression of the Mrr1-regulated genes *MGD1*, *MGD2*, and *MDR1*, and improves growth in FLZ in a partially *MRR1*- and *MDR1*-dependent manner. Furthermore, deletion of the glyoxalase I gene *GLO1* leads to increased growth in FLZ in the absence of exogenously added MG. Finally, we assess the relative MG resistance and MG-induced growth in FLZ of multiple *Candida* species and strains and show that both phenotypes are generally strain-dependent rather than species-dependent.

Chapter 3 focuses on the role of Mrr1a in *C. auris* regarding MG resistance and induction of gene expression by MG or by benomyl. We show that Mrr1a, but not Mrr1b or Mrr1c, contributes to MG resistance in the clade III *C. auris* isolate B11221, and that Mrr1a regulates basal and induced expression of the *C. auris* orthologs of *MDR1* and *MGD1*. Surprisingly, an RNA-seq analysis revealed that Mrr1a only appears to be required for expression of *MDR1* and *MGD1,* in contrast to other *Candida* species which possess larger Mrr1 regulons. Finally, we characterize the global transcriptional response of *C. auris* to MG and benomyl and show that the two compounds induce and repress genes involved in common cellular processes, independently of Mrr1a. Genes upregulated by MG and/or benomyl are involved in sulfur metabolism, amino acid metabolism and biosynthesis, and transmembrane transport, while genes downregulated by MG and/or benomyl are involved in iron homeostasis and carbohydrate metabolism.

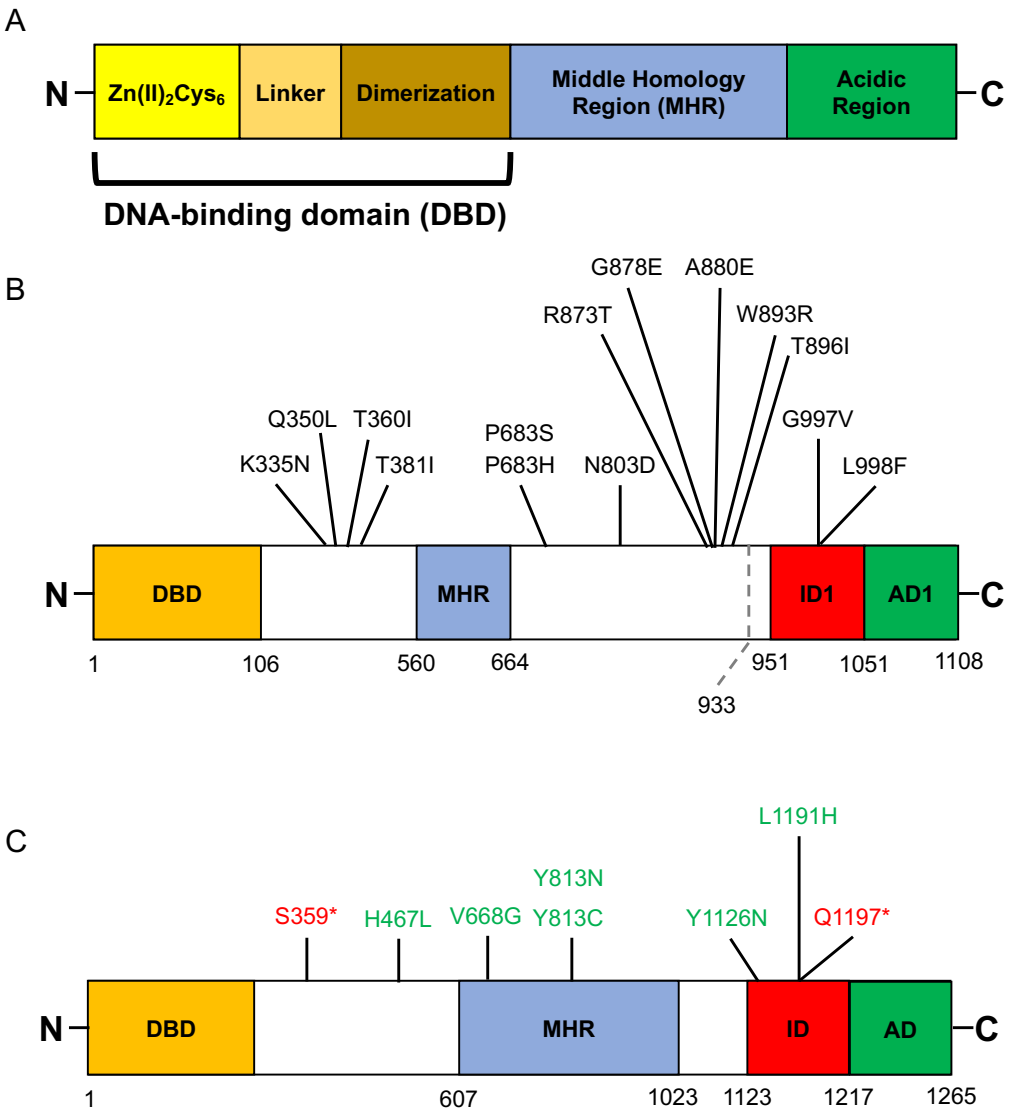

Figure 1.1. Mrr1 is a typical zinc-cluster transcription factor. (A) Conserved structural and functional domains of zinc-cluster transcription factors. **(B)** Experimentally determined structural and functional domains of *C. albicans* Mrr1 (CaMrr1). Known gain-of-function amino acid substitutions are indicated. **(C)** Predicted structural and functional domains of *C. lusitaniae* Mrr1 (ClMrr1) based on homology to CaMrr1. Known gain-of-function amino acid substitutions are indicated in green, mutations resulting in premature stop codons are indicated in red. Diagrams are not to scale.

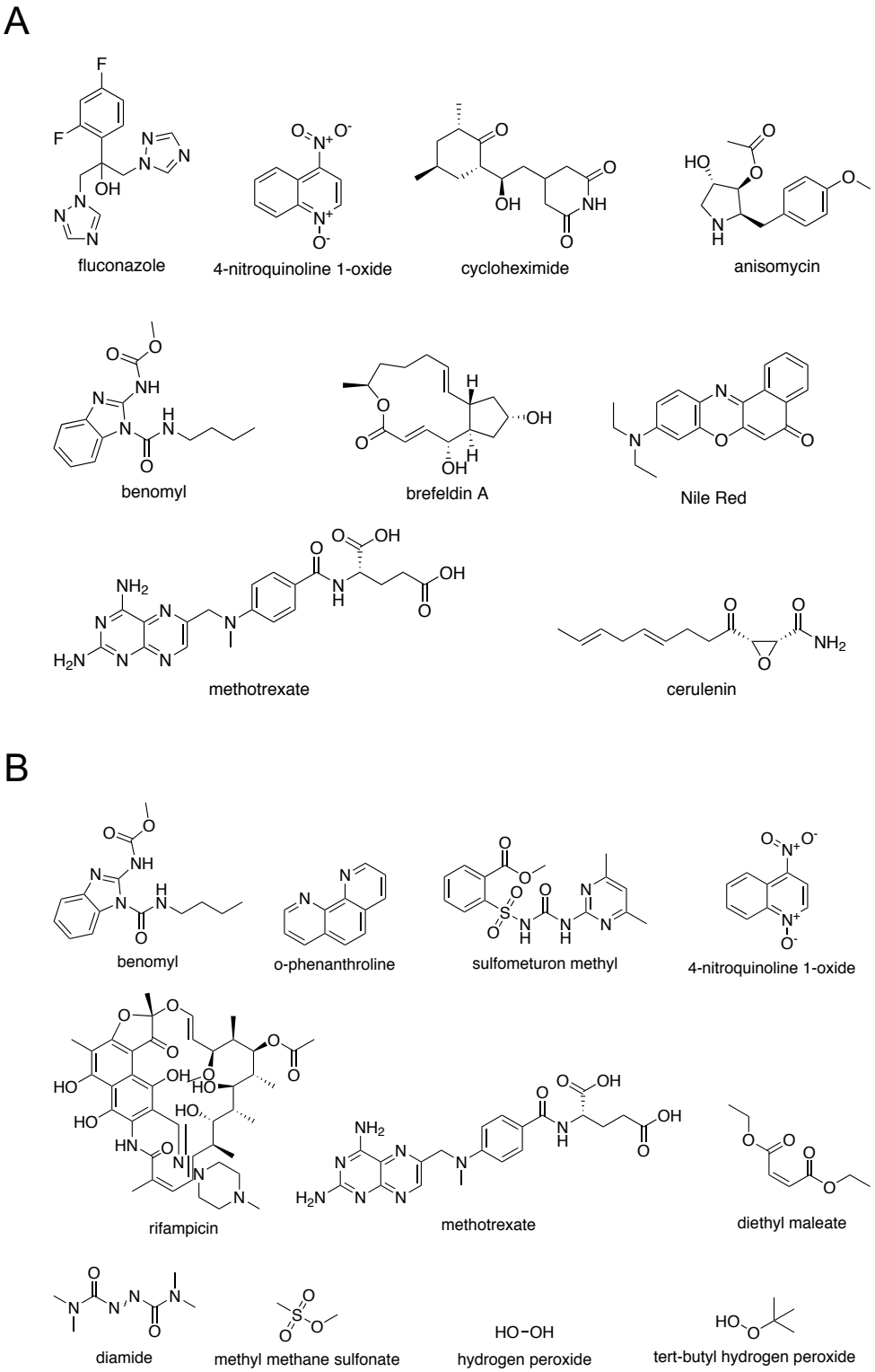

Figure 1.2. A variety of structurally and functionally unrelated molecules can act as substrates of Mdr1 or induce *MDR1* expression in *C. albicans*. (A) Experimentally

demonstrated substrates of CaMdr1. **(B)** Experimentally demonstrated inducers of *CaMDR1* expression.

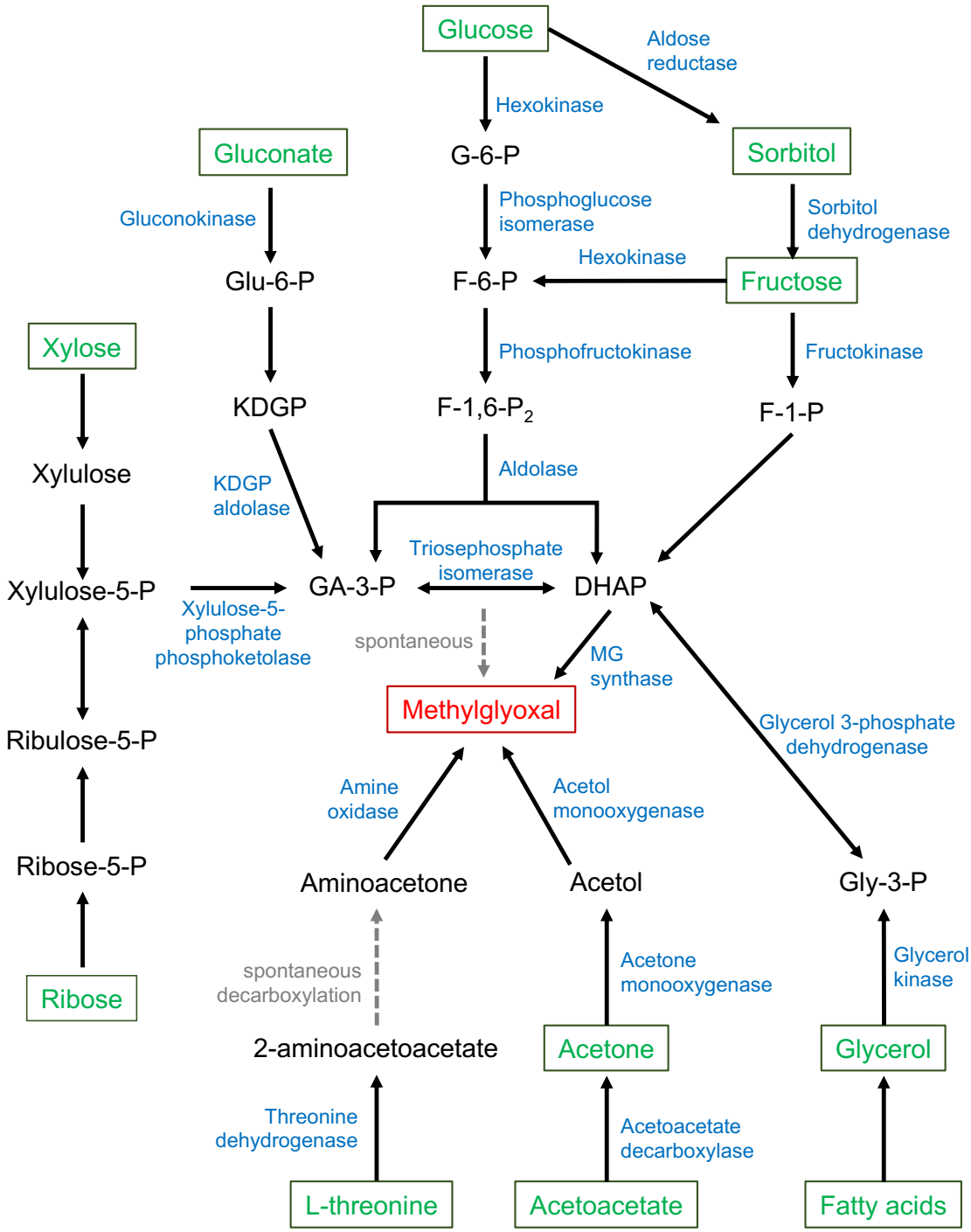

Figure 1.3. Pathways of cellular MG formation.

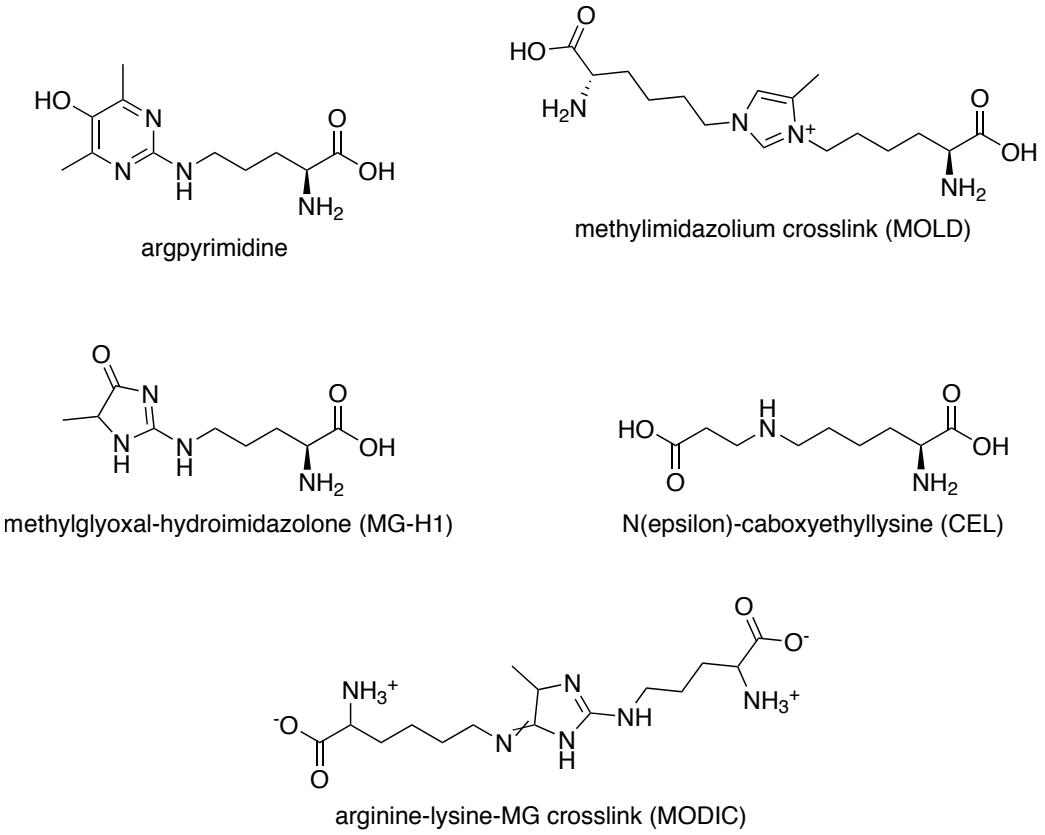

Figure 1.4. Chemical structures of the most common MG-derived advanced glycation endproducts (AGEs).

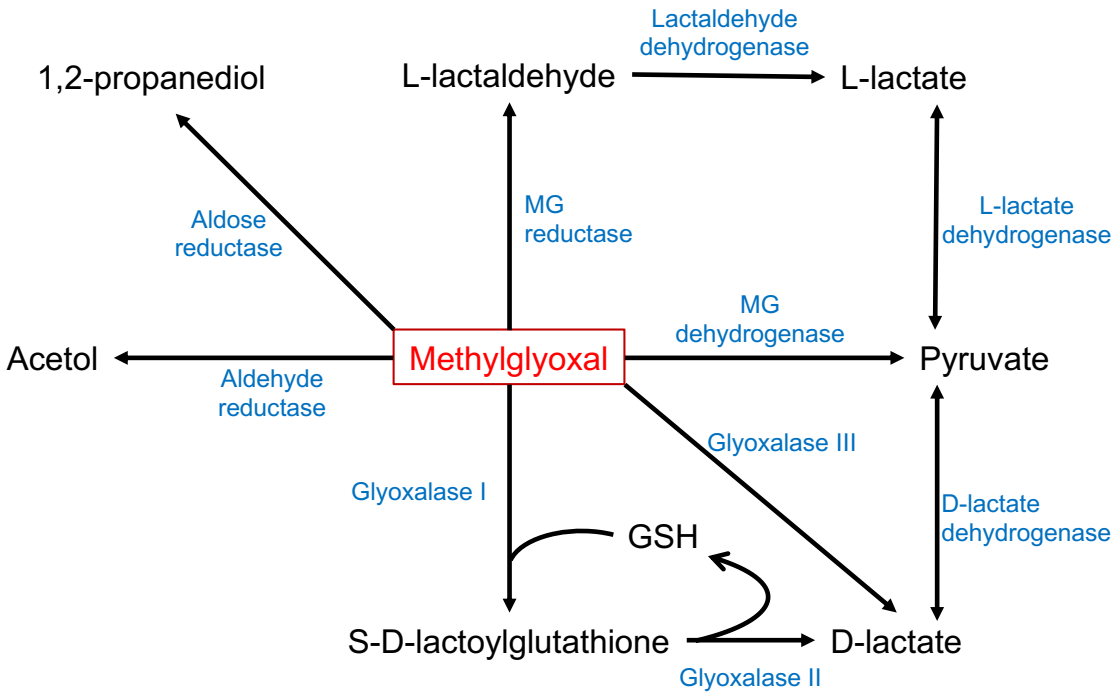

Figure 1.5. Pathways of MG detoxification and metabolism.

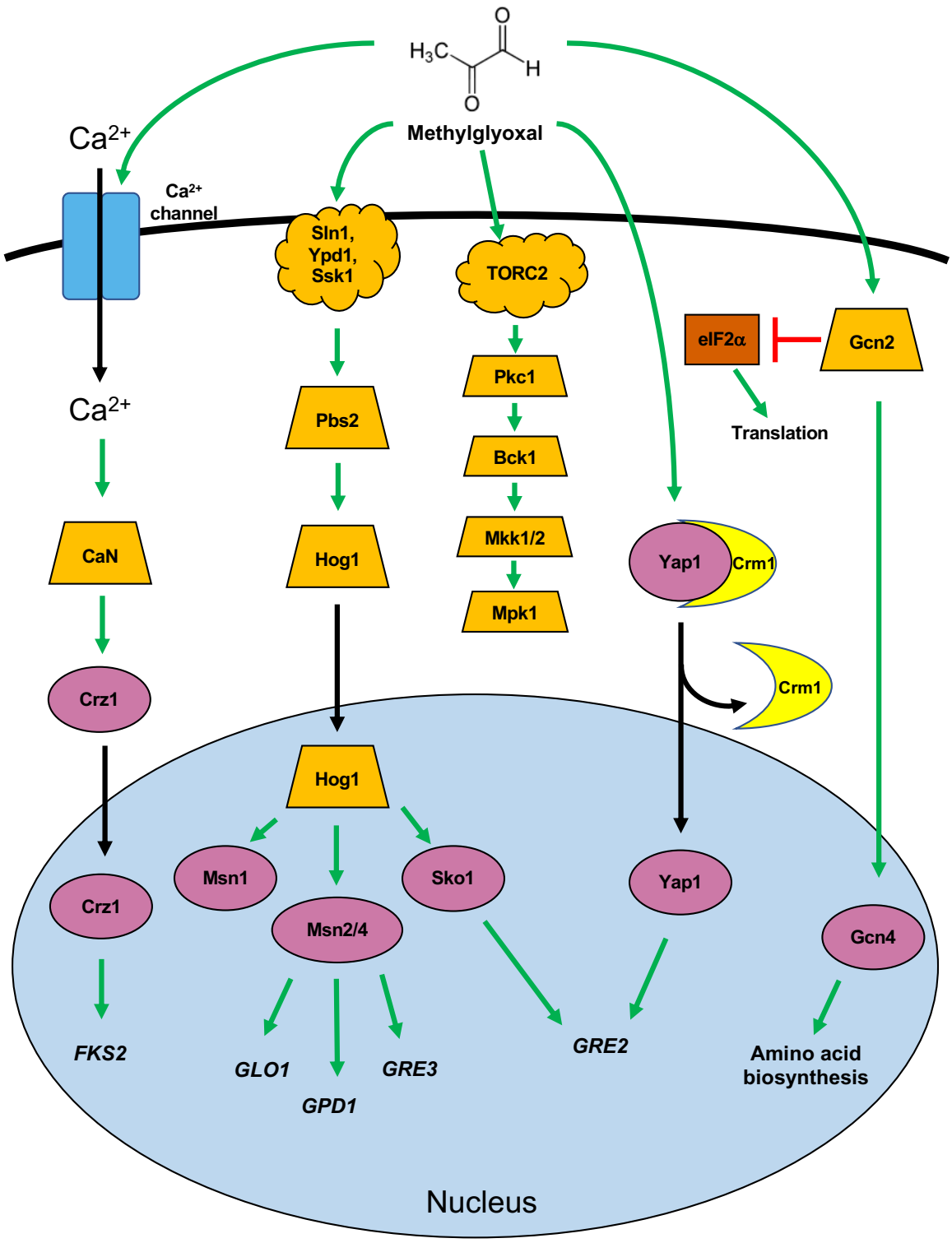

Figure 1.6. Overview of signaling pathways modulated by MG in *S. cerevisiae*. Purple ovals represent transcription factors, orange trapezoids represent protein kinases, orange clouds represent kinase complexes, green arrows represent protein activation, red lines

represent protein inhibition, and black arrows represent translocation. Further detail is provided in the text.

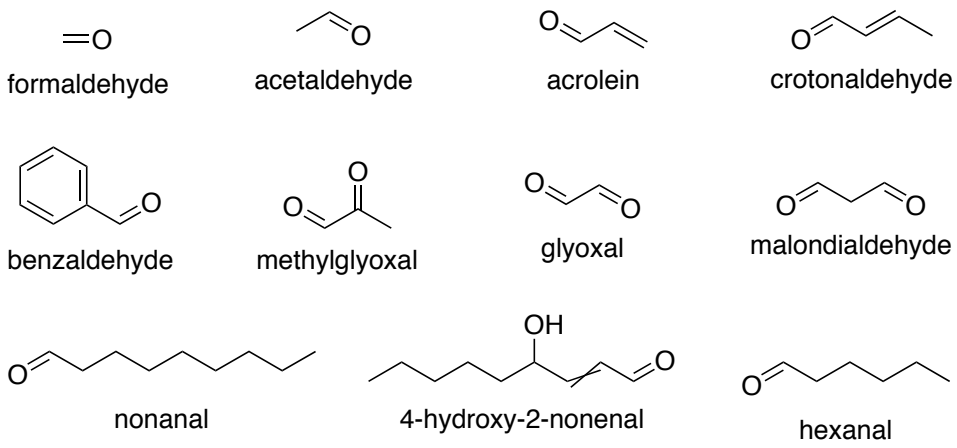

Figure 1-7. Chemical structures of physiologically relevant reactive carbonyl species (RCS).

References

1. Vallabhaneni S, Mody RK, Walker T, Chiller T. 2016. The Global Burden of Fungal Diseases. Infectious Disease Clinics of North America 30:1-11.
2. Chen X, Yang Y, Li Y, Chen J. 2021. Clinical characteristics and risk factors for death in patients with *Candida* bloodstream infection in Intensive Care Unit. Zhong Nan Da Xue Xue Bao Yi Xue Ban 46:719-724.
3. Zhang W, Song X, Wu H, Zheng R. 2019. Epidemiology, risk factors and outcomes of *Candida albicans* vs. non-albicans candidaemia in adult patients in Northeast China. Epidemiol Infect 147:e277.
4. Muderris T, Kaya S, Ormen B, Aksoy Gokmen A, Varer Akpinar C, Yurtsever Gul S. 2020. Mortality and risk factor analysis for *Candida* blood stream infection: A three-year retrospective study. J Mycol Med 30:101008.
5. Brescini L, Mazzanti S, Orsetti E, Morroni G, Masucci A, Pocognoli A, Barchiesi F. 2020. Species distribution and antifungal susceptibilities of bloodstream *Candida* isolates: a nine-years single center survey. J Chemother 32:244-250.
6. Wisplinghoff H, Ebbers J, Geurtz L, Stefanik D, Major Y, Edmond MB, Wenzel RP, Seifert H. 2014. Nosocomial bloodstream infections due to *Candida* spp. in the USA: species distribution, clinical features and antifungal susceptibilities. Int J Antimicrob Agents 43:78-81.
7. Sayeed MA, Farooqi J, Jabeen K, Mahmood SF. 2020. Comparison of risk factors and outcomes of *Candida auris* candidemia with non-*Candida auris* candidemia: A retrospective study from Pakistan. Med Mycol 58:721-729.

8. Chi HW, Yang YS, Shang ST, Chen KH, Yeh KM, Chang FY, Lin JC. 2011. *Candida albicans* versus non-albicans bloodstream infections: the comparison of risk factors and outcome. J Microbiol Immunol Infect 44:369-75.

9. Al-Rashdi A, Al-Maani A, Al-Wahaibi A, Alqayoudhi A, Al-Jardani A, Al-Abri S. 2021. Characteristics, Risk Factors, and Survival Analysis of *Candida auris* Cases: Results of One-Year National Surveillance Data from Oman. Journal of Fungi 7.

10. Sbrana F, Sozio E, Bassetti M, Ripoli A, Pieralli F, Azzini AM, Morettini A, Nozzoli C, Merelli M, Rizzardo S, Bertolino G, Carrara D, Scarparo C, Concia E, Menichetti F, Tascini C. 2018. Independent risk factors for mortality in critically ill patients with candidemia on Italian Internal Medicine Wards. Intern Emerg Med 13:199-204.

11. Esmailzadeh A, Zarrinfar H, Fata A, Sen T. 2018. High prevalence of candiduria due to non-albicans *Candida* species among diabetic patients: A matter of concern? J Clin Lab Anal 32:e22343.

12. Fisher BM, Lamey PJ, Samaranayake LP, MacFarlane TW, Frier BM. 1987. Carriage of *Candida* species in the oral cavity in diabetic patients: relationship to glycaemic control. J Oral Pathol 16:282-4.

13. Willis AM, Coulter WA, Fulton CR, Hayes JR, Bell PM, Lamey PJ. 1999. Oral candidal carriage and infection in insulin-treated diabetic patients. Diabet Med 16:675-9.

14. Patel PN, Sah P, Chandrashekar C, Vidyasagar S, Venkata Rao J, Tiwari M, Radhakrishnan R. 2017. Oral candidal speciation, virulence and antifungal susceptibility in type 2 diabetes mellitus. Diabetes Res Clin Pract 125:10-19.

15. Zaoutis TE, Foraker E, McGowan KL, Mortensen J, Campos J, Walsh TJ, Klein JD. 2005. Antifungal susceptibility of *Candida* spp. isolated from pediatric patients: a survey of 4 children's hospitals. Diagn Microbiol Infect Dis 52:295-8.

16. Gong X, Luan T, Wu X, Li G, Qiu H, Kang Y, Qin B, Fang Q, Cui W, Qin Y, Li J, Zang B. 2016. Invasive candidiasis in intensive care units in China: Risk factors and prognoses of *Candida albicans* and non-albicans *Candida* infections. Am J Infect Control 44:e59-63.

17. Ding XR, Yan DH, Sun W, Zeng ZY, Su RR, Su JR. 2015. Epidemiology and risk factors for nosocomial Non-*Candida albicans* candidemia in adult patients at a tertiary care hospital in North China. Medical Mycology 53:684-690.

18. Sharma Y, Chumber SK, Kaur M. 2017. Studying the Prevalence, Species Distribution, and Detection of In vitro Production of Phospholipase from Candida Isolated from Cases of Invasive Candidiasis. Journal of Global Infectious Diseases 9:8-11.

19. Quindos G. 2014. Epidemiology of candidaemia and invasive candidiasis. A changing face. Rev Iberoam Micol 31:42-8.

20. Quindos G, Marcos-Arias C, San-Millan R, Mateo E, Eraso E. 2018. The continuous changes in the aetiology and epidemiology of invasive candidiasis: from familiar *Candida albicans* to multiresistant *Candida auris*. Int Microbiol 21:107-119.

21. Patel PK, Erlandsen JE, Kirkpatrick WR, Berg DK, Westbrook SD, Louden C, Cornell JE, Thompson GR, Vallor AC, Wickes BL, Wiederhold NP, Redding SW, Patterson TF. 2012. The Changing Epidemiology of Oropharyngeal Candidiasis in

Patients with HIV/AIDS in the Era of Antiretroviral Therapy. AIDS Res Treat 2012:262471.

22. Lamoth F, Lockhart SR, Berkow EL, Calandra T. 2018. Changes in the epidemiological landscape of invasive candidiasis. J Antimicrob Chemother 73:i4-i13.

23. Papadimitriou-Olivgeris M, Spiliopoulou A, Fligou F, Tsiata E, Kolonitsiou F, Nikolopoulou A, Papamichail C, Spiliopoulou I, Marangos M, Christofidou M. 2021. Risk factors for isolation of fluconazole and echinocandin non-susceptible *Candida* species in critically ill patients. J Med Microbiol 70.

24. Dutta A, Palazzi DL. 2011. *Candida* non-albicans versus *Candida albicans* fungemia in the non-neonatal pediatric population. Pediatr Infect Dis J 30:664-8.

25. Lee WJ, Hsu JF, Lai MY, Chiang MC, Lin HC, Huang HR, Wu IH, Chu SM, Fu RH, Tsai MH. 2018. Factors and outcomes associated with candidemia caused by non-albicans *Candida* spp versus *Candida albicans* in children. American Journal of Infection Control 46:1387-1393.

26. Tressler AB, Markwei M, Fortin C, Yao M, Procop GW, Soper DE, Goje O. 2021. Risks for Recurrent Vulvovaginal Candidiasis Caused by Non-Albicans *Candida* Versus *Candida Albicans*. Journal of Womens Health 30:1588-1596.

27. Shigemura K, Osawa K, Jikimoto T, Yoshida H, Hayama B, Ohji G, Iwata K, Fujisawa M, Arakawa S. 2014. Comparison of the clinical risk factors between *Candida albicans* and *Candida* non-albicans species for bloodstream infection. J Antibiot (Tokyo) 67:311-4.

28. Garnacho-Montero J, Diaz-Martin A, Garcia-Cabrera E, Ruiz Perez de Pipaon M, Hernandez-Caballero C, Aznar-Martin J, Cisneros JM, Ortiz-Leyba C. 2010. Risk factors for fluconazole-resistant candidemia. Antimicrob Agents Chemother 54:3149-54.

29. Chi HW, Yang YS, Shang ST, Chen KH, Yeh KM, Chang FY, Lin JC. 2011. Candida albicans versus non-albicans bloodstream infections: The comparison of risk factors and outcome. Journal of Microbiology Immunology and Infection 44:369-375.

30. Satoh K, Makimura K, Hasumi Y, Nishiyama Y, Uchida K, Yamaguchi H. 2009. *Candida auris* sp. nov., a novel ascomycetous yeast isolated from the external ear canal of an inpatient in a Japanese hospital. Microbiol Immunol 53:41-4.

31. Lee WG, Shin JH, Uh Y, Kang MG, Kim SH, Park KH, Jang HC. 2011. First three reported cases of nosocomial fungemia caused by Candida auris. J Clin Microbiol 49:3139-42.

32. Lockhart SR, Etienne KA, Vallabhaneni S, Farooqi J, Chowdhary A, Govender NP, Colombo AL, Calvo B, Cuomo CA, Desjardins CA, Berkow EL, Castanheira M, Magobo RE, Jabeen K, Asghar RJ, Meis JF, Jackson B, Chiller T, Litvintseva AP. 2017. Simultaneous Emergence of Multidrug-Resistant Candida auris on 3 Continents Confirmed by Whole-Genome Sequencing and Epidemiological Analyses. Clin Infect Dis 64:134-140.

33. Chow NA, Munoz JF, Gade L, Berkow EL, Li X, Welsh RM, Forsberg K, Lockhart SR, Adam R, Alanio A, Alastruey-Izquierdo A, Althawadi S, Arauz AB, Ben-Ami R, Bharat A, Calvo B, Desnos-Ollivier M, Escandon P, Gardam D, Gunturu R,

Heath CH, Kurzai O, Martin R, Litvintseva AP, Cuomo CA. 2020. Tracing the Evolutionary History and Global Expansion of Candida auris Using Population Genomic Analyses. mBio 11.

34. Chow NA, de Groot T, Badali H, Abastabar M, Chiller TM, Meis JF. 2019. Potential Fifth Clade of Candida auris, Iran, 2018. Emerg Infect Dis 25:1780-1781.

35. Khan Z, Ahmad S, Benwan K, Purohit P, Al-Obaid I, Bafna R, Emara M, Mokaddas E, Abdullah AA, Al-Obaid K, Joseph L. 2018. Invasive *Candida auris* infections in Kuwait hospitals: epidemiology, antifungal treatment and outcome. Infection 46:641-650.

36. Ruiz-Gaitan A, Martinez H, Moret AM, Calabuig E, Tasias M, Alastruey-Izquierdo A, Zaragoza O, Mollar J, Frasquet J, Salavert-Lleti M, Ramirez P, Lopez-Hontangas JL, Peman J. 2019. Detection and treatment of *Candida auris* in an outbreak situation: risk factors for developing colonization and candidemia by this new species in critically ill patients. Expert Review of Anti-Infective Therapy 17:295-305.

37. Shastri PS, Shankarnarayan SA, Oberoi J, Rudramurthy SM, Wattal C, Chakrabarti A. 2020. *Candida auris* candidaemia in an intensive care unit - Prospective observational study to evaluate epidemiology, risk factors, and outcome. Journal of Critical Care 57:42-48.

38. Chowdhary A, Prakash A, Sharma C, Kordalewska M, Kumar A, Sarma S, Tarai B, Singh A, Upadhyaya G, Upadhyay S, Yadav P, Singh PK, Khillan V, Sachdeva N, Perlin DS, Meis JF. 2018. A multicentre study of antifungal susceptibility patterns among 350 *Candida auris* isolates (2009-17) in India: role of the *ERG11*

and *FKS1* genes in azole and echinocandin resistance. Journal of Antimicrobial Chemotherapy 73:891-899.

39. Osei Sekyere J. 2018. *Candida auris*: A systematic review and meta-analysis of current updates on an emerging multidrug-resistant pathogen. Microbiologyopen 7:e00578.

40. Eyre DW, Sheppard AE, Madder H, Moir I, Moroney R, Quan TP, Griffiths D, George S, Butcher L, Morgan M, Newnham R, Sunderland M, Clarke T, Foster D, Hoffman P, Borman AM, Johnson EM, Moore G, Brown CS, Walker AS, Peto TEA, Crook DW, Jeffery KJM. 2018. A *Candida auris* Outbreak and Its Control in an Intensive Care Setting. New England Journal of Medicine 379:1322-1331.

41. Taori SK, Khonyongwa K, Hayden I, Athukorala GDA, Letters A, Fife A, Desai N, Borman AM. 2019. *Candida auris* outbreak: Mortality, interventions and cost of sustaining control. J Infect 79:601-611.

42. Welsh RM, Bentz ML, Shams A, Houston H, Lyons A, Rose LJ, Litvintseva AP. 2017. Survival, Persistence, and Isolation of the Emerging Multidrug-Resistant Pathogenic Yeast *Candida auris* on a Plastic Health Care Surface. Journal of Clinical Microbiology 55:2996-3005.

43. Rutala WA, Kanamori H, Gergen MF, Sickbert-Bennett EE, Weber DJ. 2019. Susceptibility of *Candida auris* and *Candida albicans* to 21 germicides used in healthcare facilities. Infection Control and Hospital Epidemiology 40:380-382.

44. Jabeen K, Mal PB, Farooqi JQ, Hashmi M, Tharwani A. 2017. Persistence of *Candida auris* on latex and nitrile gloves and their transmission to sterile urinary catheters; Comparison with other yeasts. Mycoses 60:127-127.

45. Jabeen K, Mal PB, Tharwani A, Hashmi M, Farooqi J. 2020. Persistence of *Candida auris* on latex and nitrile gloves with transmission to sterile urinary catheters. Medical Mycology 58:128-132.

46. Kim SH, Iyer KR, Pardeshi L, Munoz JF, Robbins N, Cuomo CA, Wong KH, Cowen LE. 2019. Genetic Analysis of *Candida auris* Implicates Hsp90 in Morphogenesis and Azole Tolerance and Cdr1 in Azole Resistance (vol 10, e02529-18, 2019). Mbio 10.

47. Rybak JM, Doorley LA, Nishimoto AT, Barker KS, Palmer GE, Rogers PD. 2019. Abrogation of Triazole Resistance upon Deletion of *CDR1* in a Clinical Isolate of *Candida auris*. Antimicrobial Agents and Chemotherapy 63.

48. Wasi M, Khandelwal NK, Moorhousem AJ, Nair R, Vishwakarma P, Bravo Ruiz G, Rossz ZK, Lorenz A, Rudramurthy SM, Chakrabarti A, Lynn AM, Mondal AK, Gow NAR, Prasad R. 2019. ABC Transporter Genes Show Upregulated Expression in Drug-Resistant Clinical Isolates of *Candida auris*: A Genome-Wide Characterization of ATP-Binding Cassette (ABC) Transporter Genes. Frontiers in Microbiology 10.

49. Carolus H, Pierson S, Munoz JF, Subotic A, Cruz RB, Cuomo CA, Van Dijck P. 2021. Genome-Wide Analysis of Experimentally Evolved *Candida auris* Reveals Multiple Novel Mechanisms of Multidrug Resistance. mBio 12.

50. Mayr EM, Ramirez-Zavala B, Kruger I, Morschhauser J. 2020. A Zinc Cluster Transcription Factor Contributes to the Intrinsic Fluconazole Resistance of Candida auris. mSphere 5.

51. Rybak JM, Munoz JF, Barker KS, Parker JE, Esquivel BD, Berkow EL, Lockhart SR, Gade L, Palmer GE, White TC, Kelly SL, Cuomo CA, Rogers PD. 2020. Mutations in *TAC1B*: a Novel Genetic Determinant of Clinical Fluconazole Resistance in *Candida auris*. Mbio 11.

52. Li J, Coste AT, Liechti M, Bachmann D, Sanglard D, Lamoth F. 2021. Novel *ERG11* and *TAC1b* mutations associated with azole resistance in *Candida auris*. Antimicrob Agents Chemother doi:10.1128/AAC.02663-20.

53. Healey KR, Kordalewska M, Jimenez Ortigosa C, Singh A, Berrio I, Chowdhary A, Perlin DS. 2018. Limited *ERG11* Mutations Identified in Isolates of *Candida auris* Directly Contribute to Reduced Azole Susceptibility. Antimicrob Agents Chemother 62.

54. AlJindan R, AlEraky DM, Mahmoud N, Abdalhamid B, Almustafa M, AbdulAzeez S, Borgio JF. 2020. Drug Resistance-Associated Mutations in *ERG11* of Multidrug-Resistant *Candida auris* in a Tertiary Care Hospital of Eastern Saudi Arabia. J Fungi (Basel) 7.

55. Rybak JM, Sharma C, Doorley LA, Barker KS, Palmer GE, Rogers PD. 2021. Delineation of the Direct Contribution of *Candida auris ERG11* Mutations to Clinical Triazole Resistance. Microbiology Spectrum 9.

56. Williamson B, Wilk A, Guerrero KD, Mikulski TD, Elias TN, Sawh I, Cancino-Prado G, Gardam D, Heath CH, Govender NP, Perlin DS, Kordalewska M, Healey KR. 2022. Impact of Erg11 Amino Acid Substitutions Identified in *Candida auris* Clade III Isolates on Triazole Drug Susceptibility. Antimicrob Agents Chemother 66:e0162421.

57. Kumar A, Prakash A, Singh A, Kumar H, Hagen F, Meis JF, Chowdhary A. 2016. *Candida haemulonii* species complex: an emerging species in India and its genetic diversity assessed with multilocus sequence and amplified fragment-length polymorphism analyses. Emerg Microbes Infect 5:e49.

58. Khan ZU, Al-Sweih NA, Ahmad S, Al-Kazemi N, Khan S, Joseph L, Chandy R. 2007. Outbreak of Fungemia among neonates caused by *Candida haemulonii* resistant to amphotericin B, itraconazole, and fluconazole. Journal of Clinical Microbiology 45:2025-2027.

59. Ruan SY, Kuo YW, Huang CT, Hsiue HC, Hsueh PR. 2010. Infections due to *Candida haemulonii*: species identification, antifungal susceptibility and outcomes. International Journal of Antimicrobial Agents 35:85-88.

60. Kim S, Ko KS, Moon SY, Lee MS, Lee MY, Son JS. 2011. Catheter-related candidemia caused by *Candida haemulonii* in a patient in long-term hospital care. J Korean Med Sci 26:297-300.

61. Coles M, Cox K, Chao A. 2020. *Candida haemulonii*: An emerging opportunistic pathogen in the United States? IDCases 21:e00900.

62. Silva CM, Carvalho-Parahym AM, Macedo DP, Lima-Neto RG, Francisco EC, Melo AS, da Conceicao MSM, Juca MB, Mello LR, Amorim RM, Neves RP. 2015. Neonatal Candidemia Caused by *Candida haemulonii*: Case Report and Review of Literature. Mycopathologia 180:69-73.

63. Ben-Ami R, Berman J, Novikov A, Bash E, Shachor-Meyouhas Y, Zakin S, Maor Y, Tarabia J, Schechner V, Adler A, Finn T. 2017. Multidrug-Resistant *Candida haemulonii* and *C. auris*, Tel Aviv, Israel. Emerg Infect Dis 23.

64. Frias-De-Leon MG, Martinez-Herrera E, Acosta-Altamirano G, Arenas R, Rodriguez-Cerdeira C. 2019. Superficial candidosis by *Candida duobushaemulonii*: An emerging microorganism. Infect Genet Evol 75:103960.

65. Resendiz-Sanchez J, Ortiz-Alvarez J, Casimiro-Ramos A, Hernandez-Rodriguez C, Villa-Tanaca L. 2020. First report of a catheter-related bloodstream infection by *Candida haemulonii* in a children's hospital in Mexico City. Int J Infect Dis 92:123-126.

66. Garcia-Martos P, Dominguez I, Marin P, Garcia-Agudo R, Aoufi S, Mira J. 2001. [Antifungal susceptibility of emerging yeast pathogens]. Enferm Infecc Microbiol Clin 19:249-56.

67. Cendejas-Bueno E, Kolecka A, Alastruey-Izquierdo A, Theelen B, Groenewald M, Kostrzewa M, Cuenca-Estrella M, Gomez-Lopez A, Boekhout T. 2012. Reclassification of the *Candida haemulonii* complex as *Candida haemulonii* (*C. haemulonii* group I), *C. duobushaemulonii sp. nov.* (*C. haemulonii* group II), and *C. haemulonii var. vulnera var. nov.*: three multiresistant human pathogenic yeasts. J Clin Microbiol 50:3641-51.

68. Ramos R, Caceres DH, Perez M, Garcia N, Castillo W, Santiago E, Borace J, Lockhart SR, Berkow EL, Hayer L, Espinosa-Bode A, Moreno J, Jackson BR, Moran J, Chiller T, de Villarreal G, Sosa N, Red Nacional de Vigilancia Epidemiologica en Microbiologia C, Vallabhaneni S. 2018. Emerging Multidrug-Resistant *Candida duobushaemulonii* Infections in Panama Hospitals: Importance of Laboratory Surveillance and Accurate Identification. J Clin Microbiol 56.

69. Chow NA, Gade L, Batra D, Rowe LA, Juieng P, Loparev VN, Litvintseva AP. 2018. Genome Sequence of the Amphotericin B-Resistant *Candida duobushaemulonii* Strain B09383. Genome Announc 6.

70. Silva LN, Oliveira SSC, Magalhaes LB, Andrade Neto VV, Torres-Santos EC, Carvalho MDC, Pereira MD, Branquinha MH, Santos ALS. 2020. Unmasking the Amphotericin B Resistance Mechanisms in *Candida haemulonii* Species Complex. ACS Infect Dis 6:1273-1282.

71. Silva LN, Ramos LS, Oliveira SSC, Magalhaes LB, Squizani ED, Kmetzsch L, Vainstein MH, Branquinha MH, Santos A. 2020. Insights into the Multi-Azole Resistance Profile in *Candida haemulonii* Species Complex. J Fungi (Basel) 6.

72. Gade L, Munoz JF, Sheth M, Wagner D, Berkow EL, Forsberg K, Jackson BR, Ramos-Castro R, Escandon P, Dolande M, Ben-Ami R, Espinosa-Bode A, Caceres DH, Lockhart SR, Cuomo CA, Litvintseva AP. 2020. Understanding the Emergence of Multidrug-Resistant *Candida*: Using Whole-Genome Sequencing to Describe the Population Structure of *Candida haemulonii* Species Complex. Front Genet 11:554.

73. Silva LN, Ramos LD, Oliveira SSC, Magalhaes LB, Squizani ED, Kmetzsch L, Vainstein MH, Branquinha MH, dos Santos ALS. 2020. Insights into the Multi-Azole Resistance Profile in *Candida haemulonii* Species Complex. Journal of Fungi 6.

74. Silva LN, Oliveira SSC, Magalhaes LB, Neto VVA, Torres-Santos EC, Carvalho MDC, Pereira MD, Branquinha MH, Santos ALS. 2020. Unmasking the

Amphotericin B Resistance Mechanisms in *Candida haemulonii* Species Complex. Acs Infectious Diseases 6:1273-1282.

75. Munoz JE, Ramirez LM, Dias LDS, Rivas LA, Ramos LS, Santos ALS, Taborda CP, Parra-Giraldo CM. 2020. Pathogenicity Levels of Colombian Strains of *Candida auris* and Brazilian Strains of *Candida haemulonii* Species Complex in Both Murine and *Galleria mellonella* Experimental Models. J Fungi (Basel) 6.

76. Fakhim H, Vaezi A, Dannaoui E, Chowdhary A, Nasiry D, Faeli L, Meis JF, Badali H. 2018. Comparative virulence of *Candida auris* with *Candida haemulonii*, *Candida glabrata* and *Candida albicans* in a murine model. Mycoses 61:377-382.

77. Pharkjaksu S, Boonmee N, Mitrpant C, Ngamskulrungroj P. 2021. Immunopathogenesis of Emerging *Candida auris* and *Candida haemulonii* Strains. Journal of Fungi 7.

78. Blinkhorn RJ, Adelstein D, Spagnuolo PJ. 1989. Emergence of a new opportunistic pathogen, *Candida lusitaniae*. J Clin Microbiol 27:236-40.

79. Atkinson BJ, Lewis RE, Kontoyiannis DP. 2008. Candida lusitaniae fungemia in cancer patients: risk factors for amphotericin B failure and outcome. Med Mycol 46:541-6.

80. Minari A, Hachem R, Raad I. 2001. Candida lusitaniae: a cause of breakthrough fungemia in cancer patients. Clin Infect Dis 32:186-90.

81. Atkinson BJ, Lewis RE, Kontoyiannis DP. 2008. Candida lusitaniae fungemia in cancer patients: risk factors for amphotericin B failure and outcome. Medical Mycology 46:541-546.

82. Chen SCA, Marriott D, Playford EG, Nguyen Q, Ellis D, Meyer W, Sorrell TC, Slavin M, Study AC. 2009. Candidaemia with uncommon *Candida* species: predisposing factors, outcome, antifungal susceptibility, and implications for management. Clinical Microbiology and Infection 15:662-669.

83. Mishra R, Kelly P, Toolsie O, Ayyadurai P, Adrish M. 2017. Uncommon cause of fungemia in a patient with renal cell cancer: A case report of *Candida lusitaniae* Fungemia. Medicine (Baltimore) 96:e8510.

84. McClenny NB, Fei H, Baron EJ, Gales AC, Houston A, Hollis RJ, Pfaller MA. 2002. Change in colony morphology of *Candida lusitaniae* in association with development of amphotericin B resistance. Antimicrob Agents Chemother 46:1325-8.

85. Pappagianis D, Collins MS, Hector R, Remington J. 1979. Development of resistance to amphotericin B in *Candida lusitaniae* infecting a human. Antimicrob Agents Chemother 16:123-6.

86. Khan Z, Ahmad S, Al-Sweih N, Khan S, Joseph L. 2019. Candida lusitaniae in Kuwait: Prevalence, antifungal susceptibility and role in neonatal fungemia. PLoS One 14:e0213532.

87. Sandoval-Denis M, Pastor FJ, Capilla J, Sutton DA, Fothergill AW, Guarro J. 2014. *In vitro* pharmacodynamics and *in vivo* efficacy of fluconazole, amphotericin B and caspofungin in a murine infection by *Candida lusitaniae*. Int J Antimicrob Agents 43:161-4.

88. Favel A, Michel-Nguyen A, Datry A, Challier S, Leclerc F, Chastin C, Fallague K, Regli P. 2004. Susceptibility of clinical isolates of *Candida lusitaniae* to five systemic antifungal agents. J Antimicrob Chemother 53:526-9.

89. Prigitano A, Biraghi E, Pozzi C, Viviani MA, Tortorano AM. 2010. *In vitro* activity of amphotericin B against *Candida lusitaniae* clinical isolates. J Chemother 22:71-2.

90. Tarif N. 2004. *Candida lusitaniae* Peritonitis in a Chronic Ambulatory Peritoneal Dialysis Patient. Saudi J Kidney Dis Transpl 15:170-3.

91. Kollia K, Arabatzis M, Kostoula O, Kostourou A, Velegraki A, Belessiotou E, Lazou A, Kostourou A. 2003. *Clavispora* (*Candida*) *lusitaniae* susceptibility profiles and genetic diversity in three tertiary hospitals (1998-2001). Int J Antimicrob Agents 22:458-60.

92. Guinet R, Chanas J, Goullier A, Bonnefoy G, Ambroise-Thomas P. 1983. Fatal septicemia due to amphotericin B-resistant *Candida lusitaniae*. J Clin Microbiol 18:443-4.

93. Merz WG. 1984. Candida lusitaniae: frequency of recovery, colonization, infection, and amphotericin B resistance. J Clin Microbiol 20:1194-5.

94. Asner SA, Giulieri S, Diezi M, Marchetti O, Sanglard D. 2015. Acquired Multidrug Antifungal Resistance in *Candida lusitaniae* during Therapy. Antimicrob Agents Chemother 59:7715-22.

95. Favel A, Michel-Nguyen A, Peyron F, Martin C, Thomachot L, Datry A, Bouchara JP, Challier S, Noel T, Chastin C, Regli P. 2003. Colony morphology switching of *Candida lusitaniae* and acquisition of multidrug resistance during treatment of a

renal infection in a newborn: case report and review of the literature. Diagn Microbiol Infect Dis 47:331-9.

96. Hadfield TL, Smith MB, Winn RE, Rinaldi MG, Guerra C. 1987. Mycoses caused by *Candida lusitaniae*. Rev Infect Dis 9:1006-12.

97. Demers EG, Biermann AR, Masonjones S, Crocker AW, Ashare A, Stajich JE, Hogan DA. 2018. Evolution of drug resistance in an antifungal-naive chronic *Candida lusitaniae* infection. Proc Natl Acad Sci U S A 115:12040-12045.

98. Desnos-Ollivier M, Moquet O, Chouaki T, Guerin AM, Dromer F. 2011. Development of echinocandin resistance in *Clavispora lusitaniae* during caspofungin treatment. J Clin Microbiol 49:2304-6.

99. Young LY, Hull CM, Heitman J. 2003. Disruption of ergosterol biosynthesis confers resistance to amphotericin B in *Candida lusitaniae*. Antimicrob Agents Chemother 47:2717-24.

100. Peyron F, Favel A, Calaf R, Michel-Nguyen A, Bonaly R, Coulon J. 2002. Sterol and fatty acid composition of *Candida lusitaniae* clinical isolates. Antimicrob Agents Chemother 46:531-3.

101. Reboutier D, Piednoel M, Boisnard S, Conti A, Chevalier V, Florent M, Gibot-Leclerc S, Da Silva B, Chastin C, Fallague K, Favel A, Noel T, Ruprich-Robert G, Chapeland-Leclerc F, Papon N. 2009. Combination of different molecular mechanisms leading to fluconazole resistance in a *Candida lusitaniae* clinical isolate. Diagn Microbiol Infect Dis 63:188-93.

102. Kannan A, Asner SA, Trachsel E, Kelly S, Parker J, Sanglard D. 2019. Comparative Genomics for the Elucidation of Multidrug Resistance in *Candida lusitaniae*. mBio 10.

103. Borgeat V, Brandalise D, Grenouillet F, Sanglard D. 2021. Participation of the ABC Transporter *CDR1* in Azole Resistance of *Candida lusitaniae*. J Fungi (Basel) 7.

104. Lamey PJ, Darwaza A, Fisher BM, Samaranayake LP, Macfarlane TW, Frier BM. 1988. Secretor status, candidal carriage and candidal infection in patients with diabetes mellitus. J Oral Pathol 17:354-7.

105. Al-Attas SA, Amro SO. 2010. Candidal colonization, strain diversity, and antifungal susceptibility among adult diabetic patients. Annals of Saudi Medicine 30:101-108.

106. Kumar BV, Padshetty NS, Bai KY, Rao MS. 2005. Prevalence of *Candida* in the oral cavity of diabetic subjects. J Assoc Physicians India 53:599-602.

107. Manfredi M, McCullough MJ, Al-Karaawi ZM, Hurel SJ, Porter SR. 2002. The isolation, identification and molecular analysis of *Candida* spp. isolated from the oral cavities of patients with diabetes mellitus. Oral Microbiol Immunol 17:181-5.

108. Lydia Rajakumari M, Saravana Kumari P. 2016. Prevalence of *Candida* species in the buccal cavity of diabetic and non-diabetic individuals in and around Pondicherry. J Mycol Med 26:359-367.

109. Belazi M, Velegraki A, Fleva A, Gidarakou I, Papanaum L, Baka D, Daniilidou N, Karamitsos D. 2005. Candidal overgrowth in diabetic patients: potential predisposing factors. Mycoses 48:192-6.

110. Zomorodian K, Kavoosi F, Pishdad GR, Mehriar P, Ebrahimi H, Bandegani A, Pakshir K. 2016. Prevalence of oral Candida colonization in patients with diabetes mellitus. J Mycol Med 26:103-110.

111. DorockaBobkowska B, BudtzJorgensen E, Wloch S. 1996. Non-insulin-dependent diabetes mellitus as a risk factor for denture stomatitis. Journal of Oral Pathology & Medicine 25:411-415.

112. Jhugroo C, Divakar DD, Jhugroo P, Al-Amri SAS, Alahmari AD, Vijaykumar S, Parine NR. 2019. Characterization of oral mucosa lesions and prevalence of yeasts in diabetic patients: A comparative study. Microb Pathog 126:363-367.

113. Bianchi CM, Bianchi HA, Tadano T, Paula CR, Hoffmann-Santos HD, Leite DP, Jr., Hahn RC. 2016. Factors Related to Oral Candidiasis in Elderly Users and Non-Users of Removable Dental Prostheses. Rev Inst Med Trop Sao Paulo 58:17.

114. Goswami R, Dadhwal V, Tejaswi S, Datta K, Paul A, Haricharan RN, Banerjee U, Kochupillai NP. 2000. Species-specific prevalence of vaginal candidiasis among patients with diabetes mellitus and its relation to their glycaemic status. Journal of Infection 41:162-166.

115. Akimoto-Gunther L, Bonfim-Mendonca Pde S, Takahachi G, Irie MM, Miyamoto S, Consolaro ME, Svidzinsk TI. 2016. Highlights Regarding Host Predisposing Factors to Recurrent Vulvovaginal Candidiasis: Chronic Stress and Reduced Antioxidant Capacity. PLoS One 11:e0158870.

116. Arfiputri DS, Hidayati AN, Handayani S, Ervianti E. 2018. Risk Factors of Vulvovaginal Candidiasis in Dermato-Venereology Outpatients Clinic of Soetomo General Hospital, Surabaya, Indonesia. Afr J Infect Dis 12:90-94.

117. Stojanovic P, Stojanovic N, Stojanovic-Radic Z, Arsic Arsenijevic V, Otasevic S, Randjelovic P, Radulovic NS. 2016. Surveillance and characterization of Candida bloodstream infections in a Serbian tertiary care hospital. J Infect Dev Ctries 10:643-56.

118. Rodrigues CF, Rodrigues ME, Henriques M. 2019. *Candida* sp. Infections in Patients with Diabetes Mellitus. Journal of Clinical Medicine 8.

119. Lim SMS, Sinnollareddy M, Sime FB. 2020. Challenges in Antifungal Therapy in Diabetes Mellitus. Journal of Clinical Medicine 9.

120. Mohammed L, Jha G, Malasevskaia I, Goud HK, Hassan A. 2021. The Interplay Between Sugar and Yeast Infections: Do Diabetics Have a Greater Predisposition to Develop Oral and Vulvovaginal Candidiasis? Cureus Journal of Medical Science 13.

121. Mowat A, Baum J. 1971. Chemotaxis of polymorphonuclear leukocytes from patients with diabetes mellitus. N Engl J Med 284:621-7.

122. Delamaire M, Maugendre D, Moreno M, Le Goff MC, Allannic H, Genetet B. 1997. Impaired leucocyte functions in diabetic patients. Diabet Med 14:29-34.

123. Tater D, Tepaut B, Bercovici JP, Youinou P. 1987. Polymorphonuclear cell derangements in type I diabetes. Horm Metab Res 19:642-7.

124. Marhoffer W, Stein M, Maeser E, Federlin K. 1992. Impairment of polymorphonuclear leukocyte function and metabolic control of diabetes. Diabetes Care 15:256-60.

125. Davidson NJ, Sowden JM, Fletcher J. 1984. Defective phagocytosis in insulin controlled diabetics: evidence for a reaction between glucose and opsonising proteins. J Clin Pathol 37:783-6.

126. de Souza Ferreira C, Araujo TH, Angelo ML, Pennacchi PC, Okada SS, de Araujo Paula FB, Migliorini S, Rodrigues MR. 2012. Neutrophil dysfunction induced by hyperglycemia: modulation of myeloperoxidase activity. Cell Biochem Funct 30:604-10.

127. Wilson RM, Reeves WG. 1986. Neutrophil phagocytosis and killing in insulin-dependent diabetes. Clin Exp Immunol 63:478-84.

128. Geisler C, Almdal T, Bennedsen J, Rhodes JM, Kolendorf K. 1982. Monocyte functions in diabetes mellitus. Acta Pathol Microbiol Immunol Scand C 90:33-7.

129. Katz S, Klein B, Elian I, Fishman P, Djaldetti M. 1983. Phagocytotic activity of monocytes from diabetic patients. Diabetes Care 6:479-82.

130. Nie LLX, Zhao PF, Yue ZQ, Zhang P, Ji N, Chen QM, Wang Q. 2021. Diabetes induces macrophage dysfunction through cytoplasmic dsDNA/AIM2 associated pyroptosis. Journal of Leukocyte Biology 110:497-510.

131. Restrepo BI, Twahirwa M, Rahbar MH, Schlesinger LS. 2014. Phagocytosis via complement or Fc-gamma receptors is compromised in monocytes from type 2 diabetes patients with chronic hyperglycemia. PLoS One 9:e92977.

132. Restrepo BI, Khan A, Singh VK, Erica d-L, Aguillon-Duran GP, Ledezma-Campos E, Canaday DH, Jagannath C. 2021. Human monocyte-derived macrophage responses to *M. tuberculosis* differ by the host's tuberculosis, diabetes or obesity status, and are enhanced by rapamycin. Tuberculosis (Edinb) 126:102047.

133. Hogendorf A, Szymanska M, Krasinska J, Baranowska-Jazwiecka A, Ancuta M, Charubczyk A, Wyka K, Drozdz I, Sokolowska-Gadoux M, Zarebska J, Michalak A, Szadkowska A, Jarosz-Chobot P, Mlynarski W. 2021. Clinical heterogeneity among pediatric patients with autoimmune type 1 diabetes stratified by immunoglobulin deficiency. Pediatric Diabetes 22:707-716.

134. Eibl N, Spatz M, Fischer GF, Mayr WR, Samstag A, Wolf HM, Schernthaner G, Eibl MM. 2002. Impaired primary immune response in type-1 diabetes: results from a controlled vaccination study. Clin Immunol 103:249-59.

135. Nam HW, Cho YJ, Lim JA, Kim SJ, Kim H, Sim SY, Lim DG. 2018. Functional status of immune cells in patients with long-lasting type 2 diabetes mellitus. Clinical and Experimental Immunology 194:125-136.

136. Ahmadiafshar A, Mohsenifard MR, Mazloomzadeh S. 2015. Evaluation of serum & salivary IgA in patients with type 1 diabetes. PLoS One 10:e0122757.

137. Balasoiu D, van Kessel KC, van Kats-Renaud HJ, Collet TJ, Hoepelman AI. 1997. Granulocyte function in women with diabetes and asymptomatic bacteriuria. Diabetes Care 20:392-5.

138. Gin H, Brottier E, Aubertin J. 1984. Influence of glycaemic normalisation by an artificial pancreas on phagocytic and bactericidal functions of granulocytes in insulin dependent diabetic patients. J Clin Pathol 37:1029-31.

139. Chou MY, Shian LR, Chang FY, Shaio MF. 1989. Opsonophagocytosis of *Staphylococcus aureus* by diabetics' sera and monocytes. Taiwan Yi Xue Hui Za Zhi 88:352-9.

140. Liberatore RR, Jr., Barbosa SF, Alkimin M, Bellinati-Pires R, Florido MP, Isaac L, Kirschfink M, Grumach AS. 2005. Is immunity in diabetic patients influencing the susceptibility to infections? Immunoglobulins, complement and phagocytic function in children and adolescents with type 1 diabetes mellitus. Pediatr Diabetes 6:206-12.

141. Dostalek M, Akhlaghi F, Puzanovova M. 2012. Effect of diabetes mellitus on pharmacokinetic and pharmacodynamic properties of drugs. Clin Pharmacokinet 51:481-99.

142. Szkudlarek A, Sulkowska A, Maciazek-Jurczyk M, Chudzik M, Rownicka-Zubik J. 2016. Effects of non-enzymatic glycation in human serum albumin. Spectroscopic analysis. Spectrochim Acta A Mol Biomol Spectrosc 152:645-53.

143. Arredondo G, Suarez E, Calvo R, Vazquez JA, Garcia-Sanchez J, Martinez-Jorda R. 1999. Serum protein binding of itraconazole and fluconazole in patients with diabetes mellitus. J Antimicrob Chemother 43:305-7.

144. Mandal SM, Mahata D, Migliolo L, Parekh A, Addy PS, Mandal M, Basak A. 2014. Glucose directly promotes antifungal resistance in the fungal pathogen, Candida spp. J Biol Chem 289:25468-73.

145. Kumar AKH, Chandrasekaran V, Kannan T, Murali AL, Lavanya J, Sudha V, Swaminathan S, Ramachandran G. 2017. Anti-tuberculosis drug concentrations in tuberculosis patients with and without diabetes mellitus. European Journal of Clinical Pharmacology 73:65-70.

146. Mann SC, Morrow M, Coyle RP, Coleman SS, Saderup A, Zheng JH, Ellison L, Bushman LR, Kiser JJ, MaWhinney S, Anderson PL, Castillo-Mancilla JR. 2020.

Lower Cumulative Antiretroviral Exposure in People Living With HIV and Diabetes Mellitus. J Acquir Immune Defic Syndr 85:483-488.

147. Aitken-Saavedra J, Lund RG, Gonzalez J, Huenchunao R, Perez-Vallespir I, Morales-Bozo I, Urzua B, Tarquinio SC, Maturana-Ramirez A, Martos J, Fernandez-Ramires R, Molina-Berrios A. 2018. Diversity, frequency and antifungal resistance of *Candida* species in patients with type 2 diabetes mellitus. Acta Odontol Scand 76:580-586.

148. Kumar S, Padmashree S, Jayalekshmi R. 2014. Correlation of salivary glucose, blood glucose and oral candidal carriage in the saliva of type 2 diabetics: A case-control study. Contemp Clin Dent 5:312-7.

149. Darwazeh AM, MacFarlane TW, McCuish A, Lamey PJ. 1991. Mixed salivary glucose levels and candidal carriage in patients with diabetes mellitus. J Oral Pathol Med 20:280-3.

150. Plotkin B, Konaklieva M. 2022. Impact of host factors on susceptibility to antifungal agents. ADMET DMPK 10:153-162.

151. Rodaki A, Bohovych IM, Enjalbert B, Young T, Odds FC, Gow NA, Brown AJ. 2009. Glucose promotes stress resistance in the fungal pathogen *Candida albicans*. Mol Biol Cell 20:4845-55.

152. Bhuyan L, Hassan S, Dash KC, Panda A, Behura SS, Ramachandra S. 2018. *Candida* Species Diversity in Oral Cavity of Type 2 Diabetic Patients and their *In vitro* Antifungal Susceptibility. Contemp Clin Dent 9:S83-S88.

153. Bremenkamp RM, Caris AR, Jorge AO, Back-Brito GN, Mota AJ, Balducci I, Brighenti FL, Koga-Ito CY. 2011. Prevalence and antifungal resistance profile of

Candida spp. oral isolates from patients with type 1 and 2 diabetes mellitus. Arch Oral Biol 56:549-55.

154. Raiesi O, Siavash M, Mohammadi F, Chabavizadeh J, Mahaki B, Maherolnaghsh M, Dehghan P. 2017. Frequency of Cutaneous Fungal Infections and Azole Resistance of the Isolates in Patients with Diabetes Mellitus. Adv Biomed Res 6:71.

155. Manfredi M, McCullough MJ, Polonelli L, Conti S, Al-Karaawi ZM, Vescovi P, Porter SR. 2006. *In vitro* antifungal susceptibility to six antifungal agents of 229 *Candida* isolates from patients with diabetes mellitus. Oral Microbiol Immunol 21:177-82.

156. Manfredi M, McCullough MJ, Al-Karaawi ZM, Vescovi P, Porter SR. 2006. I*n vitro* evaluation of virulence attributes of *Candida* spp. isolated from patients affected by diabetes mellitus. Oral Microbiol Immunol 21:183-9.

157. Tsang CSP, Chu FCS, Leung WK, Jin LJ, Samaranayake LP, Siu SC. 2007. Phospholipase, proteinase and haemolytic activities of *Candida albicans* isolated from oral cavities of patients with type 2 diabetes mellitus. J Med Microbiol 56:1393-1398.

158. Fatahinia M, Poormohamadi F, Zarei Mahmoudabadi A. 2015. Comparative Study of Esterase and Hemolytic Activities in Clinically Important *Candida* Species, Isolated From Oral Cavity of Diabetic and Non-diabetic Individuals. Jundishapur J Microbiol 8:e20893.

159. Rajendran R, Robertson DP, Hodge PJ, Lappin DF, Ramage G. 2010. Hydrolytic enzyme production is associated with *Candida albicans* biofilm formation from patients with type 1 diabetes. Mycopathologia 170:229-35.

160. Morschhauser J, Barker KS, Liu TT, Bla BWJ, Homayouni R, Rogers PD. 2007. The transcription factor Mrr1p controls expression of the *MDR1* efflux pump and mediates multidrug resistance in *Candida albicans*. PLoS Pathog 3:e164.

161. Schubert S, Rogers PD, Morschhauser J. 2008. Gain-of-function mutations in the transcription factor *MRR1* are responsible for overexpression of the *MDR1* efflux pump in fluconazole-resistant *Candida dubliniensis* strains. Antimicrob Agents Chemother 52:4274-80.

162. Silva AP, Miranda IM, Guida A, Synnott J, Rocha R, Silva R, Amorim A, Pina-Vaz C, Butler G, Rodrigues AG. 2011. Transcriptional profiling of azole-resistant *Candida parapsilosis* strains. Antimicrob Agents Chemother 55:3546-56.

163. Arastehfar A, Daneshnia F, Hafez A, Khodavaisy S, Najafzadeh MJ, Charsizadeh A, Zarrinfar H, Salehi M, Shahrabadi ZZ, Sasani E, Zomorodian K, Pan W, Hagen F, Ilkit M, Kostrzewa M, Boekhout T. 2020. Antifungal susceptibility, genotyping, resistance mechanism, and clinical profile of *Candida tropicalis* blood isolates. Med Mycol 58:766-773.

164. Li J, Coste AT, Bachmann D, Sanglard D, Lamoth F. 2022. Deciphering the Mrr1/Mdr1 Pathway in Azole Resistance of *Candida auris*. Antimicrob Agents Chemother doi:10.1128/aac.00067-22:e0006722.

165. MacPherson S, Larochelle M, Turcotte B. 2006. A fungal family of transcriptional regulators: the zinc cluster proteins. Microbiol Mol Biol Rev 70:583-604.

166. Schubert S, Popp C, Rogers PD, Morschhauser J. 2011. Functional dissection of a *Candida albicans* zinc cluster transcription factor, the multidrug resistance regulator Mrr1. Eukaryot Cell 10:1110-21.

167. Dunkel N, Blass J, Rogers PD, Morschhauser J. 2008. Mutations in the multi-drug resistance regulator *MRR1*, followed by loss of heterozygosity, are the main cause of *MDR1* overexpression in fluconazole-resistant *Candida albicans* strains. Mol Microbiol 69:827-40.

168. Kusch H, Engelmann S, Albrecht D, Morschhauser J, Hecker M. 2007. Proteomic analysis of the oxidative stress response in *Candida albicans*. Proteomics 7:686-97.

169. Karababa M, Coste AT, Rognon B, Bille J, Sanglard D. 2004. Comparison of gene expression profiles of *Candida albicans* azole-resistant clinical isolates and laboratory strains exposed to drugs inducing multidrug transporters. Antimicrob Agents Chemother 48:3064-79.

170. Harry JB, Oliver BG, Song JL, Silver PM, Little JT, Choiniere J, White TC. 2005. Drug-induced regulation of the *MDR1* promoter in *Candida albicans*. Antimicrob Agents Chemother 49:2785-92.

171. Schubert S, Barker KS, Znaidi S, Schneider S, Dierolf F, Dunkel N, Aid M, Boucher G, Rogers PD, Raymond M, Morschhauser J. 2011. Regulation of efflux pump expression and drug resistance by the transcription factors Mrr1, Upc2, and Cap1 in *Candida albicans*. Antimicrob Agents Chemother 55:2212-23.

172. Schneider S, Morschhauser J. 2015. Induction of *Candida albicans* drug resistance genes by hybrid zinc cluster transcription factors. Antimicrob Agents Chemother 59:558-69.

173. Lucau-Danila A, Lelandais G, Kozovska Z, Tanty V, Delaveau T, Devaux F, Jacq C. 2005. Early expression of yeast genes affected by chemical stress. Mol Cell Biol 25:1860-8.

174. Lelandais G, Tanty V, Geneix C, Etchebest C, Jacq C, Devaux F. 2008. Genome adaptation to chemical stress: clues from comparative transcriptomics in *Saccharomyces cerevisiae* and *Candida glabrata*. Genome Biol 9:R164.

175. Wang Y, Cao YY, Jia XM, Cao YB, Gao PH, Fu XP, Ying K, Chen WS, Jiang YY. 2006. Cap1p is involved in multiple pathways of oxidative stress response in *Candida albicans*. Free Radic Biol Med 40:1201-9.

176. Kuge S, Jones N, Nomoto A. 1997. Regulation of yAP-1 nuclear localization in response to oxidative stress. EMBO J 16:1710-20.

177. Wood MJ, Storz G, Tjandra N. 2004. Structural basis for redox regulation of Yap1 transcription factor localization. Nature 430:917-21.

178. Delaunay A, Isnard AD, Toledano MB. 2000. H_2O_2 sensing through oxidation of the Yap1 transcription factor. EMBO J 19:5157-66.

179. Kuge S, Arita M, Murayama A, Maeta K, Izawa S, Inoue Y, Nomoto A. 2001. Regulation of the yeast Yap1p nuclear export signal is mediated by redox signal-induced reversible disulfide bond formation. Mol Cell Biol 21:6139-50.

180. Znaidi S, Barker KS, Weber S, Alarco AM, Liu TT, Boucher G, Rogers PD, Raymond M. 2009. Identification of the *Candida albicans* Cap1p regulon. Eukaryot Cell 8:806-20.

181. Messenguy F, Dubois E. 2003. Role of MADS box proteins and their cofactors in combinatorial control of gene expression and cell development. Gene 316:1-21.

182. Riggle PJ, Kumamoto CA. 2006. Transcriptional regulation of *MDR1*, encoding a drug efflux determinant, in fluconazole-resistant *Candida albicans* strains through an Mcm1p binding site. Eukaryot Cell 5:1957-68.

183. Tuch BB, Galgoczy DJ, Hernday AD, Li H, Johnson AD. 2008. The evolution of combinatorial gene regulation in fungi. PLoS Biol 6:e38.

184. Mogavero S, Tavanti A, Senesi S, Rogers PD, Morschhauser J. 2011. Differential requirement of the transcription factor Mcm1 for activation of the *Candida albicans* multidrug efflux pump *MDR1* by its regulators Mrr1 and Cap1. Antimicrob Agents Chemother 55:2061-6.

185. Rottmann M, Dieter S, Brunner H, Rupp S. 2003. A screen in *Saccharomyces cerevisiae* identified *CaMCM1*, an essential gene in *Candida albicans* crucial for morphogenesis. Mol Microbiol 47:943-59.

186. Jarvis EE, Clark KL, Sprague GF, Jr. 1989. The yeast transcription activator PRTF, a homolog of the mammalian serum response factor, is encoded by the *MCM1* gene. Genes Dev 3:936-45.

187. Passmore S, Maine GT, Elble R, Christ C, Tye BK. 1988. *Saccharomyces cerevisiae* protein involved in plasmid maintenance is necessary for mating of MAT alpha cells. J Mol Biol 204:593-606.

188. Mead J, Bruning AR, Gill MK, Steiner AM, Acton TB, Vershon AK. 2002. Interactions of the Mcm1 MADS box protein with cofactors that regulate mating in yeast. Mol Cell Biol 22:4607-21.

189. Althoefer H, Schleiffer A, Wassmann K, Nordheim A, Ammerer G. 1995. Mcm1 is required to coordinate G2-specific transcription in *Saccharomyces cerevisiae*. Mol Cell Biol 15:5917-28.

190. McInerny CJ, Partridge JF, Mikesell GE, Creemer DP, Breeden LL. 1997. A novel Mcm1-dependent element in the *SWI4*, *CLN3*, *CDC6*, and *CDC47* promoters activates M/G1-specific transcription. Genes Dev 11:1277-88.

191. Kuo MH, Grayhack E. 1994. A library of yeast genomic MCM1 binding sites contains genes involved in cell cycle control, cell wall and membrane structure, and metabolism. Mol Cell Biol 14:348-59.

192. Kuo MH, Nadeau ET, Grayhack EJ. 1997. Multiple phosphorylated forms of the *Saccharomyces cerevisiae* Mcm1 protein include an isoform induced in response to high salt concentrations. Mol Cell Biol 17:819-32.

193. Messenguy F, Dubois E. 1993. Genetic evidence for a role for MCM1 in the regulation of arginine metabolism in *Saccharomyces cerevisiae*. Mol Cell Biol 13:2586-92.

194. Chen Y, Tye BK. 1995. The yeast Mcm1 protein is regulated posttranscriptionally by the flux of glycolysis. Mol Cell Biol 15:4631-9.

195. Yu G, Deschenes RJ, Fassler JS. 1995. The essential transcription factor, Mcm1, is a downstream target of Sln1, a yeast "two-component" regulator. J Biol Chem 270:8739-43.

196. Fassler JS, Gray WM, Malone CL, Tao W, Lin H, Deschenes RJ. 1997. Activated alleles of yeast *SLN1* increase Mcm1-dependent reporter gene expression and

diminish signaling through the Hog1 osmosensing pathway. J Biol Chem 272:13365-71.

197. Silver PM, Oliver BG, White TC. 2004. Role of *Candida albicans* transcription factor Upc2p in drug resistance and sterol metabolism. Eukaryot Cell 3:1391-7.

198. MacPherson S, Akache B, Weber S, De Deken X, Raymond M, Turcotte B. 2005. *Candida albicans* zinc cluster protein Upc2p confers resistance to antifungal drugs and is an activator of ergosterol biosynthetic genes. Antimicrob Agents Chemother 49:1745-52.

199. Znaidi S, Weber S, Al-Abdin OZ, Bomme P, Saidane S, Drouin S, Lemieux S, De Deken X, Robert F, Raymond M. 2008. Genomewide location analysis of *Candida albicans* Upc2p, a regulator of sterol metabolism and azole drug resistance. Eukaryot Cell 7:836-47.

200. Dunkel N, Liu TT, Barker KS, Homayouni R, Morschhauser J, Rogers PD. 2008. A gain-of-function mutation in the transcription factor Upc2p causes upregulation of ergosterol biosynthesis genes and increased fluconazole resistance in a clinical *Candida albicans* isolate. Eukaryot Cell 7:1180-90.

201. Liu Z, Myers LC. 2017. *Candida albicans* Swi/Snf and Mediator Complexes Differentially Regulate Mrr1-Induced *MDR1* Expression and Fluconazole Resistance. Antimicrob Agents Chemother 61.

202. Balachandra VK, Ghosh SK. 2022. Emerging roles of SWI/SNF remodelers in fungal pathogens. Curr Genet 68:195-206.

203. Mao X, Cao F, Nie X, Liu H, Chen J. 2006. The Swi/Snf chromatin remodeling complex is essential for hyphal development in *Candida albicans*. FEBS Lett 580:2615-22.

204. Lu Y, Su C, Mao X, Raniga PP, Liu H, Chen J. 2008. Efg1-mediated recruitment of NuA4 to promoters is required for hypha-specific Swi/Snf binding and activation in *Candida albicans*. Mol Biol Cell 19:4260-72.

205. Tebbji F, Chen Y, Sellam A, Whiteway M. 2017. The Genomic Landscape of the Fungus-Specific SWI/SNF Complex Subunit, Snf6, in *Candida albicans*. mSphere 2.

206. Burgain A, Pic E, Markey L, Tebbji F, Kumamoto CA, Sellam A. 2019. A novel genetic circuitry governing hypoxic metabolic flexibility, commensalism and virulence in the fungal pathogen *Candida albicans*. PLoS Pathog 15:e1007823.

207. Moran GP, Anderson MZ, Myers LC, Sullivan DJ. 2019. Role of Mediator in virulence and antifungal drug resistance in pathogenic fungi. Curr Genet 65:621-630.

208. Tebbji F, Chen Y, Richard Albert J, Gunsalus KT, Kumamoto CA, Nantel A, Sellam A, Whiteway M. 2014. A functional portrait of Med7 and the mediator complex in *Candida albicans*. PLoS Genet 10:e1004770.

209. Lindsay AK, Morales DK, Liu Z, Grahl N, Zhang A, Willger SD, Myers LC, Hogan DA. 2014. Analysis of *Candida albicans* mutants defective in the Cdk8 module of mediator reveal links between metabolism and biofilm formation. PLoS Genet 10:e1004567.

210. Hollomon JM, Liu Z, Rusin SF, Jenkins NP, Smith AK, Koeppen K, Kettenbach AN, Myers LC, Hogan DA. 2022. The *Candida albicans* Cdk8-dependent phosphoproteome reveals repression of hyphal growth through a Flo8-dependent pathway. PLoS Genet 18:e1009622.

211. Zhang A, Liu Z, Myers LC. 2013. Differential regulation of white-opaque switching by individual subunits of *Candida albicans* mediator. Eukaryot Cell 12:1293-304.

212. Uwamahoro N, Qu Y, Jelicic B, Lo TL, Beaurepaire C, Bantun F, Quenault T, Boag PR, Ramm G, Callaghan J, Beilharz TH, Nantel A, Peleg AY, Traven A. 2012. The functions of Mediator in *Candida albicans* support a role in shaping species-specific gene expression. PLoS Genet 8:e1002613.

213. Liu Z, Myers LC. 2017. Mediator Tail Module Is Required for Tac1-Activated *CDR1* Expression and Azole Resistance in *Candida albicans*. Antimicrob Agents Chemother 61.

214. Demers EG, Stajich JE, Ashare A, Occhipinti P, Hogan DA. 2021. Balancing Positive and Negative Selection: *In Vivo* Evolution of *Candida lusitaniae MRR1*. mBio 12.

215. Iyer KR, Camara K, Daniel-Ivad M, Trilles R, Pimentel-Elardo SM, Fossen JL, Marchillo K, Liu Z, Singh S, Munoz JF, Kim SH, Porco JA, Jr., Cuomo CA, Williams NS, Ibrahim AS, Edwards JE, Jr., Andes DR, Nodwell JR, Brown LE, Whitesell L, Robbins N, Cowen LE. 2020. An oxindole efflux inhibitor potentiates azoles and impairs virulence in the fungal pathogen *Candida auris*. Nat Commun 11:6429.

216. Rogers PD, Barker KS. 2003. Genome-wide expression profile analysis reveals coordinately regulated genes associated with stepwise acquisition of azole resistance in *Candida albicans* clinical isolates. Antimicrob Agents Chemother 47:1220-7.

217. Cowen LE, Nantel A, Whiteway MS, Thomas DY, Tessier DC, Kohn LM, Anderson JB. 2002. Population genomics of drug resistance in *Candida albicans*. Proc Natl Acad Sci U S A 99:9284-9.

218. Hooshdaran MZ, Barker KS, Hilliard GM, Kusch H, Morschhauser J, Rogers PD. 2004. Proteomic analysis of azole resistance in *Candida albicans* clinical isolates. Antimicrob Agents Chemother 48:2733-5.

219. Hoehamer CF, Cummings ED, Hilliard GM, Morschhauser J, Rogers PD. 2009. Proteomic analysis of Mrr1p- and Tac1p-associated differential protein expression in azole-resistant clinical isolates of *Candida albicans*. Proteomics Clin Appl 3:968-78.

220. Kusch H, Biswas K, Schwanfelder S, Engelmann S, Rogers PD, Hecker M, Morschhauser J. 2004. A proteomic approach to understanding the development of multidrug-resistant *Candida albicans* strains. Mol Genet Genomics 271:554-65.

221. Rogers PD, Barker KS. 2002. Evaluation of differential gene expression in fluconazole-susceptible and -resistant isolates of *Candida albicans* by cDNA microarray analysis. Antimicrob Agents Chemother 46:3412-7.

222. Woolley DW. 1944. Some biological effects produced by benzimidazole and their reversal by purines. Journal of Biological Chemistry 152:225-232.

223. Holt RJ. 1976. Topical Pharmacology of Imidazole Antifungals. Journal of Cutaneous Pathology 3:45-59.

224. Richardson K. 1990. The discovery and profile of fluconazole. J Chemother 2:51-4.

225. Fling ME, Kopf J, Tamarkin A, Gorman JA, Smith HA, Koltin Y. 1991. Analysis of a *Candida albicans* Gene That Encodes a Novel Mechanism for Resistance to Benomyl and Methotrexate. Molecular & General Genetics 227:318-329.

226. Ben-Yaacov R, Knoller S, Caldwell GA, Becker JM, Koltin Y. 1994. *Candida albicans* gene encoding resistance to benomyl and methotrexate is a multidrug resistance gene. Antimicrob Agents Chemother 38:648-52.

227. Goldway M, Teff D, Schmidt R, Oppenheim AB, Koltin Y. 1995. Multidrug resistance in *Candida albicans*: disruption of the *BENr* gene. Antimicrob Agents Chemother 39:422-6.

228. Sanglard D, Kuchler K, Ischer F, Pagani JL, Monod M, Bille J. 1995. Mechanisms of resistance to azole antifungal agents in *Candida albicans* isolates from AIDS patients involve specific multidrug transporters. Antimicrob Agents Chemother 39:2378-86.

229. Albertson GD, Niimi M, Cannon RD, Jenkinson HF. 1996. Multiple efflux mechanisms are involved in *Candida albicans* fluconazole resistance. Antimicrob Agents Chemother 40:2835-41.

230. White TC. 1997. Increased mRNA levels of *ERG16*, *CDR*, and *MDR1* correlate with increases in azole resistance in *Candida albicans* isolates from a patient

infected with human immunodeficiency virus. Antimicrob Agents Chemother 41:1482-7.

231. Franz R, Kelly SL, Lamb DC, Kelly DE, Ruhnke M, Morschhauser J. 1998. Multiple molecular mechanisms contribute to a stepwise development of fluconazole resistance in clinical *Candida albicans* strains. Antimicrob Agents Chemother 42:3065-72.

232. Franz R, Ruhnke M, Morschhauser J. 1999. Molecular aspects of fluconazole resistance development in *Candida albicans*. Mycoses 42:453-8.

233. Wirsching S, Michel S, Morschhauser J. 2000. Targeted gene disruption in *Candida albicans* wild-type strains: the role of the *MDR1* gene in fluconazole resistance of clinical *Candida albicans* isolates. Molecular Microbiology 36:856-865.

234. Hiller D, Sanglard D, Morschhauser J. 2006. Overexpression of the *MDR1* gene is sufficient to confer increased resistance to toxic compounds in *Candida albicans*. Antimicrobial Agents and Chemotherapy 50:1365-1371.

235. Gupta V, Kohli A, Krishnamurthy S, Puri N, Aalamgeer SA, Panwar S, Prasad R. 1998. Identification of polymorphic mutant alleles of *CaMDR1*, a major facilitator of *Candida albicans* which confers multidrug resistance, and its *in vitro* transcriptional activation. Curr Genet 34:192-9.

236. Vogel M, Hartmann T, Koberle M, Treiber M, Autenrieth IB, Schumacher UK. 2008. Rifampicin induces *MDR1* expression in *Candida albicans*. J Antimicrob Chemother 61:541-7.

237. Suchodolski J, Krasowska A. 2021. Fructose Induces Fluconazole Resistance in *Candida albicans* through Activation of Mdr1 and Cdr1 Transporters. Int J Mol Sci 22.

238. Nett JE, Lepak AJ, Marchillo K, Andes DR. 2009. Time course global gene expression analysis of an *in vivo Candida* biofilm. J Infect Dis 200:307-13.

239. Shi C, Liu J, Li W, Zhao Y, Meng L, Xiang M. 2019. Expression of fluconazole resistance-associated genes in biofilm from 23 clinical isolates of *Candida albicans*. Braz J Microbiol 50:157-163.

240. Moran GP, Sanglard D, Donnelly SM, Shanley DB, Sullivan DJ, Coleman DC. 1998. Identification and expression of multidrug transporters responsible for fluconazole resistance in *Candida dubliniensis*. Antimicrob Agents Chemother 42:1819-30.

241. Wirsching S, Moran GP, Sullivan DJ, Coleman DC, Morschhauser J. 2001. *MDR1*-mediated drug resistance in *Candida dubliniensis*. Antimicrob Agents Chemother 45:3416-21.

242. Berkow EL, Manigaba K, Parker JE, Barker KS, Kelly SL, Rogers PD. 2015. Multidrug Transporters and Alterations in Sterol Biosynthesis Contribute to Azole Antifungal Resistance in *Candida parapsilosis*. Antimicrob Agents Chemother 59:5942-50.

243. Branco J, Silva AP, Silva RM, Silva-Dias A, Pina-Vaz C, Butler G, Rodrigues AG, Miranda IM. 2015. Fluconazole and Voriconazole Resistance in *Candida parapsilosis* Is Conferred by Gain-of-Function Mutations in *MRR1* Transcription Factor Gene. Antimicrob Agents Chemother 59:6629-33.

244. Grossman NT, Pham CD, Cleveland AA, Lockhart SR. 2015. Molecular mechanisms of fluconazole resistance in *Candida parapsilosis* isolates from a U.S. surveillance system. Antimicrob Agents Chemother 59:1030-7.

245. Souza AC, Fuchs BB, Pinhati HM, Siqueira RA, Hagen F, Meis JF, Mylonakis E, Colombo AL. 2015. *Candida parapsilosis* Resistance to Fluconazole: Molecular Mechanisms and *In Vivo* Impact in Infected *Galleria mellonella* Larvae. Antimicrob Agents Chemother 59:6581-7.

246. Choi MJ, Won EJ, Shin JH, Kim SH, Lee WG, Kim MN, Lee K, Shin MG, Suh SP, Ryang DW, Im YJ. 2016. Resistance Mechanisms and Clinical Features of Fluconazole-Nonsusceptible *Candida tropicalis* Isolates Compared with Fluconazole-Less-Susceptible Isolates. Antimicrobial Agents and Chemotherapy 60:3653-3661.

247. You LS, Qian WB, Yang Q, Mao LP, Zhu L, Huang XB, Jin J, Meng HT. 2017. *ERG11* Gene Mutations and *MDR1* Upregulation Confer Pan-Azole Resistance in *Candida tropicalis* Causing Disseminated Candidiasis in an Acute Lymphoblastic Leukemia Patient on Posaconazole Prophylaxis. Antimicrobial Agents and Chemotherapy 61.

248. Fan X, Xiao M, Zhang D, Huang JJ, Wang H, Hou X, Zhang L, Kong F, Chen SCA, Tong ZH, Xu YC. 2019. Molecular mechanisms of azole resistance in *Candida tropicalis* isolates causing invasive candidiasis in China. Clinical Microbiology and Infection 25:885-891.

249. Kohli A, Gupta V, Krishnamurthy S, Hasnain SE, Prasad R. 2001. Specificity of drug transport mediated by CaMDR1: a major facilitator of *Candida albicans*. J Biosci 26:333-9.

250. Hampe IAI, Friedman J, Edgerton M, Morschhauser J. 2017. An acquired mechanism of antifungal drug resistance simultaneously enables *Candida albicans* to escape from intrinsic host defenses. PLoS Pathog 13:e1006655.

251. Allison DL, Willems HME, Jayatilake J, Bruno VM, Peters BM, Shirtliff ME. 2016. *Candida*-Bacteria Interactions: Their Impact on Human Disease. Microbiol Spectr 4.

252. Kwak MK, Ku M, Kang SO. 2018. Inducible NAD(H)-linked methylglyoxal oxidoreductase regulates cellular methylglyoxal and pyruvate through enhanced activities of alcohol dehydrogenase and methylglyoxal-oxidizing enzymes in glutathione-depleted *Candida albicans*. Biochimica Et Biophysica Acta-General Subjects 1862:18-39.

253. Yin Z, Stead D, Walker J, Selway L, Smith DA, Brown AJ, Quinn J. 2009. A proteomic analysis of the salt, cadmium and peroxide stress responses in *Candida albicans* and the role of the Hog1 stress-activated MAPK in regulating the stress-induced proteome. Proteomics 9:4686-703.

254. Enjalbert B, Smith DA, Cornell MJ, Alam I, Nicholls S, Brown AJ, Quinn J. 2006. Role of the Hog1 stress-activated protein kinase in the global transcriptional response to stress in the fungal pathogen *Candida albicans*. Mol Biol Cell 17:1018-32.

255. Setiadi ER, Doedt T, Cottier F, Noffz C, Ernst JF. 2006. Transcriptional response of *Candida albicans* to hypoxia: linkage of oxygen sensing and Efg1p-regulatory networks. J Mol Biol 361:399-411.

256. Seneviratne CJ, Wang Y, Jin L, Abiko Y, Samaranayake LP. 2008. *Candida albicans* biofilm formation is associated with increased anti-oxidative capacities. Proteomics 8:2936-47.

257. Rosenbach A, Dignard D, Pierce JV, Whiteway M, Kumamoto CA. 2010. Adaptations of *Candida albicans* for growth in the mammalian intestinal tract. Eukaryot Cell 9:1075-86.

258. Garay-Arroyo A, Covarrubias AA. 1999. Three genes whose expression is induced by stress in *Saccharomyces cerevisiae*. Yeast 15:879-892.

259. Vido K, Spector D, Lagniel G, Lopez S, Toledano MB, Labarre J. 2001. A proteome analysis of the cadmium response in Saccharomyces cerevisiae. J Biol Chem 276:8469-74.

260. DeRisi J, van den Hazel B, Marc P, Balzi E, Brown P, Jacq C, Goffeau A. 2000. Genome microarray analysis of transcriptional activation in multidrug resistance yeast mutants. FEBS Lett 470:156-60.

261. Chen CN, Porubleva L, Shearer G, Svrakic M, Holden LG, Dover JL, Johnston M, Chitnis PR, Kohl DH. 2003. Associating protein activities with their genes: rapid identification of a gene encoding a methylglyoxal reductase in the yeast *Saccharomyces cerevisiae*. Yeast 20:545-54.

262. Hauser M, Horn P, Tournu H, Hauser NC, Hoheisel JD, Brown AJ, Dickinson JR. 2007. A transcriptome analysis of isoamyl alcohol-induced filamentation in yeast

reveals a novel role for Gre2p as isovaleraldehyde reductase. FEMS Yeast Res 7:84-92.

263. Jayakody LN, Horie K, Hayashi N, Kitagaki H. 2013. Engineering redox cofactor utilization for detoxification of glycolaldehyde, a key inhibitor of bioethanol production, in yeast *Saccharomyces cerevisiae*. Appl Microbiol Biotechnol 97:6589-600.

264. Jayakody LN, Turner TL, Yun EJ, Kong, II, Liu JJ, Jin YS. 2018. Expression of Gre2p improves tolerance of engineered xylose-fermenting *Saccharomyces cerevisiae* to glycolaldehyde under xylose metabolism. Appl Microbiol Biotechnol 102:8121-8133.

265. Moon J, Liu ZL. 2012. Engineered NADH-dependent *GRE2* from *Saccharomyces cerevisiae* by directed enzyme evolution enhances HMF reduction using additional cofactor NADPH. Enzyme Microb Technol 50:115-20.

266. Warringer J, Blomberg A. 2006. Involvement of yeast *YOL151W*/*GRE2* in ergosterol metabolism. Yeast 23:389-98.

267. Pitarch A, Abian J, Carrascal M, Sanchez M, Nombela C, Gil C. 2004. Proteomics-based identification of novel *Candida albicans* antigens for diagnosis of systemic candidiasis in patients with underlying hematological malignancies. Proteomics 4:3084-106.

268. Muheim A, Waldner R, Sanglard D, Reiser J, Schoemaker HE, Leisola MS. 1991. Purification and properties of an aryl-alcohol dehydrogenase from the white-rot fungus *Phanerochaete chrysosporium*. Eur J Biochem 195:369-75.

269. Yang DD, Francois JM, de Billerbeck GM. 2012. Cloning, expression and characterization of an aryl-alcohol dehydrogenase from the white-rot fungus *Phanerochaete chrysosporium* strain BKM-F-1767. BMC Microbiol 12:126.

270. Delneri D, Gardner DC, Bruschi CV, Oliver SG. 1999. Disruption of seven hypothetical aryl alcohol dehydrogenase genes from *Saccharomyces cerevisiae* and construction of a multiple knock-out strain. Yeast 15:1681-9.

271. Hacisalihoglu B, Holyavkin C, Topaloglu A, Kisakesen HI, Cakar ZP. 2019. Genomic and transcriptomic analysis of a coniferyl aldehyde-resistant *Saccharomyces cerevisiae* strain obtained by evolutionary engineering. Fems Yeast Research 19.

272. Lucau-Danila A, Delaveau T, Lelandais G, Devaux F, Jacq C. 2003. Competitive promoter occupancy by two yeast paralogous transcription factors controlling the multidrug resistance phenomenon. J Biol Chem 278:52641-50.

273. Singleton DR, Masuoka J, Hazen KC. 2001. Cloning and analysis of a *Candida albicans* gene that affects cell surface hydrophobicity. J Bacteriol 183:3582-8.

274. Synnott JM, Guida A, Mulhern-Haughey S, Higgins DG, Butler G. 2010. Regulation of the hypoxic response in *Candida albicans*. Eukaryot Cell 9:1734-46.

275. Hoehamer CF, Cummings ED, Hilliard GM, Rogers PD. 2010. Changes in the proteome of *Candida albicans* in response to azole, polyene, and echinocandin antifungal agents. Antimicrob Agents Chemother 54:1655-64.

276. Lorenz MC, Bender JA, Fink GR. 2004. Transcriptional response of *Candida albicans* upon internalization by macrophages. Eukaryot Cell 3:1076-87.

277. Li DD, Wang Y, Dai BD, Li XX, Zhao LX, Cao YB, Yan L, Jiang YY. 2013. *ECM17*-dependent methionine/cysteine biosynthesis contributes to biofilm formation in *Candida albicans*. Fungal Genet Biol 51:50-9.

278. Zuzuarregui A, Monteoliva L, Gil C, del Olmo M. 2006. Transcriptomic and proteomic approach for understanding the molecular basis of adaptation of *Saccharomyces cerevisiae* to wine fermentation. Appl Environ Microbiol 72:836-47.

279. Nakano M, Morita T, Yamamoto T, Sano H, Ashiuchi M, Masui R, Kuramitsu S, Yagi T. 1999. Purification, molecular cloning, and catalytic activity of *Schizosaccharomyces pombe* pyridoxal reductase. A possible additional family in the aldo-keto reductase superfamily. J Biol Chem 274:23185-90.

280. Gasch AP, Spellman PT, Kao CM, Carmel-Harel O, Eisen MB, Storz G, Botstein D, Brown PO. 2000. Genomic expression programs in the response of yeast cells to environmental changes. Mol Biol Cell 11:4241-57.

281. Rossignol T, Kobi D, Jacquet-Gutfreund L, Blondin B. 2009. The proteome of a wine yeast strain during fermentation, correlation with the transcriptome. J Appl Microbiol 107:47-55.

282. Fujisawa H, Nagata S, Misono H. 2003. Characterization of short-chain dehydrogenase/reductase homologues of *Escherichia coli* (YdfG) and *Saccharomyces cerevisiae* (YMR226C). Biochim Biophys Acta 1645:89-94.

283. Katz M, Hahn-Hagerdal B, Gorwa-Grauslund MF. 2003. Screening of two complementary collections of *Saccharomyces cerevisiae* to identify enzymes

involved in stereo-selective reductions of specific carbonyl compounds: an alternative to protein purification. Enzyme and Microbial Technology 33:163-172.

284. Phillips SA, Thornalley PJ. 1993. The formation of methylglyoxal from triose phosphates. Investigation using a specific assay for methylglyoxal. Eur J Biochem 212:101-5.

285. Pompliano DL, Peyman A, Knowles JR. 1990. Stabilization of a reaction intermediate as a catalytic device: definition of the functional role of the flexible loop in triosephosphate isomerase. Biochemistry 29:3186-94.

286. Richard JP. 1991. Kinetic parameters for the elimination reaction catalyzed by triosephosphate isomerase and an estimation of the reaction's physiological significance. Biochemistry 30:4581-5.

287. Shonk CE, Boxer GE. 1964. Enzyme Patterns in Human Tissues. I. Methods for the Determination of Glycolytic Enzymes. Cancer Res 24:709-21.

288. Hopper DJ, Cooper RA. 1972. The purification and properties of *Escherichia coli* methylglyoxal synthase. Biochem J 128:321-9.

289. Cooper RA. 1974. Methylglyoxal formation during glucose catabolism by *Pseudomonas saccharophila*. Identification of methylglyoxal synthase. Eur J Biochem 44:81-6.

290. Tsai PK, Gracy RW. 1976. Isolation and characterization of crystalline methylglyoxal synthetase from *Proteus vulgaris*. J Biol Chem 251:364-7.

291. Huang K, Rudolph FB, Bennett GN. 1999. Characterization of methylglyoxal synthase from *Clostridium acetobutylicum* ATCC 824 and its use in the formation of 1, 2-propanediol. Appl Environ Microbiol 65:3244-7.

292. Shin SM, Song SH, Lee JW, Kwak MK, Kang SO. 2017. Methylglyoxal synthase regulates cell elongation via alterations of cellular methylglyoxal and spermidine content in *Bacillus subtilis*. Int J Biochem Cell Biol 91:14-28.

293. Pazhang M, Khajeh K, Asghari SM, Falahati H, Naderi-Manesh H. 2010. Cloning, expression, and characterization of a novel methylglyoxal synthase from *Thermus* sp. strain GH5. Appl Biochem Biotechnol 162:1519-28.

294. Ray S, Ray M. 1981. Isolation of methylglyoxal synthase from goat liver. J Biol Chem 256:6230-3.

295. Kadner RJ, Murphy GP, Stephens CM. 1992. Two mechanisms for growth inhibition by elevated transport of sugar phosphates in *Escherichia coli*. J Gen Microbiol 138:2007-14.

296. Rekarte UD, Zwaig N, Isturiz T. 1973. Accumulation of methylglyoxal in a mutant of *Escherichia coli* constitutive for gluconate catabolism. J Bacteriol 115:727-31.

297. Kim I, Kim E, Yoo S, Shin D, Min B, Song J, Park C. 2004. Ribose utilization with an excess of mutarotase causes cell death due to accumulation of methylglyoxal. J Bacteriol 186:7229-35.

298. Freedberg WB, Kistler WS, Lin EC. 1971. Lethal synthesis of methylglyoxal by *Escherichia coli* during unregulated glycerol metabolism. J Bacteriol 108:137-44.

299. Penninckx MJ, Jaspers CJ, Legrain MJ. 1983. The glutathione-dependent glyoxalase pathway in the yeast *Saccharomyces cerevisiae*. J Biol Chem 258:6030-6.

300. Hasim S, Hussin NA, Alomar F, Bidasee KR, Nickerson KW, Wilson MA. 2014. A glutathione-independent glyoxalase of the DJ-1 superfamily plays an important

role in managing metabolically generated methylglyoxal in Candida albicans. J Biol Chem 289:1662-74.

301. Zeng S, Constant P, Yang D, Baulard A, Lefevre P, Daffe M, Wattiez R, Fontaine V. 2019. Cpn60.1 (GroEL1) Contributes to Mycobacterial Crabtree Effect: Implications for Biofilm Formation. Front Microbiol 10:1149.

302. Whitaker M, Ruecker N, Hartman T, Klevorn T, Andres J, Kim J, Rhee K, Ehrt S. 2020. Two interacting ATPases protect *Mycobacterium tuberculosis* from glycerol and nitric oxide toxicity. J Bacteriol doi:10.1128/JB.00202-20.

303. Xu D, Liu X, Guo C, Zhao J. 2006. Methylglyoxal detoxification by an aldo-keto reductase in the cyanobacterium *Synechococcus* sp. PCC 7002. Microbiology (Reading) 152:2013-2021.

304. Cao W, Chang T, Li X-q, Wang R, Wu L. 2017. Dual effects of fructose on ChREBP and FoxO1/3α are responsible for AldoB up-regulation and vascular remodelling. Clinical Science 131:309-325.

305. Ashton N, Dhar I, Dhar A, Wu L, Desai KM. 2013. Increased Methylglyoxal Formation with Upregulation of Renin Angiotensin System in Fructose Fed Sprague Dawley Rats. PLoS ONE 8.

306. Liu J, Wang R, Desai K, Wu L. 2011. Upregulation of aldolase B and overproduction of methylglyoxal in vascular tissues from rats with metabolic syndrome. Cardiovascular Research 92:494-503.

307. Valishkevych BV, Vasylkovska RA, Lozinska LM, Semchyshyn HM. 2016. Fructose-Induced Carbonyl/Oxidative Stress in *S. cerevisiae*: Involvement of TOR. Biochem Res Int 2016:8917270.

308. Elliott WH. 1958. A new threonine metabolite. Biochim Biophys Acta 29:446-7.

309. Elliott WH. 1959. Amino-acetone; its isolation and role in metabolism. Nature 183:1051-2.

310. Murata K, Saikusa T, Fukuda Y, Watanabe K, Inoue Y, Shimosaka M, Kimura A. 1986. Metabolism of 2-oxoaldehydes in yeasts. Possible role of glycolytic bypath as a detoxification system in L-threonine catabolism by *Saccharomyces cerevisiae*. Eur J Biochem 157:297-301.

311. Elliott WH. 1960. Methylglyoxal formation from aminoacetone by ox plasma. Nature 185:467-8.

312. Ray S, Ray M. 1983. Formation of methylglyoxal from aminoacetone by amine oxidase from goat plasma. J Biol Chem 258:3461-2.

313. Ray M, Ray S. 1987. Aminoacetone oxidase from goat liver. Formation of methylglyoxal from aminoacetone. J Biol Chem 262:5974-7.

314. Ray M, Ray S. 1985. L-Threonine dehydrogenase from goat liver. Feedback inhibition by methylglyoxal. J Biol Chem 260:5913-8.

315. Lyles GA, Chalmers J. 1992. The metabolism of aminoacetone to methylglyoxal by semicarbazide-sensitive amine oxidase in human umbilical artery. Biochem Pharmacol 43:1409-14.

316. Deng Y, Yu PH. 1999. Assessment of the deamination of aminoacetone, an endogenous substrate for semicarbazide-sensitive amine oxidase. Anal Biochem 270:97-102.

317. Deng Y, Boomsma F, Yu PH. 1998. Deamination of methylamine and aminoacetone increases aldehydes and oxidative stress in rats. Life Sci 63:2049-58.

318. Sartori A, Mano CM, Mantovani MC, Dyszy FH, Massari J, Tokikawa R, Nascimento OR, Nantes IL, Bechara EJ. 2013. Ferricytochrome (c) directly oxidizes aminoacetone to methylglyoxal, a catabolite accumulated in carbonyl stress. PLoS One 8:e57790.

319. Laffel L. 1999. Ketone bodies: a review of physiology, pathophysiology and application of monitoring to diabetes. Diabetes Metab Res Rev 15:412-26.

320. Casazza JP, Felver ME, Veech RL. 1984. The metabolism of acetone in rat. J Biol Chem 259:231-6.

321. Koop DR, Casazza JP. 1985. Identification of ethanol-inducible P-450 isozyme 3a as the acetone and acetol monooxygenase of rabbit microsomes. J Biol Chem 260:13607-12.

322. Beisswenger BG, Delucia EM, Lapoint N, Sanford RJ, Beisswenger PJ. 2005. Ketosis leads to increased methylglyoxal production on the Atkins diet. Ann N Y Acad Sci 1043:201-10.

323. Li C, Dai S, Lu J, Zhao B, Wang J, Li P, Wu Z, Mu Y, Feng C, Dong Q. 2018. Methylglyoxal: A newly detected and potentially harmful metabolite in the blood of ketotic dairy cows. J Dairy Sci 101:8513-8523.

324. Lukins HB, Foster JW. 1963. Methyl Ketone Metabolism in Hydrocarbon-Utilizing Mycobacteria. J Bacteriol 85:1074-87.

325. Kato L. 1983. *In vitro* cultivation of *Mycobacterium* X from *Mycobacterium leprae*-infected tissues in acetone-dimethylsulfoxide-tetradecane medium. Int J Lepr Other Mycobact Dis 51:77-83.

326. Burback BL, Perry JJ. 1993. Biodegradation and biotransformation of groundwater pollutant mixtures by *Mycobacterium vaccae*. Appl Environ Microbiol 59:1025-9.

327. Furuya T, Hirose S, Osanai H, Semba H, Kino K. 2011. Identification of the monooxygenase gene clusters responsible for the regioselective oxidation of phenol to hydroquinone in mycobacteria. Appl Environ Microbiol 77:1214-20.

328. Furuya T, Nakao T, Kino K. 2015. Catalytic function of the mycobacterial binuclear iron monooxygenase in acetone metabolism. FEMS Microbiol Lett 362.

329. Taylor DG, Trudgill PW, Cripps RE, Harris PR. 1980. The Microbial-Metabolism of Acetone. Journal of General Microbiology 118:159-170.

330. Awala SI, Gwak JH, Kim YM, Kim SJ, Strazzulli A, Dunfield PF, Yoon H, Kim GJ, Rhee SK. 2021. Verrucomicrobial methanotrophs grow on diverse C3 compounds and use a homolog of particulate methane monooxygenase to oxidize acetone. Isme Journal 15:3636-3647.

331. Thornalley PJ, Langborg A, Minhas HS. 1999. Formation of glyoxal, methylglyoxal and 3-deoxyglucosone in the glycation of proteins by glucose. Biochem J 344 Pt 1:109-16.

332. Takahashi K. 1977. Further studies on the reactions of phenylglyoxal and related reagents with proteins. J Biochem 81:403-14.

333. Shipanova IN, Glomb MA, Nagaraj RH. 1997. Protein modification by methylglyoxal: chemical nature and synthetic mechanism of a major fluorescent adduct. Arch Biochem Biophys 344:29-36.

334. Thornalley PJ. 2005. Dicarbonyl intermediates in the maillard reaction. Ann N Y Acad Sci 1043:111-7.

335. Thornalley PJ. 2007. Endogenous alpha-oxoaldehydes and formation of protein and nucleotide advanced glycation endproducts in tissue damage. Novartis Found Symp 285:229-43; discussion 243-6.

336. Rabbani N, Thornalley PJ. 2012. Methylglyoxal, glyoxalase 1 and the dicarbonyl proteome. Amino Acids 42:1133-42.

337. Ahmed N, Thornalley PJ, Dawczynski J, Franke S, Strobel J, Stein G, Haik GM. 2003. Methylglyoxal-derived hydroimidazolone advanced glycation end-products of human lens proteins. Invest Ophthalmol Vis Sci 44:5287-92.

338. Thornalley PJ, Battah S, Ahmed N, Karachalias N, Agalou S, Babaei-Jadidi R, Dawnay A. 2003. Quantitative screening of advanced glycation endproducts in cellular and extracellular proteins by tandem mass spectrometry. Biochem J 375:581-92.

339. Gallet X, Charloteaux B, Thomas A, Brasseur R. 2000. A fast method to predict protein interaction sites from sequences. J Mol Biol 302:917-26.

340. Bartlett GJ, Porter CT, Borkakoti N, Thornton JM. 2002. Analysis of catalytic residues in enzyme active sites. J Mol Biol 324:105-21.

341. Riordan JF, McElvany KD, Borders CL, Jr. 1977. Arginyl residues: anion recognition sites in enzymes. Science 195:884-6.

342. Lederer MO, Klaiber RG. 1999. Cross-linking of proteins by Maillard processes: characterization and detection of lysine-arginine cross-links derived from glyoxal and methylglyoxal. Bioorg Med Chem 7:2499-507.

343. Ansari NA, Moinuddin, Ali R. 2011. Glycated lysine residues: a marker for non-enzymatic protein glycation in age-related diseases. Dis Markers 30:317-24.

344. Chakraborty S, Karmakar K, Chakravortty D. 2014. Cells producing their own nemesis: understanding methylglyoxal metabolism. IUBMB Life 66:667-78.

345. Lo TW, Westwood ME, McLellan AC, Selwood T, Thornalley PJ. 1994. Binding and modification of proteins by methylglyoxal under physiological conditions. A kinetic and mechanistic study with N alpha-acetylarginine, N alpha-acetylcysteine, and N alpha-acetyllysine, and bovine serum albumin. J Biol Chem 269:32299-305.

346. Mostafa AA, Randell EW, Vasdev SC, Gill VD, Han Y, Gadag V, Raouf AA, El Said H. 2007. Plasma protein advanced glycation end products, carboxymethyl cysteine, and carboxyethyl cysteine, are elevated and related to nephropathy in patients with diabetes. Mol Cell Biochem 302:35-42.

347. Gomes RA, Vicente Miranda H, Silva MS, Graca G, Coelho AV, Ferreira AE, Cordeiro C, Freire AP. 2006. Yeast protein glycation *in vivo* by methylglyoxal. Molecular modification of glycolytic enzymes and heat shock proteins. FEBS J 273:5273-87.

348. Donnellan L, Young C, Simpson BS, Acland M, Dhillon VS, Costabile M, Fenech M, Hoffmann P, Deo P. 2022. Proteomic Analysis of Methylglyoxal Modifications Reveals Susceptibility of Glycolytic Enzymes to Dicarbonyl Stress. Int J Mol Sci 23.

349. Flores-Morales P, Diema C, Vilaseca M, Estelrich J, Luque FJ, Gutiérrez-Oliva S, Toro-Labbé A, Silva E. 2011. Enhanced reactivity of Lys182 explains the limited efficacy of biogenic amines in preventing the inactivation of glucose-6-phosphate dehydrogenase by methylglyoxal. Bioorganic & Medicinal Chemistry 19:1613-1622.

350. Sjoblom NM, Kelsey MMG, Scheck RA. 2018. A Systematic Study of Selective Protein Glycation. Angewandte Chemie International Edition 57:16077-16082.

351. Kimzey MJ, Kinsky OR, Yassine HN, Tsaprailis G, Stump CS, Monks TJ, Lau SS. 2015. Site specific modification of the human plasma proteome by methylglyoxal. Toxicology and Applied Pharmacology 289:155-162.

352. Banerjee S. 2021. Biophysical and mass spectrometry based characterization of methylglyoxal-modified myoglobin: Role of advanced glycation end products in inducing protein structural alterations. International Journal of Biological Macromolecules 193:2165-2172.

353. Muranova LK, Perfilov MM, Serebryakova MV, Gusev NB. 2016. Effect of methylglyoxal modification on the structure and properties of human small heat shock protein HspB6 (Hsp20). Cell Stress and Chaperones 21:617-629.

354. Leone S, Fonderico J, Melchiorre C, Carpentieri A, Picone D. 2019. Structural effects of methylglyoxal glycation, a study on the model protein MNEI. Mol Cell Biochem 451:165-171.

355. Venkatraman J, Aggarwal K, Balaram P. 2001. Helical peptide models for protein glycation: proximity effects in catalysis of the Amadori rearrangement. Chemistry & Biology 8:611-625.

356. Fica-Contreras SM, Shuster SO, Durfee ND, Bowe GJK, Henning NJ, Hill SA, Vrla GD, Stillman DR, Suralik KM, Sandwick RK, Choi S. 2017. Glycation of Lys-16 and Arg-5 in amyloid-β and the presence of Cu2+ play a major role in the oxidative stress mechanism of Alzheimer's disease. JBIC Journal of Biological Inorganic Chemistry 22:1211-1222.

357. Ahmed N, Dobler D, Dean M, Thornalley PJ. 2005. Peptide Mapping Identifies Hotspot Site of Modification in Human Serum Albumin by Methylglyoxal Involved in Ligand Binding and Esterase Activity. Journal of Biological Chemistry 280:5724-5732.

358. Acimovic JM, Stanimirovic BD, Todorovic N, Jovanovic VB, Mandic LM. 2010. Influence of the microenvironment of thiol groups in low molecular mass thiols and serum albumin on the reaction with methylglyoxal. Chem Biol Interact 188:21-30.

359. Pavićević ID, Jovanović VB, Takić MM, Penezić AZ, Aćimović JM, Mandić LM. 2014. Fatty acids binding to human serum albumin: Changes of reactivity and glycation level of Cysteine-34 free thiol group with methylglyoxal. Chemico-Biological Interactions 224:42-50.

360. Schneider M, Thoss G, Hubner-Parajsz C, Kientsch-Engel R, Stahl P, Pischetsrieder M. 2004. Determination of glycated nucleobases in human urine by a new monoclonal antibody specific for N2-carboxyethyl-2'-deoxyguanosine. Chem Res Toxicol 17:1385-90.

361. Frischmann M, Bidmon C, Angerer J, Pischetsrieder M. 2005. Identification of DNA adducts of methylglyoxal. Chem Res Toxicol 18:1586-92.

362. Synold T, Xi B, Wuenschell GE, Tamae D, Figarola JL, Rahbar S, Termini J. 2008. Advanced glycation end products of DNA: quantification of N2-(1-Carboxyethyl)-2'-deoxyguanosine in biological samples by liquid chromatography electrospray ionization tandem mass spectrometry. Chem Res Toxicol 21:2148-55.

363. Thornalley PJ, Waris S, Fleming T, Santarius T, Larkin SJ, Winklhofer-Roob BM, Stratton MR, Rabbani N. 2010. Imidazopurinones are markers of physiological

genomic damage linked to DNA instability and glyoxalase 1-associated tumour multidrug resistance. Nucleic Acids Res 38:5432-42.

364. Tu CY, Chen YF, Lii CK, Wang TS. 2013. Methylglyoxal induces DNA crosslinks in ECV304 cells via a reactive oxygen species-independent protein carbonylation pathway. Toxicol In Vitro 27:1211-9.

365. Petrova KV, Millsap AD, Stec DF, Rizzo CJ. 2014. Characterization of the deoxyguanosine-lysine cross-link of methylglyoxal. Chem Res Toxicol 27:1019-29.

366. Murata-Kamiya N, Kamiya H. 2001. Methylglyoxal, an endogenous aldehyde, crosslinks DNA polymerase and the substrate DNA. Nucleic Acids Res 29:3433-8.

367. Tamae D, Lim P, Wuenschell GE, Termini J. 2011. Mutagenesis and repair induced by the DNA advanced glycation end product N2-1-(carboxyethyl)-2'-deoxyguanosine in human cells. Biochemistry 50:2321-9.

368. Kasai H, Kumeno K, Yamaizumi Z, Nishimura S, Nagao M, Fujita Y, Sugimura T, Nukaya H, Kosuge T. 1982. Mutagenicity of methylglyoxal in coffee. Gan 73:681-3.

369. Fujita Y, Wakabayashi K, Nagao M, Sugimura T. 1985. Characteristics of major mutagenicity of instant coffee. Mutat Res 142:145-8.

370. Nagao M, Fujita Y, Sugimura T, Kosuge T. 1986. Methylglyoxal in beverages and foods: its mutagenicity and carcinogenicity. IARC Sci Publ:283-91.

371. Nagao M, Fujita Y, Wakabayashi K, Nukaya H, Kosuge T, Sugimura T. 1986. Mutagens in coffee and other beverages. Environ Health Perspect 67:89-91.

372. Wuenschell GE, Tamae D, Cercillieux A, Yamanaka R, Yu C, Termini J. 2010. Mutagenic potential of DNA glycation: miscoding by (R)- and (S)-N2-(1-carboxyethyl)-2'-deoxyguanosine. Biochemistry 49:1814-21.

373. Krymkiewicz N, Dieguez E, Rekarte UD, Zwaig N. 1971. Properties and mode of action of a bactericidal compound (=methylglyoxal) produced by a mutant of *Escherichia coli*. J Bacteriol 108:1338-47.

374. Ahmad MI, Ahmad S, Moinuddin. 2011. Preferential recognition of methylglyoxal-modified calf thymus DNA by circulating antibodies in cancer patients. Indian J Biochem Biophys 48:290-6.

375. Ahmad S, Uddin M, Habib S, Shahab U, Alam K, Ali A. 2014. Autoimmune response to AGE modified human DNA: Implications in type 1 diabetes mellitus. J Clin Transl Endocrinol 1:66-72.

376. Ahmad S, Moinuddin, Shahab U, Habib S, Khan MS, Alam K, Ali A. 2014. Glycoxidative damage to human DNA: Neo-antigenic epitopes on DNA molecule could be a possible reason for autoimmune response in type 1 diabetes. Glycobiology 24:281-291.

377. Kalapos MP. 2008. The tandem of free radicals and methylglyoxal. Chem Biol Interact 171:251-71.

378. Okado A, Kawasaki Y, Hasuike Y, Takahashi M, Teshima T, Fujii J, Taniguchi N. 1996. Induction of apoptotic cell death by methylglyoxal and 3-deoxyglucosone in macrophage-derived cell lines. Biochem Biophys Res Commun 225:219-24.

379. Chang T, Wang R, Wu L. 2005. Methylglyoxal-induced nitric oxide and peroxynitrite production in vascular smooth muscle cells. Free Radic Biol Med 38:286-93.

380. Kikuchi S, Shinpo K, Moriwaka F, Makita Z, Miyata T, Tashiro K. 1999. Neurotoxicity of methylglyoxal and 3-deoxyglucosone on cultured cortical neurons: synergism between glycation and oxidative stress, possibly involved in neurodegenerative diseases. J Neurosci Res 57:280-9.

381. Wittmann I, Mazak I, Poto L, Wagner Z, Wagner L, Vas T, Kovacs T, Belagyi J, Nagy J. 2001. Role of iron in the interaction of red blood cells with methylglyoxal. Modification of L-arginine by methylglyoxal is catalyzed by iron redox cycling. Chem Biol Interact 138:171-87.

382. Choudhary D, Chandra D, Kale RK. 1997. Influence of methylglyoxal on antioxidant enzymes and oxidative damage. Toxicol Lett 93:141-52.

383. Polykretis P, Luchinat E, Boscaro F, Banci L. 2020. Methylglyoxal interaction with superoxide dismutase 1. Redox Biol 30:101421.

384. Lankin VZ, Sharapov MG, Goncharov RG, Tikhaze AK, Novoselov VI. 2019. Natural Dicarbonyls Inhibit Peroxidase Activity of Peroxiredoxins. Dokl Biochem Biophys 485:132-134.

385. Zhang H, Forman HJ. 2012. Glutathione synthesis and its role in redox signaling. Semin Cell Dev Biol 23:722-8.

386. Kalapos MP, Garzo T, Antoni F, Mandl J. 1992. Accumulation of S-D-lactoylglutathione and transient decrease of glutathione level caused by methylglyoxal load in isolated hepatocytes. Biochim Biophys Acta 1135:159-64.

387. Leoncini G, Maresca M, Buzzi E. 1989. Inhibition of the glycolytic pathway by methylglyoxal in human platelets. Cell Biochem Funct 7:65-70.

388. Baskaran S, Balasubramanian KA. 1990. Effect of methylglyoxal on protein thiol and amino groups in isolated rat enterocytes and colonocytes and activity of various brush border enzymes. Indian J Biochem Biophys 27:13-7.

389. Shamsi FA, Lin K, Sady C, Nagaraj RH. 1998. Methylglyoxal-derived modifications in lens aging and cataract formation. Invest Ophthalmol Vis Sci 39:2355-64.

390. Akhand AA, Hossain K, Mitsui H, Kato M, Miyata T, Inagi R, Du J, Takeda K, Kawamoto Y, Suzuki H, Kurokawa K, Nakashima I. 2001. Glyoxal and methylglyoxal trigger distinct signals for MAP family kinases and caspase activation in human endothelial cells. Free Radic Biol Med 31:20-30.

391. Choudhary D, Chandra D, Kale RK. 1997. Influence of methylglyoxal on antioxidant enzymes and oxidative damage. Toxicology Letters 93:141-152.

392. Kalapos MP. 1999. Influence of acetone on the hepatotoxicity of methylglyoxal. Medical Science Research 27:617-620.

393. Ankrah NA, Appiah-Opong R. 1999. Toxicity of low levels of methylglyoxal: depletion of blood glutathione and adverse effect on glucose tolerance in mice. Toxicology Letters 109:61-67.

394. Vander Jagt DL, Hunsaker LA, Vander Jagt TJ, Gomez MS, Gonzales DM, Deck LM, Royer RE. 1997. Inactivation of glutathione reductase by 4-hydroxynonenal and other endogenous aldehydes. Biochem Pharmacol 53:1133-40.

395. Wu L, Juurlink BH. 2002. Increased methylglyoxal and oxidative stress in hypertensive rat vascular smooth muscle cells. Hypertension 39:809-14.

396. Neuberg C. 1913. The destruction of milk acid aldehyde and methylglyoxal through faunal organs. Biochemische Zeitschrift 49:502-506.

397. Racker E. 1951. The mechanism of action of glyoxalase. J Biol Chem 190:685-96.

398. Sousa Silva M, Gomes RA, Ferreira AE, Ponces Freire A, Cordeiro C. 2013. The glyoxalase pathway: the first hundred years... and beyond. Biochem J 453:1-15.

399. Sousa Silva M, Ferreira AE, Gomes R, Tomas AM, Ponces Freire A, Cordeiro C. 2012. The glyoxalase pathway in protozoan parasites. Int J Med Microbiol 302:225-9.

400. Cameron AD, Olin B, Ridderstrom M, Mannervik B, Jones TA. 1997. Crystal structure of human glyoxalase I--evidence for gene duplication and 3D domain swapping. EMBO J 16:3386-95.

401. Aronsson AC, Marmstal E, Mannervik B. 1978. Glyoxalase I, a zinc metalloenzyme of mammals and yeast. Biochem Biophys Res Commun 81:1235-40.

402. Barata L, Sousa Silva M, Schuldt L, da Costa G, Tomas AM, Ferreira AE, Weiss MS, Ponces Freire A, Cordeiro C. 2010. Cloning, expression, purification, crystallization and preliminary X-ray diffraction analysis of glyoxalase I from *Leishmania infantum*. Acta Crystallogr Sect F Struct Biol Cryst Commun 66:571-4.

403. Sukdeo N, Clugston SL, Daub E, Honek JF. 2004. Distinct classes of glyoxalase I: metal specificity of the *Yersinia pestis*, *Pseudomonas aeruginosa* and *Neisseria meningitidis* enzymes. Biochem J 384:111-7.

404. Greig N, Wyllie S, Vickers TJ, Fairlamb AH. 2006. Trypanothione-dependent glyoxalase I in Trypanosoma cruzi. Biochem J 400:217-23.

405. Vickers TJ, Greig N, Fairlamb AH. 2004. A trypanothione-dependent glyoxalase I with a prokaryotic ancestry in *Leishmania major*. Proc Natl Acad Sci U S A 101:13186-91.

406. Ariza A, Vickers TJ, Greig N, Armour KA, Dixon MJ, Eggleston IM, Fairlamb AH, Bond CS. 2006. Specificity of the trypanothione-dependent *Leishmania major* glyoxalase I: structure and biochemical comparison with the human enzyme. Mol Microbiol 59:1239-48.

407. Mustafiz A, Ghosh A, Tripathi AK, Kaur C, Ganguly AK, Bhavesh NS, Tripathi JK, Pareek A, Sopory SK, Singla-Pareek SL. 2014. A unique Ni2+ -dependent and methylglyoxal-inducible rice glyoxalase I possesses a single active site and functions in abiotic stress response. Plant J 78:951-63.

408. Jain M, Batth R, Kumari S, Mustafiz A. 2016. *Arabidopsis thaliana* Contains Both Ni^{2+} and Zn^{2+} Dependent Glyoxalase I Enzymes and Ectopic Expression of the Latter Contributes More towards Abiotic Stress Tolerance in *E. coli*. PLoS One 11:e0159348.

409. Bito A, Haider M, Hadler I, Breitenbach M. 1997. Identification and phenotypic analysis of two glyoxalase II encoding genes from *Saccharomyces cerevisiae*,

GLO2 and *GLO4*, and intracellular localization of the corresponding proteins. J Biol Chem 272:21509-19.

410. Akoachere M, Iozef R, Rahlfs S, Deponte M, Mannervik B, Creighton DJ, Schirmer H, Becker K. 2005. Characterization of the glyoxalases of the malarial parasite *Plasmodium falciparum* and comparison with their human counterparts. Biol Chem 386:41-52.

411. Wendler A, Irsch T, Rabbani N, Thornalley PJ, Krauth-Siegel RL. 2009. Glyoxalase II does not support methylglyoxal detoxification but serves as a general trypanothione thioesterase in African trypanosomes. Mol Biochem Parasitol 163:19-27.

412. Irsch T, Krauth-Siegel RL. 2004. Glyoxalase II of African trypanosomes is trypanothione-dependent. J Biol Chem 279:22209-17.

413. Armeni T, Cianfruglia L, Piva F, Urbanelli L, Luisa Caniglia M, Pugnaloni A, Principato G. 2014. S-D-Lactoylglutathione can be an alternative supply of mitochondrial glutathione. Free Radic Biol Med 67:451-9.

414. Misra K, Banerjee AB, Ray S, Ray M. 1995. Glyoxalase III from *Escherichia coli*: a single novel enzyme for the conversion of methylglyoxal into D-lactate without reduced glutathione. Biochem J 305 (Pt 3):999-1003.

415. Benov L, Sequeira F, Beema AF. 2004. Role of rpoS in the regulation of glyoxalase III in *Escherichia coli*. Acta Biochim Pol 51:857-60.

416. Okado-Matsumoto A, Fridovich I. 2000. The role of alpha,beta -dicarbonyl compounds in the toxicity of short chain sugars. J Biol Chem 275:34853-7.

417. Subedi KP, Choi D, Kim I, Min B, Park C. 2011. Hsp31 of *Escherichia coli* K-12 is glyoxalase III. Mol Microbiol 81:926-36.

418. Quigley PM, Korotkov K, Baneyx F, Hol WG. 2003. The 1.6-A crystal structure of the class of chaperones represented by *Escherichia coli* Hsp31 reveals a putative catalytic triad. Proc Natl Acad Sci U S A 100:3137-42.

419. Sastry MS, Korotkov K, Brodsky Y, Baneyx F. 2002. Hsp31, the *Escherichia coli yedU* gene product, is a molecular chaperone whose activity is inhibited by ATP at high temperatures. J Biol Chem 277:46026-34.

420. Mujacic M, Bader MW, Baneyx F. 2004. *Escherichia coli* Hsp31 functions as a holding chaperone that cooperates with the DnaK-DnaJ-GrpE system in the management of protein misfolding under severe stress conditions. Mol Microbiol 51:849-59.

421. Mujacic M, Baneyx F. 2006. Regulation of *Escherichia coli hchA*, a stress-inducible gene encoding molecular chaperone Hsp31. Mol Microbiol 60:1576-89.

422. Mujacic M, Baneyx F. 2007. Chaperone Hsp31 contributes to acid resistance in stationary-phase *Escherichia coli*. Appl Environ Microbiol 73:1014-8.

423. Kim HJ, Lee KY, Kwon AR, Lee BJ. 2017. Structural and functional studies of SAV0551 from Staphylococcus aureus as a chaperone and glyoxalase III. Biosci Rep 37.

424. Chandrangsu P, Dusi R, Hamilton CJ, Helmann JD. 2014. Methylglyoxal resistance in *Bacillus subtilis*: contributions of bacillithiol-dependent and independent pathways. Mol Microbiol 91:706-15.

425. Bankapalli K, Saladi S, Awadia SS, Goswami AV, Samaddar M, D'Silva P. 2015. Robust glyoxalase activity of Hsp31, a ThiJ/DJ-1/PfpI family member protein, is critical for oxidative stress resistance in *Saccharomyces cerevisiae*. J Biol Chem 290:26491-507.

426. Zhao Q, Su Y, Wang Z, Chen C, Wu T, Huang Y. 2014. Identification of glutathione (GSH)-independent glyoxalase III from Schizosaccharomyces pombe. BMC Evol Biol 14:86.

427. Lee JY, Song J, Kwon K, Jang S, Kim C, Baek K, Kim J, Park C. 2012. Human DJ-1 and its homologs are novel glyoxalases. Hum Mol Genet 21:3215-25.

428. Li T, Cheng X, Wang Y, Yin X, Li Z, Liu R, Liu G, Wang Y, Xu Y. 2019. Genome-wide analysis of glyoxalase-like gene families in grape (*Vitis vinifera L.*) and their expression profiling in response to downy mildew infection. BMC Genomics 20:362.

429. Islam T, Ghosh A. 2018. Genome-wide dissection and expression profiling of unique glyoxalase III genes in soybean reveal the differential pattern of transcriptional regulation. Sci Rep 8:4848.

430. Ghosh A, Kushwaha HR, Hasan MR, Pareek A, Sopory SK, Singla-Pareek SL. 2016. Presence of unique glyoxalase III proteins in plants indicates the existence of shorter route for methylglyoxal detoxification. Sci Rep 6:18358.

431. Jana GA, Krishnamurthy P, Kumar PP, Yaish MW. 2021. Functional characterization and expression profiling of glyoxalase III genes in date palm grown under abiotic stresses. Physiol Plant 172:780-794.

432. Smith N, Wilson MA. 2017. Structural Biology of the DJ-1 Superfamily. Adv Exp Med Biol 1037:5-24.

433. Mencke P, Boussaad I, Romano CD, Kitami T, Linster CL, Kruger R. 2021. The Role of DJ-1 in Cellular Metabolism and Pathophysiological Implications for Parkinson's Disease. Cells 10.

434. Kusch H, Engelmann S, Bode R, Albrecht D, Morschhauser J, Hecker M. 2008. A proteomic view of *Candida albicans* yeast cell metabolism in exponential and stationary growth phases. Int J Med Microbiol 298:291-318.

435. Singh RP, Prasad HK, Sinha I, Agarwal N, Natarajan K. 2011. Cap2-HAP complex is a critical transcriptional regulator that has dual but contrasting roles in regulation of iron homeostasis in *Candida albicans*. J Biol Chem 286:25154-70.

436. Amm I, Norell D, Wolf DH. 2015. Absence of the Yeast Hsp31 Chaperones of the DJ-1 Superfamily Perturbs Cytoplasmic Protein Quality Control in Late Growth Phase. PLoS One 10:e0140363.

437. Natkanska U, Skoneczna A, Sienko M, Skoneczny M. 2017. The budding yeast orthologue of Parkinson's disease-associated DJ-1 is a multi-stress response protein protecting cells against toxic glycolytic products. Biochim Biophys Acta Mol Cell Res 1864:39-50.

438. Jez JM, Bennett MJ, Schlegel BP, Lewis M, Penning TM. 1997. Comparative anatomy of the aldo-keto reductase superfamily. Biochem J 326 (Pt 3):625-36.

439. Ellis EM. 2002. Microbial aldo-keto reductases. FEMS Microbiol Lett 216:123-31.

440. Ko J, Kim I, Yoo S, Min B, Kim K, Park C. 2005. Conversion of methylglyoxal to acetol by *Escherichia coli* aldo-keto reductases. J Bacteriol 187:5782-9.

441. Grant AW, Steel G, Waugh H, Ellis EM. 2003. A novel aldo-keto reductase from *Escherichia coli* can increase resistance to methylglyoxal toxicity. FEMS Microbiol Lett 218:93-9.

442. Aguilera J, Prieto JA. 2001. The *Saccharomyces cerevisiae* aldose reductase is implied in the metabolism of methylglyoxal in response to stress conditions. Curr Genet 39:273-83.

443. Mudalkar S, Sreeharsha RV, Reddy AR. 2016. A novel aldo-keto reductase from *Jatropha curcas* L. (JcAKR) plays a crucial role in the detoxification of methylglyoxal, a potent electrophile. J Plant Physiol 195:39-49.

444. Turoczy Z, Kis P, Torok K, Cserhati M, Lendvai A, Dudits D, Horvath GV. 2011. Overproduction of a rice aldo-keto reductase increases oxidative and heat stress tolerance by malondialdehyde and methylglyoxal detoxification. Plant Mol Biol 75:399-412.

445. Songsiriritthigul C, Narawongsanont R, Tantitadapitak C, Guan HH, Chen CJ. 2020. Structure-function study of AKR4C14, an aldo-keto reductase from Thai jasmine rice (*Oryza sativa* L. ssp. indica cv. KDML105). Acta Crystallogr D Struct Biol 76:472-483.

446. Auiyawong B, Narawongsanont R, Tantitadapitak C. 2017. Characterization of AKR4C15, a Novel Member of Aldo-Keto Reductase, in Comparison with Other Rice AKR(s). Protein J 36:257-269.

447. Jain D, Khandal H, Khurana JP, Chattopadhyay D. 2016. A pathogenesis related-10 protein CaARP functions as aldo/keto reductase to scavenge cytotoxic aldehydes. Plant Mol Biol 90:171-87.

448. Kumar D, Singh P, Yusuf MA, Upadhyaya CP, Roy SD, Hohn T, Sarin NB. 2013. The *Xerophyta viscosa* aldose reductase (ALDRXV4) confers enhanced drought and salinity tolerance to transgenic tobacco plants by scavenging methylglyoxal and reducing the membrane damage. Mol Biotechnol 54:292-303.

449. Endo S, Matsunaga T, Mamiya H, Hara A, Kitade Y, Tajima K, El-Kabbani O. 2009. Characterization of a rat NADPH-dependent aldo-keto reductase (AKR1B13) induced by oxidative stress. Chem Biol Interact 178:151-7.

450. Endo S, Matsunaga T, Horie K, Tajima K, Bunai Y, Carbone V, El-Kabbani O, Hara A. 2007. Enzymatic characteristics of an aldo-keto reductase family protein (AKR1C15) and its localization in rat tissues. Arch Biochem Biophys 465:136-47.

451. Endo S, Morikawa Y, Matsunaga T, Hara A, Nishinaka T. 2022. Porcine aldo-keto reductase 1 C subfamily members AKR1C1 and AKR1C4: Substrate specificity, inhibitor sensitivity and activators. J Steroid Biochem Mol Biol doi:10.1016/j.jsbmb.2022.106113:106113.

452. Akita H, Watanabe M, Suzuki T, Nakashima N, Hoshino T. 2015. Molecular cloning and characterization of two *YGL039w* genes encoding broad specificity NADPH-dependent aldehyde reductases from *Kluyveromyces marxianus* strain DMB1. FEMS Microbiol Lett 362.

453. Akita H, Watanabe M, Suzuki T, Nakashima N, Hoshino T. 2015. Characterization of the *Kluyveromyces marxianus* strain DMB1 *YGL157w* gene product as a broad specificity NADPH-dependent aldehyde reductase. AMB Express 5:17.

454. Roberts AJ, Dunne J, Scullion P, Norval S, Fairlamb AH. 2018. A role for trypanosomatid aldo-keto reductases in methylglyoxal, prostaglandin and isoprostane metabolism. Biochem J 475:2593-2610.

455. Brophy PM, Crowley P, Barrett J. 1990. A novel NADPH/NADH-dependent aldehyde reduction enzyme isolated from the tapeworm *Moniezia expansa*. FEBS Lett 263:305-7.

456. Kavanagh KL, Jornvall H, Persson B, Oppermann U. 2008. Medium- and short-chain dehydrogenase/reductase gene and protein families : the SDR superfamily: functional and structural diversity within a family of metabolic and regulatory enzymes. Cell Mol Life Sci 65:3895-906.

457. Ting SM, Miller ON, Sellinger OZ. 1965. The Metabolism of Lactaldehyde. Vii. The Oxidation of D-Lactaldehyde in Rat Liver. Biochim Biophys Acta 97:407-15.

458. Ray M, Ray S. 1984. Purification and partial characterization of a methylglyoxal reductase from goat liver. Biochim Biophys Acta 802:119-27.

459. Shivani, Grewal SK, Gill RK, Virk HK, Bhardwaj RD. 2022. Methylglyoxal detoxification pathway - Explored first time for imazethapyr tolerance in lentil (*Lens culinaris L.*). Plant Physiology and Biochemistry 177:10-22.

460. Smits MM, Johnson MA. 1981. Methylglyoxal: Enzyme distributions relative to its presence in Douglas-fir needles and absence in Douglas-fir needle callus. Archives of Biochemistry and Biophysics 208:431-439.

461. Murata K, Fukuda Y, Simosaka M, Watanabe K, Saikusa T, Kimura A. 1985. Metabolism of 2-oxoaldehyde in yeasts. Purification and characterization of

NADPH-dependent methylglyoxal-reducing enzyme from *Saccharomyces cerevisiae*. Eur J Biochem 151:631-6.

462. Inoue Y, Rhee H, Watanabe K, Murata K, Kimura A. 1988. Metabolism of 2-oxoaldehyde in mold. Purification and characterization of two methylglyoxal reductases from *Aspergillus niger*. Eur J Biochem 171:213-8.

463. Lee HM, Seo JH, Kwak MK, Kang SO. 2017. Methylglyoxal upregulates *Dictyostelium discoideum* slug migration by triggering glutathione reductase and methylglyoxal reductase activity. Int J Biochem Cell Biol 90:81-92.

464. Ghoshal K, Banerjee AB, Ray S. 1989. Methylglyoxal-catabolizing enzymes of *Leishmania donovani* promastigotes. Molecular and Biochemical Parasitology 35:21-29.

465. Greig N, Wyllie S, Patterson S, Fairlamb AH. 2009. A comparative study of methylglyoxal metabolism in trypanosomatids. FEBS Journal 276:376-386.

466. Liu S, Skory C, Qureshi N. 2020. Ethanol tolerance assessment in recombinant *E. coli* of ethanol responsive genes from *Lactobacillus buchneri* NRRL B-30929. World Journal of Microbiology and Biotechnology 36.

467. Chen J, Yang S, Liang S, Lu F, Long K, Zhang X. 2020. *In vitro* synergistic effects of three enzymes from *Bacillus subtilis* CH-1 on keratin decomposition. 3 Biotech 10.

468. Vogel-Scheel J, Alpert C, Engst W, Loh G, Blaut M. 2010. Requirement of Purine and Pyrimidine Synthesis for Colonization of the Mouse Intestine by *Escherichia coli*. Applied and Environmental Microbiology 76:5181-5187.

469. Miller DV, Ruhlin M, Ray WK, Xu H, White RH. 2017. N^5,N^{10}-methylenetetrahydromethanopterin reductase from *Methanocaldococcus jannaschii* also serves as a methylglyoxal reductase. FEBS Letters 591:2269-2278.

470. Misra K, Banerjee AB, Ray S, Ray M. 1996. Reduction of methylglyoxal in *Escherichia coli* K12 by an aldehyde reductase and alcohol dehydrogenase. Mol Cell Biochem 156:117-24.

471. Yang CF, Brush EJ. 1993. A spectrophotometric assay for alpha-ketoaldehydes using horse liver alcohol dehydrogenase. Anal Biochem 214:124-7.

472. van der Oost J, Voorhorst WG, Kengen SW, Geerling AC, Wittenhorst V, Gueguen Y, de Vos WM. 2001. Genetic and biochemical characterization of a short-chain alcohol dehydrogenase from the hyperthermophilic archaeon *Pyrococcus furiosus*. Eur J Biochem 268:3062-8.

473. Elleuche S, Klippel B, von der Heyde A, Antranikian G. 2013. Comparative analysis of two members of the metal ion-containing group III-alcohol dehydrogenases from *Dickeya zeae*. Biotechnol Lett 35:725-33.

474. Kwak MK, Ku M, Kang SO. 2014. NAD(+)-linked alcohol dehydrogenase 1 regulates methylglyoxal concentration in *Candida albicans*. FEBS Lett 588:1144-53.

475. Monder C. 1967. Alpha-keto aldehyde dehydrogenase, an enzyme that catalyzes the enzymic oxidation of methylglyoxal to pyruvate. J Biol Chem 242:4603-9.

476. Ray S, Ray M. 1982. Purification and characterization of NAD and NADP-linked alpha-ketoaldehyde dehydrogenases involved in catalyzing the oxidation of methylglyoxal to pyruvate. J Biol Chem 257:10566-70.

477. Vander Jagt DL, Davison LM. 1977. Purification and characterization of 2-oxoaldehyde dehydrogenase from rat liver. Biochim Biophys Acta 484:260-7.

478. Rhee H-i, Watanabe K, Murata K, Kimura A. 1987. Metabolism of 2-Ketoaldehydes in Bacteria: Oxidative Conversion of Methylglyoxal to Pyruvate by an Enzyme from *Pseudomonas putida*. Agricultural and Biological Chemistry 51:1059-1066.

479. Schalkwijk CG, Stehouwer CDA. 2020. Methylglyoxal, a Highly Reactive Dicarbonyl Compound, in Diabetes, Its Vascular Complications, and Other Age-Related Diseases. Physiol Rev 100:407-461.

480. Kalapos MP. 2013. Where does plasma methylglyoxal originate from? Diabetes Research and Clinical Practice 99:260-271.

481. Wang XJ, Zhang HX, Li H, Zhu AH, Gao WY. 2019. Measurement of alpha-dicarbonyl compounds in human saliva by pre-column derivatization HPLC. Clin Chem Lab Med 57:1915-1922.

482. Piuri G, Basello K, Rossi G, Soldavini CM, Duiella S, Privitera G, Spadafranca A, Costanzi A, Tognon E, Cappelletti M, Corsetto PA, Rizzo AM, Speciani AF, Ferrazzi E. 2020. Methylglyoxal, Glycated Albumin, PAF, and TNF-alpha: Possible Inflammatory and Metabolic Biomarkers for Management of Gestational Diabetes. Nutrients 12.

483. Lyles GA. 1996. Mammalian plasma and tissue-bound semicarbazide-sensitive amine oxidases: biochemical, pharmacological and toxicological aspects. Int J Biochem Cell Biol 28:259-74.

484. Beisswenger PJ, Howell SK, O'Dell RM, Wood ME, Touchette AD, Szwergold BS. 2001. alpha-Dicarbonyls increase in the postprandial period and reflect the degree of hyperglycemia. Diabetes Care 24:726-32.

485. Nemet I, Turk Z, Duvnjak L, Car N, Varga-Defterdarovic L. 2005. Humoral methylglyoxal level reflects glycemic fluctuation. Clin Biochem 38:379-83.

486. Boomsma F, Derkx FHM, Vandenmeiracker AH, Manintveld AJ, Schalekamp MADH. 1995. Plasma Semicarbazide-Sensitive Amine Oxidase Activity Is Elevated in Diabetes-Mellitus and Correlates with Glycosylated Hemoglobin. Clinical Science 88:675-679.

487. Boomsma F, van den Meiracker AH, Winkel S, Aanstoot HJ, Batstra MR, in't Veld AJM, Bruining GJ. 1999. Circulating semicarbazide-sensitive amine oxidase is raised both in Type I (insulin-dependent), in Type II (non-insulin-dependent) diabetes mellitus and even in childhood Type I diabetes at first clinical diagnosis. Diabetologia 42:233-237.

488. Dhar A, Desai K, Kazachmov M, Yu P, Wu L. 2008. Methylglyoxal production in vascular smooth muscle cells from different metabolic precursors. Metabolism 57:1211-20.

489. Beisswenger PJ, Howell SK, Russell GB, Miller ME, Rich SS, Mauer M. 2013. Early progression of diabetic nephropathy correlates with methylglyoxal-derived advanced glycation end products. Diabetes Care 36:3234-9.

490. Hanssen NMJ, Scheijen J, Jorsal A, Parving HH, Tarnow L, Rossing P, Stehouwer CDA, Schalkwijk CG. 2017. Higher Plasma Methylglyoxal Levels Are Associated

With Incident Cardiovascular Disease in Individuals With Type 1 Diabetes: A 12-Year Follow-up Study. Diabetes 66:2278-2283.

491. Hanssen NMJ, Westerink J, Scheijen J, van der Graaf Y, Stehouwer CDA, Schalkwijk CG, Group SS. 2018. Higher Plasma Methylglyoxal Levels Are Associated With Incident Cardiovascular Disease and Mortality in Individuals With Type 2 Diabetes. Diabetes Care 41:1689-1695.

492. Hanssen NMJ, Teraa M, Scheijen JLJM, Van de Waarenburg M, Gremmels H, Stehouwer CDA, Verhaar MC, Schalkwijk CG. 2021. Plasma Methylglyoxal Levels Are Associated With Amputations and Mortality in Severe Limb Ischemia Patients With and Without Diabetes. Diabetes Care 44:157-163.

493. Kuntz S, Kunz C, Rudloff S. 2010. Carbonyl compounds methylglyoxal and glyoxal affect interleukin-8 secretion in intestinal cells by superoxide anion generation and activation of MAPK p38. Mol Nutr Food Res 54:1458-67.

494. Bezold V, Rosenstock P, Scheffler J, Geyer H, Horstkorte R, Bork K. 2019. Glycation of macrophages induces expression of pro-inflammatory cytokines and reduces phagocytic efficiency. Aging (Albany NY) 11:5258-5275.

495. Guerra BA, Bolin AP, Otton R. 2012. Carbonyl stress and a combination of astaxanthin/vitamin C induce biochemical changes in human neutrophils. Toxicol In Vitro 26:1181-90.

496. Chu JM, Lee DK, Wong DP, Wong GT, Yue KK. 2016. Methylglyoxal-induced neuroinflammatory response in in vitro astrocytic cultures and hippocampus of experimental animals. Metab Brain Dis 31:1055-64.

497. Medeiros ML, Oliveira AL, de Oliveira MG, Monica FZ, Antunes E. 2021. Methylglyoxal Exacerbates Lipopolysaccharide-Induced Acute Lung Injury via RAGE-Induced ROS Generation: Protective Effects of Metformin. J Inflamm Res 14:6477-6489.

498. Ward RA, McLeish KR. 2004. Methylglyoxal: a stimulus to neutrophil oxygen radical production in chronic renal failure? Nephrol Dial Transplant 19:1702-7.

499. Yamawaki H, Saito K, Okada M, Hara Y. 2008. Methylglyoxal mediates vascular inflammation via JNK and p38 in human endothelial cells. Am J Physiol Cell Physiol 295:C1510-7.

500. Lin CC, Chan CM, Huang YP, Hsu SH, Huang CL, Tsai SJ. 2016. Methylglyoxal activates NF-kappaB nuclear translocation and induces *COX-2* expression via a p38-dependent pathway in synovial cells. Life Sci 149:25-33.

501. Rehman S, Alouffi S, Faisal M, Qahtan AA, Alatar AA, Ahmad S. 2021. Methylglyoxal mediated glycation leads to neo-epitopes generation in fibrinogen: Role in the induction of adaptive immune response. Int J Biol Macromol 175:535-543.

502. Perween S, Abidi M, Faiz Faizy A, Moinuddin. 2022. Biophysical changes in methylglyoxal modified fibrinogen and its role in the immunopathology of type 2 diabetes mellitus. Int J Biol Macromol 202:199-214.

503. Abidi M, Mir AR, Khan F, Ali A, Uddin M. 2020. Glycoxidation of LDL Generates Cytotoxic Adducts and Elicits Humoral Response in Type 2 Diabetes Mellitus. Glycobiology doi:10.1093/glycob/cwaa077.

504. Khan MY, Alouffi S, Khan MS, Husain FM, Akhter F, Ahmad S. 2020. The neoepitopes on methylglyoxal (MG) glycated LDL create autoimmune response; autoimmunity detection in T2DM patients with varying disease duration. Cellular Immunology 351.

505. Jyoti, Mir AR, Habib S, Siddiqui SS, Ali A, Moinuddin. 2016. Neo-epitopes on methylglyoxal modified human serum albumin lead to aggressive autoimmune response in diabetes. Int J Biol Macromol 86:799-809.

506. Fan X, Subramaniam R, Weiss MF, Monnier VM. 2003. Methylglyoxal–bovine serum albumin stimulates tumor necrosis factor alpha secretion in RAW 264.7 cells through activation of mitogen-activating protein kinase, nuclear factor κB and intracellular reactive oxygen species formation. Archives of Biochemistry and Biophysics 409:274-286.

507. Watanabe M, Toyomura T, Tomiyama M, Wake H, Liu KY, Teshigawara K, Takahashi H, Nishibori M, Mori S. 2020. Advanced glycation end products (AGEs) synergistically potentiated the proinflammatory action of lipopolysaccharide (LPS) and high mobility group box-1 (HMGB1) through their direct interactions. Molecular Biology Reports 47:7153-7159.

508. Ishibashi Y, Matsui T, Nakamura N, Sotokawauchi A, Higashimoto Y, Yamagishi SI. 2017. Methylglyoxal-derived hydroimidazolone-1 evokes inflammatory reactions in endothelial cells via an interaction with receptor for advanced glycation end products. Diab Vasc Dis Res 14:450-453.

509. Lee HW, Gu MJ, Lee JY, Lee S, Kim Y, Ha SK. 2021. Methylglyoxal-Lysine Dimer, an Advanced Glycation End Product, Induces Inflammation via Interaction with RAGE in Mesangial Cells. Mol Nutr Food Res 65:e2000799.

510. Jeong S-R, Lee K-W. 2021. Methylglyoxal-Derived Advanced Glycation End Product (AGE4)-Induced Apoptosis Leads to Mitochondrial Dysfunction and Endoplasmic Reticulum Stress through the RAGE/JNK Pathway in Kidney Cells. International Journal of Molecular Sciences 22.

511. Khalid M, Petroianu G, Adem A. 2022. Advanced Glycation End Products and Diabetes Mellitus: Mechanisms and Perspectives. Biomolecules 12.

512. Jiang M, Yakupu A, Guan H, Dong J, Liu Y, Song F, Tang J, Tian M, Niu Y, Lu S. 2022. Pyridoxamine ameliorates methylglyoxal-induced macrophage dysfunction to facilitate tissue repair in diabetic wounds. Int Wound J 19:52-63.

513. Haucke E, Navarrete-Santos A, Simm A, Silber RE, Hofmann B. 2014. Glycation of extracellular matrix proteins impairs migration of immune cells. Wound Repair Regen 22:239-45.

514. Dhananjayan K, Gunawardena D, Hearn N, Sonntag T, Moran C, Gyengesi E, Srikanth V, Munch G. 2017. Activation of Macrophages and Microglia by Interferon-gamma and Lipopolysaccharide Increases Methylglyoxal Production: A New Mechanism in the Development of Vascular Complications and Cognitive Decline in Type 2 Diabetes Mellitus? J Alzheimers Dis 59:467-479.

515. Prantner D, Nallar S, Richard K, Spiegel D, Collins KD, Vogel SN. 2021. Classically activated mouse macrophages produce methylglyoxal that induces a

TLR4-and RAGE-independent proinflammatory response. Journal of Leukocyte Biology 109:605-619.

516. Rachman H, Kim N, Ulrichs T, Baumann S, Pradl L, Nasser Eddine A, Bild M, Rother M, Kuban RJ, Lee JS, Hurwitz R, Brinkmann V, Kosmiadi GA, Kaufmann SH. 2006. Critical role of methylglyoxal and AGE in mycobacteria-induced macrophage apoptosis and activation. PLoS One 1:e29.

517. Hazen SL, d'Avignon A, Anderson MM, Hsu FF, Heinecke JW. 1998. Human Neutrophils Employ the Myeloperoxidase-Hydrogen Peroxide-Chloride System to Oxidize α-Amino Acids to a Family of Reactive Aldehydes. Journal of Biological Chemistry 273:4997-5005.

518. Hazen SL, Hsu FF, d'Avignon A, Heinecke JW. 1998. Human Neutrophils Employ Myeloperoxidase To Convert α-Amino Acids to a Battery of Reactive Aldehydes: A Pathway for Aldehyde Generation at Sites of Inflammation. Biochemistry 37:6864-6873.

519. Anderson MM, Hazen SL, Hsu FF, Heinecke JW. 1997. Human neutrophils employ the myeloperoxidase-hydrogen peroxide-chloride system to convert hydroxy-amino acids into glycolaldehyde, 2-hydroxypropanal, and acrolein. A mechanism for the generation of highly reactive alpha-hydroxy and alpha,beta-unsaturated aldehydes by phagocytes at sites of inflammation. Journal of Clinical Investigation 99:424-432.

520. Anderson MM, Requena JR, Crowley JR, Thorpe SR, Heinecke JW. 1999. The myeloperoxidase system of human phagocytes generates Nε-(carboxymethyl)lysine on proteins: a mechanism for producing advanced glycation

end products at sites of inflammation. Journal of Clinical Investigation 104:103-113.

521. Hazen SL, Hsu FF, Heinecke JW. 1996. p-hydroxyphenylacetaldehyde is the major product of L-tyrosine oxidation by activated human phagocytes - A chloride-dependent mechanism for the conversion of free amino acids into reactive aldehydes by myeloperoxidase. Journal of Biological Chemistry 271:1861-1867.

522. Zhang MM, Ong CL, Walker MJ, McEwan AG. 2016. Defence against methylglyoxal in Group A *Streptococcus*: a role for Glyoxylase I in bacterial virulence and survival in neutrophils? Pathog Dis 74.

523. Maeta K, Izawa S, Inoue Y. 2005. Methylglyoxal, a metabolite derived from glycolysis, functions as a signal initiator of the high osmolarity glycerol-mitogen-activated protein kinase cascade and calcineurin/Crz1-mediated pathway in *Saccharomyces cerevisiae*. J Biol Chem 280:253-60.

524. Aguilera J, Rodriguez-Vargas S, Prieto JA. 2005. The HOG MAP kinase pathway is required for the induction of methylglyoxal-responsive genes and determines methylglyoxal resistance in *Saccharomyces cerevisiae*. Mol Microbiol 56:228-39.

525. Nomura W, Inoue Y. 2015. Methylglyoxal activates the target of rapamycin complex 2-protein kinase C signaling pathway in *Saccharomyces cerevisiae*. Mol Cell Biol 35:1269-80.

526. Nomura W, Maeta K, Inoue Y. 2017. Phosphatidylinositol 3,5-bisphosphate is involved in methylglyoxal-induced activation of the Mpk1 mitogen-activated protein kinase cascade in *Saccharomyces cerevisiae*. J Biol Chem 292:15039-15048.

527. Nomura W, Maeta K, Kita K, Izawa S, Inoue Y. 2008. Role of Gcn4 for adaptation to methylglyoxal in *Saccharomyces cerevisiae*: methylglyoxal attenuates protein synthesis through phosphorylation of eIF2alpha. Biochem Biophys Res Commun 376:738-42.

528. Nomura W, Maeta K, Kita K, Izawa S, Inoue Y. 2010. Methylglyoxal activates Gcn2 to phosphorylate eIF2alpha independently of the TOR pathway in *Saccharomyces cerevisiae*. Appl Microbiol Biotechnol 86:1887-94.

529. Maeta K, Izawa S, Okazaki S, Kuge S, Inoue Y. 2004. Activity of the Yap1 transcription factor in *Saccharomyces cerevisiae* is modulated by methylglyoxal, a metabolite derived from glycolysis. Mol Cell Biol 24:8753-64.

530. Aguilera J, Prieto JA. 2004. Yeast cells display a regulatory mechanism in response to methylglyoxal. FEMS Yeast Res 4:633-41.

531. Inoue Y, Tsujimoto Y, Kimura A. 1998. Expression of the glyoxalase I gene of *Saccharomyces cerevisiae* is regulated by high osmolarity glycerol mitogen-activated protein kinase pathway in osmotic stress response. J Biol Chem 273:2977-83.

532. Rep M, Albertyn J, Thevelein JM, Prior BA, Hohmann S. 1999. Different signalling pathways contribute to the control of *GPD1* gene expression by osmotic stress in *Saccharomyces cerevisiae*. Microbiology 145:715-727.

533. Albertyn J, Hohmann S, Thevelein JM, Prior BA. 1994. *GPD1*, which encodes glycerol-3-phosphate dehydrogenase, is essential for growth under osmotic stress in *Saccharomyces cerevisiae*, and its expression is regulated by the high-osmolarity glycerol response pathway. Molecular and Cellular Biology 14:4135-4144.

534. Roelants FM, Leskoske KL, Martinez Marshall MN, Locke MN, Thorner J. 2017. The TORC2-Dependent Signaling Network in the Yeast *Saccharomyces cerevisiae*. Biomolecules 7.

535. Semchyshyn H. 2020. Reactive Carbonyls Induce TOR- and Carbohydrate-Dependent Hormetic Response in Yeast. The Scientific World Journal 2020:1-6.

536. da Silva SM, Batista-Nascimento L, Gaspar-Cordeiro A, Vernis L, Pimentel C, Rodrigues-Pousada C. 2018. Transcriptional regulation of FeS biogenesis genes: A possible shield against arsenate toxicity activated by Yap1. Biochim Biophys Acta Gen Subj 1862:2152-2161.

537. Wiatrowski HA, Carlson M. 2003. Yap1 accumulates in the nucleus in response to carbon stress in *Saccharomyces cerevisiae*. Eukaryot Cell 2:19-26.

538. Molin M, Renault JP, Lagniel G, Pin S, Toledano M, Labarre J. 2007. Ionizing radiation induces a Yap1-dependent peroxide stress response in yeast. Free Radic Biol Med 43:136-44.

539. Lushchak OV, Inoue Y, Lushchak VI. 2010. Regulatory protein Yap1 is involved in response of yeast *Saccharomyces cerevisiae* to nitrosative stress. Biochemistry (Mosc) 75:629-64.

540. Nguyen TT, Iwaki A, Ohya Y, Izawa S. 2014. Vanillin causes the activation of Yap1 and mitochondrial fragmentation in *Saccharomyces cerevisiae*. J Biosci Bioeng 117:33-8.

541. Kim D, Hahn JS. 2013. Roles of the Yap1 transcription factor and antioxidants in *Saccharomyces cerevisiae*'s tolerance to furfural and 5-hydroxymethylfurfural,

which function as thiol-reactive electrophiles generating oxidative stress. Appl Environ Microbiol 79:5069-77.

542. Turton HE, Dawes IW, Grant CM. 1997. Saccharomyces cerevisiae exhibits a yAP-1-mediated adaptive response to malondialdehyde. J Bacteriol 179:1096-101.

543. Mata J, Anda S, Zach R, Grallert B. 2017. Activation of Gcn2 in response to different stresses. Plos One 12.

544. Yoshida A, Wei D, Nomura W, Izawa S, Inoue Y. 2012. Reduction of Glucose Uptake through Inhibition of Hexose Transporters and Enhancement of Their Endocytosis by Methylglyoxal in Saccharomyces cerevisiae. Journal of Biological Chemistry 287:701-711.

545. Roy A, Hashmi S, Li Z, Dement AD, Hong Cho K, Kim J-H, Tansey WP. 2016. The glucose metabolite methylglyoxal inhibits expression of the glucose transporter genes by inactivating the cell surface glucose sensors Rgt2 and Snf3 in yeast. Molecular Biology of the Cell 27:862-871.

546. Zuin A, Vivancos AP, Sansó M, Takatsume Y, Ayté J, Inoue Y, Hidalgo E. 2005. The Glycolytic Metabolite Methylglyoxal Activates Pap1 and Sty1 Stress Responses in *Schizosaccharomyces pombe*. Journal of Biological Chemistry 280:36708-36713.

547. Takatsume Y, Izawa S, Inoue Y. 2006. Methylglyoxal as a Signal Initiator for Activation of the Stress-activated Protein Kinase Cascade in the Fission Yeast *Schizosaccharomyces pombe*. Journal of Biological Chemistry 281:9086-9092.

548. Takatsume Y, Izawa S, Inoue Y. 2007. Modulation of Spc1 stress-activated protein kinase activity by methylglyoxal through inhibition of protein phosphatase in the

fission yeast *Schizosaccharomyces pombe*. Biochemical and Biophysical Research Communications 363:942-947.

549. Hong F-y, Bao J-f, Hao J, Yu Q, Liu J. 2015. Methylglyoxal and Advanced Glycation End-Products Promote Cytokines Expression in Peritoneal Mesothelial Cells Via MAPK Signaling. The American Journal of the Medical Sciences 349:105-109.

550. Matsumoto T, Katome T, Kojima M, Takayanagi K, Taguchi K, Kobayashi T. 2021. Methylglyoxal augments uridine diphosphate-induced contraction via activation of p38 mitogen-activated protein kinase in rat carotid artery. European Journal of Pharmacology 904.

551. Lee KM, Lee CY, Zhang G, Lyu A, Yue KKM. 2019. The dataset of methylglyoxal activating p38 and p44/42 pathway in osteoclast. Data in Brief 26.

552. Lee JH, Parveen A, Do MH, Kang MC, Yumnam S, Kim SY. 2020. Molecular mechanisms of methylglyoxal-induced aortic endothelial dysfunction in human vascular endothelial cells. Cell Death & Disease 11.

553. Wang Y, Hall LM, Kujawa M, Li H, Zhang X, O'Meara M, Ichinose T, Wang J-M. 2019. Methylglyoxal triggers human aortic endothelial cell dysfunction via modulation of the KATP/MAPK pathway. American Journal of Physiology-Cell Physiology 317:C68-C81.

554. Ward RA, McLeish KR. 2004. Methylglyoxal: a stimulus to neutrophil oxygen radical production in chronic renal failure? Nephrology Dialysis Transplantation 19:1702-1707.

555. Fukunaga M, Miyata S, Liu BF, Miyazaki H, Hirota Y, Higo S, Hamada Y, Ueyama S, Kasuga M. 2004. Methylglyoxal induces apoptosis through activation of p38 MAPK in rat Schwann cells. Biochemical and Biophysical Research Communications 320:689-695.

556. Hua X, Chi W, Su L, Li J, Zhang Z, Yuan X. 2017. ROS-induced Oxidative Injury involved in Pathogenesis of Fungal Keratitis via p38 MAPK Activation. Sci Rep 7:10421.

557. Kwak S, Choi YS, Na HG, Bae CH, Song S-Y, Kim Y-D. 2020. Glyoxal and Methylglyoxal as E-cigarette Vapor Ingredients-Induced Pro-Inflammatory Cytokine and Mucins Expression in Human Nasal Epithelial Cells. American Journal of Rhinology & Allergy 35:213-220.

558. Liu B-F, Miyata S, Hirota Y, Higo S, Miyazaki H, Fukunaga M, Hamada Y, Ueyama S, Muramoto O, Uriuhara A, Kasuga M. 2003. Methylglyoxal induces apoptosis through activation of p38 mitogen-activated protein kinase in rat mesangial cells. Kidney International 63:947-957.

559. Pal A, Bhattacharya I, Bhattacharya K, Mandal C, Ray M. 2009. Methylglyoxal induced activation of murine peritoneal macrophages and surface markers of T lymphocytes in Sarcoma-180 bearing mice: Involvement of MAP kinase, NF-κβ signal transduction pathway. Molecular Immunology 46:2039-2044.

560. Fukunaga M, Miyata S, Higo S, Hamada Y, Ueyama S, Kasuga M. 2005. Methylglyoxal Induces Apoptosis through Oxidative Stress-Mediated Activation of p38 Mitogen-Activated Protein Kinase in Rat Schwann Cells. Annals of the New York Academy of Sciences 1043:151-157.

561. Bo J, Xie S, Guo Y, Zhang C, Guan Y, Li C, Lu J, Meng QH. 2016. Methylglyoxal Impairs Insulin Secretion of Pancreaticβ-Cells through Increased Production of ROS and Mitochondrial Dysfunction Mediated by Upregulation of *UCP2* and MAPKs. Journal of Diabetes Research 2016:1-14.

562. Chang Y-C, Hsieh M-C, Wu H-J, Wu W-C, Kao Y-H. 2015. Methylglyoxal, a reactive glucose metabolite, enhances autophagy flux and suppresses proliferation of human retinal pigment epithelial ARPE-19 cells. Toxicology in Vitro 29:1358-1368.

563. Akhand A. 2001. Glyoxal and methylglyoxal trigger distinct signals for map family kinases and caspase activation in human endothelial cells. Free Radical Biology and Medicine 31:20-30.

564. Jan C-R, Chen C-H, Wang S-C, Kuo S-Y. 2005. Effect of methylglyoxal on intracellular calcium levels and viability in renal tubular cells. Cellular Signalling 17:847-855.

565. Sachdeva R, Fleming T, Schumacher D, Homberg S, Stilz K, Mohr F, Wagner AH, Tsvilovskyy V, Mathar I, Freichel M. 2019. Methylglyoxal evokes acute Ca2+ transients in distinct cell types and increases agonist-evoked Ca2+ entry in endothelial cells via CRAC channels. Cell Calcium 78:66-75.

566. Gupta S, Hadas K, Randriamboavonjy V, Elgheznawy A, Mann A, Fleming I. 2013. Methylglyoxal Induces Platelet Hyperaggregation and Reduces Thrombus Stability by Activating PKC and Inhibiting PI3K/Akt Pathway. PLoS ONE 8.

567. Hoque TS, Uraji M, Ye W, Hossain MA, Nakamura Y, Murata Y. 2012. Methylglyoxal-induced stomatal closure accompanied by peroxidase-mediated ROS production in *Arabidopsis*. Journal of Plant Physiology 169:979-986.

568. Li Z-G. 2020. Regulative role of calcium signaling on methylglyoxal-improved heat tolerance in maize (*Zea mays L*) seedlings. Plant Signaling & Behavior 15.

569. Eid BG, Abu-Sharib AT, El-Bassossy HM, Balamash K, Smirnov SV. 2018. Enhanced calcium entry via activation of NOX/PKC underlies increased vasoconstriction induced by methylglyoxal. Biochemical and Biophysical Research Communications 506:1013-1018.

570. Vasdev S, Stuckless J. 2011. Role of methylglyoxal in essential hypertension. International Journal of Angiology 19:e58-e65.

571. Gallyas F, Jia X, Chang T, Wilson TW, Wu L. 2012. Methylglyoxal Mediates Adipocyte Proliferation by Increasing Phosphorylation of Akt1. PLoS ONE 7.

572. Kim D, Kim K-A, Kim J-H, Kim E-H, Bae O-N. 2020. Methylglyoxal-Induced Dysfunction in Brain Endothelial Cells via the Suppression of Akt/HIF-1α Pathway and Activation of Mitophagy Associated with Increased Reactive Oxygen Species. Antioxidants 9.

573. Bellier J, Nokin M-J, Caprasse M, Tiamiou A, Blomme A, Scheijen JL, Koopmansch B, MacKay GM, Chiavarina B, Costanza B, Rademaker G, Durieux F, Agirman F, Maloujahmoum N, Cusumano PG, Lovinfosse P, Leung HY, Lambert F, Bours V, Schalkwijk CG, Hustinx R, Peulen O, Castronovo V, Bellahcène A. 2020. Methylglyoxal Scavengers Resensitize KRAS-Mutated Colorectal Tumors to Cetuximab. Cell Reports 30:1400-1416.e6.

574. Shin M-G, Lee J-W, Han J-S, Lee B, Jeong J-H, Park S-H, Kim J-H, Jang S, Park M, Kim S-Y, Kim S, Yang YR, Kim J-Y, Hoe K-L, Park C, Lee K-P, Kwon K-S, Kwon E-S. 2020. Bacteria-derived metabolite, methylglyoxal, modulates the longevity of *C. elegans* through TORC2/SGK-1/DAF-16 signaling. Proceedings of the National Academy of Sciences 117:17142-17150.

575. Ng S-P, Nomura W, Takahashi H, Inoue K, Kawada T, Goto T. 2021. Methylglyoxal attenuates isoproterenol-induced increase in uncoupling protein 1 expression through activation of JNK signaling pathway in beige adipocytes. Biochemistry and Biophysics Reports 28.

576. Nokin M-J, Bellier J, Durieux F, Peulen O, Rademaker G, Gabriel M, Monseur C, Charloteaux B, Verbeke L, van Laere S, Roncarati P, Herfs M, Lambert C, Scheijen J, Schalkwijk C, Colige A, Caers J, Delvenne P, Turtoi A, Castronovo V, Bellahcène A. 2019. Methylglyoxal, a glycolysis metabolite, triggers metastasis through MEK/ERK/SMAD1 pathway activation in breast cancer. Breast Cancer Research 21.

577. Bollong MJ, Lee G, Coukos JS, Yun H, Zambaldo C, Chang JW, Chin EN, Ahmad I, Chatterjee AK, Lairson LL, Schultz PG, Moellering RE. 2018. A metabolite-derived protein modification integrates glycolysis with KEAP1–NRF2 signalling. Nature 562:600-604.

578. Nishimoto S, Koike S, Inoue N, Suzuki T, Ogasawara Y. 2017. Activation of Nrf2 attenuates carbonyl stress induced by methylglyoxal in human neuroblastoma cells: Increase in GSH levels is a critical event for the detoxification mechanism. Biochemical and Biophysical Research Communications 483:874-879.

579. Dafre AL, Goldberg J, Wang T, Spiegel DA, Maher P. 2015. Methylglyoxal, the foe and friend of glyoxalase and Trx/TrxR systems in HT22 nerve cells. Free Radical Biology and Medicine 89:8-19.

580. Koike S, Nishimoto S, Ogasawara Y. 2017. Cysteine persulfides and polysulfides produced by exchange reactions with H2S protect SH-SY5Y cells from methylglyoxal-induced toxicity through Nrf2 activation. Redox Biology 12:530-539.

581. Cheng A-S, Cheng Y-H, Chiou C-H, Chang T-L. 2012. Resveratrol Upregulates Nrf2 Expression To Attenuate Methylglyoxal-Induced Insulin Resistance in Hep G2 Cells. Journal of Agricultural and Food Chemistry 60:9180-9187.

582. Lee B-H, Hsu W-H, Chang Y-Y, Kuo H-F, Hsu Y-W, Pan T-M. 2012. Ankaflavin: a natural novel PPARγ agonist upregulates Nrf2 to attenuate methylglyoxal-induced diabetes *in vivo*. Free Radical Biology and Medicine 53:2008-2016.

583. Hsu W-H, Lee B-H, Chang Y-Y, Hsu Y-W, Pan T-M. 2013. A novel natural Nrf2 activator with PPARγ-agonist (monascin) attenuates the toxicity of methylglyoxal and hyperglycemia. Toxicology and Applied Pharmacology 272:842-851.

584. Ozyamak E, Almeida C, Moura APS, Miller S, Booth IR. 2013. Integrated stress response of *Escherichia coli* to methylglyoxal: transcriptional readthrough from the *nemRA* operon enhances protection through increased expression of glyoxalase I. Molecular Microbiology 88:936-950.

585. Lee C, Shin J, Park C. 2013. Novel regulatory system *nemRA-gloA* for electrophile reduction in *Escherichia coli* K-12. Molecular Microbiology 88:395-412.

586. Gray MJ, Wholey W-Y, Parker BW, Kim M, Jakob U. 2013. NemR Is a Bleach-sensing Transcription Factor. Journal of Biological Chemistry 288:13789-13798.

587. Ray A, Edmonds KA, Palmer LD, Skaar EP, Giedroc DP. 2020. *Staphylococcus aureus* Glucose-Induced Biofilm Accessory Protein A (GbaA) Is a Monothiol-Dependent Electrophile Sensor. Biochemistry 59:2882-2895.

588. Juarez P, Jeannot K, Plésiat P, Llanes C. 2017. Toxic Electrophiles Induce Expression of the Multidrug Efflux Pump MexEF-OprN in *Pseudomonas aeruginosa* through a Novel Transcriptional Regulator, CmrA. Antimicrobial Agents and Chemotherapy 61.

589. Tang X, Bai Y, Duong A, Smith MT, Li L, Zhang L. 2009. Formaldehyde in China: production, consumption, exposure levels, and health effects. Environ Int 35:1210-24.

590. Boor PJ, Trent MB, Lyles GA, Tao M, Ansari GA. 1992. Methylamine metabolism to formaldehyde by vascular semicarbazide-sensitive amine oxidase. Toxicology 73:251-8.

591. Tong ZQ, Wang W, Luo WH, Lv JH, Li H, Luo HJ, Jia JP, He R. 2017. Urine Formaldehyde Predicts Cognitive Impairment in Post-Stroke Dementia and Alzheimer's Disease. Journal of Alzheimers Disease 55:1031-1038.

592. Tan T, Zhang Y, Luo WH, Lv JH, Han CS, Hamlin JNR, Luo HJ, Li H, Wan Y, Yang X, Song WH, Tong ZQ. 2018. Formaldehyde induces diabetes-associated cognitive impairments. Faseb Journal 32:3669-3679.

593. Yasokawa D, Murata S, Iwahashi Y, Kitagawa E, Nakagawa R, Hashido T, Iwahashi H. 2010. Toxicity of Methanol and Formaldehyde Towards

Saccharomyces cerevisiae as Assessed by DNA Microarray Analysis. Applied Biochemistry and Biotechnology 160:1685-1698.

594. Korsten MA, Matsuzaki S, Feinman L, Lieber CS. 1975. High blood acetaldehyde levels after ethanol administration. Difference between alcoholic and nonalcoholic subjects. N Engl J Med 292:386-9.

595. Wong MK, Scott BK, Peterson CM. 1992. Breath acetaldehyde following ethanol consumption. Alcohol 9:189-92.

596. Lachenmeier DW, Monakhova YB. 2011. Short-term salivary acetaldehyde increase due to direct exposure to alcoholic beverages as an additional cancer risk factor beyond ethanol metabolism. J Exp Clin Cancer Res 30:3.

597. Nuutinen H, Lindros KO, Salaspuro M. 1983. Determinants of blood acetaldehyde level during ethanol oxidation in chronic alcoholics. Alcohol Clin Exp Res 7:163-8.

598. Lachenmeier DW, Salaspuro M. 2017. *ALDH2*-deficiency as genetic epidemiologic and biochemical model for the carcinogenicity of acetaldehyde. Regul Toxicol Pharmacol 86:128-136.

599. Vakevainen S, Tillonen J, Agarwal DP, Srivastava N, Salaspuro M. 2000. High salivary acetaldehyde after a moderate dose of alcohol in *ALDH2*-deficient subjects: strong evidence for the local carcinogenic action of acetaldehyde. Alcohol Clin Exp Res 24:873-7.

600. Bae KY, Kim SW, Shin HY, Kim JM, Shin IS, Kim SJ, Kim JK, Yoon JS. 2012. The acute effects of ethanol and acetaldehyde on physiological responses after

ethanol ingestion in young healthy men with different *ALDH2* genotypes. Clin Toxicol (Phila) 50:242-9.

601. Yokoyama A, Kamada Y, Imazeki H, Hayashi E, Murata S, Kinoshita K, Yokoyama T, Kitagawa Y. 2016. Effects of *ADH1B* and *ALDH2* Genetic Polymorphisms on Alcohol Elimination Rates and Salivary Acetaldehyde Levels in Intoxicated Japanese Alcoholic Men. Alcohol Clin Exp Res 40:1241-50.

602. Tillonen J, Homann N, Rautio M, Jousimies-Somer H, Salaspuro M. 1999. Role of yeasts in the salivary acetaldehyde production from ethanol among risk groups for ethanol-associated oral cavity cancer. Alcohol Clin Exp Res 23:1409-15.

603. Salaspuro M. 1997. Microbial metabolism of ethanol and acetaldehyde and clinical consequences. Addict Biol 2:35-46.

604. Yokoi A, Ekuni D, Hata H, Yamane-Takeuchi M, Maruyama T, Yamanaka R, Morita M. 2019. Relationship between acetaldehyde concentration in mouth air and characteristics of microbiota of tongue dorsum in Japanese healthy adults: a cross-sectional study. J Appl Oral Sci 27:e20180635.

605. Visapaa JP, Tillonen J, Salaspuro M. 2002. Microbes and mucosa in the regulation of intracolonic acetaldehyde concentration during ethanol challenge. Alcohol Alcohol 37:322-6.

606. Homann N, Tillonen J, Rintamaki H, Salaspuro M, Lindqvist C, Meurman JH. 2001. Poor dental status increases acetaldehyde production from ethanol in saliva: a possible link to increased oral cancer risk among heavy drinkers. Oral Oncol 37:153-8.

607. Homann N, Tillonen J, Meurman JH, Rintamaki H, Lindqvist C, Rautio M, Jousimies-Somer H, Salaspuro M. 2000. Increased salivary acetaldehyde levels in heavy drinkers and smokers: a microbiological approach to oral cavity cancer. Carcinogenesis 21:663-8.

608. Vakevainen S, Tillonen J, Blom M, Jousimies-Somer H, Salaspuro M. 2001. Acetaldehyde production and other ADH-related characteristics of aerobic bacteria isolated from hypochlorhydric human stomach. Alcohol Clin Exp Res 25:421-6.

609. Vakevainen S, Mentula S, Nuutinen H, Salmela KS, Jousimies-Somer H, Farkkila M, Salaspuro M. 2002. Ethanol-derived microbial production of carcinogenic acetaldehyde in achlorhydric atrophic gastritis. Scand J Gastroenterol 37:648-55.

610. Jokelainen K, Roine RP, Vaananen H, Farkkila M, Salaspuro M. 1994. *In vitro* acetaldehyde formation by human colonic bacteria. Gut 35:1271-4.

611. Uittamo J, Siikala E, Kaihovaara P, Salaspuro M, Rautemaa R. 2009. Chronic candidosis and oral cancer in APECED-patients: production of carcinogenic acetaldehyde from glucose and ethanol by *Candida albicans*. Int J Cancer 124:754-6.

612. Nieminen MT, Uittamo J, Salaspuro M, Rautemaa R. 2009. Acetaldehyde production from ethanol and glucose by non-*Candida albicans* yeasts *in vitro*. Oral Oncol 45:e245-8.

613. Gainza-Cirauqui ML, Nieminen MT, Novak Frazer L, Aguirre-Urizar JM, Moragues MD, Rautemaa R. 2013. Production of carcinogenic acetaldehyde by *Candida albicans* from patients with potentially malignant oral mucosal disorders. J Oral Pathol Med 42:243-9.

614. Alnuaimi AD, Ramdzan AN, Wiesenfeld D, O'Brien-Simpson NM, Kolev SD, Reynolds EC, McCullough MJ. 2016. *Candida* virulence and ethanol-derived acetaldehyde production in oral cancer and non-cancer subjects. Oral Dis 22:805-814.

615. Marttila E, Bowyer P, Sanglard D, Uittamo J, Kaihovaara P, Salaspuro M, Richardson M, Rautemaa R. 2013. Fermentative 2-carbon metabolism produces carcinogenic levels of acetaldehyde in *Candida albicans*. Mol Oral Microbiol 28:281-91.

616. Alnuaimi AD, Wiesenfeld D, O'Brien-Simpson NM, Reynolds EC, McCullough MJ. 2015. Oral *Candida* colonization in oral cancer patients and its relationship with traditional risk factors of oral cancer: a matched case-control study. Oral Oncol 51:139-45.

617. Chauhan NM, Raut JS, Mohan Karuppayil S. 2011. Acetaldehyde inhibits the yeast-to-hypha conversion and biofilm formation in *Candida albicans*. Mycoscience 52:356-360.

618. Aranda A, del Olmo ML. 2004. Exposure of *Saccharomyces cerevisiae* to acetaldehyde induces sulfur amino acid metabolism and polyamine transporter genes, which depend on Met4p and Haa1p transcription factors, respectively. Appl Environ Microbiol 70:1913-22.

619. Aranda A, Querol A, del Olmo M. 2002. Correlation between acetaldehyde and ethanol resistance and expression of *HSP* genes in yeast strains isolated during the biological aging of sherry wines. Arch Microbiol 177:304-12.

620. Aranda A, del Olmo Ml M. 2003. Response to acetaldehyde stress in the yeast *Saccharomyces cerevisiae* involves a strain-dependent regulation of several *ALD* genes and is mediated by the general stress response pathway. Yeast 20:747-59.

621. Matsufuji Y, Fujimura S, Ito T, Nishizawa M, Miyaji T, Nakagawa J, Ohyama T, Tomizuka N, Nakagawa T. 2008. Acetaldehyde tolerance in *Saccharomyces cerevisiae* involves the pentose phosphate pathway and oleic acid biosynthesis. Yeast 25:825-33.

622. Matsufuji Y, Nakagawa T, Fujimura S, Tani A, Nakagawa J. 2010. Transcription factor Stb5p is essential for acetaldehyde tolerance in *Saccharomyces cerevisiae*. J Basic Microbiol 50:494-8.

623. Matsufuji Y, Yamamoto K, Yamauchi K, Mitsunaga T, Hayakawa T, Nakagawa T. 2013. Novel physiological roles for glutathione in sequestering acetaldehyde to confer acetaldehyde tolerance in *Saccharomyces cerevisiae*. Appl Microbiol Biotechnol 97:297-303.

624. Grigsby J, Betts B, Vidro-Kotchan E, Culbert R, Tsin A. 2012. A possible role of acrolein in diabetic retinopathy: involvement of a VEGF/TGFbeta signaling pathway of the retinal pigment epithelium in hyperglycemia. Curr Eye Res 37:1045-53.

625. Sakata K, Kashiwagi K, Sharmin S, Ueda S, Igarashi K. 2003. Acrolein produced from polyamines as one of the uraemic toxins. Biochem Soc Trans 31:371-4.

626. Park YS, Taniguchi N. 2008. Acrolein induces inflammatory response underlying endothelial dysfunction: a risk factor for atherosclerosis. Ann N Y Acad Sci 1126:185-9.

627. Sun Y, Ito S, Nishio N, Tanaka Y, Chen N, Isobe K. 2014. Acrolein induced both pulmonary inflammation and the death of lung epithelial cells. Toxicol Lett 229:384-92.

628. Kawabata C, Nagasawa T, Ono M, Tarumoto N, Katoh N, Hotta Y, Kawano H, Igarashi K, Shiokawa K, Nishimura K. 2021. Plasma acrolein level in rheumatoid arthritis increases independently of the disease characteristics. Mod Rheumatol 31:357-364.

629. Tsou HH, Hsu WC, Fuh JL, Chen SP, Liu TY, Wang HT. 2018. Alterations in Acrolein Metabolism Contribute to Alzheimer's Disease. J Alzheimers Dis 61:571-580.

630. Tully M, Tang J, Zheng L, Acosta G, Tian R, Hayward L, Race N, Mattson D, Shi R. 2018. Systemic Acrolein Elevations in Mice With Experimental Autoimmune Encephalomyelitis and Patients With Multiple Sclerosis. Front Neurol 9:420.

631. Kwolek-Mirek M, Bednarska S, Bartosz G, Bilinski T. 2009. Acrolein toxicity involves oxidative stress caused by glutathione depletion in the yeast *Saccharomyces cerevisiae*. Cell Biol Toxicol 25:363-78.

632. Ouyang X, Tran QT, Goodwin S, Wible RS, Sutter CH, Sutter TR. 2011. Yap1 activation by H_2O_2 or thiol-reactive chemicals elicits distinct adaptive gene responses. Free Radic Biol Med 50:1-13.

633. Lemar KM, Passa O, Aon MA, Cortassa S, Muller CT, Plummer S, O'Rourke B, Lloyd D. 2005. Allyl alcohol and garlic (*Allium sativum*) extract produce oxidative stress in *Candida albicans*. Microbiology (Reading) 151:3257-3265.

634. Kuloglu M, Atmaca M, Tezcan E, Gecici O, Tunckol H, Ustundag B. 2002. Antioxidant enzyme activities and malondialdehyde levels in patients with obsessive-compulsive disorder. Neuropsychobiology 46:27-32.

635. Bulut M, Selek S, Gergerlioglu HS, Savas HA, Yilmaz HR, Yuce M, Ekici G. 2007. Malondialdehyde levels in adult attention-deficit hyperactivity disorder. J Psychiatry Neurosci 32:435-8.

636. Relhan V, Gupta SK, Dayal S, Pandey R, Lal H. 2002. Blood thiols and malondialdehyde levels in psoriasis. J Dermatol 29:399-403.

637. Baskol G, Demir H, Baskol M, Kilic E, Ates F, Kocer D, Muhtaroglu S. 2005. Assessment of paraoxonase 1 activity and malondialdehyde levels in patients with rheumatoid arthritis. Clin Biochem 38:951-5.

638. Khan MA, Baseer A. 2000. Increased malondialdehyde levels in coronary heart disease. J Pak Med Assoc 50:261-4.

639. Paliogiannis P, Fois AG, Sotgia S, Mangoni AA, Zinellu E, Pirina P, Carru C, Zinellu A. 2018. Circulating malondialdehyde concentrations in patients with stable chronic obstructive pulmonary disease: a systematic review and meta-analysis. Biomark Med 12:771-781.

640. Chang JM, Kuo MC, Kuo HT, Chiu YW, Chen HC. 2005. Increased glomerular and extracellular malondialdehyde levels in patients and rats with diabetic nephropathy. J Lab Clin Med 146:210-5.

641. Gross NT, Hultenby K, Mengarelli S, Camner P, Jarstrand C. 2000. Lipid peroxidation by alveolar macrophages challenged with *Cryptococcus neoformans*, *Candida albicans* or *Aspergillus fumigatus*. Med Mycol 38:443-9.

Chapter 2

Mrr1 regulation of methylglyoxal catabolism and methylglyoxal-induced fluconazole resistance in *Candida lusitaniae*

Amy R. Biermann, Elora G. Demers, Deborah A. Hogan

Published in Molecular Microbiology, 2021 Jan;115(1):116-130; DOI: 10.1111/mmi.14604.

2.1 Abstract

Transcription factor Mrr1, best known for its regulation of *Candida* azole resistance genes such as *MDR1*, regulates other genes that are poorly characterized. Among the other Mrr1-regulated genes are putative methylglyoxal reductases. Methylglyoxal (MG) is a toxic metabolite that is elevated in diabetes, uremia, and sepsis, which are diseases that increase the risk for candidiasis, and MG serves as a regulatory signal in diverse organisms. Our studies in *Clavispora lusitaniae*, also known as *Candida lusitaniae*, showed that Mrr1 regulates expression of two paralogous MG reductases, *MGD1* and *MGD2*, and that both participate in MG resistance and MG catabolism. Exogenous MG increased Mrr1-dependent expression of *MGD1* and *MGD2* as well as expression of *MDR1*, which encodes an efflux pump that exports fluconazole. MG improved growth in the presence of fluconazole and this was largely Mrr1-dependent with contributions from a secondary transcription factor, Cap1. Increased fluconazole resistance was also observed in mutants lacking Glo1, a Mrr1-indedependent MG catabolic enzyme. Isolates from other *Candida* species displayed heterogeneity in MG resistance and MG stimulation of azole resistance. We propose endogenous and host-derived MG can induce *MDR1* and other Mrr1-regulated

genes causing increased drug resistance, which may contribute to some instances of fungal treatment failure.

2.2 Introduction

Candida species are among the most prominent fungal pathogens, with mortality rates for candidemia ranging from 28 to 72% depending on geographic location (reviewed in (1)), and recent decades have seen a worldwide increase in the overall incidence of candidemia (2). Treatment failure of invasive fungal infections remains an important clinical issue (3) due to long-term complications, high mortality rates, and elevated healthcare costs. Perplexingly, treatment may fail even in cases where isolates from a patient have tested as susceptible to a certain antifungal *in vitro*, suggesting that cryptic factors which are not present during *in vitro* testing may influence the outcome of antifungal therapy *in vivo*.

In *Candida* species, one mechanism of azole resistance is overexpression of the gene *MDR1* (4-7), which encodes an efflux pump. Overexpression of *MDR1* is usually caused by gain-of-function mutations in the gene encoding the zinc-cluster transcription factor Mrr1 (7-10). Many studies have focused on the relationship between *Candida* Mrr1 and resistance against clinical, host, and microbially-produced antifungal compounds (7, 8, 10-14). However, little is known about other genes that Mrr1 regulates and thus, the natural role of Mrr1 beyond its involvement in drug resistance is not well understood. By studying the biological functions of Mrr1-regulated genes, it is possible to gain insight into important questions such as the evolutionary purpose of Mrr1, drivers of selection for gain-of-function mutations in Mrr1, and other consequences of high Mrr1 activity aside from

drug resistance. Independent studies in *C. albicans* (10, 13, 15-17), *Candida parapsilosis* (18), and *Clavispora* (*Candida*) *lusitaniae* (7, 19) have revealed genes that appear coordinately upregulated in fluconazole (FLZ)-resistant isolates with gain-of-function mutations in *MRR1*.

Previously, we demonstrated a link between FLZ resistance and specific single nucleotide polymorphisms in the *MRR1* locus (*CLUG_00542*) among twenty clinical *C. lusitaniae* isolates from a single patient with cystic fibrosis (7). We identified multiple *MRR1* alleles containing gain-of-function mutations that correlated with elevated FLZ resistance, though the presence of *MRR1* alleles conferring high FLZ resistance within this population was unexpected, as the patient had no prior history of antifungal use. Thus, we became interested in other potential factors that could have selected for gain-of-function mutations in *MRR1*. An RNA-Seq analysis comparing several isolates with high- or low-activity Mrr1 variants identified nineteen genes that may be regulated by Mrr1 in *C. lusitaniae*, including two genes that encoded putative methylglyoxal (MG) reductases (7). Although homologs of *CaGRP2*/*MGD1* were known to be more highly expressed in FLZ-resistant *Candida* strains with high Mrr1 activity across multiple species (7, 13, 15-19), the relationship between Mrr1 and MG has not been described. Recently, genome analyses by Kannan, Sanglard, and colleagues (19) found a possible expansion of putative aldehyde reductases including MG reductases in the *C. lusitaniae* genome.

MG is a reactive compound that forms spontaneously during multiple metabolic processes in all known organisms (**Fig. 2.1**). Because it is a highly reactive electrophile, MG can irreversibly modify proteins, lipids, and nucleic acids in a nonenzymatic reaction known as glycation, resulting in cellular damage and stress (20, 21). Serum levels of MG

are elevated in patients with diabetes (22-24), sepsis (25), and uremia (26-29) relative to healthy controls. Additionally, evidence suggests that MG is generated during inflammation as part of the neutrophil respiratory burst (30). In fungi, MG can be formed during metabolism, for example, in *Saccharomyces cerevisiae,* a positive correlation has been shown between rate of glycolysis and MG levels (31). Catabolism of MG can occur through a glutathione-dependent glyoxalase system, Glo1 and Glo2 (32), or through NADH- or NADPH-dependent MG reductases (33) (**Fig. 2.1**). MG reductases have been characterized in *S. cerevisiae*, Gre2 (34), and *C. albicans*, Grp2 (35).

In the present study, we demonstrated that in *C. lusitaniae*, Mrr1 regulates *MGD1* (*CLUG_01281*) and *MGD2* (*CLUG_04991*), both of which encode proteins important for the detoxification and metabolism of MG. Deletion of one or both genes led to increased sensitivity to high concentrations of exogenous MG and decreased ability to use MG as a sole carbon source. In addition, we demonstrated that MG can induce Mrr1-dependent expression of *MGD1* and *MGD2*, as well as expression of *MDR1* in a partially Mrr1-dependent manner. MG increased growth in FLZ, and this response was largely dependent on *MRR1* and *MDR1*. Furthermore, deletion of *GLO1* increased FLZ resistance, likely due to elevated endogenous levels of MG. Finally, we showed that though MG sensitivity varies across *Candida* species, stimulation of azole resistance by MG is not exclusive to *C. lusitaniae*. Together, these data demonstrate a broader role for Mrr1 in a metabolic process and describe a mechanism by which host or microbial metabolism could increase resistance to azoles *in vivo*.

2.3 Results

C. lusitaniae MGD1 and *MGD2* contribute to the detoxification and metabolism of MG

In our previous work, an RNA-seq analysis of clinical *C. lusitaniae* isolates from a chronic lung infection showed that two genes with high sequence identity to each other, *CLUG_01281* and *CLUG_04991*, were significantly upregulated in isolates with gain-of-function mutations in *MRR1* (7). The protein sequences encoded by *CLUG_01281* and *CLUG_04991* are 88% percent identical to each other, and both have 59% and 58% identity to *C. albicans* Grp2 and *S. cerevisiae* Gre2, respectively (34, 35) (**Fig. 2.2A**). Based on sequence homology to previously characterized MG reductases and the experimental data shown below, from here forward *CLUG_01281* and *CLUG_04991* are referred to as *MGD1* and *MGD2*, respectively. We further analyzed the relationships between *MGD1, MGD2,* and other putative MG reductases with homology to *C. albicans GRP2* in select *Candida* spp. using FungiDB (36, 37) (**Fig. 2.2A**). An interesting phylogeny emerged among the homologs with at least 50% amino acid identity to *C. albicans* Grp2. *C. lusitaniae MGD1* and *MGD2* were more similar to each other than to homologs in other *Candida* species, and other *Candida* species, including *Candida auris*, *Candida parapsilosis*, and *Candida tropicalis* also had at least one set of highly similar paralogous putative MG reductases (**Fig. 2.2A**). *Candida glabrata* has a pair of related putative MG reductases that are homologous to *S. cerevisiae* Gre2 (**Fig. 2.2A**). The phylogeny of Grp2 homologs suggests that a duplication of MG reductase genes has occurred in many *Candida* species, indicating that this function may be biologically important within the natural niches of *Candida*.

To determine if *MGD1* and *MGD2* were involved in MG resistance and gain more insight into the respective roles of these two similar genes, we knocked out each gene independently and in combination in the previously characterized *C. lusitaniae* clinical isolate S18, which contains a constitutively active Mrr1 variant, H467L (referred to as H4) (7). We found that although the *mgd1*Δ*, mgd2*Δ*,* and *mgd1*Δ*/mgd2*Δ mutants grew similarly to the S18 parental strain in the absence of MG, they grew significantly worse in the presence of 15 mM MG, with a lower OD_{600} after 36 hours, slower growth rate, and longer lag time (**Fig. 2.2B, C,** and **D**; see **Fig. S2.1A** and **S2.1C** for representative growth curves). To our surprise, the double mutant did not exhibit a more severe phenotype than either single mutant, suggesting that these genes are not redundant and that both enzymes are required for full function of the cell's NADPH- or NADH-dependent MG reductase machinery. We confirmed these phenotypes in the L17 isolate, which is closely related to S18 and shares the constitutively active Mrr1-H4 variant, and similarly found that the *mgd1*Δ and *mgd2*Δ mutants were more sensitive to MG than the parental strains (**Fig. 2.2E**; see **Fig. S2.1D** and **Fig. S2.1B** for representative growth curves). We were unable to generate an *mgd1*Δ/*mgd2*Δ double mutant in the L17 background for reasons that are not yet known but do not appear to relate to the selectable markers used as each selectable marker can be used singly.

To determine if *MGD1* and *MGD2* also contributed to MG metabolism, we tested whether the *mgd1*Δ, *mgd2*Δ, or *mgd1*Δ/*mgd2*Δ mutants were deficient in utilizing MG as a sole carbon source. In minimal YNB medium with 5 mM glucose, none of the mutants displayed a significant difference in OD_{600} at 36 h relative to the WT (**Fig. S2.2A**). With 5 mM MG as the sole carbon source, neither single mutant exhibited a significant defect in

growth, but the *mgd1*Δ/*mgd2*Δ displayed a 26.8% reduction in yield ($p < 0.05$) relative to the WT (**Fig. S2.2B**). Together, these data suggest that both *MGD1* and *MGD2* play a role in the detoxification and metabolism of MG.

Mrr1 strongly regulates expression of *MGD1*, but *MGD2* is not highly expressed under standard conditions

We have previously reported (7) an RNA-seq analysis that showed that clinical isolates with constitutive Mrr1 activity had higher levels of *MGD1* and *MGD2* expression than strains with low basal Mrr1 activity. Furthermore, analyses of *C. albicans*, *C. parapsilosis*, and an independent collection of clinical *C. lusitaniae* isolates also found that expression of methylglyoxal reductase genes was elevated in azole-resistant strains with gain-of-function mutations in Mrr1 (13, 15-19). In both the S18 and L17 isolate backgrounds, the *mrr1*Δ mutant was significantly more sensitive to 15 mM MG than the WT despite no difference in growth between the isogenic parental and *mrr1*Δ strains in control conditions (**Fig. 2.3A** and **B**). Furthermore, we found that S18 *mrr1*Δ had a 32% lower yield relative to the parental strain in MG as a sole carbon source, with no defects in growth on glucose, and that S18 *mrr1*Δ phenocopied the *mgd1*Δ/*mgd2*Δ mutant in this assay (**Fig. S2.2**).

To directly assess whether Mrr1 regulates expression of *MGD1* and *MGD2*, we developed a set of isogenic strains that differed only by which *MRR1* allele was present at the native locus. These *MRR1* alleles were complemented into the *mrr1*Δ derivative of U04, which we have previously described (7). The naturally occurring *MRR1* alleles in this set included a high activity variant (Mrr1-Y813C, referred to as Y8) and a low activity

variant (Mrr1-L1191H + Q1197* referred to as L1Q1*); the strain with the high activity Mrr1-Y8 variant had a FLZ minimum inhibitory concentration (MIC) that was 64-128-fold higher than the strain with the low activity Mrr1-L1Q1* variant (**Table 2.1**). The *mrr1*Δ derivative of U04 had an 8-fold higher FLZ MIC than the strain with a low activity allele, though the mechanism for this is not known (**Table 2.1**). As expected, based on results shown in **Fig. 2.2**, we found that strains with high Mrr1 activity grew better in medium with MG compared to strains with low or no Mrr1 activity; no growth differences were observed between strains in control conditions (**Fig. 2.3C** and **D**). We found that the *mrr1*Δ mutant had significantly lower levels of basal expression of *MGD1* relative to the relative to WT and Y8 revertant, and the strain with low activity Mrr1 variant had even lower *MGD1* expression (**Fig. 2.3E**). *MGD2* levels were 10-100-fold lower than *MGD1*, as judged using a standard curve of input DNA with primer sets for *MGD1*, *MGD2*, and *ACT1* (see Methods). Surprisingly, *MGD2* levels were not different across the U04 strains with different Mrr1 variants in YPD medium without MG (**Fig. 2.3F**).

Exogenous MG induces Mrr1-regulated genes through Mrr1 with contributions from Cap1

Because of our observations that *MGD1* and *MGD2* are involved in detoxification and metabolism of MG (**Fig. 2.2** and **S2.2B**), we tested whether MG induced their expression through Mrr1 in the S18 background. As shown in **Fig. 2.4A** and **B**, 5 mM MG significantly induced expression of *MGD1* by 2-fold at 15 minutes and *MGD2* by 16-fold at 30 minutes in the unaltered S18 isolate. Expression of both genes remained elevated after 60 minutes of MG exposure, although they appeared to be trending downward and

the difference at 60 min relative to basal expression only reached statistical significance for *MGD1*. MG also induced expression of another Mrr1-regulated gene, *MDR1*, by 6-fold at 15 and 30 minutes, but as with *MGD1* and *MGD2*, relative *MDR1* levels began trending downward by 60 minutes (**Fig. 2.4C**).

As *C. albicans* Mrr1 induces *MDR1* in response to benomyl and hydrogen peroxide (H_2O_2) in conjunction with another transcription factor, Cap1 (13), we hypothesized that Cap1 may similarly contribute to Mrr1 induction of *MDR1* in *C. lusitaniae*. Furthermore, in *S. cerevisiae*, MG directly modifies the Cap1 ortholog Yap1 by reversibly oxidizing cysteines, thereby inducing nuclear translocation (38). To determine whether *C. lusitaniae MRR1* and/or *CAP1* (*CLUG_02670*) were required for the transcriptional response observed in **Fig. 2.4A-C**, we used isogenic *mrr1*Δ, *cap1*Δ, and *mrr1*Δ/*cap1*Δ mutants in the S18 background. Consistent with the results in **Fig. 2.4A** and **B**, MG induced expression of *MGD1* (**Fig. 2.4D**) and *MGD2* (**Fig. 2.4E**) by two-fold and 12-fold, respectively in the S18 parental strain, while the *mrr1*Δ*, cap1*Δ, or *mrr1*Δ/*cap1*Δ derivatives of S18 did not exhibit a significant change in expression of either gene in response to 5 mM MG (**Fig. 2.4D** and **E**). These results support the hypothesis that both Mrr1 and Cap1 are necessary for induction of *MGD1* and *MGD2* expression in response to MG. Additionally, the S18 *cap1*Δ mutant was also defective in growth in YPD + 15 mM MG (**Fig. S2.3**) providing further evidence that Cap1 plays an important role the upregulation of genes involved in MG detoxification.

Consistent with the transcriptomics evidence that Mrr1 coregulates *MGD1* and *MGD2* with *MDR1*(7), that all three genes are induced by MG (**Fig. 2.4A-C**), and that MG induction of *MGD1* and *MGD2* depended on Mrr1, we found that Mrr1 also played a

role in MG induction of *MDR1*. While there were no differences in *MDR1* levels among the WT, *mrr1*Δ, *cap1*Δ and *mrr1*Δ/*cap1*Δ in control conditions, the S18 *mrr1*Δ and the S18 *mrr1*Δ/*cap1*Δ had significantly lower *MDR1* levels than the WT and *cap1*Δ in medium with MG (**Fig. 2.4F**). To confirm these results in strain L17, we repeated our analysis of *MDR1* expression in the original isolate and its *mrr1*Δ and *cap1*Δ derivatives. In agreement with the results in **Fig. 2.4C and 2.4F**, the parental L17 exhibited a significant increase in *MDR1* expression when exposed to MG, and knocking out *MRR1* reduced *MDR1* levels in medium with MG. (**Fig S2.4**). In L17, the *cap1*Δ also had significantly lower *MDR1* levels when compared to the WT. Together, it appears that Mrr1 and Cap1 each play a role in MG-dependent *MDR1* induction, though the effects of loss of Cap1 were only significant in strain L17. The weak stimulation of *MDR1* by MG in the S18 *mrr1*Δ/*cap1*Δ background leads us to suggest that there are other factors may also influence the levels of *MDR1* in response to MG as we discuss below.

MG stimulates growth in FLZ in an Mrr1- and Mdr1-dependent manner

Due to the induction of *MDR1* expression by MG (**Fig. 2.4F**), we hypothesized that MG could increase *MDR1*-dependent FLZ resistance in *C. lusitaniae*. To test this, we used FLZ at a concentration equal to the MIC (**Table 2.1**) and 5 mM MG. While MG alone did not alter the growth of S18 WT (**Fig. S2.5A**), it drastically improved growth in the presence of FLZ (**Fig. 2.5A**), resulting in a OD_{600} at 16 h that was, on average, 5.2-fold higher than in FLZ alone (**Fig. 2.5**). The S18 *mrr1*Δ and *mrr1*Δ/*cap1*Δ mutants exhibited a significantly lower fold increase in yield at 16 h in FLZ upon amendment of the medium with MG compared to the S18 parental strain, 2.4- and 1.8-fold, respectively and S18 *mdr1*Δ was

similar to the *mrr1*Δ and *mrr1*Δ/*cap1*Δ mutants (**Fig. 2.5B**). The *cap1*Δ mutant exhibited on average a 4.6-fold increase in growth in FLZ with MG which was not significantly different from the parental S18 in these analyses, but trended lower (**Fig. 2.5B**).

We repeated these growth assays in the L17 background with strains lacking *MRR1*, *CAP1*, or *MDR1*. Again, MG did not alter growth for any of the strains relative to the YPD control (**Fig. S2.5B**), but it did lead to a robust stimulation of growth in FLZ, with an average fold change in OD_{600} of 8.5 (**Fig. S2.5 C** and **D**). The stimulation of growth in FLZ by MG was partially dependent on Mrr1 as the *mrr1*Δ mutant exhibited a fold change in OD_{600} of 4.2 which was significantly lower than the S18 WT (**Fig. S2.5D**). Similar to the S18 background, the L17 *mdr1*Δ mutant exhibited a fold change in OD_{600} at 16h that was significantly lower than the parental isolate (2.7-fold). Consistent with the *MDR1* expression analysis of L17 strains that found that both Mrr1 and Cap1 contributed to the induction of *MDR1* (**Fig. S2.4**), both Mrr1 and Cap1 contributed to increased FLZ resistance in the presence of MG (**Fig. S2.5D**). The differences between the S18 and L17 backgrounds in the robustness of the *cap1*Δ mutant phenotype, with Cap1 appearing to play a greater role in *MDR1* regulation in L17, suggest that strain-dependent variables may influence the relative importance of the two transcription factors in the MG response.

Strains with constitutively active Mrr1 variants exhibit greater growth with MG in FLZ than strains with low activity Mrr1 variants

Given our discovery of repeated selection for Mrr1 variants with constitutive activity within a chronic *C. lusitaniae* lung infection (7), we sought to determine if higher basal Mrr1 activity effected the magnitude of stimulation of FLZ resistance by MG. We

compared the effects of a sub-inhibitory concentration of MG on growth in the presence of inhibitory concentrations of FLZ for *C. lusitaniae* strains S18 and L17, which both express the constitutively active Mrr1-H4 variant, to previously published strains U05 and L14, which express the low activity Mrr1-L1Q1* variant. While there were no differences in growth among strains in reference conditions, the combination of FLZ and MG significantly increased the growth of isolates with high Mrr1 activity (S18 and L17) by ~6-fold relative to growth with FLZ alone and isolates with low Mrr1 activity (U05 and L14) showed similar trends, though the differences were not significant (**Fig. 2.6B**). These results show strains with highly active Mrr1 variants were able to reach more robust levels of FLZ resistance in response to MG than strains with low Mrr1 activity.

Absence of *GLO1* causes increased sensitivity to MG and increased resistance to FLZ

The experiments above focused on the effects of exogenous MG, but endogenously generated MG is also an important signal that modulates cell behavior (39-42). Disruption of the glyoxalase pathway in *S. cerevisiae* has been shown to cause an accumulation of intracellular MG (38, 43) and render cells highly sensitive to exogenous MG (44). The glyoxalase pathway, which consists of the glutathione-dependent enzymes Glo1 and Glo2, is widely recognized as a major mechanism for MG catabolism in eukaryotic cells (see **Fig. 2.1**) (45). Thus, we were interested in whether the S18 *glo1*Δ mutant (lacking *CLUG_04105*) was more resistant to FLZ than its parent in the absence of exogenously added MG. We found that S18 *glo1*Δ was highly sensitive to 15 mM MG (**Fig. 2.7A**), even more so than the S18 *mgd1*Δ, *mgd2*Δ, and *mgd1*Δ/*mgd2*Δ mutants (**Fig. S2.2C**). Although S18 *glo1*Δ had similar growth kinetics in YPD as the S18 WT (**Fig. 2.7A**), the *glo1*Δ mutant

grew substantially better in FLZ compared to its parent strain (**Fig 2.7B**). These data lead us to speculate that the absence of *GLO1* in *C. lusitaniae* leads to an accumulation of intracellular MG, which may influence the activity of Mrr1, causing an increase in FLZ resistance.

C. lusitaniae is more resistant to MG than many other *Candida* species, and some strains of other species exhibit induction of azole resistance by MG

To assess intrinsic MG resistance across multiple *Candida* species, we assessed growth for a panel of isolates representing seven *Candida* species on YPD agar plates in the presence and absence of 15 mM MG. As controls, we included the *C. lusitaniae* S18 isolate and S18 *glo1*Δ, shown above to be highly sensitive to MG (**Fig. 2.7**). We found that *C. lusitaniae* and *Candida dubliniensis* strains were only minimally inhibited by 15 mM MG on plates. There was, however, heterogeneity in growth on MG among *C. auris* and *C. albicans* strains, and the tested *Candida guilliermondii*, *C. glabrata*, and *C. parapsilosis* strains were highly sensitive to MG (**Fig. 2.8A**). Overall, the results in **Fig. 2.8A**, using a limited number of strains, suggest that intrinsic MG resistance varies between *Candida* species and strains.

We used the same strains as in **Fig. 2.8A** to determine if the increase in FLZ resistance in the presence of MG was conserved across *Candida* species. Using 3 mM MG, a lower concentration of MG than in **Fig. 2.8A** because of high MG sensitivity of some species, we determined resistance to increasing concentrations of either FLZ or voriconazole (VOR) depending on the species. As shown in **Fig. 2.8B**, *C. parapsilosis* RC-601 and *C. dubliniensis* CM2 displayed a striking increase of growth on FLZ with MG and

C. glabrata ATCC 2001 exhibited a striking increase of growth on VOR with MG. *C. auris* CAU-01 demonstrated a more subtle increase in growth with MG (**Fig. 2.8B**). Strains that did not demonstrate visible stimulation of growth on FLZ or VOR by MG under the tested conditions are shown in **Fig S2.6**. These results suggest that MG stimulation of azole resistance is not exclusive to *C. lusitaniae*, but not every strain within a species can be stimulated under the conditions tested. Future studies are required to determine what factors determine whether a strain is or is not capable of being induced by MG to have higher azole resistance.

2.4 Discussion

The findings from this study show that Mrr1 plays an important role in regulating genes other than *MDR1* in ways that impact growth and fitness, thereby adding to the growing appreciation of MG as an important biological signal across the tree of life. Although the serum concentrations of MG reported in humans are lower than those used *in vitro* for this study (46, 47), local MG levels at sites of infection are hard to measure as MG is highly reactive. At the site of a chronic infection, it is likely that microbes are exposed to MG from a variety of exogenous and endogenous sources including the host immune system, other microbes, and the pathogen's own metabolic activity (see **Fig. 2.1** and reviewed in (48)). Evidence for the generation of MG *in vivo* comes from the fact that group A *Streptococci* require glyoxalase I for resistance to neutrophil killing, suggesting that neutrophils may be a source of MG *in vivo* (30). In addition, *CaGRP2*, along with other stress-response genes, was upregulated in *C. albicans* cells grown in the murine cecum (49). Even low levels of exogenous MG may stimulate a transcriptional response if

endogenous MG is already high due to basal metabolism or depletion of the reducing agents required for MG detoxification. Production of MG can be affected by the local environment with low carbon or phosphate increasing MG production in mammalian and bacterial cells, respectively (50-52). In addition, MG reaction with arginine, lysine, and cysteine residues on proteins forms both reversible and irreversible adducts, and thus some effects of MG on transcriptional activation may increase over time upon low level exposure (20, 21). Our demonstration of the induction of azole resistance by MG could be an important step toward understanding and preventing treatment failure in populations who are susceptible to *Candida* infection.

Previous studies of Mrr1 in multiple *Candida* species have focused on the regulation and biological significance of only a small number of Mrr1-regulated genes, primarily the two efflux pumps encoded by *MDR1* (4-7) and *FLU1* (14, 53, 54). Here, we show that isogenic *C. lusitaniae* strains with gain-of-function mutations in Mrr1 led to higher levels of *MGD1* and *MGD2* transcripts, and higher resistance to exogenous MG (**Fig. 2.3D**) than strains with low Mrr1 activity. Furthermore, we showed that MG induced Mrr1 activity to increase the expression of not just *MGD1* and *MGD2*, but also *MDR1*. The co-regulation of genes involved in the detoxification of metabolic by-products with efflux pumps may highlight a broad coordination of a stress response that could be important *in vivo*. Future studies will determine whether MG enhances FLZ resistance *in vivo* and if MG exposure can contribute to the selection for high activity Mrr1 variants.

While multiple chemical inducers of Mrr1 activity have been described, including methotrexate, 4-nitroquinoline-N-oxide, *o*-phenanthroline, benomyl, diethyl maleate, diamide, and H_2O_2, (12, 13, 55), little is known about why or how these inducers activate

Mrr1. It has been postulated that many of these compounds many directly or indirectly induce oxidative stress, which then activates Mrr1. MG is especially interesting as a natural inducer of Mrr1 activity because i) it is produced by cells during metabolism and *in vivo* as an antimicrobial agent, ii) Mrr1 regulates enzymes that specifically metabolize and detoxify this compound, and iii) it has similarly been documented to cause oxidative stress like other known inducers of Mrr1 activity. Though the mechanism by which MG activates transcription in *C. lusitaniae* will be the subject of future work, in *S. cerevisiae* MG has been shown to activate the Cap1 homolog Yap1 by reversibly modifying cysteine residues (38). Multiple studies have established that the transcription factors Mrr1 and Cap1, a regulator of oxidative stress, can cooperate to regulate the expression of *MDR1* in *C. albicans* (12, 13) and we found evidence that this can be the case in *C. lusitaniae*. We do not yet know if Mrr1 or Cap1 is directly modified by MG. *C. lusitaniae* Mrr1 contains many cysteine residues near the C-terminal portion that could be react with MG in a manner similar to *S. cerevisiae* Yap1. Furthermore, the observation that MG slightly induced *MDR1* even in the absence of both *MRR1* and *CAP1* (**Fig. 2.4F**) suggests that other transcription regulators may play a role in *MDR1* induction in response to MG. Other known regulators of *MDR1* expression in *C. albicans* include the transcription factors Mcm1, which is required for induction of *MDR1* by benomyl and by hyperactive Mrr1, but not induction by H_2O_2 (12), and Upc2 (13, 56), as well as the Swi/Snf chromatin remodeling complex (11).

As MG is elevated in many diseases associated with *Candida* infections, we were struck by the implications of subinhibitory levels of exogenous MG inducing Mrr1 activity and by extension FLZ treatment outcomes. Diabetes (reviewed in (57)) and uremia (58,

59) are considered risk factors for infection by a variety of *Candida* species, and both are associated with higher levels of MG. Our studies with the *C. lusitaniae glo1*Δ mutant suggest that intracellular MG can also influence FLZ resistance (38, 43). The glyoxalase system, utilizing Glo1 and Glo2, requires reduced glutathione (GSH) to function (**Fig. 2.1**), so it is possible that oxidants encountered *in vivo* could deplete GSH and cause increased intracellular MG. In fact, GSH levels are lower in chronic infections, such as those associated with cystic fibrosis (60, 61). It is also worth noting that diethyl maleate, a compound shown to induce *MDR1* expression in *C. albicans* (55), is commonly used in laboratory studies to deplete GSH (62-66).

Importantly, we found that MG induction of azole resistance was not specific to *C. lusitaniae* but more broadly applicable to other *Candida* species though with clear strain-to-strain differences in MG sensitivity (**Fig. 2.8B**). Interestingly, several species of bacteria exhibit an increase of drug resistance-related genes in response to MG; for example, MG induces expression of the MexEF-OprN multidrug efflux system in *Pseudomonas aerguinosa* (67), and derepresses *Escherichia coli* TetR family repressor NemR (68). Clearly, MG is an important stimulus and stressor that many microbes encounter and understanding how MG affects microbial physiology and drug resistance can open doors to novel means of modulating pathogenic and/or commensal microbes for better health outcomes. For example, it would be interesting to investigate whether supplementation with carnosine, a known scavenger of MG (69) that is readily available as a dietary supplement, could improve the efficacy when treating infection by *Candida* species, particularly in patients who are predisposed to elevated serum MG.

2.5 Methods

Generation of MG reductase phylogenetic tree

Orthologs of CaGrp2 from *S. cerevisiae* and multiple *Candida* species were identified in FungiDB (https://fungidb.org) (36, 37) and selected for a protein Clustal Omega multiple sequence alignment (70). The resulting alignment was then used to generate a phylogenetic tree using the Interactive Tree of Life (ITOL) tool (https://itol.embl.de) (71).

Strains, media, and growth conditions

The sources of all strains used in this study are listed in **Table S2.1**. All strains were stored long term in a final concentration of 25% glycerol at -80°C and freshly streaked onto yeast extract peptone dextrose (YPD) agar (10 g/L yeast extract, 20 g/L peptone, 2% glucose, 1.5% agar) once every seven days and maintained at room temperature. Cells were grown in YPD, yeast nitrogen base (YNB) (0.67% yeast nitrogen base medium with ammonium sulfate (RPI Corp)) supplemented with either 5 mM dextrose or 5 mM MG (Sigma-Aldrich, 5.55 M), or RPMI-1640 (Sigma, containing L-glutamine, 165 mM MOPS, 2% glucose at pH 7) liquid as noted. Media was supplemented with FLZ (Sigma-Aldrich, stock 4 mg mL^{-1} in DMSO) or 3 mM, 5 mM or 15 mM MG as noted. Unless otherwise noted, all overnight cultures were grown in 5 mL YPD liquid medium (10 g/L yeast extract, 20 g/L peptone, 2% glucose) on a rotary wheel at 30°C. *E. coli* strains were grown in LB with either 100 µg mL^{-1} carbenicillin (carb) or 15 µg mL^{-1} gentamycin (gent) as necessary.

Plasmids for complementation of *MRR1*

We amplified i) the *MRR1* gene and terminator with ~1150 bp upstream for homology from the appropriate strain's genomic DNA, ii) the selective marker, *HygB* from pYM70 (72), and iii) ~950 bp downstream of *MRR1* for homology from genomic U05 (identical sequence for all relevant strains using primers listed in **Table S2.2**. PCR products were cleaned up using the Zymo DNA Clean & Concentrator kit (Zymo Research) and assembled using the *S. cerevisiae* recombination technique previously described (73). Plasmids created in *S. cerevisiae* were isolated using a yeast plasmid miniprep kit (Zymo Research) and transformed into High Efficiency NEB®5-alpha competent *E. coli* (New England BioLabs). *E. coli* containing pMQ30 derived plasmids were selected for on LB containing 15 μg mL^{-1} gentamycin. Plasmids from *E. coli* were isolated using a Zyppy Plasmid Miniprep kit (Zymo Research) and subsequently verified by Sanger sequencing with the Dartmouth College Genomics and Molecular Biology Shared Resources Core. *MRR1* complementation plasmids were linearized with Not1-HF (New England BioLabs), cleaned up the Zymo DNA Clean & Concentrator kit (Zymo Research) and eluted in molecular biology grade water (Corning) before transformation of 2 μg into *C. lusitaniae* strain U04 *mrr1*Δ as described below.

All plasmids for complementing *MRR1* were constructed using the *S. cerevisiae* recombination technique previously described (73) and primers listed in **Table S2.2**. To create the precursor plasmid pMQ30$^{MRR1\text{-}L1191H+Q1197*}$-*URA3*, *MRR1* with ~1150 bp upstream of *MRR1* and separately ~950 bp downstream of *MRR1* were amplified from genomic U05 (containing *MRR1*$^{L1191H+Q1197*}$*)* DNA and *C. albicans URA3* under the controls of a TEF1 promoter was amplified from pTEF1-*URA3*. This construct did not

restore growth of 5-FOA resistant *C. lusitaniae* strains on uracil deplete medium, so we replaced *URA3* with a different selectable marker. Linearized pMQ30$^{MRR1\text{-}L1191H+Q1197*}$-*URA3* (using XbaI) and PCR amplified HygB, the hygromycin B resistance gene from pYM70 (72), were combined using the *S. cerevisiae* recombination technique to create pMQ30$^{MRR1\text{-}L1191H+Q1197*}$-*HygB*. To create the pMQ30$^{MRR1\text{-}Y813C}$-*HygB* plasmid, pMQ30$^{MRR1\text{-}L1191H+Q1197*}$-*HygB* was linearized with XbaI and NotI to remove *MRR1* and the upstream sequence. Replacement sequence including *MRR1* with ~1150 bp upstream of *MRR1* were amplified from U04 (*MRR1*^{Y813C}) gDNA.

Plasmids created in *S. cerevisiae* were isolated using a yeast plasmid miniprep kit (Zymo Research) and transformed into High Efficiency NEB®5-alpha competent *E. coli* (New England BioLabs). *E. coli* containing pMQ30 derived plasmids were selected for on LB containing 15 μg mL^{-1} gentamycin. Plasmids from *E. coli* were isolated using a Zyppy Plasmid Miniprep kit (Zymo Research) and subsequently verified by Sanger sequencing with the Dartmouth College Genomics and Molecular Biology Shared Resources Core. All restriction enzymes were purchased from New England BioLabs and used as recommended by the manufacturer.

Mutant construction

Mutants were generated using an expression-free CRISPR-Cas9 method, as previously described (74), with the exception of the *mgd1*Δ/*mgd2*Δ double mutant, as detailed below. In brief, cultures were grown to exponential phase in 50 mL YPD on a shaker at 150 rpm, then washed and incubated in TE buffer and 0.1 M lithium acetate at 30°C for one hour. Dithiothreitol was added to a final concentration of 100 mM and

cultures were incubated for an additional 30 minutes at 30°C. Cells were washed and resuspended in 1 M sorbitol before being transferred to electroporation cuvettes. To each cuvette was added 1.5 µg of DNA for the knockout or *MRR1* complementation construct and Cas9 ribonucleoprotein containing crRNA specific to the target gene. Following electroporation, cells were allowed to recover in YPD at 30°C for four to six hours. Cells were then plated on YPD agar supplemented with 200 µg mL^{-1} nourseothricin (NAT) or 600 µg mL^{-1} hygromycin B (HYG) and incubated at 30°C for two days. The *mgd1*Δ/*mgd2*Δ double mutant was generated from the S18 *mgd1*Δ single mutant using the microhomology repair method (75). In brief, the knockout construct containing 50 bp homology to the flanking regions of *MGD2* was transformed alongside Cas9 complexed with two crRNA, targeting the 5' and 3' region immediately adjacent to *MGD2*. PCR with primers inside the *NAT1* or *HygB* cassette and in the flanking regions of the genes outside of each construct were used to confirm all mutants. Primers (IDT) used to create knockout constructs and verify mutants are listed in **Table S2.2**.

Minimum Inhibitory Concentration (MIC) Assay

MIC assays for FLZ were performed as described in (7) using the broth microdilution method. In brief, overnight cultures were diluted to an OD_{600} of 0.1 in 200 µL dH_2O and 60 µL of each dilution were added to 5 mL RPMI-1640 medium. FLZ was serially diluted across a clear, flat-bottom 96-well plate (Falcon) from 128 µg mL^{-1} down to 0.25 µg mL^{-1} in RPMI-1640. To each well was added 100 µL of cell suspension in RPMI-1640. Upon addition of cells, the final concentration of FLZ ranged from 64 µg mL^{-1} to 0.125 µg mL^{-1}. Plates were incubated at 35°C and scored for growth at 24 hours; the

results are summarized in **Table 2.1**. The MIC was defined as the drug concentration that abolished visible growth compared to a drug-free control.

Growth Kinetics

C. lusitaniae cultures were grown overnight, diluted 1:50 into 5 mL fresh YPD, and grown for four to six hours at 30°C. After washing, the cultures were diluted to OD_{600} of 1 in 200 µL dH_2O. Each inoculum was prepared by pipetting 60 µL of the OD_{600} of 1 suspension into 5 mL YPD. Clear 96-well flat-bottom plates (Falcon) were prepared by adding 100 µl per well YPD or YPD with MG and/or FLZ at twice the desired final concentrations. 100 µL of inoculum was added to each row of the plate. Each plate was set up in technical triplicate for each strain and condition. The plates were incubated in a Synergy Neo2 Microplate Reader (BioTek, USA) to generate a kinetic curve. The plate reader protocol was as follows: heat to 37°C, start kinetic, read OD_{600} every 60 minutes for 16 or 36 hours, end kinetic.

Spot Assays

Candida cultures were grown overnight, diluted 1:50 into 5 mL fresh YPD, and grown for four to six hours at 30°C. Cultures were diluted to OD_{600} of 1 in 200 µL dH_2O. Each strain was then serially diluted by 1:10 down to an OD_{600} of approximately 1×10^{-6}. 5 µL of each dilution was spotted onto YPD alone or YPD containing the specified concentrations of MG, FLZ or VOR (Cayman Chemical Company, stock 1 mg mL^{-1} in DMSO). Plates were incubated at 37°C for two days before imaging.

Quantitative Real-Time PCR

C. lusitaniae cultures were grown overnight, diluted 1:50 into 5 mL fresh YPD, and grown for four hours at 30°C. Control cultures were harvested at this point and MG was added to a final concentration of 5 mM to all other cultures, which were returned to 30°C on a roller drum. Cultures were then harvested after 15, 30, or 60 minutes. To harvest, 2 mL of culture was spun in a tabletop centrifuge at 13.2 x *g* for 5 min and supernatant was discarded. RNA isolation, gDNA removal, cDNA synthesis, and quantitative real-time PCR were performed as previously described (7). Transcripts were normalized to *ACT1* expression. Primers are listed in **Table S2.2**.

Statistical analysis and figure preparation

All graphs were prepared with GraphPad Prism 8.3.0 (GraphPad Software). One- and two-way analysis of variance (ANOVA) tests were performed in Prism; details on each test are described in the corresponding figure legends. All p values were two-tailed and $p < 0.05$ were considered to be significant for all analyses performed and are indicated with asterisks or letters in the text: *p<0.05, **p<0.01, ***p<0.001, ****p<0.0001. The graphical abstract was prepared using BioRender (biorender.com).

Data availability

The data that support the findings of this study are available from the corresponding author upon request.

2.6 Acknowledgements

We thank Theodore White, Richard Calderone, Lawrence Myers, Joachim Morschhäuser, Isabel Miranda, Kyria Boundy-Mills and the FDA-CDC Antimicrobial Resistance Isolate Bank for providing strains. We thank Judith Berman for the pGEM-*URA3* plasmid.

Author contributions. ARB, EGD, and DAH conceived and designed the experiments and wrote the paper. ARB and EGD performed the experiments. ARB, EGD, and DAH analyzed the data.

Funding. This study was supported by grants R01 5R01 AI127548 to DAH and AI133956 to EGD. Core services were provided by STANTO19R0 to CFF RDP, P30-DK117469 to DartCF, and P20-GM113132 to BioMT. Sequencing services and specialized equipment were provided by the Genomics and Molecular Biology Shared Resource Core at Dartmouth, NCI Cancer Center Support Grant 5P30 CA023108-41. The content is solely the responsibility of the authors and does not necessarily represent the official views of the NIH.

Competing interests. The authors have declared that no competing interests exist.

Table 2.1. FLZ MIC and relative Mrr1 activity of *C. lusitaniae* strains used in this paper

Strain	FLZ MIC (μg mL^{-1})	Relative Mrr1 activity
S18	8	High
S18 *mgd1*Δ	8	High
S18 *mgd2*Δ	8	High
S18 *mgd1*Δ/*mgd2*Δ	8	High
S18 *mrr1*Δ	4	N/A
S18 *cap1*Δ	8	High
S18 *mrr1*Δ/*cap1*Δ	4	N/A
S18 *mdr1*Δ	2	High
S18 *glo1*Δ	8	High
L17	8	High
L17 *mgd1*Δ	8	High
L17 *mgd2*Δ	8	High
L17 *mrr1*Δ	4	N/A
L17 *cap1*Δ	8	High
L17 *mdr1*Δ	2	High
U04	32	High
U04 *mrr1*Δ	4-8	N/A
U04 *mrr1*Δ + *MRR1*-Y8	32	High
U04 *mrr1*Δ + *MRR1*-L1Q1*	0.25 – 0.5	Low
U05	0.5 - 1	Low
L14	0.5 - 1	Low

Table S2.1. Strains and plasmids used in this study

Strain	Lab #	Species	Parent	Relevant Characteristics or Genotype	Source
Fungal Strains					
U04 (A04)	DH2949	*C. lusitaniae*		Clinical isolate, FLZ-resistant, *MRR1*^{Y813C}	(7, 74)
U04 *mrr1*Δ	DH3306	*C. lusitaniae*	U04	*mrr1*Δ::*NAT1*	(7)
U04 *mrr1*Δ + *MRR1*^{Y813C} (Y8)	DH3613	*C. lusitaniae*	U04 *mrr1*Δ	*MRR1*^{Y813C}-*HygB*	This study
U04 *mrr1*Δ + *MRR1*$^{L1191H+Q1197*}$ (L1Q1*)	DH3628	*C. lusitaniae*	U04 *mrr1*Δ	*MRR1*$^{L1191H+Q1197*}$-*HygB*	This study
U05	DH3087	*C. lusitaniae*		Clinical isolate, FLZ-susceptible, *MRR1*$^{L1191H+Q1197*}$	(7)
L14	DH3088	*C. lusitaniae*		Clinical isolate, FLZ-susceptible, *MRR1*$^{L1191H+Q1197*}$	(7)
L17	DH3101	*C. lusitaniae*		Clinical isolate, FLZ-resistant, *MRR1*^{H467L}	(7)
L17 *mrr1*Δ	DH3110	*C. lusitaniae*	L17	*mrr1*Δ::*NAT1*	(7)
L17 *cap1*Δ	DH3720	*C. lusitaniae*	L17	*cap1*Δ::*NAT1*	This study
L17 *mgd1*Δ	DH3724	*C. lusitaniae*	L17	*mgd1*Δ::*NAT1*	This study
L17 *mgd2*Δ	DH3726	*C. lusitaniae*	L17	*mgd2*Δ::*NAT1*	This study
S18	DH3102	*C. lusitaniae*		Clinical isolate, FLZ-resistant, *MRR1*^{H467L}	(7)
S18 *mrr1*Δ	DH3718	*C. lusitaniae*	S18	*mrr1*Δ::*NAT1*	This study
S18 *cap1*Δ	DH3719	*C. lusitaniae*	S18	*cap1*Δ::*HygB*	This study
S18 *mrr1*Δ/*cap1*Δ	DH3721	*C. lusitaniae*	S18 *cap1*Δ	*cap1*Δ::*HygB*/*mrr1*Δ::*NAT1*	This study
S18 *mdr1*Δ	DH3722	*C. lusitaniae*	S18	*mdr1*Δ::*HygB*	This study
S18 *mgd1*Δ	DH3723	*C. lusitaniae*	S18	*mgd1*Δ::*NAT1*	This study
S18 *mgd2*Δ	DH3725	*C. lusitaniae*	S18	*mgd2*Δ::*HygB*	This study
S18 *mgd1*Δ/*mgd2*Δ	DH3727	*C. lusitaniae*	S18 *mgd1*Δ	*mgd1*Δ::*NAT1*/*mgd2*Δ::*HygB*	This study
S18 *glo1*Δ	DH3728	*C. lusitaniae*	S18	*glo1*Δ::*NAT1*	This study

SC5314	DH35	*C. albicans*	Wild-type *C. albicans* lab strain	(76)
F2	DH3550	*C. albicans*	Clinical isolate, FLZ-susceptible	(77)
F5	DH3551	*C. albicans*	Clinical isolate, FLZ-resistant	(77)
Wü284	DH2178	*C. dubliniensis*	Clinical isolate	(78)
CM1	DH3575	*C. dubliniensis*	Clinical isolate, FLZ-susceptible	(79)
CM2	DH3576	*C. dubliniensis*	Clinical isolate, FLZ-resistant	(79)
RC-601	DH1989	*C. parapsilosis*	Clinical isolate	(80)
JB6	DH3595	*C. parapsilosis*	CLIB24 *mrr1*Δ + $MRR1^{Q1064P}$	(81)
JB12	DH3596	*C. parapsilosis*	CLIB24 *mrr1*Δ + $MRR1^{K873N}$	(81)
ATCC 6260 (RC-401)	DH1984	*C. guilliermondii*	Clinical isolate	(80)
RC-201	DH1986	*C. glabrata*	Clinical isolate	(80)
ATCC 2001	DH2788	*C. glabrata*	Clinical isolate	(82)
CAU-01	DH2768	*C. auris*	Clinical isolate	(83)
CAU-02	DH2769	*C. auris*	Clinical isolate	(83)
CAU-03	DH2770	*C. auris*	Clinical isolate	(83)
CAU-04	DH2771	*C. auris*	Clinical isolate	(83)
CAU-05	DH2772	*C. auris*	Clinical isolate	(83)
Y533	DH1981	*C. lusitaniae*	Clinical isolate	(84)
RC-301	DH1987	*C. lusitaniae*	Clinical isolate	(80)
UCDFST 80-11	DH3119	*C. lusitaniae*	Environmental isolate	[a]
UCDFST 80-12	DH3120	*C. lusitaniae*	Environmental isolate	[a]
Plasmids in *E. coli* (DH5α)				
$pMQ30^{MRR1\text{-}L1191H+Q1197*}$	DH3829	*E. coli*	$MRR1^{L1191H+Q1197*}$-*HygB* complementation, $Gent^R$	This study
$pMQ30^{MRR1\text{-}Y813C}$	DH3831	*E. coli*	$MRR1^{Y813C}$-*HygB* complementation, $Gent^R$	This study
pNAT	DH2664	*E. coli*	TEF1p-*NAT1*, $Amp/Carb^R$	(85)
pYM70	DH3352	*E. coli*	TEF2p-*HygB*, $Amp/Carb^R$	(72)
pGEM-*URA3*	DH3316	*E. coli*	pGEM-T (Promega) containing *CaURA3,* $Gent^R$	(86)
pMQ30	DH2620	*E. coli*	Plasmid that replicates in *S. cerevisiae* and *E. coli*, using uracil or gentamycin selection, respectively	(73)

[a] UCDFST, Phaff Yeast Culture Collection, Food Science and Technology, University of California Davis; ATCC, American Type Culture Collection.

Table S2.2. Oligonucleotides used in this study

Name	Description	Sequence	Ref
AB001	Forward to make left flank of knockout construct for *MRR1*	5'- AAG GCG TGT CCT TCA TGT T - 3'	(7)
AB003	Reverse to make left flank of knockout construct for *MRR1*	5' - AAC GTC GTG ACT GGG AAA AAT CAT TAG CTT CGC TGG AAT TTC TGT TT - 3'	(7)
AB004	Forward to make right flank of knockout construct for *MRR1*	5' - TAT CCG CTC ACA ATT CCA CTG CTC GGT TCT GGT TCT ATA TG - 3'	(7)
AB006	Reverse to make right flank of knockout construct for *MRR1*	5' - GAG TAC GTG GAT CTC TAC TTG ATG - 3'	(7)
AB007	Nested forward to amplify across stitched *MRR1* knockout construct	5' - CTT TGC TTG TTT GGG AAA CCT C - 3'	(7)
AB008	Nested reverse to amplify across stitched *MRR1* knockout construct	5' - TGG CAT TGA ACC CGG AAA - 3'	(7)
AB009	Forward to amplify *NAT1* for *MRR1* knockout construct	5' - AAA CAG AAA TTC CAG CGA AGC TAA TGA TTT TTC CCA GTC ACG ACG TT - 3'	(7)
AB010	Reverse to amplify *NAT1* for *MRR1* knockout construct	5' - CAT ATA GAA CCA GAA CCG AGC AGT GGA ATT GTG AGC GGA TA - 3'	(7)
ED058	Forward for RT-PCR of *MDR1*	5’ - TCCATCCATGGGTCCATTATTC	(7)
ED059	Reverse for RT-PCR of *MDR1*	5’ – CTCAACACAAGGAAAGCACATC – 3’	(7)
ACT1-F	Forward for RT-PCR of *ACT1*	5’ – GTA TCG CTG AGC GTA TGC AA – 3’	(87)
ACT1-R	Reverse for RT-PCR of *ACT1*	5’ – GAT GGA TGG TCC AGA CTC GT – 3’	(87)
AB023	Forward to make left flank of knockout construct for *MGD1*	5' - CCG AAG AAT GAG CTA CGA GAA T - 3'	This study
AB024	Reverse to make left flank of knockout construct for *MGD1*	5' - AAC GTC GTG ACT GGG AAA AAT CAT TAT TTG GGT TGC TCT CGT GTT - 3'	This study
AB025	Forward to make right flank of knockout construct for *MGD1*	5' - TAT CCG CTC ACA ATT CCA CAA ATC CGG ACA TTG AGG ACT ATC - 3'	This study
AB026	Reverse to make right flank of knockout construct for *MGD1*	5' - CGG AGT ATC GTA TCC CAA CAA TAA - 3'	This study
AB027	Nested forward to amplify across stitched *MGD1* knockout construct	5' - AAC GAA GTG TAT GCA CAT TTG AC - 3'	This study

AB028	Nested reverse to amplify across stitched *MGD1* knockout construct	5' - AGA TCG CAA TCT CCT TAA TGC T - 3'	This study
AB029	Forward to amplify *NAT1* for *MGD1* knockout construct	5' - AAC ACG AGA GCA ACC CAA ATA ATG ATT TTT CCC AGT CAC GAC GTT - 3'	This study
AB030	Reverse to amplify *NAT1* for *MGD1* knockout construct	5' - GAT AGT CCT CAA TGT CCG GAT TTG TGG AAT TGT GAG CGG ATA - 3'	This study
AB039	Forward for RT-PCR of *MGD1*	5' - CGC AGA AAT CCC TAA AGT AAA T - 3'	This study
AB040	Reverse for RT-PCR of *MGD1*	5' - TAC CCT TTG CTT CGT TCT T - 3'	This study
AB043	Forward to make left flank of knockout construct for *GLO1*	5' - GGC ATA TCT GCC ACT AGG AAA G - 3'	This study
AB044	Reverse to make left flank of knockout construct for *GLO1*	5' - AAC GTC GTG ACT GGG AAA AAT CAT TAC TTT AAT AAG CAG GCC GGA GT - 3'	This study
AB045	Forward to make right flank of knockout construct for *GLO1*	5' - TAT CCG CTC ACA ATT CCA TTG TAC GAG GAA GCG AGA A - 3'	This study
AB046	Reverse to make right flank of knockout construct for *GLO1*	5' - CCT TGA TCT TAG GCT CCA ACT T - 3'	This study
AB047	Nested forward to amplify across stitched *GLO1* knockout construct	5' - GAT CGG TGA GTG TGG TTC TTT - 3'	This study
AB048	Nested reverse to amplify across stitched *GLO1* knockout construct	5' - GCC GCC AAT GAA GAT GTT TG - 3'	This study
AB049	Forward to amplify *NAT1* for *GLO1* knockout construct	5' - ACT CCG GCC TGC TTA TTA AAG TAA TGA TTT TTC CCA GTC ACG ACG TT - 3'	This study
AB050	Reverse to amplify *NAT1* for *GLO1* knockout construct	5' - TTC TCG CTT CCT CGT ACA ATG GTG GAA TTG TGA GCG GAT A - 3'	This study
AB051	Forward for RT-PCR of *MGD2*	5' - CAG AGA TAC CTA AAG CCT TT - 3'	This study
AB052	Reverse for RT-PCR of *MGD2*	5' - TCC AAG ATG GTC TGT TGT G - 3'	This study
AB053	Forward to make left flank of knockout construct for *MGD2*	5' – GCT GTA GTC TGT AAG GTT AGG TC - 3'	This study
AB054	Reverse to make left flank of knockout construct for *MGD2* using *NAT1*	5' – AAC GTC GTG ACT GGG AAA AAT CAT TAG GTT CAG GCC ATA TTG ACT TTG - 3'	This study
AB055	Forward to make right flank of knockout construct for *MGD2* using *NAT1*	5' - TAT CCG CTC ACA ATT CCA CGG TTT CAA GCT ACT TAG TGT ATG G -3'	This study

AB056	Reverse to make right flank of knockout construct for *MGD2*	5' – TGA GTA TGA GGA AGG GTG ATA TTC - 3'	This study
AB057	Nested forward to amplify across stitched *MGD2* knockout construct	5' – GCA TTT ATT GGA GTA TTG GAG ATG G - 3'	This study
AB058	Nested reverse to amplify across stitched *MGD2* knockout construct	5' – GTG TTC ATG ATC ATT GGG CAT AG - 3'	This study
AB059	Forward to amplify *NAT1* for *MGD2* knockout construct	5' – CAA AGT CAA TAT GGC CTG AAC CTA ATG ATT TTT CCC AGT CAC GAC GTT - 3'	This study
AB060	Reverse to amplify *NAT1* for *MGD2* knockout construct	5' – CCA TAC ACT AAG TAG CTT GAA ACC GTG GAA TTG TGA GCG GAT A - 3'	This study
AB069	Forward to make left flank of knockout construct for *CAP1*	5' - TCA ACA GAA GTA GTG CCT GTA T - 3'	This study
AB070	Reverse to make left flank of knockout construct for *CAP1* using *NAT1*	5' - AAC GTC GTG ACT GGG AAA AAT CAT TAG CTT TAA CGG CAA GGA GTT AG - 3'	This study
AB071	Forward to make right flank of knockout construct for *CAP1* using *NAT1*	5' - TAT CCG CTC ACA ATT CCA CGA AAC GGA CAG CGT AGT TAG T - 3'	This study
AB072	Reverse to make right flank of knockout construct for *CAP1*	5' - CAG CTT CTC CGT GTA TCG TTT A - 3'	This study
AB073	Nested forward to amplify across stitched *CAP1* knockout construct	5' - CGC TTC TTT ACG CAT TGT AAC C - 3'	This study
AB074	Nested reverse to amplify across stitched *CAP1* knockout construct	5' - CAG CGT ATT CGA CCC ATC TT - 3'	This study
AB075	Forward to amplify *NAT1* for *CAP1* knockout construct	5' - CTA ACT CCT TGC CGT TAA AGC TAA TGA TTT TTC CCA GTC ACG ACG TT - 3'	This study
AB076	Reverse to amplify *NAT1* for *CAP1* knockout construct	5' - ACT AAC TAC GCT GTC CGT TTC GTG GAA TTG TGA GCG GAT A - 3'	This study
AB092	Reverse to make left flank of knockout construct for *CAP1* using *HygB*	5' - GAC GTC AGG TGG CAC TTT TCG GGG GCT TTA ACG GCA AGG AGT TAG - 3'	This study
AB093	Forward to amplify *HygB* for *CAP1* knockout construct	5' - CTA ACT CCT TGC CGT TAA AGC CCC CGA AAA GTG CCA CCT GAC GTC - 3'	This study
AB094	Reverse to amplify *HygB* for *CAP1* knockout construct	5' - ACT AAC TAC GCT GTC CGT TTC GGC CTC GTG ATA CGC CTA TT - 3'	This study
AB095	Forward to make right flank of knockout	5' - AAT AGG CGT ATC ACG AGG CCG AAA CGG ACA GCG TAG TTA GT - 3'	This study

	construct for *CAP1* using *HygB*		
AB122	Forward to amplify *MGD2* MMEJ construct with *HygB*	5' - GCG TAT AAT TAT TCC GTG TAT GTT GAA CTT CGG AAT TAA ACC CAA CGG GGT ATA GTG CTT GCT GTT CGA T - 3'	This study
AB123	Reverse to amplify *MGD2* MMEJ construct with *HygB*	5' - CCT TAA TTG TGC GAA CGT ACA TGA AAT CCT CAG TAT ATC ACA AAT CTT GCA TTT TAT GAT GGA ATG AAT G - 3'	This study
ED038	Forward to make left flank of knockout construct for *MDR1*	5’ – CAG TAG TGT GTT CGT CTC CTT AG – 3’	(7)
ED042	Nested forward to amplify across stitched *MDR1* knockout construct	5’ – CGG CGG AGT TAT ATC CGT TTC – 3’	(7)
ED043	Nested reverse to amplify across stitched *MDR1* knockout construct	5’ – GGC TTC CGT ATT TAA GCT GTA CT – 3’	(7)
ED048	Reverse to make right flank of knockout construct for *MDR1*	5’ – CCG ACC CTC CCA TTC AAT C – 3’	(7)
ED103	Forward to amplify *MRR1* and 1kb upstream w/ homology to pMQ30	5’ – TTT TCC CAG TCA CGA CGT TGT AAA ACG ACG GCC GCG GCC GCA AGG CGT GTC CTT CAT GTT – 3’	This study
ED110	Reverse to amplify 1 kb downstream *MRR1* w/ homology to pMQ30	5’ – CGG ATA ACA ATT TCA CAC AGG AAA CAG CTA TGA CCC GGA GCT TTT CAT CAC CAC CA – 3’	This study
ED115	Reverse to amplify *MRR1* and 1kb upstream w/ homology to *HygB*	5’ – AGC AAT ATC GAA CAG CAA GCA CTA TAT CTA GAG GTT TAC GAC GGA ACT AGC TGC T – 3’	This study
ED121	Forward to amplify *HygB* w/ homology to *MRR1* (swap for *URA3*)	5’ – TAG TTC AAC TCA GCA GCT AGT TCC GTC GTA AAC CTC TAG ATA TAG TGC TTG CTG TTC GAT – 3’	This study
ED122	Reverse to amplify *HygB* w/ homology to *MRR1* downstream (swap for *URA3*)	5’ – CTG ATG TGC CGA TCA ATG AGT CAG AAA CAG CCT GTA TTT TAT GAT GGA ATG AAT GGG ATG – 3’	This study
ED125	Forward upstream of *MRR1* to validate complement	5’ – GAA AAA GAA GCC AGC AGA CC – 3’	This study
ED126	Reverse downstream of *MRR1* to validate complement	5’ – GGG TAA AGC CAT TGC AGA C – 3’	This study
ED187	Reverse to make left flank of knockout construct for *MDR1* using *HygB*	5’ – GCA ATA TCG AAC AGC AAG CAC TAT AGC GAT TAG GTA TTA GAT GGA TGT TTG – 3’	This study
ED188	Forward to amplify *HygB* for *MDR1* knockout construct	5’ – CAA ACA TCC ATC TAA TAC CTA ATC GCT ATA GTG CTT GCT GTT CGA TAT TGC – 3’	This study
ED189	Reverse to amplify *HygB* for *MDR1* knockout construct	5’ – CCT GAA CAA TTA CCT TGT GAA CTC ATT TTA TGA TGG AAT GAA TGG G – 3’	This study

ED190	Forward to make right flank of knockout construct for *MDR1* using *HygB*	5’ – CCC ATT CAT TCC ATC ATA AAA TGA GTT CAC AAG GTA ATT GTT CAG G – 3’	This study
NG_087	Reverse *NAT1* internal, for validation	5’ – GAA GTT CCA GTT GAT CCA CCA TTG A – 3’	(74)
rev seq *NAT1*	Forward *NAT1* internal, for validation	5’ – CGA TGG TAC TGC TTC CGA TGG – 3’	(74)
ED123	Reverse *HygB* internal, for validation	5’ – CAT AAC CTC TAC CAC CAA CAT C – 3’	This study
ED124	Forward *HygB* internal, for validation	5’ – GCT CAA GGT AGA TGT GAT GC – 3’	This study
POP01	Forward to amplify *CaURA3* w/ homology to pNAT	5’ – ACA TCC GAA CAT AAA CAA CCA TGA CAG TCA ACA CTA AG – 3’	This study
POP02	Reverse to amplify *CaURA3* w/ homology to pNAT	5’ – AAT CTT TTT ATT GTC AGT ATT TAT AAT TGG CCA GTT TTT TTC – 3’	This study
POP03	Forward to amplify pNAT, replacing *NAT1* w/ *CaURA3*	5’ – ATA CTG ACA ATA AAA AGA TTC TTG TTT TCA AGA ACT TGT CAT TTG TAT AG – 3’	This study
POP04	Reverse to amplify pNAT, replacing *NAT1* w/ *CaURA3*	5’ – GGT TGT TTA TGT TCG GAT GTG ATG TGA GAA CTG TAT C – 3’	This study
POP18	Reverse to validate pTEF1-*URA3*	5’ - CAG GAA ACA GCT ATG ACC ATG – 3’	This study
POP19	Forward to validate pTEF1-*URA3*	5’ - CGT ACA TTT AGC CCA TAC ATC C – 3’	This study
***MDR1* crRNA**	crRNA for *MDR1*	5’ – AGT CCT TGC TTG GCC ACA GG – 3’	(7)
***MRR1* crRNA**	crRNA for *MRR1*	5’ – TTC ATC ACT AAA GAT GAT GG – 3’	(7)
***CAP1* crRNA**	crRNA for *CAP1*	5’ – AAC CAC ACA CAA AAC CAG GG – 3’	This study
***MGD1* crRNA**	crRNA for *MGD1*	5’ – GGA GAA AGG ATA CTC CGT GG – 3’	This study
***MGD2* crRNA**	crRNA for *MGD2* (used with *NAT1* construct)	5’ – GAA AAA GTT TGC TGA AAA GG– 3’	This study
***MGD2* 5’ crRNA**	crRNA for *MGD2* (used with *HYGB* construct)	5’ – GGG AAA GAC TAC AGA TAA GG – 3’	This study
***MGD2* 3’ crRNA**	crRNA for *MGD2* (used with *HYGB* construct)	5’ – CTA TAC CGA TAA TCT GGA CT – 3’	This study
***GLO1* crRNA**	crRNA for *GLO1*	5’ – TGG CCA CAT TTG TAT CAC GG – 3’	This study
NAT1* *crRNA	crRNA for *NAT1* (making *MRR1* complement strains)	5’ – GGG AAA ACC TTA GTC AAT GG – 3’	This study

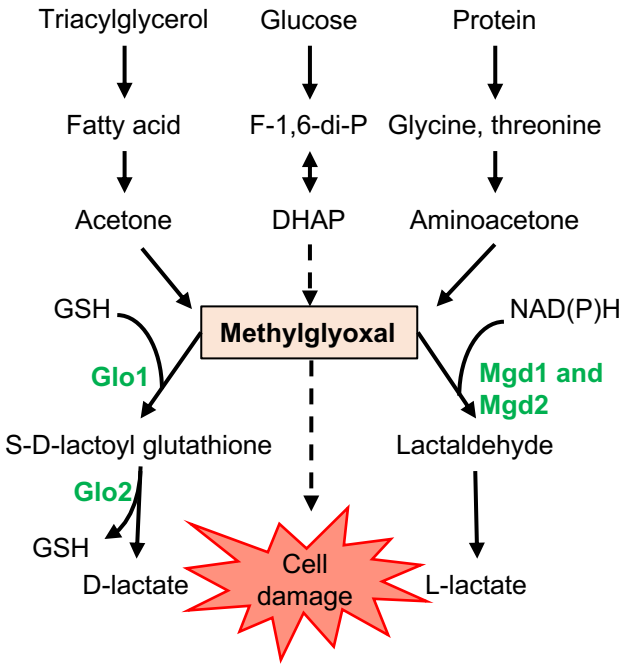

Figure 2.1. Schematic of methylglyoxal (MG) metabolism and catabolism. MG is a highly reactive, toxic product that forms spontaneously during the catabolism of sugars, fatty acids, and proteins. It can be detoxified to D-lactate via the GSH-dependent glyoxalase system, consisting of Glo1 and Glo2, or to lactaldehyde through NAD(P)H-dependent MG reductases such as Mgd1 and Mgd2, which are homologs of C. albicans Grp2. F-1,6-di-P, fructose 1,6-bisphosphate; DHAP, dihydroxyacetone phosphate; GSH, reduced glutathione. Solid arrows represent enzymatic processes; dashed arrows represent nonenzymatic processes.

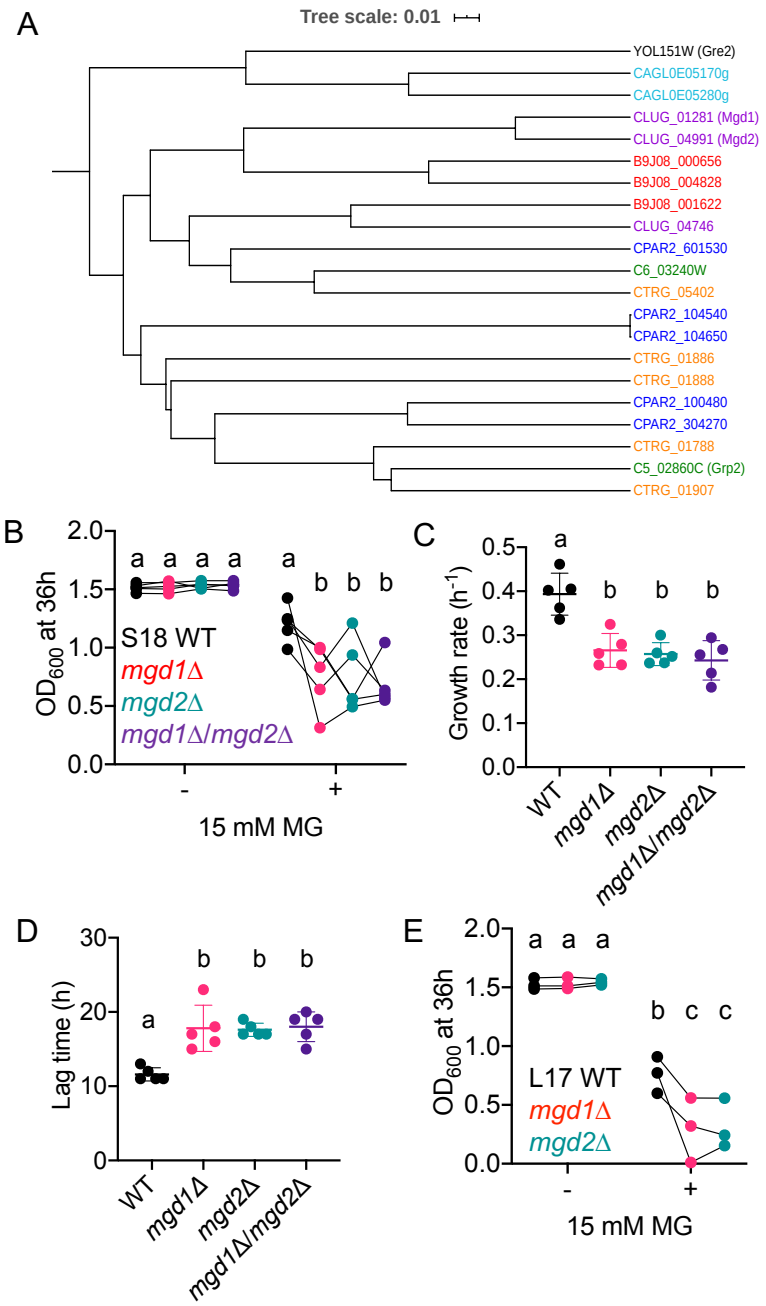

Figure 2.2. *MGD1* and *MGD2* are required for fitness in the presence of high MG. (A) Phylogeny of known and putative MG reductase based on amino acid sequences with homology to *C. albicans* Grp2, *S. cerevisiae* Gre2, and *C. lusitaniae* Mgd1 and Mgd2. *Candida* species is denoted by color: *C. lusitaniae* (purple); *C. auris* (red); *C. tropicalis* (orange); *C. parapsilosis* (blue); *C. glabrata* (teal) and *C. albicans* (green). **(B-D)** Growth

of *C. lusitaniae* S18 WT (black), *mgd1*Δ (red), *mgd2*Δ (teal), and *mgd1*Δ/*mgd2*Δ (purple) strains in YPD with or without 15 mM MG in terms of OD_{600} after 36 h **(B)**, exponential growth rate **(C)**, and lag time **(D)**. Data shown represent the mean ± SD from five independent experiments. **(E)** OD_{600} after 36 h of strain L17 WT (black), *mgd*1Δ (red), and *mgd2*Δ (teal) in YPD with or without 15 mM MG. Data shown represent the mean ± SD from three independent experiments. Ordinary two-way ANOVA with Tukey's multiple comparison test was used for statistical evaluation in **(B)** and **(E)**; a-b, a-c, b-c, $p < 0.05$. Data points connected by line in **(B)** and **(E)** are from the same experiment. Ordinary one-way ANOVA with Tukey's multiple comparison test was used for statistical evaluation in **(C)** and **(D)**; a-b, $p < 0.01$.

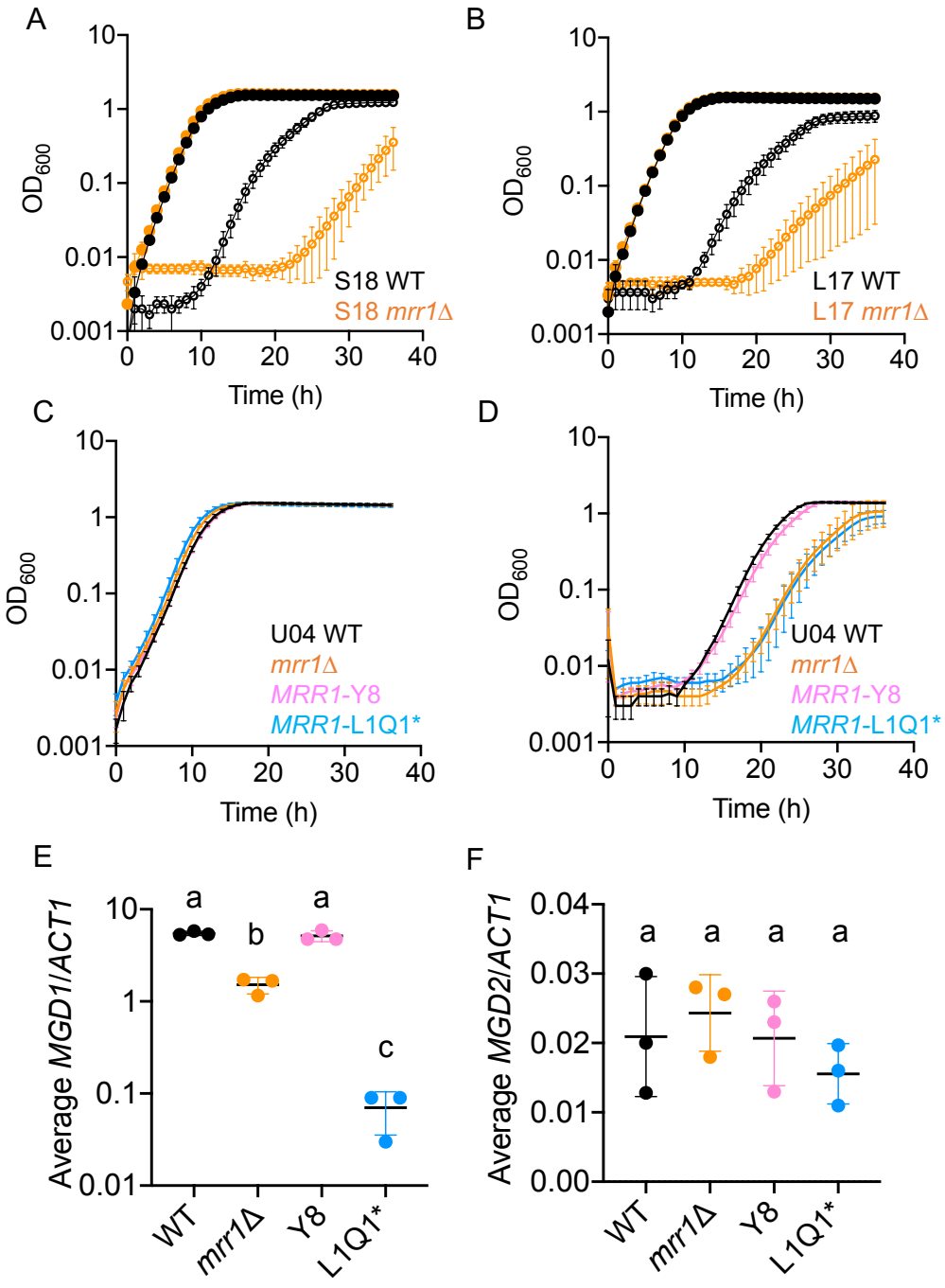

Figure 2.3. Mrr1 regulates MG resistance and basal expression of *MGD1* but not *MGD2*. (A-B) Growth curves of *C. lusitaniae* S18 **(A)** and L17 **(B)** wild type (black) and *mrr1*Δ (orange) in YPD alone (closed circles) or with 15 mM MG (open circles). One representative experiment out of three independent experiments is shown; error bars

represent the standard deviation of technical replicates within the experiment. **(C-D)** Growth curves of *C. lusitaniae* U04 (black), U04 *mrr1*Δ (orange), U04 *mrr1*Δ + $MRR1^{Y8}$ (pink) and U04 *mrr1*Δ + $MRR1^{L1Q1*}$ (light blue) in YPD alone **(C)** or with 15 mM MG **(D)**. One representative experiment out of three independent experiments is shown; error bars represent the standard deviation of technical replicates within the experiment. **(E-F)** Expression of *MGD1* **(E)** and *MGD2* **(F)** in *C. lusitaniae* U04 WT (black), U04 *mrr1*Δ (orange), U04 *mrr1*Δ + $MRR1^{Y8}$ (pink) and U04 *mrr1*Δ + $MRR1^{L1Q1*}$ (light blue). Data shown represent the mean ± SD from three independent experiments. Ordinary one-way ANOVA with Tukey's multiple comparison test was used for statistical evaluation in **(E-F)**; a-b and a-c, $p < 0.0001$; b-c, $p < 0.01$.

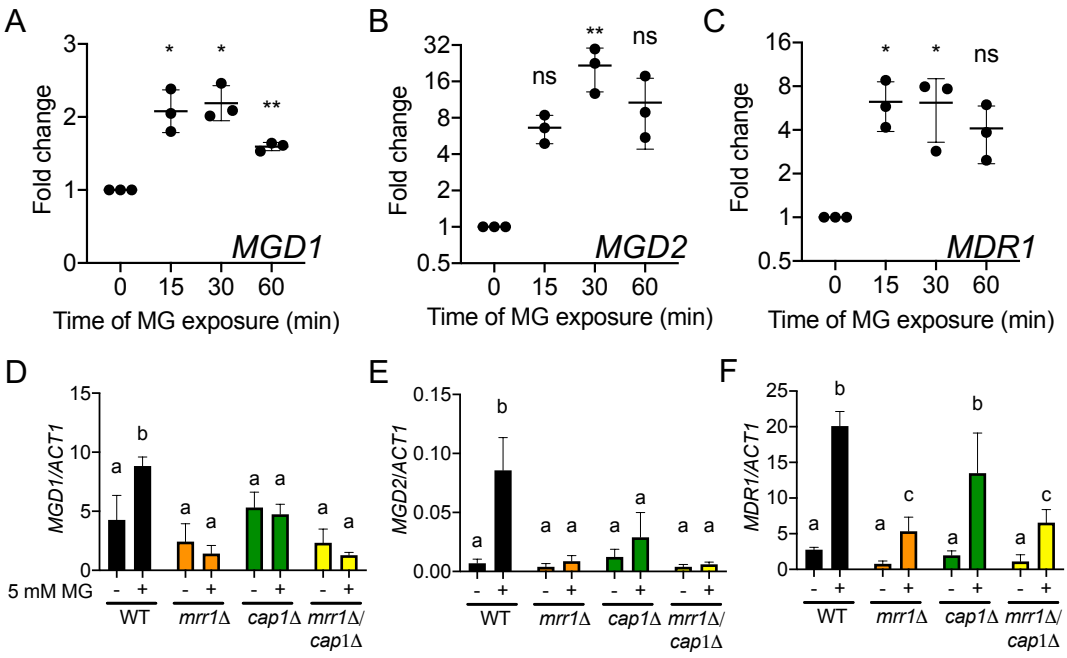

Figure 2.4. Levels of *MGD1*, *MGD2*, and *MDR1* transcripts were increased in response to MG in a partially Mrr1- and Cap1-dependent manner. (A-C) *C. lusitaniae* isolate S18 was grown to exponential phase at 30°C and treated with 5 mM MG for the time indicated prior to analysis of *MGD1* **(A)**, *MGD2* **(B)**, and *MDR1* **(C)** transcript levels by qRT-PCR. Transcript levels are normalized to levels of *ACT1* and presented as ratio at each time point relative to 0 min for three independent experiments. Data shown represent the mean ± SD from three independent experiments. Ordinary one-way ANOVA with Dunnett's multiple comparison test was used for statistical evaluation of each time point compared to 0 min; * $p < 0.05$, ** $p < 0.01$, ns not significant. **(D-F)** *C. lusitaniae* S18 wild type (black) and *mrr1*Δ (orange), *cap1*Δ (green), and *mrr1*Δ/*cap1*Δ (yellow) mutants were grown to exponential phase at 30°C and treated with 5 mM MG for 15 minutes prior to analysis of *MGD1* **(D)**, *MGD2* **(E)**, and *MDR1* **(F)** transcript levels by qRT-PCR. Transcript levels are normalized to *ACT1*. Data shown represent the mean ± SD for three

independent experiments. Ordinary two-way ANOVA with Tukey's multiple comparison test was used for statistical evaluation; a-b, a-c, and b-c $p < 0.05$.

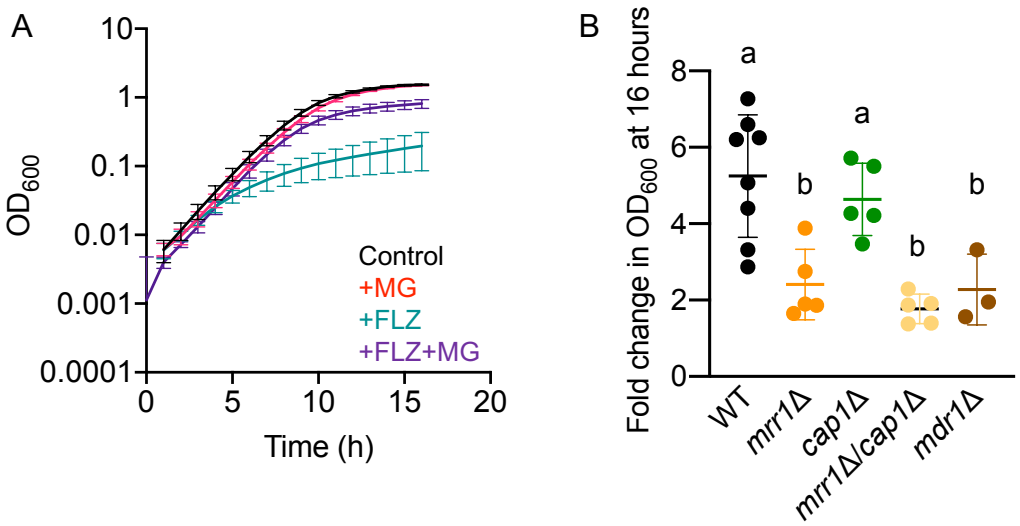

Figure 2.5. MG increases FLZ resistance via Mrr1 and Mdr1. (A) *C. lusitaniae* isolate S18 was grown at 37°C in YPD alone (black), or with 5 mM MG (red), FLZ (equal to the MIC) (teal), or FLZ + 5 mM MG (purple). Data shown represent the mean ± SD for eight independent experiments. **(B)** Fold change in OD_{600} after 16 hours of growth for each indicated strain at 37°C in FLZ versus FLZ + 5 mM MG. Data shown represent the mean ± SD from at least three independent experiments. Ordinary one-way ANOVA with Tukey's multiple comparison test was used for statistical evaluation; a-b, $p < 0.05$.

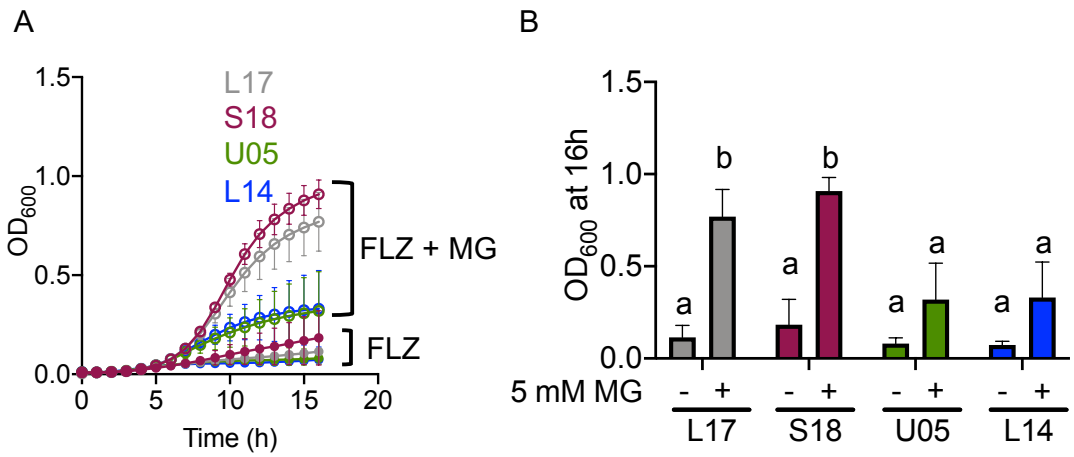

Figure 2.6. Strains with a constitutively active Mrr1 variant show a greater increase in growth with FLZ by MG than strains with low activity Mrr1 variants. *C. lusitaniae* isolates with low activity Mrr1 variants, U05 (green) and L14 (blue), or with constitutively active Mrr1 variants, L17 (grey) and S18 (dark red), were grown at 37°C in YPD with FLZ in the presence or absence of 5 mM MG. **(A)** Growth kinetics of isolates U05, L14, S18, and L17 in FLZ with (open circles) or without (closed circles) 5 mM MG. Data shown represent the mean ± SD from three independent experiments. **(B)** OD_{600} after 16 hours of growth for each indicated strain at 37°C in FLZ with or without 5 mM MG as indicated. Data shown represent the mean ± SD from three independent experiments. Ordinary two-way ANOVA Tukey's multiple comparison test was used for statistical analysis; a-b, $p < 0.05$.

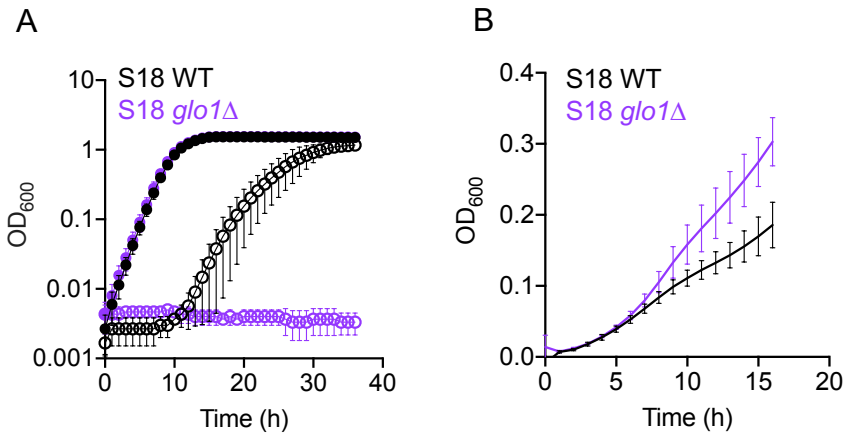

Figure 2.7. The absence of *GLO1*, which encodes a MG catabolizing enzyme, leads to increased sensitivity to MG and increased resistance to FLZ. (A) *C. lusitaniae* S18 wild type (WT, black) and its *glo1*Δ derivative (purple) were grown in YPD with (open circles) or without (closed circles) 15 mM MG. **(B)** Growth of S18 wild type (WT, black) and *glo1*Δ (purple) derivative in YPD with 8 µg mL-1 FLZ. Data shown represent the mean ± SD from three independent experiments.

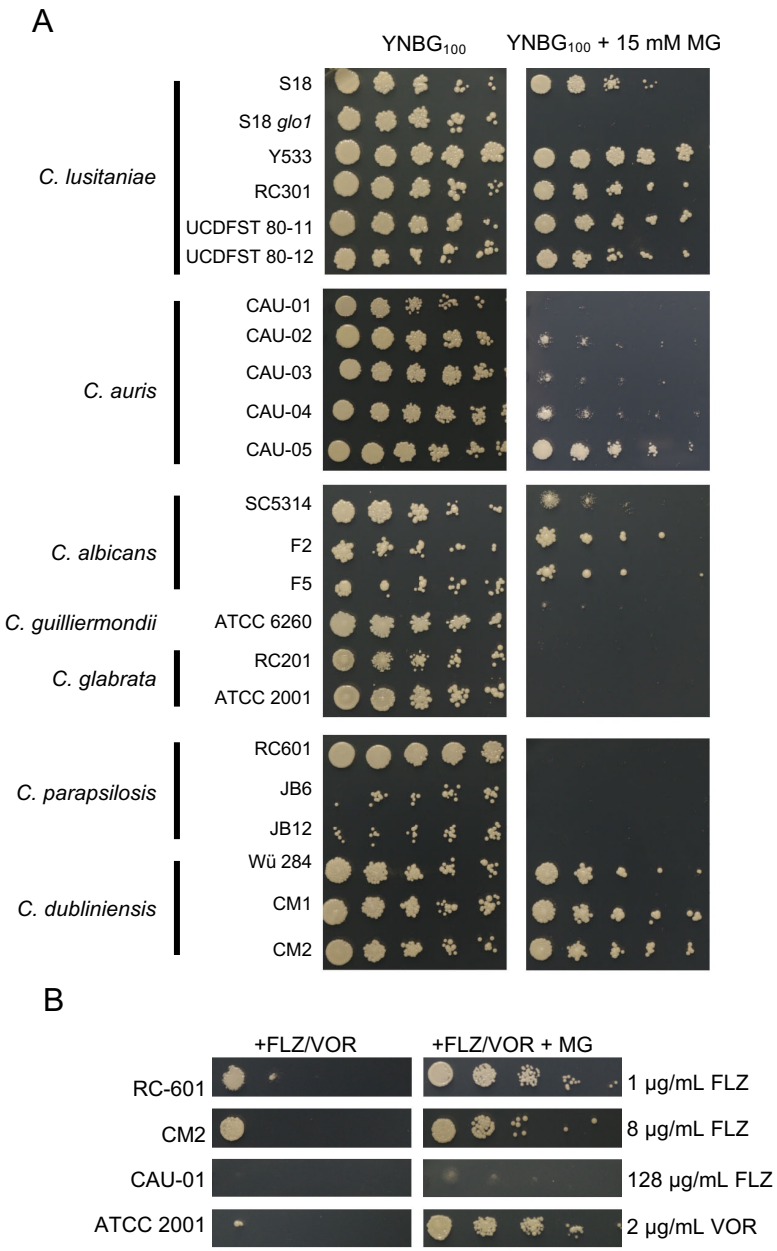

Figure 2.8. MG sensitivity and MG stimulation of azole resistance varies among *Candida* species and strains. (A) Serial 1:10 dilutions of each *Candida* strain were spotted onto $YNBG_{100}$ plates without or with 15 mM MG, then grown at 37°C for two days. One representative out of three independent experiments is shown. **(B)** Serial 1:10 dilutions of *Candida* strains were spotted onto $YNBG_{100}$ plates containing the indicated concentration of FLZ or VOR without or with 3 mM MG. Only strains that demonstrated improved

growth with the presence of 3 mM MG are shown here, the other strains are shown in **Fig. S2.6**. One representative experiment out of two independent experiments is shown.

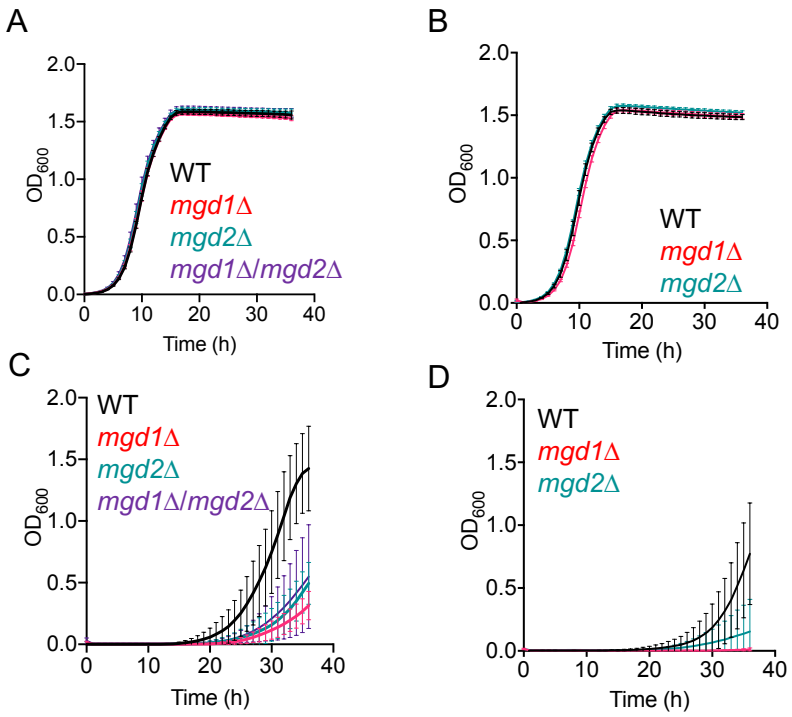

Figure S2.1. 15 mM MG inhibits growth in a strain-dependent manner. Representative growth kinetics for *C. lusitaniae* strains grown in YPD in the absence **(A, B)** or presence **(C, D)** of 15 mM MG. S18 **(A, C)** or L17 **(B, D)** parental (black) and isogenic *mgd1*Δ (red), *mgd2*Δ (teal), and *mgd1*Δ/*mgd2*Δ (purple) mutants are shown. One representative experiment out of three **(B, D)** or five **(A, C)** independent experiments is shown, data summarized in **Fig. 2.2B** and **D**. Error bars indicate the standard deviation of technical replicates from the same experiment.

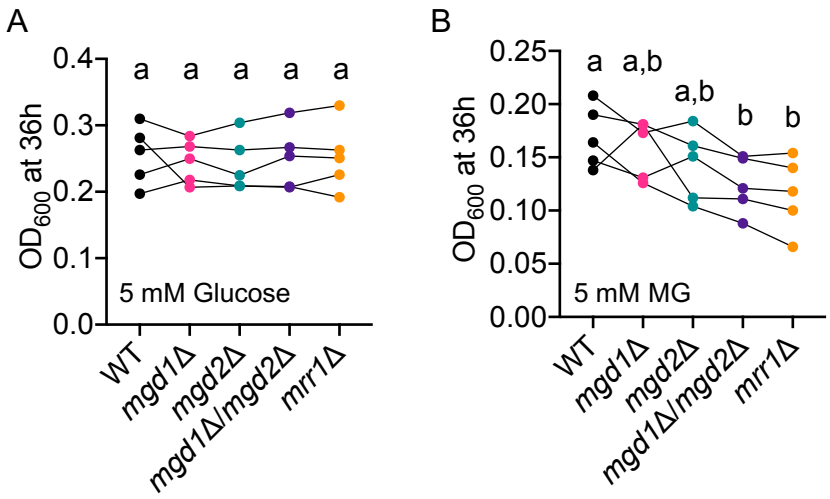

Figure S2.2. *MGD1*, *MGD2*, and *MRR1* play a role in MG catabolism. *C. lusitaniae* S18 strains were grown in YNB medium supplemented with either 5 mM glucose **(A)** or 5 mM MG **(B)**, and OD_{600} was measured after 36 h of growth. RM one-way ANOVA with Geisser-Greenhouse correction and Tukey's multiple comparison test was used for statistical analysis; a-b, a-c, and b-c, $p < 0.05$. Data shown represent the mean OD_{600} at 36 h from each of five independent experiments. Data points connected by line are from the same experiment.

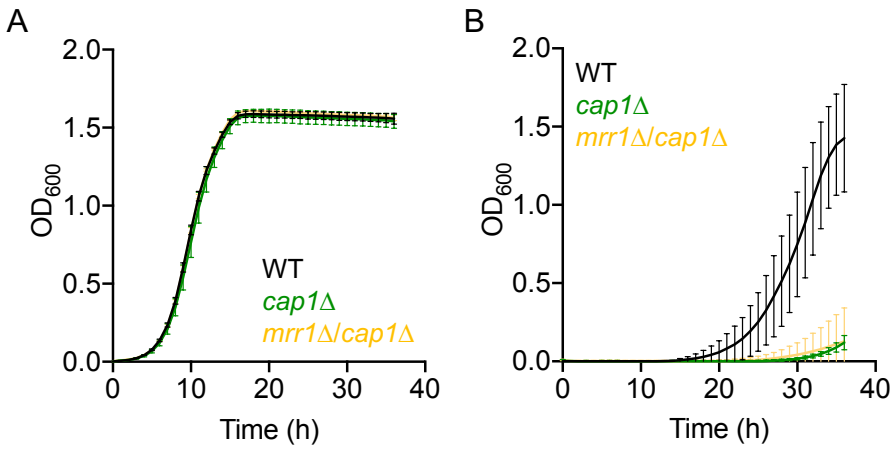

Figure S2.3. Loss of *CAP1* increases sensitivity to high concentrations of exogenous MG regardless of whether *MRR1* is present. *C. lusitaniae* S18 (black), *cap1*Δ (green), and *mrr1*Δ/*cap1*Δ (gold) were grown in YPD alone **(A)** or with 15 mM MG **(B)**. One representative experiment out of three is shown. Error bars indicate the standard deviation of technical replicates from the same experiment.

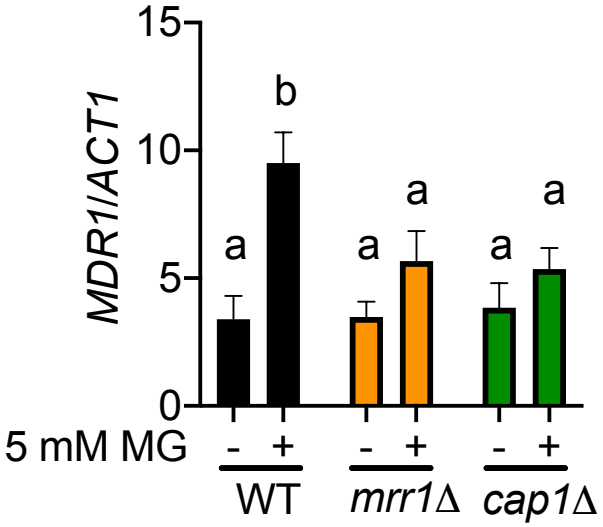

Figure S2.4. *MRR1* and *CAP1* play a role in MG-dependent *MDR1* induction in *C. lusitaniae* isolate L17. Induction of *MDR1* in L17 WT (black), *mrr1*Δ (orange), and *cap1*Δ (green) following 15 minutes of exposure to 5 mM MG in YPD-grown exponential phase cells. Data shown represent the mean ± SD from three independent experiments. Ordinary two-way ANOVA with Tukey's multiple comparison test was used for statistical evaluation; a-b $p < 0.01$.

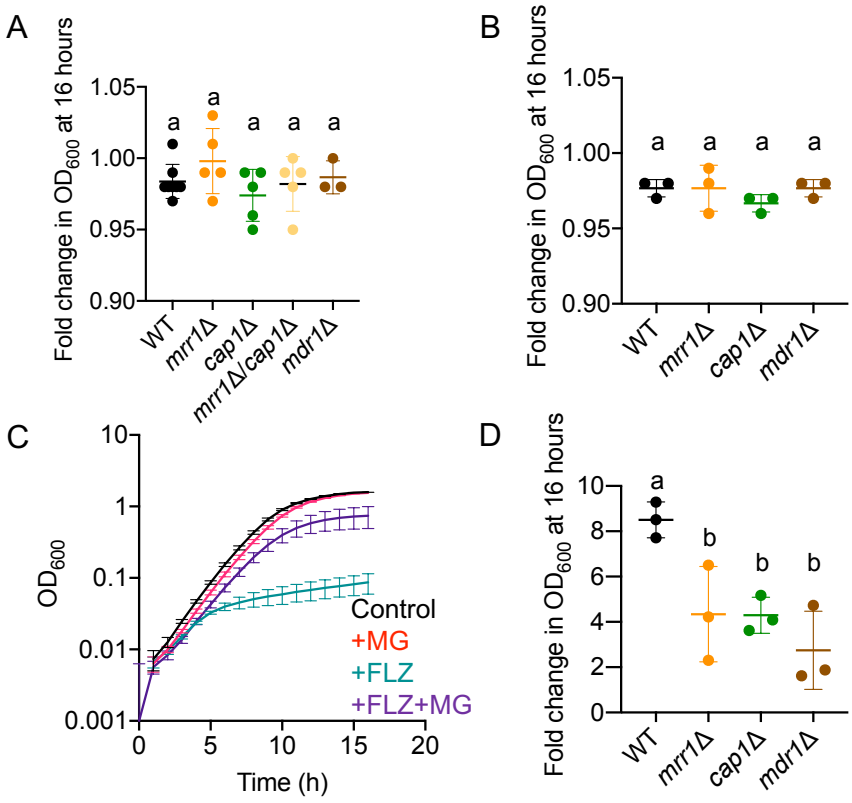

Figure S2.5. 5 mM MG increases growth in FLZ but not in YPD alone in isolates S18 and L17. (A) Fold change in OD_{600} after 16 hours of growth for indicated S18 strains in YPD versus YPD supplemented with 5 mM MG. Data shown represent the mean ± SD from at least three independent experiments. Ordinary one-way ANOVA with Tukey's multiple comparison test was used for statistical evaluation; no strains were significantly different from one another. **(B)** Fold change in OD_{600} after 16 hours of growth for indicated L17 strains in YPD versus YPD supplemented with 5 mM MG. Data shown represent the mean ± SD from three independent experiments. Ordinary one-way ANOVA with Tukey's multiple comparison test was used for statistical evaluation; no strains were significantly different from one another. **(C)** Growth curve for L17 WT in YPD alone (black), or with 5 mM MG (red), FLZ (equal to the MIC) (teal), or FLZ + 5 mM MG (purple). Data shown represent the mean ± SD from three independent experiments. **(D)** Fold difference in OD_{600}

after 16 hours of growth for indicated L17 strains in FLZ alone versus FLZ with 5 mM MG. Data shown represent the mean ± SD from three independent experiments. Ordinary one-way ANOVA with Tukey's multiple comparison test was used for statistical evaluation; a-b, $p < 0.05$.

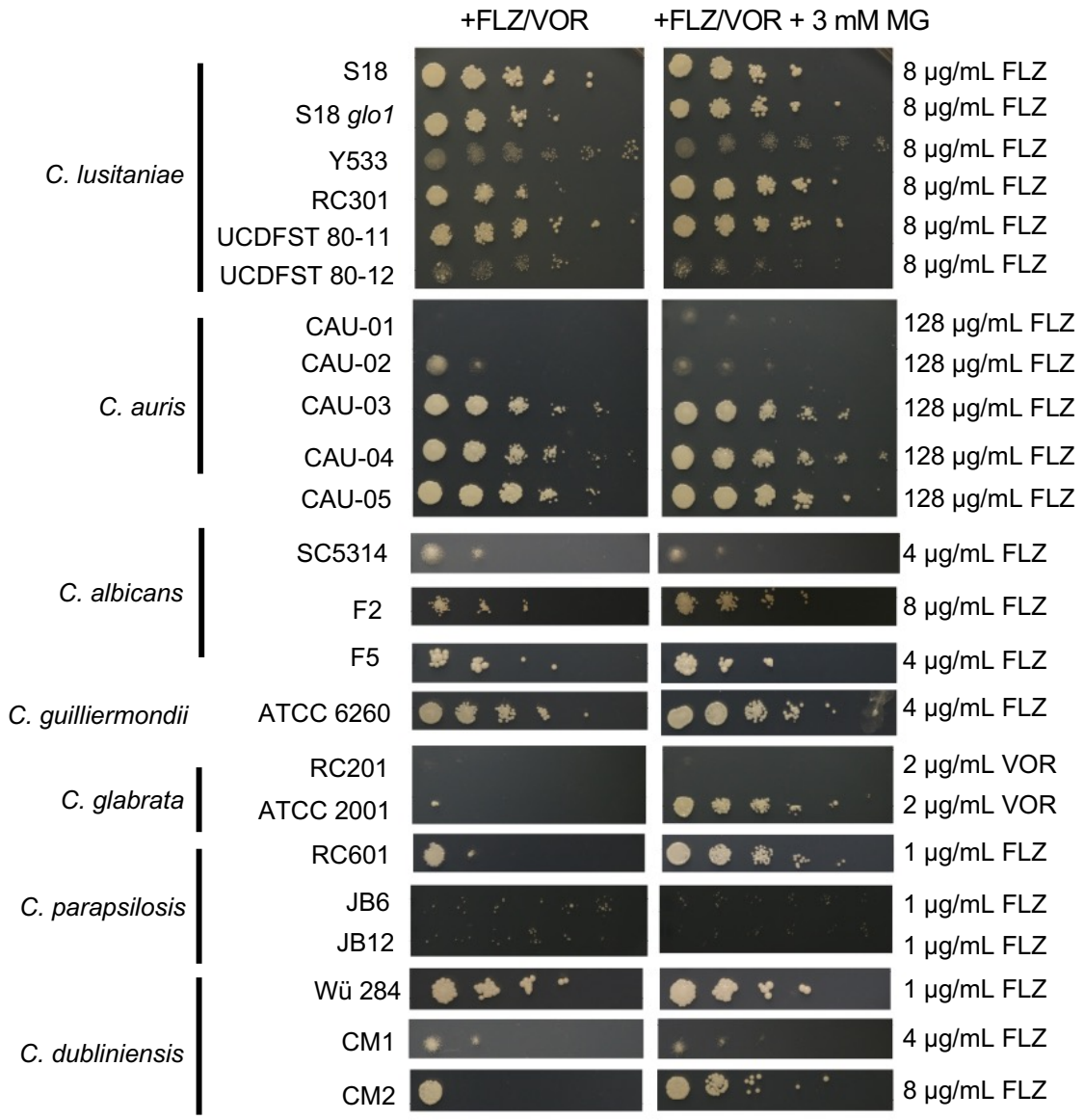

Fig S2.6. Growth of all tested *Candida* strains on azoles with or without 3 mM MG. Serial 1:10 dilutions of each *Candida* strain were spotted onto $YNBG_{100}$ with FLZ or VOR in the absence and presence of 3 mM MG, then grown at 37°C for two days. One representative experiment out of two independent experiments is shown.

References

1. Lamoth F, Lockhart SR, Berkow EL, Calandra T. 2018. Changes in the epidemiological landscape of invasive candidiasis. J Antimicrob Chemother 73:i4-i13.
2. Arendrup MC. 2010. Epidemiology of invasive candidiasis. Curr Opin Crit Care 16:445-52.
3. Nucci M, Perfect JR. 2008. When primary antifungal therapy fails. Clinical Infectious Diseases 46:1426-1433.
4. Hiller D, Sanglard D, Morschhauser J. 2006. Overexpression of the *MDR1* gene is sufficient to confer increased resistance to toxic compounds in *Candida albicans*. Antimicrob Agents Chemother 50:1365-71.
5. Jin L, Cao Z, Wang Q, Wang Y, Wang X, Chen H, Wang H. 2018. *MDR1* overexpression combined with *ERG11* mutations induce high-level fluconazole resistance in *Candida tropicalis* clinical isolates. BMC Infect Dis 18:162.
6. Wirsching S, Moran GP, Sullivan DJ, Coleman DC, Morschhauser J. 2001. *MDR1*-mediated drug resistance in *Candida dubliniensis*. Antimicrob Agents Chemother 45:3416-21.
7. Demers EG, Biermann AR, Masonjones S, Crocker AW, Ashare A, Stajich JE, Hogan DA. 2018. Evolution of drug resistance in an antifungal-naive chronic *Candida lusitaniae* infection. Proc Natl Acad Sci U S A 115:12040-12045.
8. Dunkel N, Blass J, Rogers PD, Morschhauser J. 2008. Mutations in the multi-drug resistance regulator *MRR1*, followed by loss of heterozygosity, are the main cause

of *MDR1* overexpression in fluconazole-resistant *Candida albicans* strains. Mol Microbiol 69:827-40.

9. Schubert S, Rogers PD, Morschhauser J. 2008. Gain-of-function mutations in the transcription factor *MRR1* are responsible for overexpression of the *MDR1* efflux pump in fluconazole-resistant *Candida dubliniensis* strains. Antimicrob Agents Chemother 52:4274-80.

10. Morschhauser J, Barker KS, Liu TT, Bla BWJ, Homayouni R, Rogers PD. 2007. The transcription factor Mrr1p controls expression of the *MDR1* efflux pump and mediates multidrug resistance in *Candida albicans*. PLoS Pathog 3:e164.

11. Liu Z, Myers LC. 2017. *Candida albicans* Swi/Snf and Mediator complexes differentially regulate Mrr1-induced *MDR1* expression and fluconazole resistance. Antimicrob Agents Chemother 61.

12. Mogavero S, Tavanti A, Senesi S, Rogers PD, Morschhauser J. 2011. Differential requirement of the transcription factor Mcm1 for activation of the *Candida albicans* multidrug efflux pump *MDR1* by its regulators Mrr1 and Cap1. Antimicrob Agents Chemother 55:2061-6.

13. Schubert S, Barker KS, Znaidi S, Schneider S, Dierolf F, Dunkel N, Aid M, Boucher G, Rogers PD, Raymond M, Morschhauser J. 2011. Regulation of efflux pump expression and drug resistance by the transcription factors Mrr1, Upc2, and Cap1 in *Candida albicans*. Antimicrob Agents Chemother 55:2212-23.

14. Hampe IAI, Friedman J, Edgerton M, Morschhauser J. 2017. An acquired mechanism of antifungal drug resistance simultaneously enables *Candida albicans* to escape from intrinsic host defenses. PLoS Pathog 13:e1006655.

15. Karababa M, Coste AT, Rognon B, Bille J, Sanglard D. 2004. Comparison of gene expression profiles of *Candida albicans* azole-resistant clinical isolates and laboratory strains exposed to drugs inducing multidrug transporters. Antimicrob Agents Chemother 48:3064-79.

16. Hoehamer CF, Cummings ED, Hilliard GM, Morschhauser J, Rogers PD. 2009. Proteomic analysis of Mrr1p- and Tac1p-associated differential protein expression in azole-resistant clinical isolates of *Candida albicans*. Proteomics Clin Appl 3:968-78.

17. Rogers PD, Barker KS. 2003. Genome-wide expression profile analysis reveals coordinately regulated genes associated with stepwise acquisition of azole resistance in *Candida albicans* clinical isolates. Antimicrob Agents Chemother 47:1220-7.

18. Silva AP, Miranda IM, Guida A, Synnott J, Rocha R, Silva R, Amorim A, Pina-Vaz C, Butler G, Rodrigues AG. 2011. Transcriptional profiling of azole-resistant *Candida parapsilosis* strains. Antimicrob Agents Chemother 55:3546-56.

19. Kannan A, Asner SA, Trachsel E, Kelly S, Parker J, Sanglard D. 2019. Comparative genomics for the elucidation of multidrug resistance in *Candida lusitaniae*. mBio 10.

20. Zuin A, Vivancos AP, Sanso M, Takatsume Y, Ayte J, Inoue Y, Hidalgo E. 2005. The glycolytic metabolite methylglyoxal activates Pap1 and Sty1 stress responses in *Schizosaccharomyces pombe*. J Biol Chem 280:36708-13.

21. Takatsume Y, Izawa S, Inoue Y. 2006. Methylglyoxal as a signal initiator for activation of the stress-activated protein kinase cascade in the fission yeast *Schizosaccharomyces pombe*. J Biol Chem 281:9086-92.

22. Lu J, Randell E, Han Y, Adeli K, Krahn J, Meng QH. 2011. Increased plasma methylglyoxal level, inflammation, and vascular endothelial dysfunction in diabetic nephropathy. Clin Biochem 44:307-11.

23. Wang XJ, Ma SB, Liu ZF, Li H, Gao WY. 2019. Elevated levels of alpha-dicarbonyl compounds in the plasma of type II diabetics and their relevance with diabetic nephropathy. J Chromatogr B Analyt Technol Biomed Life Sci 1106-1107:19-25.

24. McLellan AC, Thornalley PJ, Benn J, Sonksen PH. 1994. Glyoxalase system in clinical diabetes mellitus and correlation with diabetic complications. Clin Sci (Lond) 87:21-9.

25. Brenner T, Fleming T, Uhle F, Silaff S, Schmitt F, Salgado E, Ulrich A, Zimmermann S, Bruckner T, Martin E, Bierhaus A, Nawroth PP, Weigand MA, Hofer S. 2014. Methylglyoxal as a new biomarker in patients with septic shock: an observational clinical study. Crit Care 18:683.

26. Mukhopadhyay S, Ghosh A, Kar M. 2008. Methylglyoxal increase in uremia with special reference to snakebite-mediated acute renal failure. Clin Chim Acta 391:13-7.

27. Lapolla A, Flamini R, Lupo A, Arico NC, Rugiu C, Reitano R, Tubaro M, Ragazzi E, Seraglia R, Traldi P. 2005. Evaluation of glyoxal and methylglyoxal levels in uremic patients under peritoneal dialysis. Ann N Y Acad Sci 1043:217-24.

28. Karg E, Papp F, Tassi N, Janaky T, Wittmann G, Turi S. 2009. Enhanced methylglyoxal formation in the erythrocytes of hemodialyzed patients. Metabolism 58:976-82.

29. Odani H, Shinzato T, Usami J, Matsumoto Y, Brinkmann Frye E, Baynes JW, Maeda K. 1998. Imidazolium crosslinks derived from reaction of lysine with glyoxal and methylglyoxal are increased in serum proteins of uremic patients: evidence for increased oxidative stress in uremia. FEBS Lett 427:381-5.

30. Zhang MM, Ong CL, Walker MJ, McEwan AG. 2016. Defence against methylglyoxal in Group A *Streptococcus*: a role for Glyoxylase I in bacterial virulence and survival in neutrophils? Pathog Dis 74.

31. Stewart BJ, Navid A, Kulp KS, Knaack JLS, Bench G. 2013. D-Lactate production as a function of glucose metabolism in *Saccharomyces cerevisiae*. Yeast 30:81-91.

32. Thornalley PJ. 1990. The glyoxalase system: new developments towards functional characterization of a metabolic pathway fundamental to biological life. Biochem J 269:1-11.

33. Ray M, Ray S. 1984. Purification and partial characterization of a methylglyoxal reductase from goat liver. Biochim Biophys Acta 802:119-27.

34. Chen CN, Porubleva L, Shearer G, Svrakic M, Holden LG, Dover JL, Johnston M, Chitnis PR, Kohl DH. 2003. Associating protein activities with their genes: rapid identification of a gene encoding a methylglyoxal reductase in the yeast *Saccharomyces cerevisiae*. Yeast 20:545-54.

35. Kwak MK, Ku M, Kang SO. 2018. Inducible NAD(H)-linked methylglyoxal oxidoreductase regulates cellular methylglyoxal and pyruvate through enhanced

activities of alcohol dehydrogenase and methylglyoxal-oxidizing enzymes in glutathione-depleted *Candida albicans*. Biochim Biophys Acta Gen Subj 1862:18-39.

36. Stajich JE, Harris T, Brunk BP, Brestelli J, Fischer S, Harb OS, Kissinger JC, Li W, Nayak V, Pinney DF, Stoeckert CJ, Jr., Roos DS. 2012. FungiDB: an integrated functional genomics database for fungi. Nucleic Acids Res 40:D675-81.

37. Basenko EY, Pulman JA, Shanmugasundram A, Harb OS, Crouch K, Starns D, Warrenfeltz S, Aurrecoechea C, Stoeckert CJ, Jr., Kissinger JC, Roos DS, Hertz-Fowler C. 2018. FungiDB: An Integrated Bioinformatic Resource for Fungi and Oomycetes. J Fungi (Basel) 4.

38. Maeta K, Izawa S, Okazaki S, Kuge S, Inoue Y. 2004. Activity of the Yap1 transcription factor in *Saccharomyces cerevisiae* is modulated by methylglyoxal, a metabolite derived from glycolysis. Mol Cell Biol 24:8753-64.

39. Moraru A, Wiederstein J, Pfaff D, Fleming T, Miller AK, Nawroth P, Teleman AA. 2018. Elevated levels of the reactive metabolite methylglyoxal recapitulate progression of type 2 diabetes. Cell Metab 27:926-934 e8.

40. Irshad Z, Xue M, Ashour A, Larkin JR, Thornalley PJ, Rabbani N. 2019. Activation of the unfolded protein response in high glucose treated endothelial cells is mediated by methylglyoxal. Sci Rep 9:7889.

41. Nokin MJ, Bellier J, Durieux F, Peulen O, Rademaker G, Gabriel M, Monseur C, Charloteaux B, Verbeke L, van Laere S, Roncarati P, Herfs M, Lambert C, Scheijen J, Schalkwijk C, Colige A, Caers J, Delvenne P, Turtoi A, Castronovo V, Bellahcene A. 2019. Methylglyoxal, a glycolysis metabolite, triggers metastasis

through MEK/ERK/SMAD1 pathway activation in breast cancer. Breast Cancer Res 21:11.

42. Antognelli C, Moretti S, Frosini R, Puxeddu E, Sidoni A, Talesa VN. 2019. Methylglyoxal Acts as a Tumor-Promoting Factor in Anaplastic Thyroid Cancer. Cells 8.

43. Penninckx MJ, Jaspers CJ, Legrain MJ. 1983. The glutathione-dependent glyoxalase pathway in the yeast *Saccharomyces cerevisiae*. J Biol Chem 258:6030-6.

44. Inoue Y, Kimura A. 1996. Identification of the structural gene for glyoxalase I from *Saccharomyces cerevisiae*. J Biol Chem 271:25958-65.

45. Thornalley PJ. 1996. Pharmacology of methylglyoxal: formation, modification of proteins and nucleic acids, and enzymatic detoxification--a role in pathogenesis and antiproliferative chemotherapy. Gen Pharmacol 27:565-73.

46. Beisswenger PJ, Howell SK, Touchette AD, Lal S, Szwergold BS. 1999. Metformin reduces systemic methylglyoxal levels in type 2 diabetes. Diabetes 48:198-202.

47. Ogasawara Y, Tanaka R, Koike S, Horiuchi Y, Miyashita M, Arai M. 2016. Determination of methylglyoxal in human blood plasma using fluorescence high performance liquid chromatography after derivatization with 1,2-diamino-4,5-methylenedioxybenzene. J Chromatogr B Analyt Technol Biomed Life Sci 1029-1030:102-105.

48. Allaman I, Belanger M, Magistretti PJ. 2015. Methylglyoxal, the dark side of glycolysis. Front Neurosci 9:23.

49. Rosenbach A, Dignard D, Pierce JV, Whiteway M, Kumamoto CA. 2010. Adaptations of *Candida albicans* for growth in the mammalian intestinal tract. Eukaryot Cell 9:1075-86.

50. Liu J, Wang R, Desai K, Wu L. 2011. Upregulation of aldolase B and overproduction of methylglyoxal in vascular tissues from rats with metabolic syndrome. Cardiovasc Res 92:494-503.

51. Masterjohn C, Park Y, Lee J, Noh SK, Koo SI, Bruno RS. 2013. Dietary fructose feeding increases adipose methylglyoxal accumulation in rats in association with low expression and activity of glyoxalase-2. Nutrients 5:3311-28.

52. Ferguson GP, Totemeyer S, MacLean MJ, Booth IR. 1998. Methylglyoxal production in bacteria: suicide or survival? Arch Microbiol 170:209-18.

53. Calabrese D, Bille J, Sanglard D. 2000. A novel multidrug efflux transporter gene of the major facilitator superfamily from *Candida albicans* (*FLU1*) conferring resistance to fluconazole. Microbiology 146 (Pt 11):2743-2754.

54. Li R, Kumar R, Tati S, Puri S, Edgerton M. 2013. *Candida albicans* Flu1-mediated efflux of salivary histatin 5 reduces its cytosolic concentration and fungicidal activity. Antimicrob Agents Chemother 57:1832-9.

55. Harry JB, Oliver BG, Song JL, Silver PM, Little JT, Choiniere J, White TC. 2005. Drug-induced regulation of the *MDR1* promoter in *Candida albicans*. Antimicrob Agents Chemother 49:2785-92.

56. Znaidi S, Weber S, Al-Abdin OZ, Bomme P, Saidane S, Drouin S, Lemieux S, De Deken X, Robert F, Raymond M. 2008. Genomewide location analysis of *Candida*

albicans Upc2p, a regulator of sterol metabolism and azole drug resistance. Eukaryot Cell 7:836-47.

57. Rodrigues CF, Rodrigues ME, Henriques M. 2019. *Candida* sp. infections in patients with diabetes mellitus. J Clin Med 8.

58. Pyrgos V, Ratanavanich K, Donegan N, Veis J, Walsh TJ, Shoham S. 2009. *Candida* bloodstream infections in hemodialysis recipients. Med Mycol 47:463-7.

59. Jawale C, Ramani K, Biswas PS. 2018. Defect in neutrophil function accounts for impaired anti-fungal immunity in kidney dysfunction. Journal of Immunology 200.

60. Kettle AJ, Turner R, Gangell CL, Harwood DT, Khalilova IS, Chapman AL, Winterbourn CC, Sly PD, Arest CF. 2014. Oxidation contributes to low glutathione in the airways of children with cystic fibrosis. Eur Respir J 44:122-9.

61. Dickerhof N, Pearson JF, Hoskin TS, Berry LJ, Turner R, Sly PD, Kettle AJ, Arest CF. 2017. Oxidative stress in early cystic fibrosis lung disease is exacerbated by airway glutathione deficiency. Free Radic Biol Med 113:236-243.

62. Yamauchi S, Kiyosawa N, Ando Y, Watanabe K, Niino N, Ito K, Yamoto T, Manabe S, Sanbuissho A. 2011. Hepatic transcriptome and proteome responses against diethyl maleate-induced glutathione depletion in the rat. Arch Toxicol 85:1045-56.

63. Urban N, Tsitsipatis D, Hausig F, Kreuzer K, Erler K, Stein V, Ristow M, Steinbrenner H, Klotz LO. 2017. Non-linear impact of glutathione depletion on *C. elegans* life span and stress resistance. Redox Biol 11:502-515.

64. Enkvetchakul B, Bottje WG. 1995. Influence of diethyl maleate and cysteine on tissue glutathione and growth in broiler chickens. Poult Sci 74:864-73.

65. Mitchell JB, Russo A, Biaglow JE, Mcpherson SJ. 1983. Cellular glutathione depletion by diethyl maleate or buthionine sulfoximine and its effects on the oxygen enhancement ratio. Radiation Research 94:612-612.

66. Zheng J, Hu CL, Shanley KL, Bizzozero OA. 2018. Mechanism of protein carbonylation in glutathione-depleted rat brain slices. Neurochem Res 43:609-618.

67. Juarez P, Jeannot K, Plesiat P, Llanes C. 2017. Toxic Electrophiles Induce Expression of the Multidrug Efflux Pump MexEF-OprN in *Pseudomonas aeruginosa* through a Novel Transcriptional Regulator, CmrA. Antimicrob Agents Chemother 61.

68. Lee C, Shin J, Park C. 2013. Novel regulatory system *nemRA-gloA* for electrophile reduction in *Escherichia coli* K-12. Mol Microbiol 88:395-412.

69. Hipkiss AR, Chana H. 1998. Carnosine protects proteins against methylglyoxal-mediated modifications. Biochem Biophys Res Commun 248:28-32.

70. Sievers F, Wilm A, Dineen D, Gibson TJ, Karplus K, Li W, Lopez R, McWilliam H, Remmert M, Soding J, Thompson JD, Higgins DG. 2011. Fast, scalable generation of high-quality protein multiple sequence alignments using Clustal Omega. Mol Syst Biol 7:539.

71. Letunic I, Bork P. 2007. Interactive Tree Of Life (iTOL): an online tool for phylogenetic tree display and annotation. Bioinformatics 23:127-8.

72. Basso LR, Jr., Bartiss A, Mao Y, Gast CE, Coelho PS, Snyder M, Wong B. 2010. Transformation of *Candida albicans* with a synthetic hygromycin B resistance gene. Yeast 27:1039-48.

73. Shanks RM, Caiazza NC, Hinsa SM, Toutain CM, O'Toole GA. 2006. Saccharomyces cerevisiae-based molecular tool kit for manipulation of genes from gram-negative bacteria. Appl Environ Microbiol 72:5027-36.

74. Grahl N, Demers EG, Crocker AW, Hogan DA. 2017. Use of RNA-protein complexes for genome editing in non-*albicans Candida* species. mSphere 2.

75. Al Abdallah Q, Ge W, Fortwendel JR. 2017. A Simple and Universal System for Gene Manipulation in *Aspergillus fumigatus*: *In Vitro*-Assembled Cas9-Guide RNA Ribonucleoproteins Coupled with Microhomology Repair Templates. mSphere 2.

76. Gillum AM, Tsay EYH, Kirsch DR. 1984. Isolation of the *Candida-Albicans* gene for orotidine-5'-phosphate decarboxylase by complementation of *S. Cerevisiae* Ura3 and *Escherichia Coli* Pyrf mutations. Molecular & General Genetics 198:179-182.

77. Franz R, Kelly SL, Lamb DC, Kelly DE, Ruhnke M, Morschhauser J. 1998. Multiple molecular mechanisms contribute to a stepwise development of fluconazole resistance in clinical *Candida albicans* strains. Antimicrob Agents Chemother 42:3065-72.

78. Morschhauser J, Ruhnke M, Michel S, Hacker J. 1999. Identification of CARE-2-negative *Candida* albicans isolates as *Candida dubliniensis*. Mycoses 42:29-32.

79. Moran GP, Sullivan DJ, Henman MC, McCreary CE, Harrington BJ, Shanley DB, Coleman DC. 1997. Antifungal drug susceptibilities of oral *Candida dubliniensis* isolates from human immunodeficiency virus (HIV)-infected and non-HIV-

infected subjects and generation of stable fluconazole-resistant derivatives in vitro. Antimicrob Agents Chemother 41:617-23.

80. Alex D, Gay-Andrieu F, May J, Thampi L, Dou DF, Mooney A, Groutas W, Calderone R. 2012. Amino acid-derived 1,2-benzisothiazolinone derivatives as novel small-molecule antifungal inhibitors: identification of potential genetic targets. Antimicrobial Agents and Chemotherapy 56:4630-4639.

81. Branco J, Silva AP, Silva RM, Silva-Dias A, Pina-Vaz C, Butler G, Rodrigues AG, Miranda IM. 2015. Fluconazole and voriconazole resistance in *Candida parapsilosis* is conferred by gain-of-function mutations in *MRR1* transcription factor gene. Antimicrob Agents Chemother 59:6629-33.

82. Gregori C, Schueller C, Roetzer A, Schwarzmuller T, Ammerer G, Kuchler K. 2007. The high-osmolarity glycerol response pathway in the human fungal pathogen *Candida glabrata* strain ATCC 2001 lacks a signaling branch that operates in baker's yeast. Eukaryotic Cell 6:1635-1645.

83. Pathirana RU, Friedman J, Norris HL, Salvatori O, McCall AD, Kay J, Edgerton M. 2018. Fluconazole-resistant *Candida auris* Is susceptible to salivary histatin 5 killing and to intrinsic host defenses. Antimicrobial Agents and Chemotherapy 62.

84. Rex JH, Cooper CR, Jr., Merz WG, Galgiani JN, Anaissie EJ. 1995. Detection of amphotericin B-resistant *Candida* isolates in a broth-based system. Antimicrob Agents Chemother 39:906-9.

85. Min K, Ichikawa Y, Woolford CA, Mitchell AP. 2016. Candida albicans Gene Deletion with a Transient CRISPR-Cas9 System. mSphere 1.

86. Wilson RB, Davis D, Mitchell AP. 1999. Rapid hypothesis testing with Candida albicans through gene disruption with short homology regions. Journal of Bacteriology 181:1868-1874.

87. Asner SA, Giulieri S, Diezi M, Marchetti O, Sanglard D. 2015. Acquired Multidrug Antifungal Resistance in Candida lusitaniae during Therapy. Antimicrob Agents Chemother 59:7715-22.

Chapter 3

Transcriptional response of *Candida auris* to the Mrr1 inducers methylglyoxal and benomyl

Amy R. Biermann, Deborah A. Hogan

Published in mSphere, 2022 Apr 27:e0012422. doi: 10.1128/msphere.00124-22.

3.1 Abstract

Candida auris is an urgent threat to human health due to its rapid spread in healthcare settings and its repeated development of multidrug resistance. Diseases that increase risk for *C. auris* infection, such as diabetes, kidney failure, or immunocompromising conditions, are associated with elevated levels of methylglyoxal (MG), a reactive dicarbonyl compound derived from several metabolic processes. In other *Candida* species, expression of MG reductase enzymes that catabolize and detoxify MG are controlled by Mrr1, a multidrug resistance-associated transcription factor, and MG induces Mrr1 activity. Here, we used transcriptomics and genetic assays to determine that *C. auris MRR1a* contributes to MG resistance, and that the main Mrr1a targets are an MG reductase and *MDR1*, which encodes a drug efflux protein. The *C. auris* Mrr1a regulon is smaller than Mrr1 regulons described in other species. In addition to MG, benomyl (BEN), a known Mrr1 stimulus, induces *C. auris* Mrr1 activity, and characterization of the *MRR1a*-dependent and independent transcriptional responses revealed substantial overlap in genes that were differentially expressed in response to each compound. Additionally, we found that an *MRR1* allele specific to one *C. auris* phylogenetic clade, clade III, encodes a hyperactive Mrr1 variant, and this activity correlated with higher MG resistance. *C. auris*

MRR1a alleles were functional in *Candida lusitaniae* and were inducible by BEN, but not by MG, suggesting that the two Mrr1 inducers act via different mechanisms. Together, the data presented in this work contribute to the understanding Mrr1 activity and MG resistance in *C. auris.*

3.2 Introduction

Although *Candida albicans* has historically been the most prominent *Candida* species associated with both superficial and invasive fungal infections, worldwide incidence of non-albicans *Candida* (NAC) species is increasing (1-10). Of particular concern is *Candida auris*, which the CDC classifies as an urgent threat due to its relatively high frequency of resistance to multiple different classes of drugs including amphotericin B, echinocandins and azoles (reviewed in (11)). Since its recognition as a novel *Candida* species in 2009, *C. auris*, has been reported in at least 40 countries (12-14). Whole-genome sequencing (WGS) analyses of *C. auris* isolates collected from across the globe indicate the concurrent emergence of four genetically distinct clades (15) with a potential fifth clade defined more recently (16). *C. auris* is thought to primarily colonize the skin (17-19) in addition to a diverse array of body sites, and most clinical isolates to date have been isolated from blood (20). Once *C. auris* has disseminated to the bloodstream, it can cause potentially fatal candidemia which has an estimated global mortality rate ranging from about 30 – 60% (15, 21, 22).

The resistance to azoles in *C. auris* is multifactorial; it has been shown that certain mutations in *ERG11* (15, 23-31) and overproduction of Cdr1 (32-36) contribute to resistance to fluconazole (FLZ). In multiple *Candida* species, the transcriptional regulator

Mrr1 also plays a role in FLZ resistance (37-45), and Mayr and colleagues (46) found three *C. auris* homologs of the transcriptional regulator Mrr1, and showed that one of them, *MRR1a*, modestly affected fluconazole resistance. Previously, we demonstrated that in *Candida* (*Clavispora*) *lusitaniae*, which is more closely related to *C. auris* relative to other well-studied *Candida* species (12, 47), Mrr1 regulates the expression of *MDR1*, and overexpression of *MDR1* confers resistance to FLZ (40, 48-55), the host antimicrobial peptide histatin-5 (40, 56), bacterially produced phenazines (40), and other toxic compounds (57) in multiple *Candida* species. *C. lusitaniae* Mrr1 also regulates dozens of other genes with two of the most strongly regulated genes encoding methylglyoxal (MG) reductase enzymes, *MGD1* and *MGD2* (37, 40, 58). Mrr1 contributes to *C. lusitaniae* resistance to MG (58), which is a spontaneously formed dicarbonyl electrophile generated as a byproduct of several metabolic processes by all living cells (reviewed in (59)). Via its carbonyl groups, MG reacts non-enzymatically with biomolecules, which can lead to cellular stress and toxicity (reviewed in (59)). Some of the risk factors (60-69) for candidiasis caused by *C. auris* or other *Candida* spp., such as diabetes (70-72), kidney disease (73-76), or septic shock (77), are associated with elevated MG in human serum. MG resistance across clinical isolates of the same *Candida* species, including *C. auris*, can vary (58).

Through specific regulators, MG and other reactive electrophiles induce stress responses in bacteria (78-80), plants (reviewed in (81)), mammals (reviewed in (82)), and the yeasts *Saccharomyces cerevisiae* (83-87) and *Schizosaccharomyces pombe* (88, 89) at subinhibitory concentrations. We found in *C. lusitaniae*, MG induces expression of *MGD1* and *MGD2* as well as *MDR1*, through a mechanism that involved Mrr1 (58), and that MG

increased fluconazole (FLZ) resistance. *C. auris* displays nosocomial transmission (61-63, 65-69), in part due to its resistance to high temperatures (90) and common surface antiseptics (91), and persistence on abiotic surfaces including latex and nitrile gloves (92), plastics (90), and axillary temperature probes (93). The factors that control *C. auris* stress resistance are not yet known.

In the present study, we show that *C. auris MRR1a* regulates resistance to MG and that MG is an inducer of Mrr1-regulated gene expression. Mrr1a regulates the gene orthologous to the methylglyoxal reductase genes *C. lusitaniae MGD1* in addition to *MDR1*, which regulates FLZ efflux, but the Mrr1a regulon is smaller than that described for other species. Furthermore, we characterize Mrr1a in both Clade I and Clade III isolates and show that the Mrr1 variant in Clade III is constitutively active. Transcriptomics analysis shows that MG elicits a large transcriptional response that is similar in both Clade I and Clade III, and that there are commonalities in the responses elicited by MG and the Mrr1 inducer benomyl. These data support the model that Mrr1 is a regulator of MG resistance in coordination with efflux proteins such as Mdr1 and provides the basis for future studies on the roles of Mrr1 and MG in survival of *C. auris* in hospital settings.

3.3 Results

Mrr1a regulates expression of orthologs to *MDR1* and *MGD1* in *C. auris* strain B11221 and is involved in MG resistance.

To determine whether the *C. auris MRR1* orthologs *MRR1a*, *MRR1b*, and *MRR1c* contributed to resistance to MG, we performed growth kinetic assays in YPD +/- 5 mM, 10 mM, or 15 mM MG. At MG concentrations of 10 mM (**Fig. 3.1A**) and 15 mM (**Fig.**

S3.1), the *mrr1a*Δ mutant displayed a substantial growth defect relative to WT, while the *mrr1b*Δ and *mrr1c*Δ mutants exhibited growth comparable to WT. None of the mutants (*mrr1a*Δ, *mrr1b*Δ, and *mrr1c*Δ) differed from the parental isolate B11221 (WT) in YPD alone or in the presence of 5 mM MG (**Fig. S3.1**). Like *C. lusitaniae*, the *C. auris* genome encodes multiple putative MG reductases; the closest orthologs to *MGD1* and *MGD2* were *CJI97_000658* and *CJI97_004624*, respectively, in the B11221 genome assembly (58) and we will henceforth refer to these genes as *MGD1* and *MGD2*. For reference, *MGD1* and *MGD2* correspond to *B9J08_000656* and *B9J08_004828* respectively in the genome assembly of the *C. auris* reference strain B8441. By quantitative real-time PCR (qRT-PCR), basal expression of *MGD1* was significantly decreased 24-fold in the *mrr1a*Δ mutant relative to B11221 WT (**Fig. 3.1B)**, and expression of *MGD2* trended lower in the *mrr1a*Δ mutant (~1.2-fold) but this difference did not reach statistical significance (**Fig. 3.1C**). *MGD1* was also more highly expressed than *MGD2* in the WT B11221 as in *C. lusitaniae* (58). Consistent with the transcriptional patterns, *C. auris* Mgd1 shares slightly more identity with *C. lusitaniae* Mgd1 than does *C. auris* Mgd2 (63% identity versus 61% identity).

In the *C. auris* B11221 background, expression of *MDR1*, another target of Mrr1 in other species including *C. lusitaniae*, also depended on Mrr1a, as the *mrr1a*Δ mutant exhibited a significant 21-fold decrease in *MDR1* expression compared to the WT parent (**Fig. 3.1D**). These results indicate that in *C. auris MDR1* and *MGD1* are co-regulated, as has been reported in *C. albicans* (44, 45, 94-96), *C. parapsilosis* (97), and *C. lusitaniae* (37, 39, 40, 58, 98) and that higher expression of *MGD1* and/or *MDR1* contributes to growth in high concentrations of MG (**Fig. 3.1A)**.

In *C. lusitaniae* and other *Candida* species, Mrr1 regulates dozens of genes in addition to *MDR1* and *MGD1* (37, 40). To further elucidate the Mrr1a regulon in *C. auris* isolate B11221, we performed an RNA-seq analysis of in B11221 WT and its *mrr1a*Δ derivative in cells from exponential phase cultures grown at 37˚C in YPD. In the control condition (YPD + dH_2O), only four genes, including *MDR1* and *MGD1*, were differentially expressed between the two strains with the cutoff of a $\log_2$ fold change ($\log_2$FC) ≥ 1.00 or ≤ -1.00 and a p-value less than 0.05 (**Fig 3.1E**). *MGD1* and *MDR1* showed a 22- and 24-fold decrease, respectively, in *mrr1a*Δ compared to WT, consistent with our qRT-PCR data. *CJI97_005632*, which was 2.25-fold lower in *mrr1*aΔ, is orthologous to the *C. albicans* genes *RIM11* and *C2_04280W_A*, both of which are predicted to encode proteins with serine/threonine kinase activity, though it is worth noting that levels of the transcript were much lower than levels of *MDR1* and *MGD1*. *CJI97_000852*, which was 2.77-fold higher in *mrr1a*Δ than in WT, has 16 orthologs of diverse predicted or known functions in *C. albicans*, including *USO5*, *USO6*, and *RBF1* (**Fig. 3.1E**). Notably, *MGD2* was not differentially expressed between B11221 WT and the *mrr1a*Δ mutant in our RNA-seq data, consistent with our qRT-PCR results described above.

Mrr1a regulates only *MDR1* and *MGD1* in response to MG and benomyl

We have previously shown in *C. lusitaniae* that MG induces expression of the Mrr1-regulated genes *MGD1* and *MGD2* in an Mrr1-dependent manner, and *MDR1* in a partially Mrr1-dependent manner (58). To determine if MG would induce expression of *MGD1*, *MGD2*, and/or *MDR1* in *C. auris*, we purified RNA for qRT-PCR from exponential-phase cultures of B11221 WT and *mrr1a*Δ treated with 5 mM MG or an equal

volume of dH_2O for 15 minutes. We found that MG treatment significantly enhanced expression of *MGD1* in WT by 2.4-fold but not in *mrr1a*Δ (**Fig. 3.2A**). *MGD1* was also induced by a 30-min treatment with 25 μg/mL benomyl (BEN), a known inducer of Mrr1-regulated genes in other *Candida* species (37, 41, 43, 95, 99-104), by 7.5-fold in the WT (**Fig. 3.2A**). The different treatment times for MG and BEN were used to be consistent with previous studies using either compound in the related species *C. lusitaniae* (37, 58). Expression of *MDR1* was also more highly induced by treatment with either MG or BEN in WT compared to the *mrr1a*Δ mutant by 6- and 14.5- fold respectively (**Fig. 3.2B**). Although *MDR1* expression was significantly induced by MG and BEN in the *mrr1a*Δ, transcript levels of *MDR1* were approximately 20-fold higher in the WT than in the *mrr1a*Δ under these conditions (**Fig. 3.2B**), suggesting that Mrr1a is required for maximum expression of *MDR1* in response to stimuli.

To describe the complete Mrr1-dependent MG- and BEN- response regulon under our test conditions in *C. auris*, we also performed RNA-seq on exponential-phase cultures of B11221 WT and *mrr1a*Δ treated with MG or BEN as described above. In B11221 WT, MG led to the upregulation of 319 genes and downregulation of 133 genes compared to the control condition **(Fig. 3.2C**). In the *mrr1a*Δ mutant, MG led to the upregulation of 349 genes and downregulation of 143 genes compared to the control condition (**Fig. S3.2A**). Consistent with our qRT-PCR data in **Fig. 3.2A**, MG induced expression of *MGD1* in the WT but not in the *mrr1a*Δ mutant (**Table S3.1**). Although expression of *MDR1* was significantly induced by MG in both the WT and the *mrr1a*Δ mutant (**Table S3.1**), levels of *MDR1* were substantially lower in the *mrr1a*Δ mutant even in the presence of MG (**Fig.**

3.2D), also in agreement with our qRT-PCR data. *MGD1* and *MDR1* strongly stood out as the only two genes in the MG response that were strongly dependent on Mrr1a (**Fig. 3.2D**).

Treatment with BEN led to upregulation of 160 genes and downregulation of 163 genes in the WT (**Fig. 3.2E**). In the *mrr1a*Δ mutant, 181 genes were upregulated, and 229 genes were downregulated in response to BEN (**Fig. S3.2B**). Like MG, induction of *MGD1* by BEN was completely dependent on Mrr1a (**Table S3.1**) and *MGD2* expression was not induced by BEN. Expression of *MDR1* was also induced by BEN in both the WT and the *mrr1a*Δ mutant, but as with MG, *MDR1* levels in the *mrr1a*Δ mutant did not reach that of the WT even with BEN treatment **(Fig. 3.2F**). Again, *MGD1* and *MDR1* appear to be the only genes in *C. auris* whose induction of expression by either MG or BEN is dependent on Mrr1a. The Mrr1a-independent responses to MG and BEN are discussed further below.

B11221 has higher basal expression of *MDR1* and of putative MG reductase genes compared to the Clade I isolate AR0390.

Many Clade III isolates, including B11221, contain an N647T single nucleotide polymorphism (SNP) in *MRR1a* (25, 105). In (105), this SNP was proposed to be a gain-of-function mutation due to the resistance of Clade III isolates against azoffluxin, a novel antifungal compound that inhibits expression and activity of *C. auris* efflux pumps. As a first step to determine if there were activity differences between the Mrr1a variant that was found Clade III strains was different from that encoded by the alleles found in Clade I, II, and IV strains, we compared MG sensitivity of B11221 to that of Clade I isolate AR0390. Interestingly, AR0390 grew substantially better than B11221 in the YPD control but showed a greater reduction in growth in YPD with 5 mM MG than did B11221 (**Fig. S3.3**).

At concentrations of 10 mM (**Fig. 3.3A**) and 15 mM MG (**Fig. S3.3**), AR0390 exhibited a profound growth defect compared to B11221. To determine if differences in MG sensitivity were due to differences in *MGD1* expression, we measured basal expression of *MGD1* and its co-regulated gene *MDR1* in B11221 and AR0390 using qRT-PCR. Both genes were significantly more highly expressed in B11221 by 42- and 4.2-fold, respectively (**Fig. 3.3B-C**).

To gain a deeper understanding of the broader transcriptional differences between B11221 and AR0390, we compared the basal global gene expression in YPD of the two strains using RNA-seq. First, we matched the 5227 syntenic orthologs between the genomes of B11221 and the Clade I reference strain B8441 to compare expression of each gene under the control condition. Of these, 755 genes were differentially expressed between B11221 and AR0390 in the control condition ($|\log_2 FC| \geq 1.00$, FDR-corrected $p < 0.05$) (**Fig. 3.3D**). The top twenty differentially expressed genes whose orthologs have known or predicted functions in *C. albicans* are reported in **Table S3.2**. Strikingly, the two genes which exhibited the largest difference in expression between B11221 and AR0390 were *MGD2* ($\log_2 FC = 11.29$) and *MGD1* ($\log_2 FC = 8.53$) (**Fig. 3.3D** and **Table S3.2**). A third gene with homology to MG reductases, *CJI97_001800*/*B9J08_002257*, was also more highly expressed in B11221, although the $\log_2 FC$ in expression of this gene in B11221 vs AR0390 was only 1.41. Low expression of *MGD1*, *MGD2*, and/or *B9J08_002257* may contribute to the severe growth defect of AR0390 in the presence of MG. Consistent with our qRT-PCR data, *MDR1* was also significantly more highly expressed in B11221 relative to AR0390 ($\log_2 FC = 4.42$) (**Fig. 3.3D** and **Table S3.2**). Although *MGD2* and *B9J08_002257* do not appear to be regulated by Mrr1a in our studies,

it is nonetheless interesting to note the elevated expression of three putative MG reductases in the *MDR1*-overexpressing *C. auris* isolate B11221, as the co-expression of *MDR1* with at least one MG reductase has been reported in numerous studies in other *Candida* species (37, 40, 44, 45, 58, 94-97).

Clade III Mrr1a^{N647T} exhibits a gain-of-function phenotype compared to Clade I Mrr1a when expressed in *C. lusitaniae*.

To compare the activities of the proteins encoded by the *MRR1a* alleles of B11221 and AR0390 more directly, we heterologously expressed each allele, henceforth referred to as *CauMRR1a^{N647T}* and *CauMRR1a* respectively, independently in a *C. lusitaniae mrr1*Δ mutant previously generated and characterized by our lab (37, 40, 58). All three *C. lusitaniae* clones expressing *CauMRR1a^{N647T}* which we tested exhibited a four-fold increase in fluconazole (FLZ) MIC relative to the U04 *mrr1*Δ parent (16 µg/mL versus 4 µg/mL), confirming that *C. auris* Clade III *MRR1a* can complement *MRR1*-dependent FLZ resistance in *C. lusitaniae* and adding support to the hypothesis that the N647T substitution in Clade III *MRR1a* confers increased activity. However, the FLZ MIC of the three tested *C. lusitaniae* clones expressing *CauMRR1a* did not differ from that of U04 *mrr1*Δ (4 µg/mL), so FLZ MIC alone could not indicate whether this allele is functional in *C. lusitaniae*. One clone expressing each *C. auris MRR1a* allele was chosen at random for the remaining experiments described in this paper: clone #1 for *CauMRR1a^{N647T}* and clone #5 for *CauMRR1a*. Using qRT-PCR, we then examined basal expression levels of *C. lusitaniae MGD1* (*CLUG_01281*) and *MDR1* (*CLUG_01938/CLUG_01939*) in the heterologous complements and the U04 *mrr1*Δ parent. Complementation with

CauMRR1a^{N647T} conferred a significant increase in basal expression of both *MGD1* (**Fig. 3.3E**) and *MDR1* (**Fig. 3.3F**) compared to the *mrr1*Δ parent, while complementation with *CauMRR1a* led to a small, but significant, decrease in expression of both genes relative to *mrr1*Δ (**Fig. 3.3E-F**). These results are consistent with our previous observations that *C. lusitaniae* strains expressing certain Mrr1 variants with low basal activity demonstrate lower expression of some Mrr1-regulated genes, including *MDR1* and *MGD1*, compared to an isogenic *mrr1*Δ strain suggesting that Mrr1 has both repressing and activating roles (37, 58). Finally, we assessed the relative MG resistance of the isogenic *C. lusitaniae* strains expressing *CauMRR1a*^{N647T} or *CauMRR1a* and the U04 *mrr1*Δ parent. The *CauMRR1a*^{N647T} complement grew markedly better in 15 mM MG compared to U04 *mrr1*Δ whereas the *CauMRR1a* complement grew substantially worse than U04 *mrr1*Δ (**Fig. 3.3G**), consistent with the pattern of *MGD1* expression we observed in these strains via qRT-PCR. None of the *C. lusitaniae* strains demonstrated growth differences in the YPD control, or in the presence of MG at concentrations of 5 mM or 10 mM (**Fig. S3.4**).

MG induces expression of *MGD1* and *MDR1* in *C. auris* B11221 and AR0390, but not in *C. lusitaniae* strains expressing *C. auris MRR1a* alleles.

Next, we compared induction of *MGD1* and *MDR1* by MG in the *C. auris* strains B11221 and AR0390 via qRT-PCR. MG significantly induced expression of *MGD1* by 2.4-fold in *C. auris* strain B11221 and by 4.0-fold in *C. auris* strain AR0390 (**Fig. 3.4A**) and expression of *MDR1* by 6.0-fold in B11221 and 9.3-fold in AR0390 (**Fig. 3.4B**). AR0390 displayed lower expression of both genes in MG, but a higher fold change

compared to B11221, further supporting the hypothesis that the N647T allele is gain-of function.

Finally, we compared induction of *MGD1* and *MDR1* by MG in the isogenic *C. lusitaniae* strains expressing either *CauMRR1a*^{N647T} or *CauMRR1a* and the *mrr1*Δ parent. Additionally, we tested induction by BEN in these strains as a control. While the *mrr1*Δ parent exhibited a significant 1.8- fold induction of *MDR1*, neither *C. lusitaniae* strain expressing a *C. auris* Mrr1a allele demonstrated a significant change in *MGD1* or *MDR1* expression in response to MG (**Fig. 3.4C-D**), indicating that *C. auris* Mrr1a may repress *MRR1*-independent MG induction of *MDR1* in *C. lusitaniae* and that induction of *MGD1* by MG in *C. lusitaniae* requires a functional *MRR1* allele from its own species. Treatment with BEN led to significant increase in expression of *MGD1* (**Fig. 3.4E**) and *MDR1* (**Fig. 3.4F**) in all three *C. lusitaniae* strains. In response to BEN, *MGD1* was induced by 1.9-fold in *mrr1*Δ, 2.9-fold in the *CauMRR1a*^{N647T} complement, and 6.1-fold in the *CauMRR1a* complement (**Fig. 3.4E**). Likewise, expression of *MDR1* was induced by 2.3-fold in *mrr1*Δ, 3.5-fold in the *CauMRR1a*^{N647T} complement, and 5.0-fold in the *CauMRR1a* complement in response to BEN (**Fig. 3.4F**). The striking difference in the ability of the *C. lusitaniae* strains expressing *C. auris MRR1a* alleles to respond to BEN versus MG suggests that there are differences in the mechanisms by which BEN and MG induce Mrr1-dependent transcriptional activation and that MG induction of *C. auris* Mrr1a is not supported by *C. lusitaniae* factors. These potential differences are a topic of future study and may shed light on mechanisms of Mrr1 activation in *Candida* species.

MG and BEN induced Mrr1a-independent transcriptional responses in *C. auris*

We have previously observed heterogeneity in MG resistance as well as MG-induced FLZ resistance among several *C. auris* isolates from different clades (58), and thus we were interested in whether the overall transcriptional response to MG was more similar or different in B11221 and AR0390. AR0390 had greater number of genes differentially expressed by MG compared to B11221; 438 genes were significantly upregulated, and 242 genes were significantly downregulated by MG (see **Fig. S3.5** for the volcano plot of all genes). More genes had a larger fold change in response to MG in AR0390 compared to B11221, including *MGD1* and *MDR1* (**Fig. 3.5A**), consistent with the qRT-PCR results in **Fig. 3.4A-B**. However, there was a large overlap of 254 genes which were induced by MG in both strains (**Fig. 3.5B**), suggesting a common response across these two genetically distinct clades. These commonly induced genes include many with putative roles in amino acid biosynthesis; transmembrane transport; or acquisition and usage of sulfur (**Fig. 3.5C** and **Table S3.3**).

Only 68 genes with syntenic orthologs across both strains were commonly repressed by MG (**Fig 3.5B**). These genes include some with putative roles in metal transport or carbohydrate uptake and metabolism (**Fig. 3.5C** and **Table S3.3**). We did not observe obvious patterns in genes that were only induced or repressed in one strain, and some genes that are listed as only induced or repressed in one strain were close to the cutoff in the other strain.

The groups of genes that were differentially expressed in response to MG in both B11221 and AR0390 were also evident in the response of B11221 to BEN as well as the response of the *mrr1a*Δ mutant in response to MG and BEN. In B11221, a total of 46 genes

exhibited significant induction by both MG and BEN, including *MGD1* and *MDR1*. Many of the 44 other genes have predicted roles in assimilation and biosynthesis of sulfur-containing compounds or xenobiotic transport (**Fig. 3.5C** and **Table S3.1**). MG also induced expression of many genes with predicted roles in the biosynthesis of amino acids. The two genes most highly upregulated upon MG treatment, in terms of fold change, in this strain were orthologous to the arginine biosynthesis genes *ARG3* ($log_2FC = 4.77$) and *ARG1* ($log_2FC = 4.72$) (**Fig. 3.2C** and **Table S3.1**). Conversely, BEN had a limited effect on expression of amino acid biosynthesis genes (**Table S3.1**). There were also common themes among the genes that were significantly repressed by both MG and BEN in B11221. Genes that were repressed by both MG and BEN included four orthologs of the *HGT* glucose transporter family, five genes with a predicted role in uptake of iron and/or copper, and *ERG6*, which encodes an enzyme in the ergosterol biosynthesis pathway (**Fig. 3.5C** and **Table S3.1**). The genes that were repressed by only one stimulus, MG or BEN, also included those involved in ergosterol biosynthesis and the uptake of iron, copper, or glucose (**Fig. 3.5C**, **Table S3.1**). In general, the transcriptional response of the *mrr1a*Δ mutant to MG and BEN was similar to that of B11221 WT (**Fig. S3.2** and **Table S3.1**).

3.4 Discussion

In this work, we have demonstrated that in *C. auris*, the zinc-cluster transcription factor Mrr1a, which is orthologous to Mrr1 in other *Candida* species, strongly regulates expression of a putative MG reductase *MGD1* in addition to *MDR1*, and that Mrr1a plays a role in MG resistance, highlighting a function of Mrr1 that is distinct from antifungal resistance. We also compared basal global gene expression in B11221 and AR0390 and

found that *MDR1*, *MGD1*, and *MGD2* were among the genes significantly more highly expressed in B11221, consistent with the higher MG resistance of this isolate relative to AR0390. These differences were explained by our finding that *MRR1a* from B11221 encoded a higher activity variant than that from AR0390 as evidenced by a higher FLZ MIC, higher expression of *MDR1* and *MGD1*, and higher MG resistance in the strain expressing *CauMRR1a*^{N647T} compared to the isogenic strain expressing *CauMRR1a*. The allele from B11221, which contains an N647T amino acid substitution (25, 105) which is in the central region of the regulator where other gain of function substitutions have been found. Both alleles result in induction of *MDR1* and *MGD1* in response to BEN but not to MG in *C. lusitaniae*, suggesting that these two compounds activate Mrr1-dependent transcription through different mechanisms.

Under the conditions tested, Mrr1a regulation in the *C. auris* B11221 background was mainly of *MGD1* and *MDR1*. Homologs of *MDR1* and at least one gene encoding a known or predicted MG reductase are co-regulated by Mrr1 in *C. albicans* (44, 45, 94-96), *C. parapsilosis* (97), and *C. lusitaniae* (37, 40, 58), suggesting that the co-regulation of these two genes has been conserved throughout multiple *Candida* species. Gaining a deeper understanding of the evolutionary and biochemical relationship between methylglyoxal reductases and efflux pumps, particularly Mdr1, may shed light on how *Candida* species sense and respond to environmental or physiological stresses, evade host defense mechanisms, and develop antifungal resistance. In all other *Candida* species with published Mrr1 regulons, however, Mrr1 appears to regulate expression of many more genes than the four we have described here in the *C. auris* strain B11221 (37, 40, 44, 45, 97). The surprisingly small number of *C. auris* genes whose expression was significantly altered by

genetic deletion of *MRR1a* may be due to possible redundancy between *MRR1a* and the other two *MRR1* orthologs in *C. auris*, *MRR1b* and *MRR1c*, although further studies would be necessary to test this hypothesis. It is striking, however, that *MRR1a* alone seems to be necessary for expression and induction of *MGD1*, which is further supported by our observation that only the *mrr1a*Δ mutant had a growth defect in MG compared to parental B11221 (**Fig. 3.1A**).

Our demonstration of increased basal activity of the *CauMRR1a*^{N647T} allele compared to the allele from AR0390 supports the hypothesis put forth by Iyer et al. (105) that the N647T substitution found in many Clade III isolates is a gain-of-function mutation. Furthermore, this may explain why deletion of *MRR1a* leads to a mild decrease in azole resistance in B11221, but not in the Clade IV isolate B11243 (46). In *C. albicans*, knocking out gain-of-function *MRR1* causes a significant decrease in FLZ resistance, but knocking out *MRR1* with wild-type transcriptional activity does not alter FLZ resistance (41, 44, 45, 106). Similarly, knocking out gain-of-function *MRR1* in *C. lusitaniae* also decreases FLZ resistance, although knocking out *MRR1* alleles that do not encode a constitutively active protein generally leads to increased FLZ resistance (37).

Although Mrr1a does not appear to play a major role in *C. auris* azole resistance (46), our findings suggest that it contributes to resistance against MG, which may be encountered in the host environment. We have previously shown that Mrr1 also contributes to MG resistance in *C. lusitaniae* in a manner that is partially dependent on *MGD1* and *MGD2* (58). Indeed, gain-of-function mutations in *MRR1* may arise in various *Candida* species due to selective pressures other than azoles. In *C. lusitaniae*, we have reported the emergence of gain-of-function mutations in *MRR1* among isolates from a patient with no

prior history of clinical antifungal use (40). In *C. auris*, most sequenced clade III isolates exhibit both the *MRR1a*^{N647T} allele and the *ERG11*^{F126L} allele (25), the latter of which has been shown to be a major contributor to azole resistance (31). Although it is not known whether the *MRR1a* or *ERG11* mutation occurred first in the clade III lineage, it seems plausible that if the *ERG11* mutation did occur first, evolution of the *MRR1a*^{N647T} allele in *C. auris* is likely to be the result of selection for *MGD1* expression and/or an unknown role for Mdr1 that is unrelated to azole resistance. Therefore, we hypothesize that Mrr1 may act, either directly or indirectly, as a response regulator for carbonyl stress in *Candida* species, and future studies will investigate a possible role for Mrr1 in resistance against other physiologically relevant reactive carbonyl compounds.

Curiously, although both variants of *C. auris* Mrr1a were inducible by BEN when expressed in *C. lusitaniae*, they were not inducible by MG under the conditions tested (**Fig. 3.4E-F**). One possible hypothesis for this observation is that Mrr1 must interact with at least one particular binding partner to induce transcription in response to MG, and that *C. auris* Mrr1a does not bind efficiently to this *C. lusitaniae* Mrr1-binding protein or complex. Differential requirements for Mrr1-dependent transcriptional activation by chemical stressors have reported in *C. albicans*. For example, the transcription factor Mcm1 is required for Mrr1-dependent induction of *MDR1* in response to BEN but not to H_2O_2 (101), and the redox-sensing transcription factor Cap1 is required for *MDR1* induction by H_2O_2 and may play a role in *MDR1* induction by BEN (44). Furthermore, gain-of-function Mrr1 in *C. albicans* requires the Swi/Snf chromatin remodeling complex to maintain promoter occupancy, and the kinase Ssn3, which is a subunit of the Mediator complex, may act in opposition to Mrr1 or its coactivators (38). Thus, although *C. auris* Mrr1a can complement

Mrr1-dependent basal and BEN-induced expression of *MDR1* and *MGD1* in *C. lusitaniae*, it may be incompatible with certain elements of the *C. lusitaniae* MG-responsive transcriptional machinery. Further studies on the differences between *C. lusitaniae* and *C. auris* Mrr1, particularly in the presence of MG, may elucidate more detailed mechanisms of Mrr1 activation.

In general, we observed substantial upregulation of genes with predicted roles in transmembrane transport, sulfur metabolism, and amino acid biosynthesis in response to MG in all three strains tested. Many genes downregulated in response to MG in all three strains have predicted roles in metal acquisition, particularly iron, and carbohydrate metabolism. In both B11221 WT and *mrr1a*Δ, BEN treatment led to differential expression of similar groups of genes as MG in addition to induction of genes with predicted roles in oxidative stress response. Our studies of the transcriptional response of *C. auris* to MG and BEN contribute to the understanding of how *Candida* species may adapt to oxidative and/or carbonyl stress, two types of stress that a pathogen is likely to encounter in the host environment. In humans, elevated serum MG has been reported in diabetes as well as in renal failure, which are both risk factors for *Candida* infection (107, 108). There is also evidence that neutrophils (109) and macrophages (110, 111) generate MG during the inflammatory response, consistent with elevated levels of MG in sepsis patients (77). In our transcriptomics analysis of three *C. auris* strains exposed to 5 mM MG for 15 min, upregulation of numerous genes involved in amino acid uptake, metabolism, and biosynthesis was one of the most striking responses to MG (**Table S3.1** for comparison of MG and BEN in B11221 WT and *mrr1a*Δ and **Table S3.2** for the comparison of genes induced by MG in B11221 and/or AR0390). In particular, induction of *ARG* genes is

interesting considering the report that *C. albicans* upregulates expression of arginine biosynthesis genes when phagocytosed by macrophages or in response to sublethal concentrations of hydrogen peroxide, tert-butyl hydroperoxide, or menadione *in vitro* (112). This induction of *ARG* genes in *C. albicans* by macrophages is dependent on the $gp91^{phox}$ subunit of the macrophage oxidase, and thus is likely a direct response to oxidative stress rather than arginine depletion (112). In our dataset, *ARG3* and *ARG1* exhibited the highest $\log_2$FC in response to MG in the B11221 background, independently of *MRR1a* (**Table S3.1**). We also observed, in all three *C. auris* strains, induction of several *MET* genes, which are involved in methionine synthesis and are an important branch of sulfur assimilation in yeast. Other genes involved in sulfur acquisition and assimilation that were induced by MG include the sulfate importer *SUL2*, a gene orthologous to both *CYS3* and *STR3* of *S. cerevisiae*, and numerous genes associated with iron-sulfur cluster formation (**Table S3.1**). A gene orthologous to *MUP1* of *S. cerevisiae* and *C. albicans* was induced by MG in B11221 WT and AR0390 but fell short of the $\log_2\text{FC} \geq 1.00$ cutoff in *mrr1a*Δ (**Table S3.1**). Induction of genes involved in sulfur metabolism, including the *MET* pathway, *SUL2, CYS3*, *STR3*, and *MUP1*, has previously been observed in *Saccharomyces cerevisiae* exposed to 1g/L acetaldehyde (113), another reactive aldehyde metabolite that is structurally similar to MG. Thus, sulfur acquisition and metabolism may be an important part of the carbonyl stress response in yeast.

In the B11221 background, we observed modest overlap in the genes and groups of genes that were up- or down- regulated in response to either MG or BEN. *MDR1* and *MGD1* were among the genes induced by both compounds, and induction of *MGD1* by either MG or BEN was completely dependent on *MRR1a*. Although BEN, which originated

as an agricultural fungicide, is widely recognized as an inducer of expression of Mrr1-regulated genes in *Candida* species (37, 41, 43, 95, 99-104), the mechanism by which this induction occurs is not yet known. BEN is thought to cause oxidative stress in yeast (114, 115), which is consistent with our observation of an upregulation of genes with a predicted role in oxidative stress response in BEN-treated *C. auris* cultures (**Table S3.1**). Additionally, in mammalian cells, BEN exposure has been shown to inhibit aldehyde dehydrogenase enzymes (116-119), which may lead to an accumulation of reactive aldehydes, although this possible mechanism has not yet been investigated in fungi.

We also note similarities between the results of our study of MG- and BEN- treated *C. auris* and the recently published transcriptional analysis of the Clade I *C. auris* strain NCPF 8973 exposed to 75 μM farnesol (120). In response to farnesol, the authors reported upregulation of many genes with predicted roles in transmembrane transport, such as *MDR1* and *CDR1*, and downregulation of numerous genes predicted to be involved in metal acquisition and homeostasis, including multiple ferric reductases and iron permeases (120). As farnesol may cause oxidative stress in *Candida* species (120-123) and in *S. cerevisiae* (124, 125), the overlap in transcriptional changes in response to MG, BEN, and farnesol likely provides valuable insight into how *C. auris* and other *Candida* species sense and adapt to physiologically relevant stressors. In fact, MG itself may serve as a stress signal in various organisms. In plants, for example, intracellular MG increases in response to drought (126, 127), salinity (126, 128-131), cold stress (126), heavy metals (128), or phosphorous deficiency (131), and overexpression of certain genes involved in MG detoxification has been shown to enhance salt tolerance in tobacco (126) and in *Brassica juncea* (132). Investigating whether MG detoxification is linked to abiotic stressors such

as salt, temperature, or desiccation in *Candida* species would be an interesting avenue of future research, particularly in *C. auris* due to its persistence on hospital surfaces and high salt tolerance.

3.5 Methods

Strains, media, and growth conditions

The sources of all strains used in this study are listed in **Table S3.4**. All strains were stored long term in a final concentration of 25% glycerol at -80°C and freshly streaked onto yeast extract peptone dextrose (YPD) agar (10 g/L yeast extract, 20 g/L peptone, 2% glucose, 1.5% agar) once every seven days and maintained at room temperature. Unless otherwise noted, all overnight cultures were grown in 5 mL YPD liquid medium (10 g/L yeast extract, 20 g/L peptone, 2% glucose) on a rotary wheel at 30°C. Media was supplemented with 25 µg/mL BEN (stock 10 mg/ml in DMSO) or 5 mM, 10 mM, or 15 mM MG (Sigma-Aldrich, 5.55 M) as noted. *E. coli* strains were grown in LB with 15 µg/mL gentamycin (gent).

Plasmids for complementation of *C. auris MRR1a*

Plasmids for complementing *C. auris MRR1a* into *C. lusitaniae* were created as follows: the open reading frame of *MRR1a* was amplified from the genomic DNA of *C. auris* isolates B11221 (for $CauMRR1a^{N647T}$) and AR0390 (for *CauMRR1a*) using a forward primer with homology to the 5' flank of *C. lusitaniae MRR1* and a reverse primer with homology to the 3' flank of *C. lusitaniae MRR1* for recombination into the *C. lusitaniae MRR1* complementation plasmid $pMQ30^{MRR1\text{-}L1191H+Q1197*}$ (58). Plasmid $pMQ30^{MRR1\text{-}}$

*L1191H+Q1197** was digested with AscI (New England BioLabs) and AgeI-HF (New England BioLabs). The PCR products and digested plasmid were cleaned using the Zymo DNA Clean & Concentrator kit (Zymo Research) and assembled using the *S. cerevisiae* recombination technique described in (133). Recombined plasmids were isolated from *S. cerevisiae* using a yeast plasmid miniprep kit (Zymo Research) before transformation into NEB®5-alpha competent *E. coli* (New England BioLabs). *E. coli* containing pMQ30-derived plasmids were selected for on LB containing 15 µg/mL gentamycin. Plasmids from *E. coli* were isolated using a Zyppy Plasmid Miniprep kit (Zymo Research) and subsequently verified by Sanger sequencing with the Dartmouth College Genomics and Molecular Biology Shared Resources Core. *MRR1a* complementation plasmids containing the correct sequences were linearized with Not1-HF (New England BioLabs), cleaned up with the Zymo DNA Clean & Concentrator kit (Zymo Research) and eluted in molecular biology grade water (Corning) before transformation of 1.5 µg into *C. lusitaniae* strain U04 *mrr1*Δ as described below. All plasmids and primers used and created in this study are listed in **Table S3.4**.

Transformation of *C. lusitaniae* with *C. auris MRR1a* complementation constructs

Mutants in *C. lusitaniae* were generated using an expression-free CRISPR-Cas9 method as previously described (37, 58, 134). In brief, cells suspended in 1M sorbitol were electroporated immediately following the addition of 1.5 µg of *C. auris MRR1a* complementation plasmid that had been previously linearized with NotI-HF (New England BioLabs) and Cas9 ribonucleoprotein containing crRNA targeting the *NAT1* gene. Transformants were selected on YPD agar containing 600 µg/ml hygromycin B (HygB).

Successful transformants were identified via PCR of the *C. lusitaniae MRR1* locus as previously described (37, 58). CRISPR RNAs (crRNAs; IDT) and primers used to validate transformants are listed in **Table S3.4**.

Minimum Inhibitory Concentration (MIC) Assay

MIC assays for FLZ were performed in RPMI-1640 medium (Sigma, containing L-glutamine, 165 mM MOPS, 2% glucose at pH 7) as described in (40) and (58) using the broth microdilution method. The final concentration of FLZ in each well ranged from 64 µg/mL to 0.125 µg/mL. Plates were incubated at 35°C and scored for growth at 24 and 48 hours; the results are reported in **Table S3.4**. The MIC was defined as the drug concentration that abolished visible growth compared to a drug-free control.

Growth Kinetics

Growth kinetic assays were performed as previously described in (58). In brief, exponential-phase cultures of *C. auris* or *C. lusitaniae* were washed and diluted in dH_2O to an OD_{600} of 1; 60 µL of each diluted cell suspension was added to 5 mL fresh YPD. To each well of a clear 96-well flat-bottom plate (Falcon) was added 100 µL of YPD or YPD with MG at twice the desired final concentration and 100 µL of cell inoculum in YPD. Plates were arranged in technical triplicate for each strain and condition and incubated in a Synergy Neo2 Microplate Reader (BioTek, USA) according to the following protocol: heat to 37°C, start kinetic, read OD_{600} every 60 minutes for 36 hours, end kinetic. Results were calculated in Microsoft Excel and plotted in GraphPad Prism 9.0.0 (GraphPad Software).

Quantitative Real-Time PCR

Overnight cultures of *C. auris* or *C. lusitaniae* were diluted 1:50 into 5 mL fresh YPD, and grown to for four hours at 37°C. To each culture was added MG to a final concentration of 5 mM (4.5 µL stock), BEN to a final concentration of 25 µg/mL (12.5 µL stock), or 4.5 µL molecular biology grade dH_2O. Cultures were returned to the roller drum at 37˚C for 15 min (MG or dH_2O) or 30 min (BEN), then centrifuged at 5000 rpm for 5 min. The differences in time of exposure in the experimental scheme was used to maintain consistency with published experiments in other species, and not because of known differences in kinetics of activity for the two inducers. RNA isolation, gDNA removal, cDNA synthesis, and quantitative real-time PCR were performed as previously described (40). Transcripts were normalized to *C. auris* or *C. lusitaniae ACT1* expression as appropriate. Results were calculated in Microsoft Excel and plotted in GraphPad Prism 9.0.0 (GraphPad Software). Primers are listed in **Table S3.4**.

RNA sequencing

Overnight cultures of *C. auris* were diluted to an OD_{600} of 0.1 in 5 mL fresh, pre-warmed YPD, and incubated on a roller drum at 37˚C for 5-6 doublings (approx. 6 hours). Cultures were diluted once more to an OD_{600} of 1 in 5 mL fresh, pre-warmed YPD and returned to the roller drum at 37˚C for another 5-6 doublings. To each culture was added MG to a final concentration of 5 mM (4.5 µL), BEN to a final concentration of 25 µg/mL (12.5 µL), or 4.5 µL molecular biology grade dH_2O. Cultures were returned to the roller drum at 37˚C for 15 min (MG or dH_2O) or 30 min (BEN), then centrifuged at 5000 rpm for 5 min. Supernatants were discarded and RNA isolation was performed on cell pellets

as described above for qRT-PCR. gDNA was removed from RNA samples as described above. DNA-free RNA samples were sent to the Microbial Genome Sequencing Center (https://www.migscenter.com/) for RNA sequencing.

Analysis of RNAseq

RNAseq data were analyzed by the Microbial Genome Sequencing Center (https://www.migscenter.com/) as follows: Quality control and adapter trimming was performed with bcl2fastq (https://support.illumina.com/sequencing/sequencing_software/bcl2fastq-conversion-software.html). Read mapping was performed with HISAT2 (135). Read quantification was performed using Subread's featureCounts (136) functionality. Read counts were loaded into R (https://www.R-project.org/) and normalized using edgeR's (137) Trimmed Mean of M values (TMM) algorithm. Subsequent values were then converted to counts per million (cpm). Differential expression analysis was performed using edgeR's Quasi Linear F-Test. In the supplementary file, the sheet named "All Quantified Genes" contain the results of the exact test for all genes in addition to the normalized counts per million for all samples. Differentially expressed genes were determined using the cutoff of $|\log_2 FC| > 1$ and $p < .05$.

Identification of orthologs

Orthologs of *C. auris* genes in *C. albicans*, *C. lusitaniae*, and *S. cerevisiae*, as well as orthologs between B11221 and the Clade I reference strain B8441, were identified using FungiDB (https://fungidb.org) (138, 139).

Generation of Venn diagrams

Venn diagrams of differentially expressed genes across different strains and conditions were computed using the Venn diagram tool from UGent Bioinformatics & Evolutionary Genomics, which is accessible at https://bioinformatics.psb.ugent.be/webtools/Venn/.

Statistical analysis and figure preparation

All graphs were prepared with GraphPad Prism 9.0.0 (GraphPad Software). Ratio paired t-tests and one-way ANOVA tests were performed in Prism; details on each test are described in the corresponding figure legends. All p-values were two-tailed and $p < 0.05$ were considered significant for all analyses performed and are indicated with asterisks in the text: * $p < 0.05$, ** $p < 0.01$, *** $p < 0.001$, **** $p < 0.0001$.

Data availability

The data supporting the findings in this study are available within the paper and its supplemental material and are also available from the corresponding author upon request. The raw sequence reads from the RNA-Seq analysis have been deposited into NCBI sequence read archive under BioProject PRJNA801628 (https://www.ncbi.nlm.nih.gov/sra/PRJNA801628).

3.6 Acknowledgements

We thank Joachim Morschhäuser and the FDA-CDC Antimicrobial Resistance Isolate Bank for providing strains. We thank Judith Berman for the pGEM-*URA3* plasmid used for yeast cloning. We thank Elora Demers for primers.

Author contributions. ARB and DAH conceived and designed the experiments and wrote the paper. ARB performed the experiments. ARB and DAH analyzed the data.

Funding. This study was supported by grants R01 5R01 AI127548 to DAH. Core services were provided by STANTO19R0 to CFF RDP, P30-DK117469 to DartCF, and P20-GM113132 to BioMT. Sequencing services and specialized equipment were provided by the Genomics and Molecular Biology Shared Resource Core at Dartmouth, NCI Cancer Center Support Grant 5P30 CA023108-41. The content is solely the responsibility of the authors and does not necessarily represent the official views of the NIH.

Competing interests. The authors have declared that no competing interests exist.

Table S3.1. Select genes differentially expressed in response to MG and/or BEN in the *C. auris* B11221 background. Differentially expressed genes were determined using a cutoff of $|\log_2 FC| \geq 1.00$ and p-value < 0.05.

Sulfur compound assimilation and biosynthesis

Locus Tag	Gene Name	Predicted function	WT MG Log_2FC	WT BEN Log_2FC	*mrr1a*Δ MG Log_2FC	*mrr1a*Δ BEN Log_2FC
CJI97_001242	*AGP3*	Serine transporter	1.06	0.80	1.36	0.42
CJI97_002494	*DUG1*	Glutathione hydrolase	1.42	-0.02	1.38	-0.46
CJI97_001665	*CYS3*	Peroxisomal cystathionine beta-lyase	1.37	0.42	1.39	0.30
CJI97_001939	*CFD1*	Role in Fe-S cluster assembly	-0.02	1.17	0.26	1.31
CJI97_001514	*CIA1*	Role in protein maturation by Fe-S cluster transfer	0.40	1.12	0.34	1.20
CJI97_004156	*DRE2*	Cytosolic Fe-S protein assembly protein	1.09	1.08	1.15	0.98
CJI97_001503	*ECM4*	Cytoplasmic glutathione S-transferase	0.48	1.55	0.33	1.73
CJI97_001382	*ECM17*	Sulfite reductase beta subunit	1.14	0.76	1.45	0.33
CJI97_001705	*GCS1*	Gamma-glutamylcysteine synthetase	0.78	2.00	1.06	1.75
CJI97_003892	*GLR1*	Glutathione reductase	-0.04	1.17	0.06	1.11
CJI97_005081	*GSH2*	Glutathione synthase	1.07	1.41	0.98	1.13
CJI97_003274	*GTO1*	Cytoplasmic glutathione S-transferase	1.39	3.93	1.93	4.27
CJI97_001739	*JLP1*	Sulfonate dioxygenase	0.38	1.44	0.42	1.32
CJI97_002076	*MET1*	Uroporphyrin-3 C-methyltransferase	1.18	1.55	1.99	1.33
CJI97_002761	*MET2*	Homoserine acetyltransferase	2.20	0.49	2.31	0.30
CJI97_004689	*MET8*	Dehydrogenase, ferrochelatase	1.83	0.30	1.65	0.65
CJI97_003625	*MET10*	Sulfite reductase	1.01	0.94	1.31	0.86
CJI97_003066	*MET14*	Adenylylsulfate kinase	1.08	0.27	1.50	0.61
CJI97_005391	*MET16*	3'-phosphoadenylsulfate reductase	1.63	1.44	1.95	1.29
CJI97_003613	*MUP1*	High affinity methionine permease	1.05	0.36	0.94	-0.06

CJI97_004493	*MUP3*	L-methionine transmembrane transporter	0.31	1.65	0.20	1.59
CJI97_004842	N/A	Role in Fe-S cluster assembly	-0.08	1.00	0.08	0.60
CJI97_005600	N/A	Cystathionine gamma-synthase	1.56	0.34	1.45	0.52
CJI97_001635	N/A	Glutathione S-conjugate transporter	0.05	1.10	0.12	0.90
CJI97_000433	*SPE2*	S-adenosylmethionine decarboxylase	1.11	0.19	1.14	0.05
CJI97_000171	*SRX1*	Sulfiredoxin	2.21	3.07	2.03	3.47
CJI97_003300	*STR2*	Cystathionine gamma-synthase	1.15	0.21	1.11	0.15
CJI97_001014	*SUL2*	Sulfate transporter	1.98	1.42	3.01	1.17
CJI97_003257	*TES1*	Acyl-CoA thioesterase	1.27	0.59	1.06	0.38
CJI97_001516	*TRR1*	Thioredoxin reductase	0.40	1.60	0.48	1.82
CJI97_000545	*TRX1*	Thioredoxin	-0.33	1.20	-0.82	2.05

Xenobiotic/Drug Transport

Locus Tag	Gene Name	Predicted function	WT MG Log_2FC	WT BEN Log_2FC	*mrr1a*Δ MG Log_2FC	*mrr1a*Δ BEN Log_2FC
CJI97_002597	*AMF1*	MFS family transporter	0.35	1.28	0.71	1.29
CJI97_000167	*CDR1*	ABC family multidrug transporter	0.30	1.88	0.40	1.76
CJI97_000479	*CDR4*	ABC family multidrug transporter	1.34	1.13	1.27	1.14
CJI97_004181	*ERC1*	Xenobiotic transmembrane transporter	1.47	1.46	1.96	1.44
CJI97_004982	*ESBP6*	MFS membrane transporter	3.97	0.66	3.90	0.20
CJI97_002850	*FLU1*	Multidrug efflux pump of the plasma membrane	0.18	1.25	0.35	1.17
CJI97_002639	*MCH2*	MFS membrane transporter	1.36	0.04	1.24	-0.01
CJI97_000609	*MCH4*	MFS membrane transporter	2.13	0.47	2.14	0.33
CJI97_004042	*MDR1*	Plasma membrane MDR/MFS multidrug efflux protein	3.83	5.60	3.65	6.65
CJI97_000797	N/A	MFS membrane transporter	3.29	1.68	3.17	0.98
CJI97_005702	N/A	ABC family multidrug transporter	1.22	1.94	1.10	2.42
CJI97_005706	N/A	ABC family multidrug transporter	0.86	1.93	0.78	1.99
CJI97_005256	*QDR3*	MFS membrane transporter	2.83	-1.94	2.63	-2.88

CJI97_005513	*ROA1*	PDR-subfamily ABC transporter	2.86	0.05	3.58	0.01
CJI97_001481	*SNQ2*	ABC family multidrug transporter	1.50	2.56	1.34	2.19
CJI97_001817	*VBA1*	MFS transporter	0.68	1.18	0.64	0.95

Amino acid biosynthesis, excluding sulfur-containing amino acids

Locus Tag	Gene Name	Predicted function	WT MG Log_2FC	WT BEN Log_2FC	*mrr1a*Δ MG Log_2FC	*mrr1a*Δ BEN Log_2FC
CJI97_000687	*ARG1*	Argininosuccinate synthase	4.72	0.81	4.63	0.55
CJI97_004654	*ARG3*	Ornithine carbamoyltransferase	4.77	1.52	4.74	0.91
CJI97_002308	*ARG4*	Argininosuccinate lyase	1.75	0.39	1.67	0.21
CJI97_001846	*ARG5, 6*	Arginine biosynthetic enzyme	1.50	0.60	1.46	0.19
CJI97_005293	*ARG8*	Acetylornithine aminotransferase	1.58	0.23	1.67	0.17
CJI97_002234	*ARO1*	Pentafunctional arom enzyme	1.49	-0.06	1.32	-0.20
CJI97_000465	*ARO2*	Chorismate synthase	2.40	0.53	2.37	0.12
CJI97_001597	*ARO3*	3-deoxy-D-arabinoheptulosonate -7-phosphate synthase	1.74	-0.12	1.64	-0.02
CJI97_003954	*ARO4*	3-deoxy-D-arabinoheptulosonate -7-phosphate synthase	2.50	0.36	2.38	0.18
CJI97_003913	*ARO7*	Chorismate mutase	1.51	0.08	1.30	0.37
CJI97_001973	*ASN1*	Asparagine synthetase	2.32	-0.20	2.06	-0.39
CJI97_001997	*BAT21*	Branched chain amino acid aminotransferase	2.51	0.24	2.61	0.10
CJI97_002013	*CPA2*	Carbamoyl-phosphate synthase subunit	1.78	0.15	1.83	-0.37
CJI97_005329	*HIS1*	ATP phosphoribosyl transferase	3.40	0.97	3.27	0.57
CJI97_003017	*HIS3*	Imidazoleglycerol-phosphate dehydratase	3.20	1.31	2.97	1.46
CJI97_003537	*HIS4*	Phosphoribosyl-AMP cyclohydrolase, phosphoribosyl-ATP diphosphatase, and histidinol dehydrogenase	2.86	0.94	2.73	0.33
CJI97_003604	*HIS5*	Histidinol-phosphate aminotransferase	2.72	0.73	2.60	0.49
CJI97_003946	*HIS7*	Imidazole glycerol phosphate synthase	2.39	0.63	2.34	0.55

CJI97_003721	*HOM2*	Aspartate-semialdehyde dehydrogenase	1.52	0.23	1.40	0.20
CJI97_003292	*HOM3*	L-aspartate 4-P-transferase	3.04	0.61	3.08	0.35
CJI97_003178	*ILV1*	Threonine dehydratase	2.06	0.53	1.93	0.28
CJI97_002682	*ILV2*	Acetolactate synthase	2.59	0.23	2.40	-0.17
CJI97_000020	*ILV3*	Dihydroxyacid dehydratase	2.77	0.75	2.60	0.37
CJI97_003514	*ILV5*	Ketol-acid reductoisomerase	1.99	-0.29	2.04	-0.50
CJI97_004523	*ILV6*	Regulatory subunit of acetolacetate synthase	1.50	0.30	1.25	0.31
CJI97_004671	*LEU1*	3-isopropylmalate dehydratase	1.45	-0.06	1.30	-0.31
CJI97_001329	*LEU4*	2-isopropylmalate synthase	4.41	0.44	4.13	-0.12
CJI97_003280	*LYS1*	Saccharopine dehydrogenase	2.89	0.33	2.81	0.11
CJI97_003346	*LYS2*	Alpha-aminoadipate reductase, large subunit	2.47	0.38	2.24	-0.31
CJI97_002417	*LYS4*	Homoaconitase	3.08	1.06	2.92	0.50
CJI97_002151	*LYS5*	Phosphopantetheinyl transferase	2.70	0.24	2.55	0.29
CJI97_001920	*LYS9*	Saccharopine dehydrogenase	1.13	0.07	0.96	-0.06
CJI97_003796	*LYS22*	Homocitrate synthase	2.91	0.07	2.82	-0.33
CJI97_003176	*SER1*	3-phosphoserine aminotransferase	2.11	0.16	2.05	0.15
CJI97_003156	*SER2*	Phosphoserine phosphatase	1.29	0.14	1.34	0.34
CJI97_000320	*SER33*	Enzyme of amino acid biosynthesis	1.05	-0.29	1.03	-0.51
CJI97_003863	*SHM1*	Mitochondrial serine hydroxymethyltransferase	1.30	-0.11	1.22	-0.01
CJI97_001157	*THR1*	Homoserine kinase	1.82	0.41	1.75	0.25
CJI97_000379	*TRP2*	Anthranilate synthase	1.05	0.42	0.91	0.08
CJI97_003979	*TRP3*	Indole-3-glycerol-phosphate synthase, anthranilate synthase	1.33	-0.02	1.27	0.12
CJI97_003855	*TRP4*	Enzyme of amino acid biosynthesis	1.25	0.06	1.17	-0.05
CJI97_003424	*TRP5*	Tryptophan synthase	2.45	0.28	2.25	0.17

Redox homeostasis and stress response

Locus Tag	Gene Name	Predicted function	WT MG Log_2FC	WT BEN Log_2FC	*mrr1a*Δ MG Log_2FC	*mrr1a*Δ BEN Log_2FC
CJI97_001841	*CAT1*	Catalase	0.54	2.49	0.67	2.38
CJI97_003095	*CIP1*	Oxidoreductase	0.51	8.04	1.33	8.70

CJI97_002824	*FDH3*	Oxidoreductase and zinc ion binding activity	-0.61	1.14	1.22	1.22
CJI97_000658	*MGD1*	NAD(H)-linked methylglyoxal oxidoreductase	1.35	2.46	-0.46	0.66
CJI97_002022	N/A	Quinone oxidoreductase	0.36	1.98	0.53	2.18
CJI97_002187	N/A	Oxidoreductase	-0.04	1.07	-0.07	0.97
CJI97_004869	N/A	Oxidoreductase	0.33	1.58	0.16	1.57
CJI97_004704	*POS5*	Mitochondrial NADH kinase	1.41	-0.46	1.54	-0.59
CJI97_004613	*PST3*	Flavodoxin-like protein	0.41	6.37	0.38	6.71
CJI97_000530	*SOD2*	Mitochondrial superoxide dismutase	-0.26	1.02	-0.39	1.41
CJI97_001282	*YAH1*	Oxidoreductase	1.01	0.99	0.87	1.07
CJI97_002560	*YCF1*	Glutathione S-conjugate transporter	4.58	0.85	0.12	0.90
CJI97_004612	*YCP4*	Flavodoxin-like protein	0.63	5.35	0.60	5.61

Ergosterol biosynthesis

Locus Tag	Gene Name	Predicted function	WT MG Log_2FC	WT BEN Log_2FC	*mrr1a*Δ MG Log_2FC	*mrr1a*Δ BEN Log_2FC
CJI97_000262	*ERG1*	Squalene epoxidase	-0.85	-1.43	-0.68	-1.38
CJI97_003811	*ERG3*	C-5 sterol desaturase	-0.96	-1.11	-0.70	-0.73
CJI97_005423	*ERG6*	Delta(24)-sterol C-methyltransferase	-1.01	-1.53	-0.78	-1.09
CJI97_005634	*ERG10*	Acetyl-CoA acetyltransferase	-0.93	-1.04	-1.07	-0.77
CJI97_005638	*ERG10*	Acetyl-CoA acetyltransferase	-1.48	-0.63	-0.71	-1.63
CJI97_001156	*ERG11*	Lanosterol 14-alpha-demethylase	-0.24	-1.40	-0.13	-1.09

Metal acquisition, including regulation

Locus Tag	Gene Name	Predicted function	WT MG Log_2FC	WT BEN Log_2FC	*mrr1a*Δ MG Log_2FC	*mrr1a*Δ BEN Log_2FC
CJI97_002517	*CTR1*	Copper transporter	-1.13	-0.26	-1.24	0.01
CJI97_000015	*FRE7*	Ferric reductase	-1.23	-0.11	-1.43	-0.40
CJI97_003972	*FRE8*	Iron/copper reductase	-1.03	-1.18	-0.90	-1.30
CJI97_004532	*FRP1*	Ferric reductase	-1.41	-1.39	-0.85	-1.66
CJI97_001154	N/A	Ferric or cupric reductase	-0.57	-1.79	-0.97	-2.16
CJI97_004566	N/A	Ferric or cupric reductase	-1.43	-1.46	-1.51	-1.81
CJI97_005148	N/A	Ferric or cupric reductase	-1.56	-0.18	-1.81	-0.50
CJI97_002299	N/A	High affinity iron transporter for intravacuolar stores of iron	-0.19	-1.79	-0.16	-1.54

CJI97_001085	N/A	Transporter of ferrochrome siderophores	-0.06	-1.10	-0.57	-1.83
CJI97_001117	N/A	Transporter of ferrochrome siderophores	-1.90	-2.52	-1.67	-2.30
CJI97_001762	N/A	Transporter of ferrochrome siderophores	-1.94	-2.41	-1.87	-2.31
CJI97_004100	N/A	Transporter of ferrochrome siderophores	-0.26	-1.47	-0.21	-1.70
CJI97_004165	N/A	Transporter of ferrochrome siderophores	0.58	-1.14	0.83	-0.62
CJI97_001499	*SEF1*	Zn2-Cys6 transcription factor, regulates iron uptake	-1.13	0.31	-1.10	0.02
CJI97_000010	*ZRT2*	Zinc transporter	-0.38	-2.50	-0.80	-2.32

Carbohydrate metabolism and biosynthesis

Locus Tag	Gene Name	Predicted function	WT MG Log_2FC	WT BEN Log_2FC	*mrr1a*Δ MG Log_2FC	*mrr1a*Δ BEN Log_2FC
CJI97_003911	*DAC1*	N-acetylglucosamine-6-phosphate deacetylase	-0.35	-2.02	0.20	-2.05
CJI97_005247	*FBP1*	Fructose-1,6-bisphosphatase	-1.33	-1.11	-1.06	-0.96
CJI97_003057	*GLC3*	1,4-glucan branching enzyme	-1.05	-1.86	-0.95	-1.62
CJI97_001045	*GSY1*	Glycogen synthase	-1.17	-1.40	-1.10	-1.25
CJI97_003909	*HXK1*	N-acetylglucosamine kinase	-0.53	-1.15	-0.36	-1.37
CJI97_005579	*MAE1*	Mitochondrial malic enzyme	-1.44	-1.41	-1.36	-1.49
CJI97_000695	*MDH1*	Mitochondrial malate dehydrogenase	-1.23	-0.73	-1.09	-0.51
CJI97_003910	*NAG1*	Glucosamine-6-phosphate deaminase	-0.28	-1.76	0.03	-1.42
CJI97_001805	N/A	Role in beta-1,6 glucan biosynthesis	-1.16	-0.30	-0.95	-0.84
CJI97_000696	*NTH1*	Neutral trehalase	-1.07	-1.46	-1.20	-1.43
CJI97_002722	*PCK1*	Phosphoenolpyruvate carboxykinase	-2.03	-1.92	-1.68	-1.77
CJI97_002654	*PMM1*	Phosphomannomutase	-1.05	-1.33	-1.12	-0.73

Glucose transport, including regulation

Locus Tag	Gene Name	Predicted function	WT MG Log_2FC	WT BEN Log_2FC	*mrr1a*Δ MG Log_2FC	*mrr1a*Δ BEN Log_2FC
CJI97_000584	*HGT16*	MFS glucose transporter	1.38	-1.96	1.28	-2.14

CJI97_002713	*HGT17*	MFS glucose transporter	0.76	-3.05	-0.60	-2.46
CJI97_005108/ CJI97_005109	*HGT19*	MFS glucose/myo-inositol transporter	-1.71	-2.78	-1.95	-2.14
CJI97_001793	N/A	MFS glucose transporter	-2.00	-6.23	-2.27	-4.76
CJI97_001794	N/A	MFS glucose transporter	0.85	-2.17	-0.21	-1.41
CJI97_002023	N/A	MFS glucose transporter	-1.57	-5.00	-1.58	-5.13
CJI97_002024	N/A	MFS glucose transporter	-2.02	-2.80	-1.69	-2.70
CJI97_002448	*RGT1*	Transcriptional repressor of glucose transport	-1.26	-1.50	-1.29	-1.56
CJI97_005617	*SHA3*	Ser/thr kinase involved in glucose transport	-1.14	-0.65	-0.87	-1.09

Table S3.2. Top 20 genes with predicted functions differentially expressed between *C. auris* isolates B11221 and AR0390 in the control condition. Differentially expressed genes were determined using a cutoff of $|\log_2 FC| \geq 1.00$ and p-value < 0.05.

Genes more highly expressed in B11221

B11221 Locus Tag	AR0390 Locus Tag	Gene Name	Predicted Function	Log_2FC (B11221 vs AR0390)	B11221 average (CPM)	AR0390 average (CPM)
CJI97_004624	*B9J08_004828*	*MGD2*	NAD(H)-linked methylglyoxal oxidoreductase	11.29	1657	0.66
CJI97_000658	*B9J08_000656*	*MGD1*	NAD(H)-linked methylglyoxal oxidoreductase	8.53	4335	11.7
CJI97_004768	*B9J08_004684*	N/A	Role in histone deacetylation	7.87	51.9	0.22
CJI97_000946	*B9J08_000928*	*AQY1*	Aquaporin water channel, osmotic shock resistance	7.33	581	3.60
CJI97_004767	*B9J08_004685*	N/A	Curved DNA-binding protein	5.36	279	6.78
CJI97_003833	*B9J08_003761*	N/A	DNA topoisomerase	5.31	96.8	2.43
CJI97_002880	*B9J08_002824*	N/A	DNA replication licensing factor required for pre-replication complex assembly	4.49	316	14.1
CJI97_004042	*B9J08_003981*	*MDR1*	Plasma membrane MDR/MFS multidrug efflux pump	4.42	190	8.88
CJI97_002740	*B9J08_002688*	*FDH1*	Formate dehydrogenase	4.33	131	6.50
CJI97_004770	*B9J08_004682*	*ECM42*	Ornithine acetyltransferase	4.24	99.9	5.28

Genes more highly expressed in AR0390

B11221 Locus Tag	AR0390 Locus Tag	Gene Name	Predicted Function	Log_2FC (B11221 vs AR0390)	B11221 average (CPM)	AR0390 average (CPM)
CJI97_001302	*B9J08_001303*	*BDF1*	Essential chromatin-binding bromodomain protein	-10.21	0.48	563
CJI97_004515	*B9J08_004451*	N/A	ALS family protein	-9.61	1.98	1546
CJI97_004556	*B9J08_005565*	*PRD1*	Proteinase	-7.29	0.14	22.6
CJI97_001865	*B9J08_002322*	*BMH1*	Role in morphology	-7.01	12.7	1639
CJI97_002974	*B9J08_002900*	*RMD9*	Mitochondrial protein with a predicted role in respiratory growth	-6.86	6.41	745

CJI97_003073	*B9J08_003002*	N/A	Iron permease	-6.51	36.8	3350
CJI97_002817	*B9J08_002762*	*INO1*	Inositol-1-phosphate synthase	-5.48	28.7	1281
CJI97_004514	*B9J08_004450*	*THI13*	Thiamin pyrimidine synthase	-4.95	2.34	72.4
CJI97_004654	*B9J08_004798*	*ARG3*	Ornithine carbamoyltransferase	-4.95	0.70	21.5
CJI97_000838	*B9J08_000820*	*SAM4*	S-adenosylmethionine-homocysteine methyltransferase	-4.43	1.93	41.5

Table S3.3. Comparison of select genes differentially expressed in response to MG in *C. auris* isolates B11221 and/or AR0390. Differentially expressed genes were determined using a cutoff of $|Log_2FC| \geq 1.00$ and p-value < 0.05.

B11221 Locus Tag	AR0390 Locus Tag	Gene Name	Predicted Function	B11221 Log_2FC	AR0390 Log_2FC
CJI97_005163	*B9J08_005078*	*AAH1*	Adenine deaminase, purine salvage and nitrogen catabolism	0.29	1.10
CJI97_002719	*B9J08_002666*	*AGP2*	Amino acid permease	0.45	1.16
CJI97_001242	*B9J08_001362*	*AGP3*	Serine transporter; sulfur assimilation	1.06	0.00
CJI97_004654	*B9J08_004798*	*ARG3*	Ornithine carbamoyltransferase	4.77	3.02
CJI97_003828	*B9J08_003754*	*ARG11*	Ornithine transporter of the mitochondrial inner membrane	0.94	1.70
CJI97_003954	*B9J08_003882*	*ARO4*	3-deoxy-D-arabinoheptulosonate-7-phosphate synthase; aromatic amino acid biosynthesis	2.50	2.22
CJI97_001997	*B9J08_002453*	*BAT21*	Branched chain amino acid aminotransferase	2.51	2.56
CJI97_005185	*B9J08_005101*	*BNA1*	3-hydroxyanthranilic acid dioxygenase; NAD biosynthesis	1.54	-0.33
CJI97_000479	*B9J08_000479*	*CDR4*	ABC transporter superfamily	1.34	1.01
CJI97_003095	*B9J08_003024*	*CIP1*	Oxidoreductase	0.51	1.30
CJI97_004156	*B9J08_004088*	*DRE2*	Cytosolic Fe-S protein assembly protein	1.09	2.52
CJI97_004181	*B9J08_004118*	*ERC1*	Xenobiotic transmembrane transporter	1.47	0.00
CJI97_002824	*B9J08_002769*	*FDH3*	Oxidoreductase and zinc ion binding activity	1.25	0.90
CJI97_005329	*B9J08_005247*	*HIS1*	ATP phosphoribosyl transferase; histidine biosynthesis	3.40	2.90
CJI97_001933	*B9J08_002388*	*HST6*	ABC transporter related to mammalian P-glycoproteins	0.66	1.18
CJI97_003449	*B9J08_003374*	*ICL1*	Isocitrate lyase; glyoxylate cycle enzyme	0.79	1.33
CJI97_000020	*B9J08_000013*	*ILV3*	Dihydroxyacid dehydratase	2.77	2.73
CJI97_004268	*B9J08_004204*	*JEN1*	Lactate transporter	1.84	-0.24
CJI97_001329	*B9J08_001277*	*LEU4*	2-isopropylmalate synthase	4.41	4.31
CJI97_001920	*B9J08_002375*	*LYS9*	Saccharopine dehydrogenase; lysine biosynthesis	1.13	0.52
CJI97_004689	*B9J08_004763*	*MET8*	Bifunctional dehydrogenase and ferrochelatase; siroheme biosynthesis	1.83	0.94
CJI97_003625	*B9J08_003552*	*MET10*	Sulfite reductase; sulfur amino acid metabolism	1.01	0.90
CJI97_000409	*B9J08_000409*	*MET13*	Methionine biosynthesis protein	0.04	1.65
CJI97_003066	*B9J08_002995*	*MET14*	Adenylylsulfate kinase; sulfur metabolism	1.08	0.93
CJI97_005391	*B9J08_005307*	*MET16*	3'-phosphoadenylsulfate reductase; sulfur amino acid metabolism	1.63	1.75
CJI97_004042	*B9J08_003981*	*MDR1*	Plasma membrane MDR/MFS multidrug efflux protein	3.83	5.27

CJI97_000658	*B9J08_000656*	*MGD1*	NAD(H)-linked methylglyoxal oxidoreductase	1.35	2.04
CJI97_004624	*B9J08_004828*	*MGD2*	NAD(H)-linked methylglyoxal oxidoreductase	-0.06	1.60
CJI97_002730	*B9J08_002677*	*MIS12*	Mitochondrial C1-tetrahydrofolate synthase precursor	1.05	0.87
CJI97_004904	*B9J08_004548*	*NAR1*	Cytosolic iron-sulfur protein assembly machinery protein	0.84	2.13
CJI97_003488	*B9J08_003413*	*OPT7*	Oligopeptide transporter, may transport GSH or related compounds	1.09	0.90
CJI97_001481	*B9J08_001125*	*SNQ2*	Putative ABC transporter superfamily	1.50	2.25
CJI97_003300	*B9J08_003225*	*STR2*	Cystathionine gamma-synthase; sulfur compound metabolism	1.15	1.32
CJI97_001014	*B9J08_000995*	*SUL2*	Sulfate transporter	1.98	2.03
CJI97_004677	*B9J08_004775*	*TPO3*	Polyamine transporter, MFS-MDR family	0.91	1.24
CJI97_002495	*B9J08_001834*	*TPO4*	Spermidine transporter	0.48	1.49
CJI97_003424	*B9J08_003349*	*TRP5*	Tryptophan synthase	2.45	2.52
CJI97_002560	*B9J08_001899*	*YCF1*	Glutathione S-conjugate transporter	4.58	4.57
CJI97_005451	*B9J08_005368*	*YDJ1*	Type I HSP40 co-chaperone	0.25	1.20
CJI97_001435	*B9J08_001171*	*ADH5*	Alcohol dehydrogenase	-1.54	-1.34
CJI97_002591	*B9J08_001930*	*AOX1*	Alternative oxidase, cyanide-resistant respiration	-1.31	-0.01
CJI97_004799	*B9J08_004653*	*ARP2*	Component of the Arp2/3 complex	-0.79	-1.11
CJI97_001469	*B9J08_001137*	*ARP3*	Protein with Myo5p-dependent localization to cortical actin patches at hyphal tip	-0.55	-1.05
CJI97_000089	*B9J08_000084*	*ATP14*	Mitochondrial F1F0 ATP synthase subunit	-0.45	-1.02
CJI97_002664	*B9J08_002610*	*ATP17*	Mitochondrial ATPase complex subunit	-0.33	-1.25
CJI97_003777	*B9J08_003702*	*CDG1*	Cysteine dioxygenases, role in conversion of cysteine to sulfite	-2.12	-2.65
CJI97_004336	*B9J08_004273*	*COX6*	Cytochrome c oxidase	-0.64	-1.03
CJI97_002184	*B9J08_001993*	*COX11*	Cytochrome oxidase assembly protein	-0.43	-1.43
CJI97_004817	*B9J08_004635*	*COX19*	Cytochrome c oxidase assembly protein	-0.39	-1.16
CJI97_002517	*B9J08_001856*	*CTR1*	Copper transporter	-1.13	-2.07
CJI97_005423	*B9J08_005340*	*ERG6*	Delta(24)-sterol C-methyltransferase, converts zymosterol to fecosterol, ergosterol biosynthesis	-1.01	-0.46
CJI97_005321	*B9J08_005239*	*FBA1*	Fructose-bisphosphate aldolase	-0.72	-1.13
CJI97_005247	*B9J08_005163*	*FBP1*	Fructose-1,6-bisphosphatase, key gluconeogenesis enzyme	-1.33	-1.48
CJI97_000015	*B9J08_000008*	*FRE7*	Ferric reductase	-1.23	-0.86
CJI97_003972	*B9J08_004052*	*FRE8*	Iron/copper reductase	-1.03	-0.23
CJI97_004532	*B9J08_004468*	*FRP1*	Ferric reductase	-1.41	-0.53
CJI97_002942	*B9J08_002886*	*GIT3*	Glycerophosphocholine permease	-1.18	-0.13
CJI97_003057	*B9J08_002986*	*GLC3*	1,4-glucan branching enzyme	-1.05	-0.93
CJI97_004438	*B9J08_004375*	*GPM1*	Phosphoglycerate mutase	-0.53	-1.40
CJI97_001045	*B9J08_001025*	*GSY1*	Glycogen synthase	-1.17	-1.36

CJI97_005108/ CJI97_005109	*B9J08_005025*	*HGT19*	MFS glucose/myo-inositol transporter	-1.71	-0.98
CJI97_002699	*B9J08_002646*	*HXT5*	Sugar transporter	0.13	-1.13
CJI97_002817	*B9J08_002762*	*INO1*	Inositol-1-phosphate synthase	-0.36	-1.41
CJI97_001658	*B9J08_001652*	*JAC1*	ATPase activator activity	-0.25	-1.04
CJI97_005579	*B9J08_005497*	*MAE1*	Mitochondrial malic enzyme	-1.44	-1.10
CJI97_000695	*B9J08_000694*	*MDH1*	Mitochondrial malate dehydrogenase	-1.23	-1.26
CJI97_002683	*B9J08_002630*	*MEP1*	Ammonium permease	-1.81	-1.38
CJI97_003663	*B9J08_003590*	*MIG2*	Transcription factor involved in glucose repression	-1.17	-1.44
CJI97_002101	*B9J08_002556*	*MIX14*	Role in aerobic respiration and mitochondrial intermembrane space localization	-0.20	-1.38
CJI97_002993	*B9J08_002919*	*MLS1*	Malate synthase, glyoxylate cycle enzyme	-0.84	-1.11
CJI97_001141	*B9J08_001463*	*MYO1*	Component of actomyosin ring at neck of newly emerged bud	-0.98	-1.22
CJI97_001117	*B9J08_001487*	N/A	Transporter of ferrochrome siderophores	-1.90	-1.06
CJI97_001762	*B9J08_001547*	N/A	Transporter of ferrochrome siderophores	-1.94	-1.07
CJI97_000596	*B9J08_000675*	N/A	Adhesin-like protein	-1.12	0.15
CJI97_002126	*B9J08_002582*	N/A	Adhesin-like protein	-1.48	1.00
CJI97_003987	*B9J08_004037*	N/A	Adhesin-like protein	-1.19	-0.35
CJI97_004240	*B9J08_004176*	N/A	Secreted lipase	-1.69	-0.78
CJI97_001776	*B9J08_001533*	N/A	NAD-aldehyde dehydrogenase	-1.57	-1.55
CJI97_003161	*B9J08_003088*	N/A	NAD-aldehyde dehydrogenase	-1.76	-1.89
CJI97_001793	*B9J08_002250*	N/A	MFS glucose transporter	-2.00	-1.41
CJI97_002024	*B9J08_002481*	N/A	MFS glucose transporter	-2.02	-1.52
CJI97_004566	*B9J08_004886*	N/A	Protein similar to ferric reductases and cupric reductases	-1.43	-1.43
CJI97_005148	*B9J08_005064*	N/A	Protein similar to ferric reductases and cupric reductases	-1.56	-1.84
CJI97_000696	*B9J08_000695*	*NTH1*	Neutral trehalase	-1.07	-0.98
CJI97_002722	*B9J08_002669*	*PCK1*	Phosphoenolpyruvate carboxykinase	-2.03	-2.01
CJI97_002521	*B9J08_001860*	*PGK1*	Phosphoglycerate kinase	-0.77	-1.19
CJI97_001140	*B9J08_001464*	*PHO84*	High-affinity phosphate transporter	-2.74	-2.72
CJI97_001580	*B9J08_002202*	*PHO89*	Phosphate permease	-1.48	-0.73
CJI97_001697	*B9J08_001613*	*PHO100*	Putative inducible acid phosphatase	-1.38	-1.60
CJI97_004666	*B9J08_004786*	*PIR1*	1,3-beta-glucan-linked cell wall protein	-0.44	-1.12
CJI97_002654	*B9J08_002600*	*PMM1*	Phosphomannomutase, enzyme of O- and N-linked mannosylation	-1.05	-0.94
CJI97_002321	*B9J08_002130*	*PUT1*	Putative proline oxidase	-2.49	-1.79
CJI97_004379	*B9J08_004317*	*PUT2*	Putative delta-1-pyrroline-5-carboxylate dehydrogenase	-1.01	-1.45
CJI97_002448	*B9J08_001787*	*RGT1*	Transcriptional repressor involved in the regulation of glucose transporter genes	-1.26	-1.62
CJI97_002974	*B9J08_002900*	*RMD9*	Mitochondrial protein with a predicted role in respiratory growth	-0.25	-1.09
CJI97_004415	*B9J08_004352*	*SAH1*	S-adenosyl-L-homocysteine hydrolase	-1.46	-1.22
CJI97_004940	*B9J08_004512*	*SCO1*	Copper transporter	-0.79	-1.06

CJI97_001499	*B9J08_001107*	*SEF1*	Zn2-Cys6 transcription factor, regulates iron uptake	-1.13	-0.81
CJI97_005617	*B9J08_005567*	*SHA3*	Ser/thr kinase involved in glucose transport	-1.14	0.10
CJI97_002536	*B9J08_001875*	*TPI1*	Triose-phosphate isomerase	-0.36	-1.42
CJI97_003198	*B9J08_003126*	*QCR8*	Ubiquinol cytochrome c reductase	-0.22	-1.12
CJI97_002481	*B9J08_001820*	*QCR10*	Ubiquinol-cytochrome-c reductase	-0.31	-1.01
CJI97_003997	*B9J08_004027*	*WOR1*	Transcription factor of white-opaque phenotypic switching in *C. albicans*	-1.22	-0.33

Table S3.4. Strains and oligonucleotides used in this study.

Fungal Strains

Strain	Lab #	Species	Parent	Relevant Characteristics (FLZ MIC)	Source
AR0390	DH2777	*C. auris*		Clinical isolate, clade I	(140)
B11221	DH3880	*C. auris*		Clinical isolate, clade III	(46)
*mrr1a*Δ	DH3881	*C. auris*	B11221	*mrr1a*Δ::*caSAT1*	(46)
*mrr1b*Δ	DH3882	*C. auris*	B11221	*mrr1b*Δ::*caSAT1*	(46)
*mrr1c*Δ	DH3883	*C. auris*	B11221	*mrr1c*Δ::*caSAT1*	(46)
U04 *mrr1*Δ	DH3306	*C. lusitaniae*	U04	*mrr1*Δ::*NAT1* (4 μg/mL)	(40)
U04 *mrr1*Δ + *CauMRR1a*^{N647T} clone #1	DH3914	*C. lusitaniae*	U04 *mrr1*Δ	*CauMRR1a*^{N647T}*-HygB* (16 μg/mL)	This study
U04 *mrr1*Δ + *CauMRR1a*^{N647T} clone #2	DH3915	*C. lusitaniae*	U04 *mrr1*Δ	*CauMRR1a*^{N647T}*-HygB* (16 μg/mL)	This study
U04 *mrr1*Δ + *CauMRR1a*^{N647T} clone #8	DH3916	*C. lusitaniae*	U04 *mrr1*Δ	*CauMRR1a*^{N647T}*-HygB* (16 μg/mL)	This study
U04 *mrr1*Δ + *CauMRR1a* clone #4	DH3917	*C. lusitaniae*	U04 *mrr1*Δ	*CauMRR1a-HygB* (4 μg/mL)	This study
U04 *mrr1*Δ + *CauMRR1a* clone #5	DH3918	*C. lusitaniae*	U04 *mrr1*Δ	*CauMRR1a-HygB* (4 μg/mL)	This study
U04 *mrr1*Δ + *CauMRR1a* clone #7	DH3919	*C. lusitaniae*	U04 *mrr1*Δ	*CauMRR1a-HygB* (4 μg/mL)	This study

Plasmids in *E. coli* (DH5α)

Strain	Lab #	Species	Description	Source
pMQ30$^{MRR1\text{-}L1191H+Q1197*}$	DH3829	*E. coli*	*MRR1*$^{L1191H+Q1197*}$*-HygB* complementation, Gent^{R}	(58)
pMQ30^{CauMRR1aN647T}	DH3912	*E. coli*	*CauMRR1a*^{N647T}*-HygB* complementation, Gent^{R}	This study
pMQ30^{CauMRR1a}	DH3913	*E. coli*	*CauMRR1a-HygB* complementation, Gent^{R}	This study

Primers

Name	Description	Sequence	Source
ED222	*C. auris ACT1* qRT Fwd	5' – GAA GGA GAT CAC TGC TTT AGC C – 3'	This study
ED223	*C. auris ACT1* qRT Rev	5' – GAG CCA CCA ATC CAC ACA G – 3'	This study
ED224	*C. auris MDR1* qRT Fwd	5' – GAA GTA TGA TGG CGG GTG – 3'	This study

ED225	*C. auris MDR1* qRT Rev	5’ – CCC AAG AGA GAC GAG CCC – 3’	This study
AB126	*C. auris MGD1* qRT Fwd	5’ – TTC CCC TGA AAT GGA TTT GA – 3’	This study
AB127	*C. auris MGD1* qRT Rev	5’ – GTC TTG GAG CCA TAG TAA CC – 3’	This study
AB130	Amplify *C. auris MRR1a* for heterologous complementation, Fwd	5’ – CTT CAA CTC CGC AAC ACC TGG AAA CTT CAT TAC TAA AGA TGA TGG TAT CTT CGA AAG ATC – 3’	This study
AB131	Amplify *C. auris MRR1a* for heterologous complementation, Rev	5’ – CTT TAC CAG TAA AGT ATC CTT GCC AAA TTT CGT TCC ATA ATT ACA CAT CAA GCA TCT CTT C – 3’	This study
ED125	Forward upstream of *C. lusitaniae MRR1* to validate complements	5’ – GAA AAA GAA GCC AGC AGA CC – 3’	(58)
ED126	Reverse upstream of *C. lusitaniae MRR1* to validate complements	5’ – GGG TAA AGC CAT TGC AGA C – 3’	(58)
ACT1-F	*C. lusitaniae ACT1* qRT Fwd	5’ – GTA TCG CTG AGC GTA TGC AA – 3’	(141)
ACT1-R	*C. lusitaniae ACT1* qRT Rev	5’ – GAT GGA TGG TCC AGA CTC GT – 3’	(141)
ED058	*C. lusitaniae MDR1* qRT Fwd	5’ – TCC ATC CAT GGG TCC ATT ATT C – 3’	(40)
ED059	*C. lusitaniae MDR1* qRT Rev	5’ – CTC AAC ACA AGG AAA GCA CAT C – 3’	(40)
AB039	*C. lusitaniae MGD1* qRT Fwd	5' – CGC AGA AAT CCC TAA AGT AAA T – 3'	(58)
AB040	*C. lusitaniae MGD1* qRT Rev	5' – TAC CCT TTG CTT CGT TCT T – 3'	(58)

Other Oligonucleotides

Name	Description	Sequence	Source
NAT1 crRNA	crRNA targeting *NAT1*; used to complement *C. auris MRR1a* alleles into *C. lusitaniae mrr1Δ::NAT1* mutant	5’ – GGG AAA ACC TTA GTC AAT GG – 3’	(58)

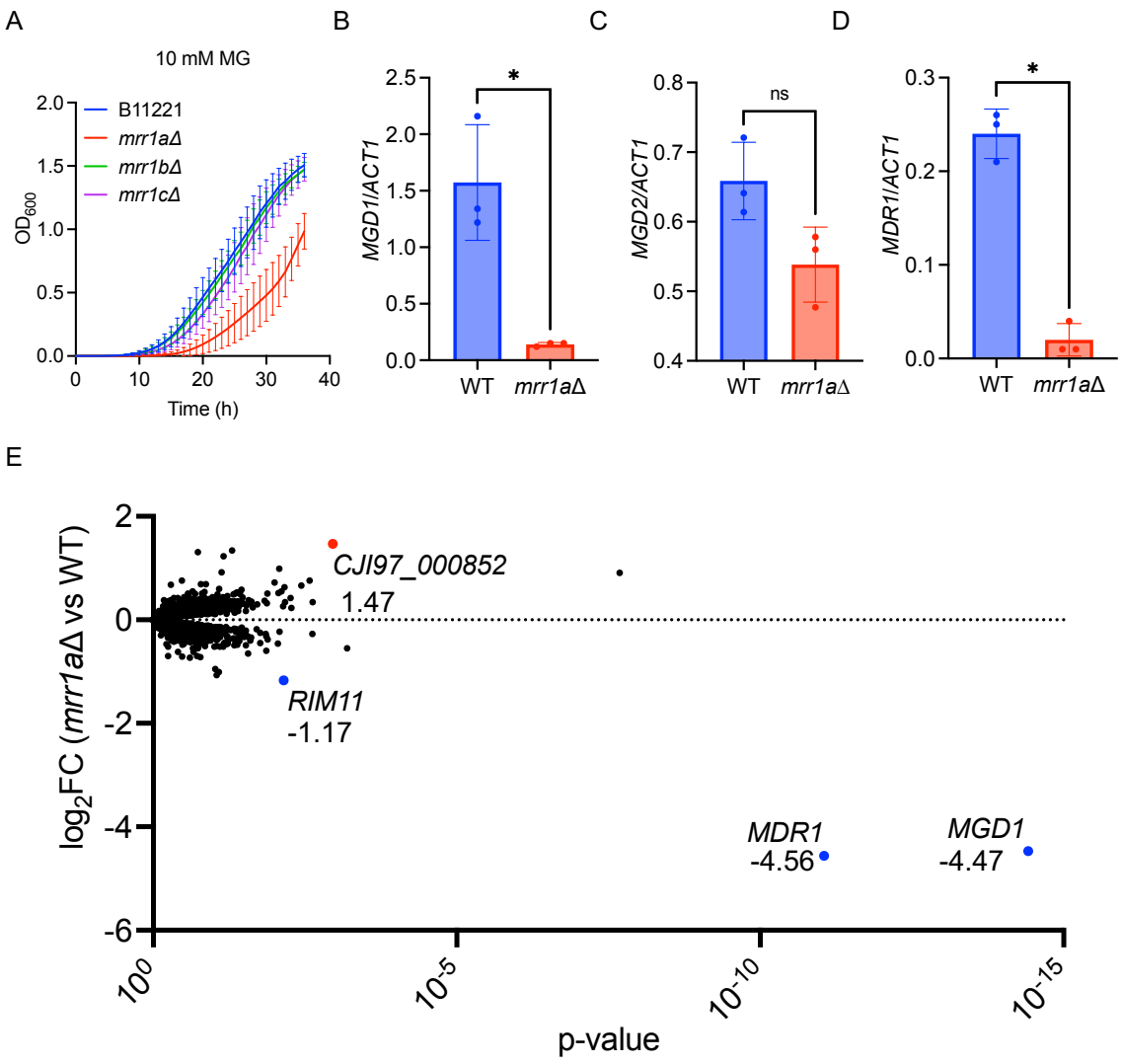

Figure 3.1. Mrr1a regulates expression of *MGD1* and *MDR1* in *C. auris* isolate B11221. **(A)** Growth curves of B11221 WT (blue) and its *mrr1a*Δ (red), *mrr1b*Δ (green), and *mrr1c*Δ (purple) derivatives in YPD + 10 mM MG. Data shown represent the mean ± SD for three independent experiments. **(B-C)** qRT-PCR assessment of *MGD1* **(B)** and *MDR1* **(C)** expression in B11221 WT (blue) and *mrr1a*Δ (red) cultures grown to exponential phase in YPD at 37˚C. Data shown represent the mean ± SD for three independent experiments. Ratio paired t-test was used for statistical evaluation; * $p < 0.05$. **(D)** Volcano plot of all quantified genes in B11221 WT vs *mrr1a*Δ in the control condition.

Each point represents a single gene; blue points indicate genes significantly more highly expressed in WT; red points indicate genes significantly more highly expressed in *mrr1a*Δ. Numbers adjacent to each colored point indicate the $\log_2$FC in *mrr1a*Δ versus WT.

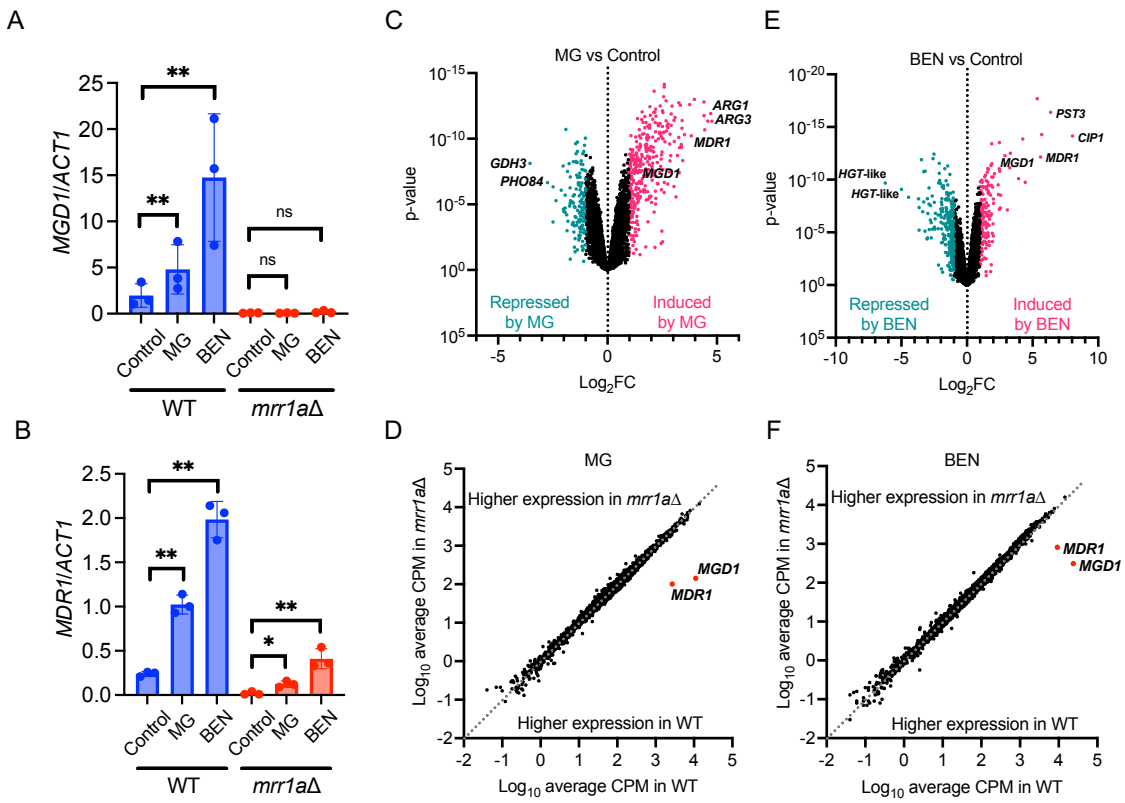

Figure 3.2. MG and BEN both lead to a vast transcriptional response in *C. auris* B11221, which includes upregulation of *MDR1* and *MGD1*. A-B) qRT-PCR analysis for expression of *MGD1* **(A)** and *MDR1* **(B)** in exponential-phase cultures of B11221 WT (blue) or *mrr1a*Δ (red) treated with MG or BEN as indicated. Data shown represent the mean ± SD for three independent experiments. Ratio paired t-test was used for statistical evaluation; ns $p > 0.05$, * $p < 0.05$, ** $p < 0.01$. **(C-D)** Volcano plots of all quantified genes in B11221 WT treated with either MG **(C)** or BEN **(D)**. Each point represents a single gene; magenta points indicate genes that were significantly upregulated compared to the control condition, teal points indicate genes that were significantly downregulated compared to the control condition. *MDR1* and *MGD1* are shown along with the two most up- and down- regulated genes in each condition. **(E-F)** Scatter plots of the average CPMs of all quantified genes in *mrr1a*Δ vs. B11221 WT treated with MG **(E)** or BEN **(F)**. Each

point represents a single gene. Points below the dotted line indicate genes that were more highly expressed in the WT, and points above the dotted line indicated genes that were more highly expressed in the *mrr1a*Δ mutant. *MDR1* and *MGD1* are shown with red dots for reference.

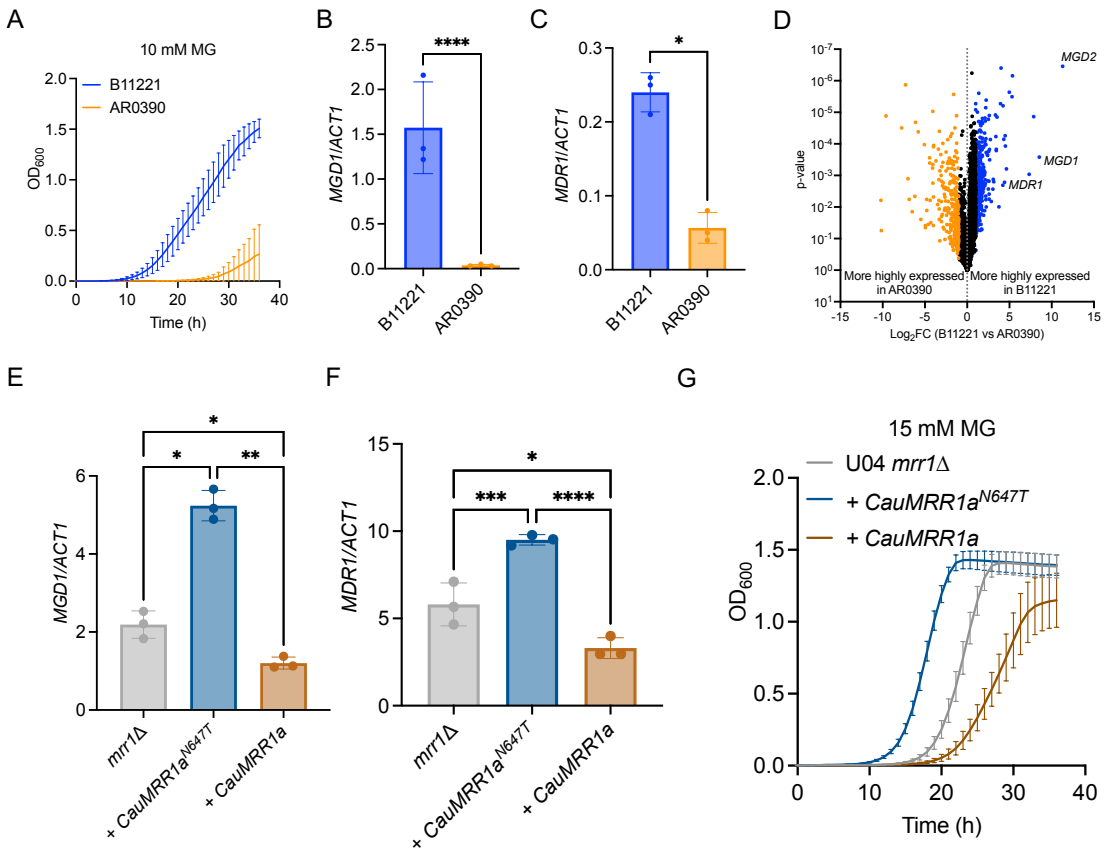

Figure 3.3. *MDR1* and *MGD1* are among the genes significantly more highly expressed in isolate B11221 compared to isolate AR0390. **(A)** Growth curves of B11221 (blue) and AR#0390 (orange) in YPD + 10 mM MG. Data shown represent the mean ± SD for three independent experiments. **(B-C)** qRT-PCR assessment of *MGD1* **(B)** and *MDR1* **(C)** expression in B11221 (blue) and AR0390 (orange) grown to exponential phase in YPD at 37˚C. Data shown represent the mean ± SD for three independent experiments. Ratio paired t-test was used for statistical evaluation; * $p < 0.05$, **** $p < 0.0001$. **(D)** Volcano plot of all quantified genes, matched by syntenic ortholog, in B11221 and AR0390 in the control condition (YPD). Each point represents a single gene; blue points indicate genes significantly more highly expressed in B11221; orange points indicate genes significantly more highly expressed in AR0390. **(E-F)** qRT-PCR expression analysis for *MGD1* **(E)** and

MDR1 **(F)** in *C. lusitaniae* U04 *mrr1*Δ (grey) and its derivatives expressing *CauMRR1a*^{N647T} (dark blue) or *CauMRR1a* (brown). Data shown represent the mean ± SD for three independent experiments. One-way ANOVA was used for statistical evaluation; * $p < 0.05$, ** $p < 0.01$, *** $p < 0.001$, **** $p < 0.0001$. (**G)** Growth curves of *C. lusitaniae* U04 *mrr1*Δ (grey) and its derivatives expressing *CauMRR1a*^{N647T} (dark blue) or *CauMRR1a* (brown) in YPD + 15 mM MG. One representative experiment of three independent experiments is shown; error bars represent the standard deviation of technical replicates within the experiment.

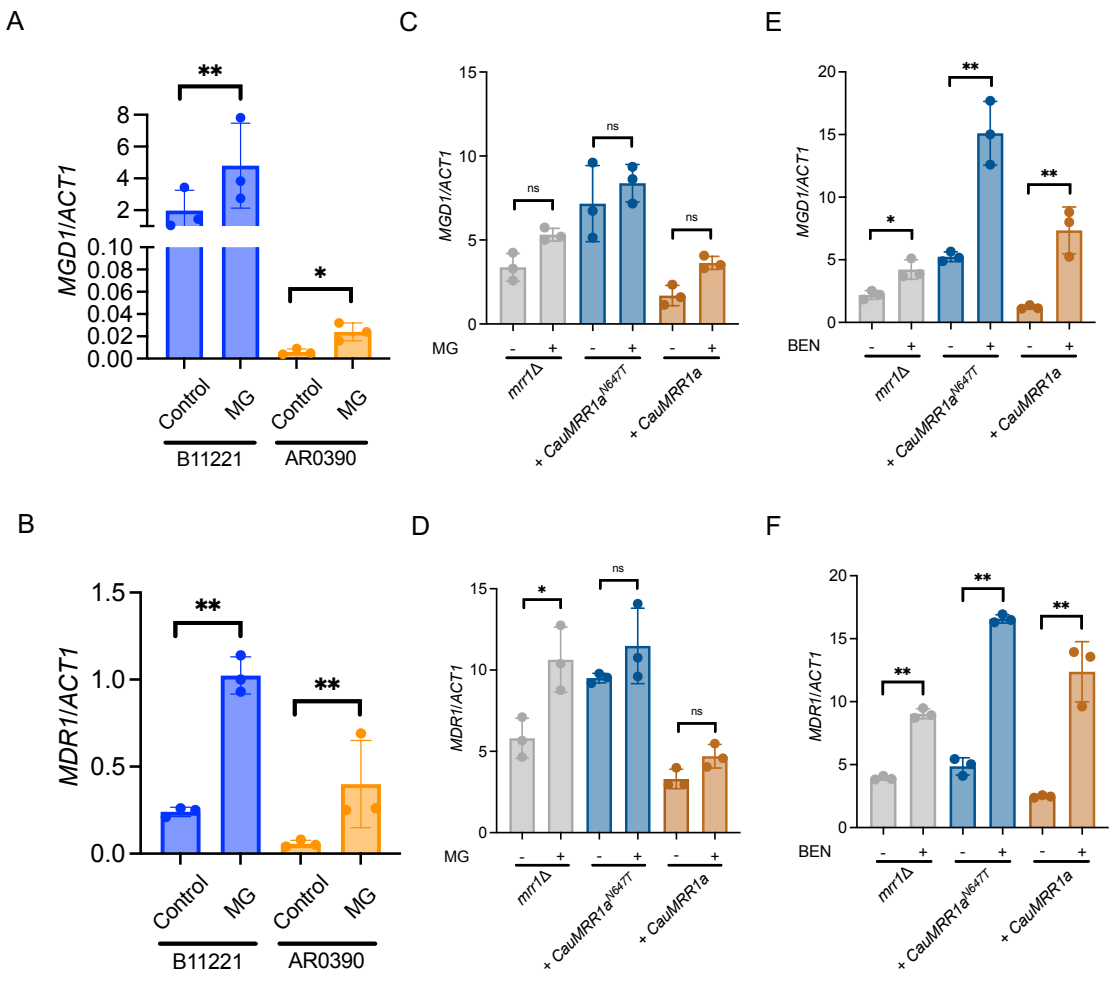

Figure 3.4. MG induces expression of *MGD1* and *MDR1* in *C. auris* isolates B11221 and AR0390, but *C. auris MRR1a* is not inducible by MG when heterologously expressed in *C. lusitaniae*. **(A-B)** qRT-PCR analysis for expression of *MGD1* **(A)** and *MDR1* **(B)** in exponential-phase cultures of B11221 (blue) or AR0390 (orange) treated with MG as indicated. Data shown represent the mean ± SD for three independent experiments. Ratio paired t-test was used for statistical evaluation; ns $p > 0.05$, * $p < 0.05$, ** $p < 0.01$. **(C-F)** qRT-PCR analysis for expression of *MGD1* **(C, E)** and *MDR1* **(D, F)** in exponential-phase cultures of *C. lusitaniae* U04 *mrr1*Δ (grey) and its derivatives expressing *CauMRR1a*^{N647T} (dark blue) or *CauMRR1a* (brown) treated with 5 mM MG for 15 min **(C, D)** or 25 µg/mL BEN for 30 min **(E, F)**. Data shown represent the mean ± SD for three

independent experiments. Ratio paired t-test was used for statistical evaluation; ns $p > 0.05$, * $p < 0.05$, ** $p < 0.01$.

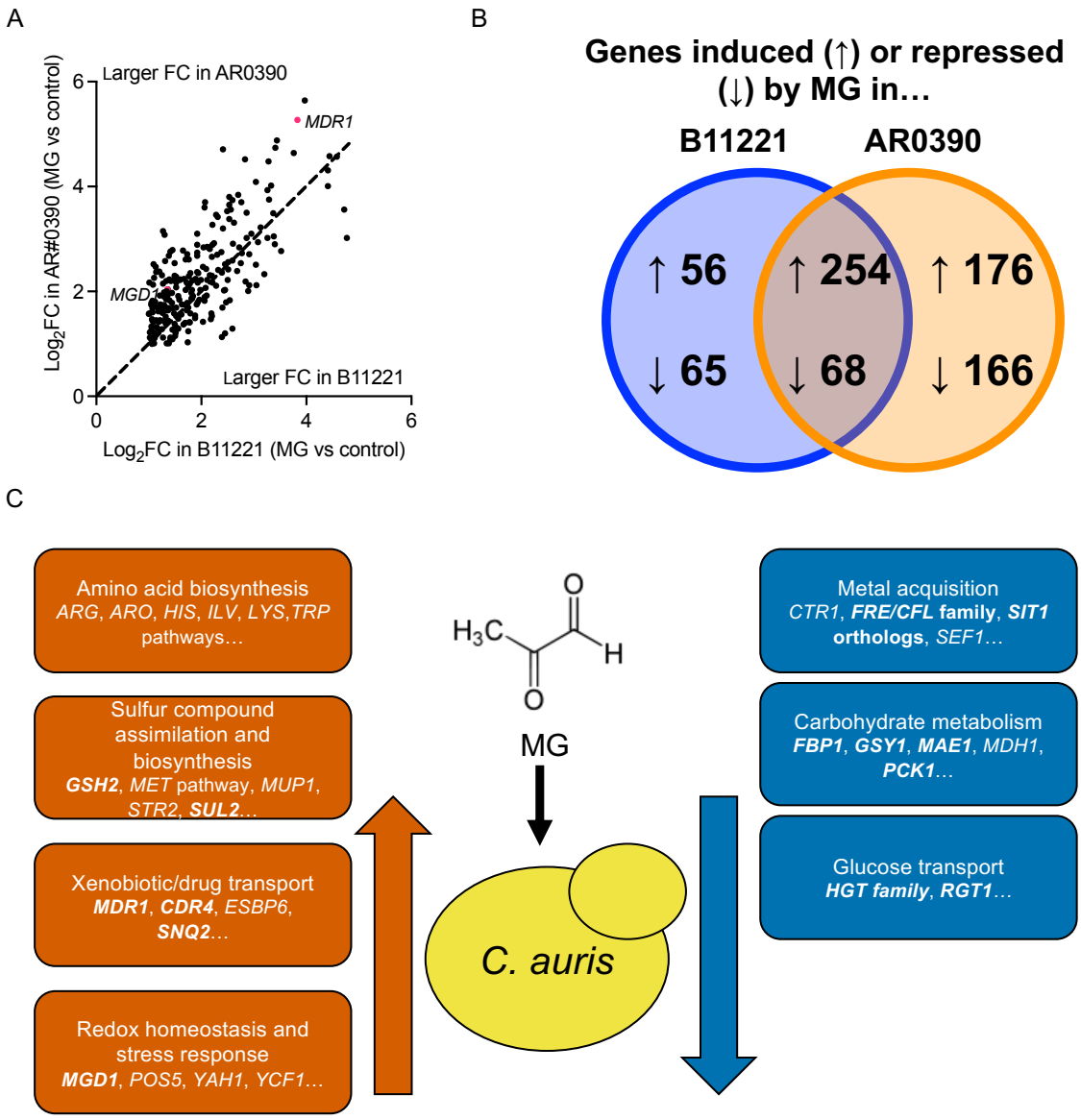

Figure 3.5. MG induces and represses common pathways across B11221 and AR0390. (**A**) Venn diagram of genes with syntenic orthologs between B11221 and AR0390 that were significantly induced (indicated by "up" arrows) or repressed (indicated by "down" arrows) by MG in either or both strains. (**B**) Scatter plot of the log_2FC of genes significantly induced by MG in AR0390 vs the log_2FC of genes induced by MG in B11221. Only genes with syntenic orthologs between the two strains are shown. Each point represents a single gene; points above the dotted line indicate genes which exhibited a greater Log_2FC in

AR0390, and points below the dotted line indicate genes which exhibited a greater log_2FC in B11221. *MGD1* and *MDR1* are indicated with red dots for reference. (**C)** Graphic summary of major groups of genes that were significantly up- or down-regulated in response to MG in both B11221 and AR0390. Genes in bold text were also up- or down-regulated in response to BEN in B11221.

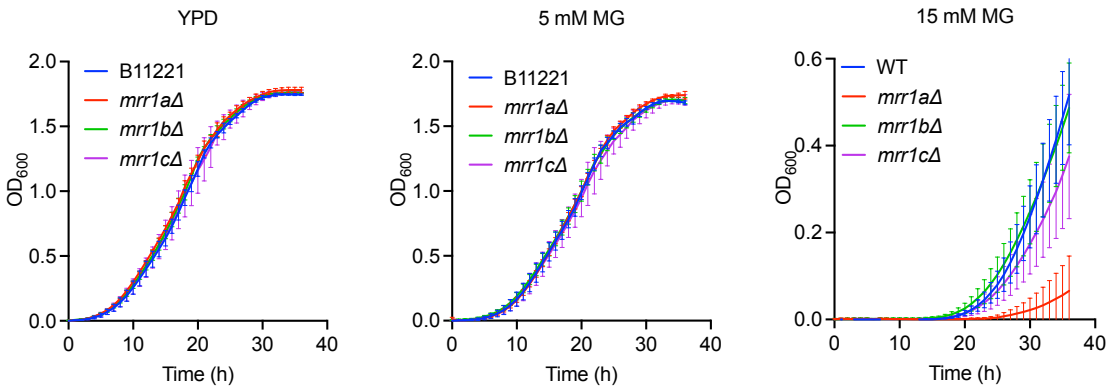

Figure S3.1. The *mrr1a*Δ mutant has a growth defect in high concentrations of MG, but not at 5 mM MG or in the YPD control. Growth curves of B11221 WT (blue) and its *mrr1a*Δ (red), *mrr1b*Δ (green), and *mrr1c*Δ (purple) derivatives in YPD (left), or YPD supplemented with 5 mM (middle), or 15 mM (right) MG. Data shown represent the mean ± SD for three independent experiments.

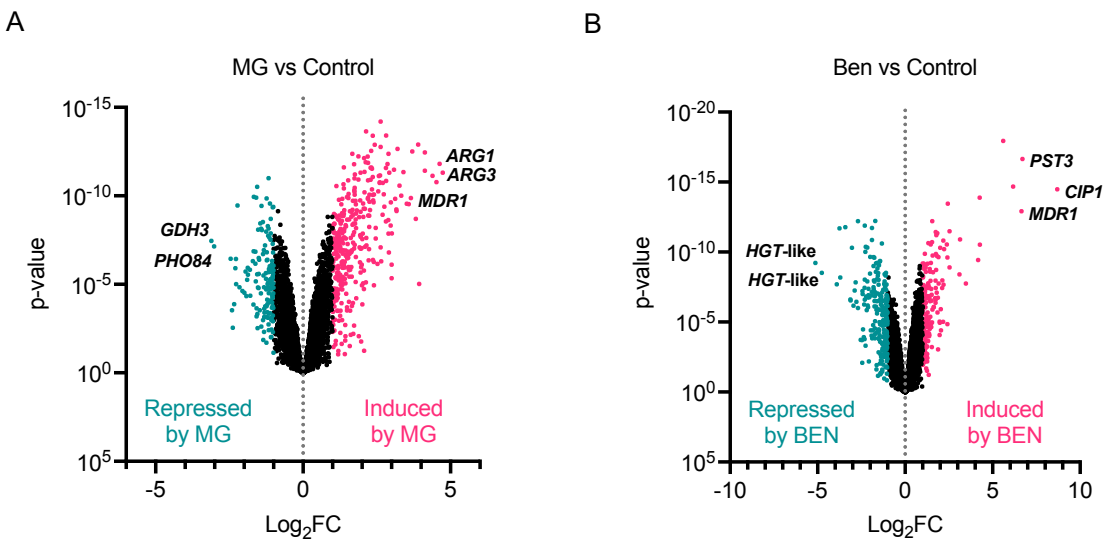

Figure S3.2. The transcriptional response of *mrr1a*Δ to either MG or BEN is overall similar to that of the B11221 WT parent strain. Volcano plots of all quantified genes in the *mrr1a*Δ mutant treated with either MG **(A)** or BEN **(B)**. Each point represents a single gene; magenta points indicate genes that were significantly upregulated compared to the control condition, teal points indicate genes that were significantly downregulated compared to the control condition. *MDR1* is shown along with the two most up- and down-regulated genes in each condition.

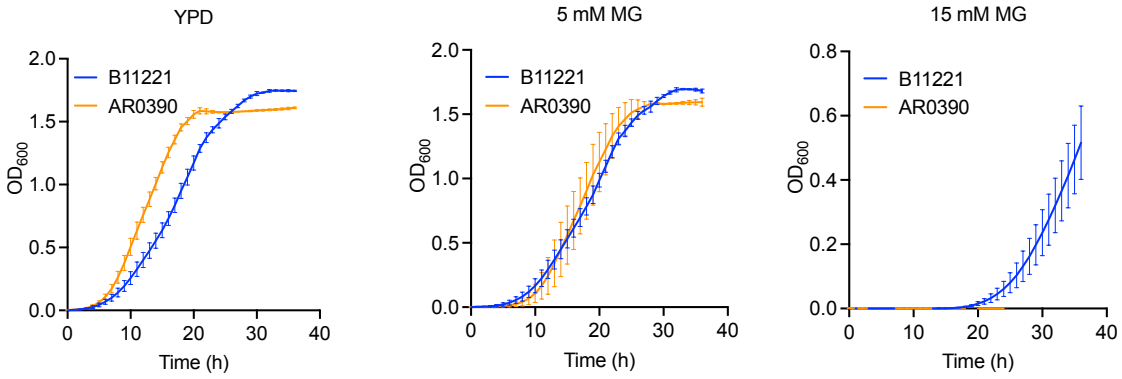

Figure S3.3. *C. auris* strain AR0390 has a growth advantage over B11221 in YPD but loses that advantage in the presence of increasing concentrations of MG. Growth curves of B11221 (blue) and AR0390 (orange) in YPD (left), or YPD supplemented with 5 mM (middle), or 15 mM (right) MG. Data shown represent the mean ± SD for three independent experiments.

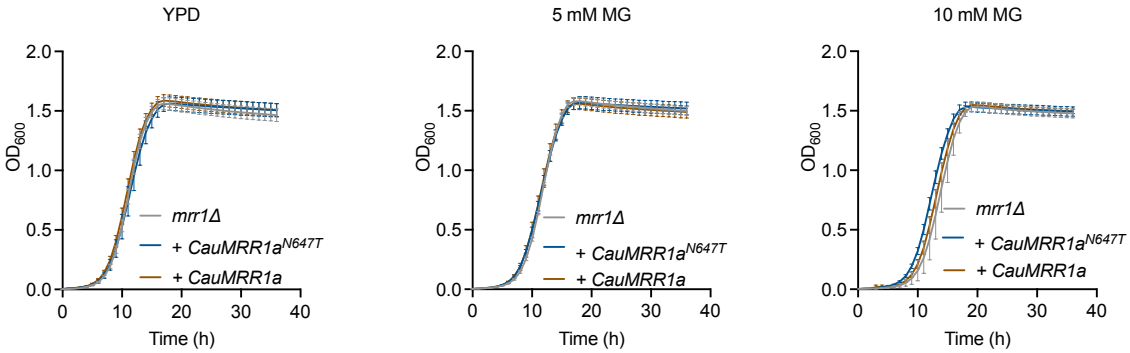

Figure S3.4. ***C. lusitaniae*** **strains complemented with** ***CauMRR1aN647T*** **or** ***CauMRR1a*** **do not differ in growth from the mrr1Δ parent at MG concentrations below 15 mM.** Growth curves of *C. lusitaniae* U04 *mrr1*Δ (grey) and its derivatives expressing *CauMRR1a*^{N647T} (dark blue) or *CauMRR1a* (brown) in YPD (left) or YPD supplemented with 5 mM (middle), or 10 mM (right) MG. Data shown represent the mean ± SD for three independent experiments.

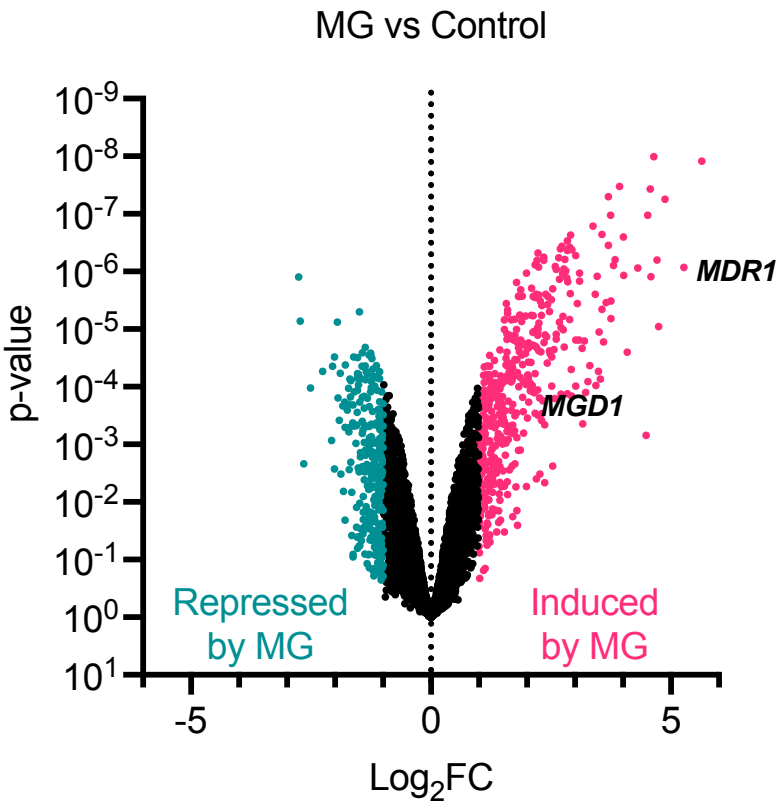

Figure S3.5. Treatment with 5 mM MG leads to the differential expression of more genes in AR0390 than in B11221. Volcano plot of all quantified genes in AR0390 treated with MG. Each point represents a single gene; magenta points indicate genes that were significantly upregulated compared to the control condition, teal points indicate genes that were significantly downregulated compared to the control condition. *MDR1* and *MGD1* are shown for reference.

References

1. Pfaller MA, Andes DR, Diekema DJ, Horn DL, Reboli AC, Rotstein C, Franks B, Azie NE. 2014. Epidemiology and outcomes of invasive candidiasis due to non-albicans species of *Candida* in 2,496 patients: data from the Prospective Antifungal Therapy (PATH) registry 2004-2008. PLoS One 9:e101510.
2. Pfaller MA, Diekema DJ. 2007. Epidemiology of invasive candidiasis: a persistent public health problem. Clin Microbiol Rev 20:133-63.
3. Quindos G, Marcos-Arias C, San-Millan R, Mateo E, Eraso E. 2018. The continuous changes in the aetiology and epidemiology of invasive candidiasis: from familiar *Candida albicans* to multiresistant *Candida auris*. Int Microbiol 21:107-119.
4. Abe M, Kinjo Y, Ueno K, Takatsuka S, Nakamura S, Ogura S, Kimura M, Araoka H, Sadamoto S, Shinozaki M, Shibuya K, Yoneyama A, Kaku M, Miyazaki Y. 2018. Differences in Ocular Complications Between *Candida albicans* and Non-albicans *Candida* Infection Analyzed by Epidemiology and a Mouse Ocular Candidiasis Model. Front Microbiol 9:2477.
5. Leeyaphan C, Bunyaratavej S, Foongladda S, Rujitharanawong C, Maneeprasopchoke P, Surawan T, Muanprasat C, Matthapan L. 2016. Epidemiology, Clinical Characteristics, Sites of Infection and Treatment Outcomes of Mucocutaneous Candidiasis Caused by Non-albicans Species of *Candida* at a Dermatologic Clinic. J Med Assoc Thai 99:406-11.
6. Quindos G. 2014. Epidemiology of candidaemia and invasive candidiasis. A changing face. Rev Iberoam Micol 31:42-8.

7. Patel PK, Erlandsen JE, Kirkpatrick WR, Berg DK, Westbrook SD, Louden C, Cornell JE, Thompson GR, Vallor AC, Wickes BL, Wiederhold NP, Redding SW, Patterson TF. 2012. The Changing Epidemiology of Oropharyngeal Candidiasis in Patients with HIV/AIDS in the Era of Antiretroviral Therapy. AIDS Res Treat 2012:262471.

8. Hachem R, Hanna H, Kontoyiannis D, Jiang Y, Raad I. 2008. The changing epidemiology of invasive candidiasis: *Candida glabrata* and *Candida krusei* as the leading causes of candidemia in hematologic malignancy. Cancer 112:2493-9.

9. Redding SW, Kirkpatrick WR, Dib O, Fothergill AW, Rinaldi MG, Patterson TF. 2000. The epidemiology of non-albicans *Candida* in oropharyngeal candidiasis in HIV patients. Spec Care Dentist 20:178-81.

10. Abi-Said D, Anaissie E, Uzun O, Raad I, Pinzcowski H, Vartivarian S. 1997. The epidemiology of hematogenous candidiasis caused by different *Candida* species. Clin Infect Dis 24:1122-8.

11. Bravo Ruiz G, Lorenz A. 2021. What do we know about the biology of the emerging fungal pathogen of humans *Candida auris*? Microbiol Res 242:126621.

12. Du H, Bing J, Hu T, Ennis CL, Nobile CJ, Huang G. 2020. *Candida auris*: Epidemiology, biology, antifungal resistance, and virulence. PLoS Pathog 16:e1008921.

13. Satoh K, Makimura K, Hasumi Y, Nishiyama Y, Uchida K, Yamaguchi H. 2009. *Candida auris* sp. nov., a novel ascomycetous yeast isolated from the external ear canal of an inpatient in a Japanese hospital. Microbiol Immunol 53:41-4.

14. Lee WG, Shin JH, Uh Y, Kang MG, Kim SH, Park KH, Jang HC. 2011. First three reported cases of nosocomial fungemia caused by *Candida auris*. J Clin Microbiol 49:3139-42.

15. Lockhart SR, Etienne KA, Vallabhaneni S, Farooqi J, Chowdhary A, Govender NP, Colombo AL, Calvo B, Cuomo CA, Desjardins CA, Berkow EL, Castanheira M, Magobo RE, Jabeen K, Asghar RJ, Meis JF, Jackson B, Chiller T, Litvintseva AP. 2017. Simultaneous Emergence of Multidrug-Resistant *Candida auris* on 3 Continents Confirmed by Whole-Genome Sequencing and Epidemiological Analyses. Clin Infect Dis 64:134-140.

16. Chow NA, de Groot T, Badali H, Abastabar M, Chiller TM, Meis JF. 2019. Potential Fifth Clade of *Candida auris*, Iran, 2018. Emerg Infect Dis 25:1780-1781.

17. Proctor DM, Dangana T, Sexton DJ, Fukuda C, Yelin RD, Stanley M, Bell PB, Baskaran S, Deming C, Chen Q, Conlan S, Park M, Program NCS, Welsh RM, Vallabhaneni S, Chiller T, Forsberg K, Black SR, Pacilli M, Kong HH, Lin MY, Schoeny ME, Litvintseva AP, Segre JA, Hayden MK. 2021. Integrated genomic, epidemiologic investigation of *Candida auris* skin colonization in a skilled nursing facility. Nat Med 27:1401-1409.

18. Horton MV, Johnson CJ, Kernien JF, Patel TD, Lam BC, Cheong JZA, Meudt JJ, Shanmuganayagam D, Kalan LR, Nett JE. 2020. *Candida auris* Forms High-Burden Biofilms in Skin Niche Conditions and on Porcine Skin. mSphere 5.

19. Uppuluri P. 2020. *Candida auris* Biofilm Colonization on Skin Niche Conditions. mSphere 5.

20. Osei Sekyere J. 2018. *Candida auris*: A systematic review and meta-analysis of current updates on an emerging multidrug-resistant pathogen. Microbiologyopen 7:e00578.

21. Taori SK, Khonyongwa K, Hayden I, Athukorala GDA, Letters A, Fife A, Desai N, Borman AM. 2019. *Candida auris* outbreak: Mortality, interventions and cost of sustaining control. J Infect 79:601-611.

22. Arensman K, Miller JL, Chiang A, Mai N, Levato J, LaChance E, Anderson M, Beganovic M, Dela Pena J. 2020. Clinical Outcomes of Patients Treated for *Candida auris* Infections in a Multisite Health System, Illinois, USA. Emerg Infect Dis 26:876-880.

23. AlJindan R, AlEraky DM, Mahmoud N, Abdalhamid B, Almustafa M, AbdulAzeez S, Borgio JF. 2020. Drug Resistance-Associated Mutations in *ERG11* of Multidrug-Resistant *Candida auris* in a Tertiary Care Hospital of Eastern Saudi Arabia. J Fungi (Basel) 7.

24. Carolus H, Pierson S, Munoz JF, Subotic A, Cruz RB, Cuomo CA, Van Dijck P. 2021. Genome-Wide Analysis of Experimentally Evolved *Candida auris* Reveals Multiple Novel Mechanisms of Multidrug Resistance. mBio 12.

25. Chow NA, Munoz JF, Gade L, Berkow EL, Li X, Welsh RM, Forsberg K, Lockhart SR, Adam R, Alanio A, Alastruey-Izquierdo A, Althawadi S, Arauz AB, Ben-Ami R, Bharat A, Calvo B, Desnos-Ollivier M, Escandon P, Gardam D, Gunturu R, Heath CH, Kurzai O, Martin R, Litvintseva AP, Cuomo CA. 2020. Tracing the Evolutionary History and Global Expansion of Candida auris Using Population Genomic Analyses. mBio 11.

26. Chowdhary A, Prakash A, Sharma C, Kordalewska M, Kumar A, Sarma S, Tarai B, Singh A, Upadhyaya G, Upadhyay S, Yadav P, Singh PK, Khillan V, Sachdeva N, Perlin DS, Meis JF. 2018. A multicentre study of antifungal susceptibility patterns among 350 *Candida auris* isolates (2009-17) in India: role of the *ERG11* and *FKS1* genes in azole and echinocandin resistance. J Antimicrob Chemother 73:891-899.

27. Healey KR, Kordalewska M, Jimenez Ortigosa C, Singh A, Berrio I, Chowdhary A, Perlin DS. 2018. Limited *ERG11* Mutations Identified in Isolates of *Candida auris* Directly Contribute to Reduced Azole Susceptibility. Antimicrob Agents Chemother 62.

28. Li J, Coste AT, Liechti M, Bachmann D, Sanglard D, Lamoth F. 2021. Novel *ERG11* and *TAC1b* mutations associated with azole resistance in *Candida auris*. Antimicrob Agents Chemother doi:10.1128/AAC.02663-20.

29. Munoz JF, Gade L, Chow NA, Loparev VN, Juieng P, Berkow EL, Farrer RA, Litvintseva AP, Cuomo CA. 2018. Genomic insights into multidrug-resistance, mating and virulence in *Candida auris* and related emerging species. Nat Commun 9:5346.

30. Rybak JM, Sharma C, Doorley LA, Barker KS, Palmer GE, Rogers PD. 2021. Delineation of the Direct Contribution of *Candida auris ERG11* Mutations to Clinical Triazole Resistance. Microbiol Spectr 9:e0158521.

31. Williamson B, Wilk A, Guerrero KD, Mikulski TD, Elias TN, Sawh I, Cancino-Prado G, Gardam D, Heath CH, Govender NP, Perlin DS, Kordalewska M, Healey KR. 2022. Impact of Erg11 Amino Acid Substitutions Identified in *Candida auris*

Clade III Isolates on Triazole Drug Susceptibility. Antimicrob Agents Chemother 66:e0162421.

32. Rybak JM, Doorley LA, Nishimoto AT, Barker KS, Palmer GE, Rogers PD. 2019. Abrogation of Triazole Resistance upon Deletion of *CDR1* in a Clinical Isolate of *Candida auris*. Antimicrob Agents Chemother 63.

33. Kim SH, Iyer KR, Pardeshi L, Munoz JF, Robbins N, Cuomo CA, Wong KH, Cowen LE. 2019. Genetic Analysis of *Candida auris* Implicates Hsp90 in Morphogenesis and Azole Tolerance and Cdr1 in Azole Resistance. mBio 10.

34. Kim SH, Iyer KR, Pardeshi L, Munoz JF, Robbins N, Cuomo CA, Wong KH, Cowen LE. 2019. Erratum for Kim et al., "Genetic Analysis of *Candida auris* Implicates Hsp90 in Morphogenesis and Azole Tolerance and Cdr1 in Azole Resistance". mBio 10.

35. Rybak JM, Munoz JF, Barker KS, Parker JE, Esquivel BD, Berkow EL, Lockhart SR, Gade L, Palmer GE, White TC, Kelly SL, Cuomo CA, Rogers PD. 2020. Mutations in *TAC1B*: a Novel Genetic Determinant of Clinical Fluconazole Resistance in *Candida auris*. mBio 11.

36. Wasi M, Khandelwal NK, Moorhouse AJ, Nair R, Vishwakarma P, Bravo Ruiz G, Ross ZK, Lorenz A, Rudramurthy SM, Chakrabarti A, Lynn AM, Mondal AK, Gow NAR, Prasad R. 2019. ABC Transporter Genes Show Upregulated Expression in Drug-Resistant Clinical Isolates of *Candida auris*: A Genome-Wide Characterization of ATP-Binding Cassette (ABC) Transporter Genes. Front Microbiol 10:1445.

37. Demers EG, Stajich JE, Ashare A, Occhipinti P, Hogan DA. 2021. Balancing Positive and Negative Selection: *In Vivo* Evolution of *Candida lusitaniae MRR1*. mBio 12.

38. Liu Z, Myers LC. 2017. *Candida albicans* Swi/Snf and Mediator Complexes Differentially Regulate Mrr1-Induced *MDR1* Expression and Fluconazole Resistance. Antimicrob Agents Chemother 61.

39. Kannan A, Asner SA, Trachsel E, Kelly S, Parker J, Sanglard D. 2019. Comparative Genomics for the Elucidation of Multidrug Resistance in *Candida lusitaniae*. mBio 10.

40. Demers EG, Biermann AR, Masonjones S, Crocker AW, Ashare A, Stajich JE, Hogan DA. 2018. Evolution of drug resistance in an antifungal-naive chronic *Candida lusitaniae* infection. Proc Natl Acad Sci U S A 115:12040-12045.

41. Schubert S, Popp C, Rogers PD, Morschhauser J. 2011. Functional dissection of a *Candida albicans* zinc cluster transcription factor, the multidrug resistance regulator Mrr1. Eukaryot Cell 10:1110-21.

42. Schubert S, Rogers PD, Morschhauser J. 2008. Gain-of-function mutations in the transcription factor *MRR1* are responsible for overexpression of the *MDR1* efflux pump in fluconazole-resistant *Candida dubliniensis* strains. Antimicrob Agents Chemother 52:4274-80.

43. Schneider S, Morschhauser J. 2015. Induction of *Candida albicans* drug resistance genes by hybrid zinc cluster transcription factors. Antimicrob Agents Chemother 59:558-69.

44. Schubert S, Barker KS, Znaidi S, Schneider S, Dierolf F, Dunkel N, Aid M, Boucher G, Rogers PD, Raymond M, Morschhauser J. 2011. Regulation of efflux pump expression and drug resistance by the transcription factors Mrr1, Upc2, and Cap1 in *Candida albicans*. Antimicrob Agents Chemother 55:2212-23.

45. Morschhauser J, Barker KS, Liu TT, Bla BWJ, Homayouni R, Rogers PD. 2007. The transcription factor Mrr1p controls expression of the *MDR1* efflux pump and mediates multidrug resistance in *Candida albicans*. PLoS Pathog 3:e164.

46. Mayr EM, Ramirez-Zavala B, Kruger I, Morschhauser J. 2020. A Zinc Cluster Transcription Factor Contributes to the Intrinsic Fluconazole Resistance of *Candida auris*. mSphere 5.

47. Spivak ES, Hanson KE. 2018. *Candida auris*: an Emerging Fungal Pathogen. J Clin Microbiol 56.

48. Jin L, Cao Z, Wang Q, Wang Y, Wang X, Chen H, Wang H. 2018. *MDR1* overexpression combined with *ERG11* mutations induce high-level fluconazole resistance in *Candida tropicalis* clinical isolates. BMC Infect Dis 18:162.

49. Liston SD, Whitesell L, Kapoor M, Shaw KJ, Cowen LE. 2020. Enhanced Efflux Pump Expression in *Candida* Mutants Results in Decreased Manogepix Susceptibility. Antimicrob Agents Chemother 64.

50. Wirsching S, Moran GP, Sullivan DJ, Coleman DC, Morschhauser J. 2001. *MDR1*-mediated drug resistance in *Candida dubliniensis*. Antimicrob Agents Chemother 45:3416-21.

51. You L, Qian W, Yang Q, Mao L, Zhu L, Huang X, Jin J, Meng H. 2017. *ERG11* Gene Mutations and *MDR1* Upregulation Confer Pan-Azole Resistance in *Candida*

tropicalis Causing Disseminated Candidiasis in an Acute Lymphoblastic Leukemia Patient on Posaconazole Prophylaxis. Antimicrob Agents Chemother 61.

52. Wirsching S, Michel S, Morschhauser J. 2000. Targeted gene disruption in *Candida albicans* wild-type strains: the role of the *MDR1* gene in fluconazole resistance of clinical *Candida albicans* isolates. Mol Microbiol 36:856-65.

53. Berkow EL, Manigaba K, Parker JE, Barker KS, Kelly SL, Rogers PD. 2015. Multidrug Transporters and Alterations in Sterol Biosynthesis Contribute to Azole Antifungal Resistance in *Candida parapsilosis*. Antimicrob Agents Chemother 59:5942-50.

54. Souza AC, Fuchs BB, Pinhati HM, Siqueira RA, Hagen F, Meis JF, Mylonakis E, Colombo AL. 2015. *Candida parapsilosis* Resistance to Fluconazole: Molecular Mechanisms and *In Vivo* Impact in Infected *Galleria mellonella* Larvae. Antimicrob Agents Chemother 59:6581-7.

55. Grossman NT, Pham CD, Cleveland AA, Lockhart SR. 2015. Molecular mechanisms of fluconazole resistance in *Candida parapsilosis* isolates from a U.S. surveillance system. Antimicrob Agents Chemother 59:1030-7.

56. Hampe IAI, Friedman J, Edgerton M, Morschhauser J. 2017. An acquired mechanism of antifungal drug resistance simultaneously enables *Candida albicans* to escape from intrinsic host defenses. PLoS Pathog 13:e1006655.

57. Hiller D, Sanglard D, Morschhauser J. 2006. Overexpression of the *MDR1* gene is sufficient to confer increased resistance to toxic compounds in *Candida albicans* (vol 50, pg 1365, 2006). Antimicrobial Agents and Chemotherapy 50:2591-2591.

58. Biermann AR, Demers EG, Hogan DA. 2021. Mrr1 regulation of methylglyoxal catabolism and methylglyoxal-induced fluconazole resistance in *Candida lusitaniae*. Mol Microbiol 115:116-130.

59. Chakraborty S, Karmakar K, Chakravortty D. 2014. Cells Producing Their Own Nemesis: Understanding Methylglyoxal Metabolism. Iubmb Life 66:667-678.

60. Tian S, Rong C, Nian H, Li F, Chu Y, Cheng S, Shang H. 2018. First cases and risk factors of super yeast *Candida auris* infection or colonization from Shenyang, China. Emerg Microbes Infect 7:128.

61. Sayeed MA, Farooqi J, Jabeen K, Mahmood SF. 2020. Comparison of risk factors and outcomes of *Candida auris* candidemia with non-*Candida auris* candidemia: A retrospective study from Pakistan. Med Mycol 58:721-729.

62. Shastri PS, Shankarnarayan SA, Oberoi J, Rudramurthy SM, Wattal C, Chakrabarti A. 2020. *Candida auris* candidaemia in an intensive care unit - Prospective observational study to evaluate epidemiology, risk factors, and outcome. J Crit Care 57:42-48.

63. Rudramurthy SM, Chakrabarti A, Paul RA, Sood P, Kaur H, Capoor MR, Kindo AJ, Marak RSK, Arora A, Sardana R, Das S, Chhina D, Patel A, Xess I, Tarai B, Singh P, Ghosh A. 2017. *Candida auris* candidaemia in Indian ICUs: analysis of risk factors. J Antimicrob Chemother 72:1794-1801.

64. Ruiz-Gaitan A, Martinez H, Moret AM, Calabuig E, Tasias M, Alastruey-Izquierdo A, Zaragoza O, Mollar J, Frasquet J, Salavert-Lleti M, Ramirez P, Lopez-Hontangas JL, Peman J. 2019. Detection and treatment of *Candida auris* in an

outbreak situation: risk factors for developing colonization and candidemia by this new species in critically ill patients. Expert Rev Anti Infect Ther 17:295-305.

65. Al-Rashdi A, Al-Maani A, Al-Wahaibi A, Alqayoudhi A, Al-Jardani A, Al-Abri S. 2021. Characteristics, Risk Factors, and Survival Analysis of *Candida auris* Cases: Results of One-Year National Surveillance Data from Oman. J Fungi (Basel) 7.

66. Caceres DH, Rivera SM, Armstrong PA, Escandon P, Chow NA, Ovalle MV, Diaz J, Derado G, Salcedo S, Berrio I, Espinosa-Bode A, Varon C, Stuckey MJ, Marino A, Villalobos N, Lockhart SR, Chiller TM, Prieto FE, Jackson BR. 2020. Case-Case Comparison of *Candida auris* Versus Other *Candida* Species Bloodstream Infections: Results of an Outbreak Investigation in Colombia. Mycopathologia 185:917-923.

67. Khan Z, Ahmad S, Benwan K, Purohit P, Al-Obaid I, Bafna R, Emara M, Mokaddas E, Abdullah AA, Al-Obaid K, Joseph L. 2018. Invasive *Candida auris* infections in Kuwait hospitals: epidemiology, antifungal treatment and outcome. Infection 46:641-650.

68. Pandya N, Cag Y, Pandak N, Pekok AU, Poojary A, Ayoade F, Fasciana T, Giammanco A, Caskurlu H, Rajani DP, Gupta YK, Balkan, II, Khan EA, Erdem H. 2021. International Multicentre Study of *Candida auris* Infections. J Fungi (Basel) 7.

69. Rossow J, Ostrowsky B, Adams E, Greenko J, McDonald R, Vallabhaneni S, Forsberg K, Perez S, Lucas T, Alroy KA, Jacobs Slifka K, Walters M, Jackson BR, Quinn M, Chaturvedi S, Blog D, New York Candida auris Investigation W. 2021. Factors Associated With *Candida auris* Colonization and Transmission in Skilled

Nursing Facilities With Ventilator Units, New York, 2016-2018. Clin Infect Dis 72:e753-e760.

70. Wang XJ, Ma SB, Liu ZF, Li H, Gao WY. 2019. Elevated levels of alpha-dicarbonyl compounds in the plasma of type II diabetics and their relevance with diabetic nephropathy. Journal of Chromatography B-Analytical Technologies in the Biomedical and Life Sciences 1106:19-25.

71. McLellan AC, Thornalley PJ, Benn J, Sonksen PH. 1994. Glyoxalase system in clinical diabetes mellitus and correlation with diabetic complications. Clin Sci (Lond) 87:21-9.

72. Lu J, Randell E, Han Y, Adeli K, Krahn J, Meng QH. 2011. Increased plasma methylglyoxal level, inflammation, and vascular endothelial dysfunction in diabetic nephropathy. Clin Biochem 44:307-11.

73. Odani H, Shinzato T, Usami J, Matsumoto Y, Brinkmann Frye E, Baynes JW, Maeda K. 1998. Imidazolium crosslinks derived from reaction of lysine with glyoxal and methylglyoxal are increased in serum proteins of uremic patients: evidence for increased oxidative stress in uremia. FEBS Lett 427:381-5.

74. Karg E, Papp F, Tassi N, Janaky T, Wittmann G, Turi S. 2009. Enhanced methylglyoxal formation in the erythrocytes of hemodialyzed patients. Metabolism 58:976-82.

75. Lapolla A, Flamini R, Lupo A, Arico NC, Rugiu C, Reitano R, Tubaro M, Ragazzi E, Seraglia R, Traldi P. 2005. Evaluation of glyoxal and methylglyoxal levels in uremic patients under peritoneal dialysis. Ann N Y Acad Sci 1043:217-24.

76. Mukhopadhyay S, Ghosh A, Kar M. 2008. Methylglyoxal increase in uremia with special reference to snakebite-mediated acute renal failure. Clin Chim Acta 391:13-7.

77. Brenner T, Fleming T, Uhle F, Silaff S, Schmitt F, Salgado E, Ulrich A, Zimmermann S, Bruckner T, Martin E, Bierhaus A, Nawroth PP, Weigand MA, Hofer S. 2014. Methylglyoxal as a new biomarker in patients with septic shock: an observational clinical study. Critical Care 18.

78. Juarez P, Jeannot K, Plesiat P, Llanes C. 2017. Toxic Electrophiles Induce Expression of the Multidrug Efflux Pump MexEF-OprN in *Pseudomonas aeruginosa* through a Novel Transcriptional Regulator, CmrA. Antimicrobial Agents and Chemotherapy 61.

79. Ozyamak E, de Almeida C, de Moura AP, Miller S, Booth IR. 2013. Integrated stress response of *Escherichia coli* to methylglyoxal: transcriptional readthrough from the nemRA operon enhances protection through increased expression of glyoxalase I. Mol Microbiol 88:936-50.

80. Lee C, Shin J, Park C. 2013. Novel regulatory system nemRA-gloA for electrophile reduction in *Escherichia coli* K-12. Mol Microbiol 88:395-412.

81. Mostofa MG, Ghosh A, Li ZG, Siddiqui MN, Fujita M, Tran LP. 2018. Methylglyoxal - a signaling molecule in plant abiotic stress responses. Free Radic Biol Med 122:96-109.

82. Kosmachevskaya OV, Shumaev KB, Topunov AF. 2017. Signal and regulatory effects of methylglyoxal in eukaryotic cells (review). Applied Biochemistry and Microbiology 53:273-289.

83. Maeta K, Izawa S, Okazaki S, Kuge S, Inoue Y. 2004. Activity of the Yap1 transcription factor in *Saccharomyces cerevisiae* is modulated by methylglyoxal, a metabolite derived from glycolysis. Mol Cell Biol 24:8753-64.

84. Aguilera J, Prieto JA. 2004. Yeast cells display a regulatory mechanism in response to methylglyoxal. FEMS Yeast Res 4:633-41.

85. Roy A, Hashmi S, Li Z, Dement AD, Cho KH, Kim JH. 2016. The glucose metabolite methylglyoxal inhibits expression of the glucose transporter genes by inactivating the cell surface glucose sensors Rgt2 and Snf3 in yeast. Mol Biol Cell 27:862-71.

86. Anonymous. 2016. Correction for The glucose metabolite methylglyoxal inhibits expression of the glucose transporter genes by inactivating the cell surface glucose sensors Rgt2 and Snf3 in yeast. Mol Biol Cell 27:3178-3179.

87. Maeta K, Izawa S, Inoue Y. 2005. Methylglyoxal, a metabolite derived from glycolysis, functions as a signal initiator of the high osmolarity glycerol-mitogen-activated protein kinase cascade and Calcineurin/Crz1-mediated pathway in *Saccharomyces cerevisiae*. Journal of Biological Chemistry 280:253-260.

88. Takatsume Y, Izawa S, Inoue Y. 2007. Modulation of Spc1 stress-activated protein kinase activity by methylglyoxal through inhibition of protein phosphatase in the fission yeast *Schizosaccharomyces pombe*. Biochem Biophys Res Commun 363:942-7.

89. Takatsume Y, Izawa S, Inoue Y. 2006. Methylglyoxal as a signal initiator for activation of the stress-activated protein kinase cascade in the fission yeast *Schizosaccharomyces pombe*. J Biol Chem 281:9086-92.

90. Welsh RM, Bentz ML, Shams A, Houston H, Lyons A, Rose LJ, Litvintseva AP. 2017. Survival, Persistence, and Isolation of the Emerging Multidrug-Resistant Pathogenic Yeast *Candida auris* on a Plastic Health Care Surface. J Clin Microbiol 55:2996-3005.

91. Rutala WA, Kanamori H, Gergen MF, Sickbert-Bennett EE, Weber DJ. 2019. Susceptibility of *Candida auris* and *Candida albicans* to 21 germicides used in healthcare facilities. Infect Control Hosp Epidemiol 40:380-382.

92. Jabeen K, Mal PB, Tharwani A, Hashmi M, Farooqi J. 2020. Persistence of *Candida auris* on latex and nitrile gloves with transmission to sterile urinary cathetersdouble dagger. Med Mycol 58:128-132.

93. Eyre DW, Sheppard AE, Madder H, Moir I, Moroney R, Quan TP, Griffiths D, George S, Butcher L, Morgan M, Newnham R, Sunderland M, Clarke T, Foster D, Hoffman P, Borman AM, Johnson EM, Moore G, Brown CS, Walker AS, Peto TEA, Crook DW, Jeffery KJM. 2018. A *Candida auris* Outbreak and Its Control in an Intensive Care Setting. N Engl J Med 379:1322-1331.

94. Hoehamer CF, Cummings ED, Hilliard GM, Morschhauser J, Rogers PD. 2009. Proteomic analysis of Mrr1p- and Tac1p-associated differential protein expression in azole-resistant clinical isolates of *Candida albicans*. Proteomics Clin Appl 3:968-78.

95. Karababa M, Coste AT, Rognon B, Bille J, Sanglard D. 2004. Comparison of gene expression profiles of *Candida albicans* azole-resistant clinical isolates and laboratory strains exposed to drugs inducing multidrug transporters. Antimicrob Agents Chemother 48:3064-79.

96. Rogers PD, Barker KS. 2003. Genome-wide expression profile analysis reveals coordinately regulated genes associated with stepwise acquisition of azole resistance in *Candida albicans* clinical isolates. Antimicrob Agents Chemother 47:1220-7.

97. Silva AP, Miranda IM, Guida A, Synnott J, Rocha R, Silva R, Amorim A, Pina-Vaz C, Butler G, Rodrigues AG. 2011. Transcriptional profiling of azole-resistant *Candida parapsilosis* strains. Antimicrob Agents Chemother 55:3546-56.

98. Kannan A, Asner SA, Trachsel E, Kelly S, Parker J, Sanglard D. 2020. Erratum for Kannan et al., "Comparative Genomics for the Elucidation of Multidrug Resistance in *Candida lusitaniae*". mBio 11.

99. Rognon B, Kozovska Z, Coste AT, Pardini G, Sanglard D. 2006. Identification of promoter elements responsible for the regulation of *MDR1* from *Candida albicans*, a major facilitator transporter involved in azole resistance. Microbiology (Reading) 152:3701-3722.

100. Ramirez-Zavala B, Mogavero S, Scholler E, Sasse C, Rogers PD, Morschhauser J. 2014. SAGA/ADA complex subunit Ada2 is required for Cap1- but not Mrr1-mediated upregulation of the *Candida albicans* multidrug efflux pump *MDR1*. Antimicrob Agents Chemother 58:5102-10.

101. Mogavero S, Tavanti A, Senesi S, Rogers PD, Morschhauser J. 2011. Differential requirement of the transcription factor Mcm1 for activation of the *Candida albicans* multidrug efflux pump *MDR1* by its regulators Mrr1 and Cap1. Antimicrob Agents Chemother 55:2061-6.

102. Hiller D, Stahl S, Morschhauser J. 2006. Multiple cis-acting sequences mediate upregulation of the *MDR1* efflux pump in a fluconazole-resistant clinical *Candida albicans* isolate. Antimicrob Agents Chemother 50:2300-8.

103. Harry JB, Oliver BG, Song JL, Silver PM, Little JT, Choiniere J, White TC. 2005. Drug-induced regulation of the *MDR1* promoter in *Candida albicans*. Antimicrob Agents Chemother 49:2785-92.

104. Gupta V, Kohli A, Krishnamurthy S, Puri N, Aalamgeer SA, Panwar S, Prasad R. 1998. Identification of polymorphic mutant alleles of *CaMDR1*, a major facilitator of *Candida albicans* which confers multidrug resistance, and its *in vitro* transcriptional activation. Curr Genet 34:192-9.

105. Iyer KR, Camara K, Daniel-Ivad M, Trilles R, Pimentel-Elardo SM, Fossen JL, Marchillo K, Liu Z, Singh S, Munoz JF, Kim SH, Porco JA, Jr., Cuomo CA, Williams NS, Ibrahim AS, Edwards JE, Jr., Andes DR, Nodwell JR, Brown LE, Whitesell L, Robbins N, Cowen LE. 2020. An oxindole efflux inhibitor potentiates azoles and impairs virulence in the fungal pathogen *Candida auris*. Nat Commun 11:6429.

106. Dunkel N, Blass J, Rogers PD, Morschhauser J. 2008. Mutations in the multi-drug resistance regulator *MRR1*, followed by loss of heterozygosity, are the main cause of *MDR1* overexpression in fluconazole-resistant *Candida albicans* strains. Mol Microbiol 69:827-40.

107. Rodrigues CF, Rodrigues ME, Henriques M. 2019. *Candida* sp. Infections in Patients with Diabetes Mellitus. J Clin Med 8.

108. Pyrgos V, Ratanavanich K, Donegan N, Veis J, Walsh TJ, Shoham S. 2009. *Candida* bloodstream infections in hemodialysis recipients. Med Mycol 47:463-7.

109. Zhang MM, Ong CL, Walker MJ, McEwan AG. 2016. Defence against methylglyoxal in Group A *Streptococcus*: a role for Glyoxylase I in bacterial virulence and survival in neutrophils? Pathog Dis 74.

110. Rachman H, Kim N, Ulrichs T, Baumann S, Pradl L, Nasser Eddine A, Bild M, Rother M, Kuban RJ, Lee JS, Hurwitz R, Brinkmann V, Kosmiadi GA, Kaufmann SH. 2006. Critical role of methylglyoxal and AGE in mycobacteria-induced macrophage apoptosis and activation. PLoS One 1:e29.

111. Prantner D, Nallar S, Richard K, Spiegel D, Collins KD, Vogel SN. 2021. Classically activated mouse macrophages produce methylglyoxal that induces a TLR4- and RAGE-independent proinflammatory response. J Leukoc Biol 109:605-619.

112. Jimenez-Lopez C, Collette JR, Brothers KM, Shepardson KM, Cramer RA, Wheeler RT, Lorenz MC. 2013. *Candida albicans* induces arginine biosynthetic genes in response to host-derived reactive oxygen species. Eukaryot Cell 12:91-100.

113. Aranda A, del Olmo ML. 2004. Exposure of *Saccharomyces cerevisiae* to acetaldehyde induces sulfur amino acid metabolism and polyamine transporter genes, which depend on Met4p and Haa1p transcription factors, respectively. Appl Environ Microbiol 70:1913-22.

114. Lucau-Danila A, Lelandais G, Kozovska Z, Tanty V, Delaveau T, Devaux F, Jacq C. 2005. Early expression of yeast genes affected by chemical stress. Mol Cell Biol 25:1860-8.

115. Lelandais G, Tanty V, Geneix C, Etchebest C, Jacq C, Devaux F. 2008. Genome adaptation to chemical stress: clues from comparative transcriptomics in *Saccharomyces cerevisiae* and *Candida glabrata*. Genome Biol 9:R164.

116. Staub RE, Quistad GB, Casida JE. 1998. Mechanism for benomyl action as a mitochondrial aldehyde dehydrogenase inhibitor in mice. Chemical Research in Toxicology 11:535-543.

117. Fitzmaurice AG, Rhodes SL, Lulla A, Murphy NP, Lam HA, O'Donnell KC, Barnhill L, Casida JE, Cockburn M, Sagasti A, Stahl MC, Maidment NT, Ritz B, Bronstein JM. 2013. Aldehyde dehydrogenase inhibition as a pathogenic mechanism in Parkinson disease. Proceedings of the National Academy of Sciences of the United States of America 110:636-641.

118. Casida JE, Ford B, Jinsmaa Y, Sullivan P, Cooney A, Goldstein DS. 2014. Benomyl, aldehyde dehydrogenase, DOPAL, and the catecholaldehyde hypothesis for the pathogenesis of Parkinson's disease. Chem Res Toxicol 27:1359-61.

119. Leiphon LJ, Picklo MJ, Sr. 2007. Inhibition of aldehyde detoxification in CNS mitochondria by fungicides. Neurotoxicology 28:143-9.

120. Jakab A, Balla N, Ragyak A, Nagy F, Kovacs F, Sajtos Z, Toth Z, Borman AM, Pocsi I, Baranyai E, Majoros L, Kovacs R. 2021. Transcriptional Profiling of the *Candida auris* Response to Exogenous Farnesol Exposure. mSphere doi:10.1128/mSphere.00710-21:e0071021.

121. Nagy F, Vitalis E, Jakab A, Borman AM, Forgacs L, Toth Z, Majoros L, Kovacs R. 2020. *In vitro* and *in vivo* Effect of Exogenous Farnesol Exposure Against *Candida auris*. Front Microbiol 11:957.

122. Shirtliff ME, Krom BP, Meijering RA, Peters BM, Zhu J, Scheper MA, Harris ML, Jabra-Rizk MA. 2009. Farnesol-induced apoptosis in *Candida albicans*. Antimicrob Agents Chemother 53:2392-401.

123. Hasim S, Vaughn EN, Donohoe D, Gordon DM, Pfiffner S, Reynolds TB. 2018. Influence of phosphatidylserine and phosphatidylethanolamine on farnesol tolerance in *Candida albicans*. Yeast 35:343-351.

124. Machida K, Tanaka T, Fujita K, Taniguchi M. 1998. Farnesol-induced generation of reactive oxygen species via indirect inhibition of the mitochondrial electron transport chain in the yeast *Saccharomyces cerevisiae*. J Bacteriol 180:4460-5.

125. Fairn GD, MacDonald K, McMaster CR. 2007. A chemogenomic screen in *Saccharomyces cerevisiae* uncovers a primary role for the mitochondria in farnesol toxicity and its regulation by the Pkc1 pathway. J Biol Chem 282:4868-4874.

126. Yadav SK, Singla-Pareek SL, Ray M, Reddy MK, Sopory SK. 2005. Methylglyoxal levels in plants under salinity stress are dependent on glyoxalase I and glutathione. Biochem Biophys Res Commun 337:61-7.

127. Nahar K, Hasanuzzaman M, Alam MM, Fujita M. 2015. Glutathione-induced drought stress tolerance in mung bean: coordinated roles of the antioxidant defence and methylglyoxal detoxification systems. AoB Plants 7.

128. Melvin P, Bankapalli K, D'Silva P, Shivaprasad PV. 2017. Methylglyoxal detoxification by a DJ-1 family protein provides dual abiotic and biotic stress tolerance in transgenic plants. Plant Mol Biol 94:381-397.

129. Vemanna RS, Babitha KC, Solanki JK, Amarnatha Reddy V, Sarangi SK, Udayakumar M. 2017. Aldo-keto reductase-1 (*AKR1*) protect cellular enzymes from salt stress by detoxifying reactive cytotoxic compounds. Plant Physiol Biochem 113:177-186.

130. Mahmud JA, Hasanuzzaman M, Khan MIR, Nahar K, Fujita M. 2020. beta-Aminobutyric Acid Pretreatment Confers Salt Stress Tolerance in *Brassica napus L*. by Modulating Reactive Oxygen Species Metabolism and Methylglyoxal Detoxification. Plants (Basel) 9.

131. Rohman MM, Islam MR, Monsur MB, Amiruzzaman M, Fujita M, Hasanuzzaman M. 2019. Trehalose Protects Maize Plants from Salt Stress and Phosphorus Deficiency. Plants (Basel) 8.

132. Veena, Reddy VS, Sopory SK. 1999. Glyoxalase I from *Brassica juncea*: molecular cloning, regulation and its over-expression confer tolerance in transgenic tobacco under stress. Plant J 17:385-95.

133. Shanks RM, Caiazza NC, Hinsa SM, Toutain CM, O'Toole GA. 2006. *Saccharomyces cerevisiae*-based molecular tool kit for manipulation of genes from gram-negative bacteria. Appl Environ Microbiol 72:5027-36.

134. Grahl N, Demers EG, Crocker AW, Hogan DA. 2017. Use of RNA-Protein complexes for genome editing in non-albicans *Candida* Species. mSphere 2:00218-17.

135. Kim D, Paggi JM, Park C, Bennett C, Salzberg SL. 2019. Graph-based genome alignment and genotyping with HISAT2 and HISAT-genotype. Nat Biotechnol 37:907-915.

136. Liao Y, Smyth GK, Shi W. 2014. featureCounts: an efficient general purpose program for assigning sequence reads to genomic features. Bioinformatics 30:923-30.

137. Robinson MD, McCarthy DJ, Smyth GK. 2010. edgeR: a Bioconductor package for differential expression analysis of digital gene expression data. Bioinformatics 26:139-40.

138. Basenko EY, Pulman JA, Shanmugasundram A, Harb OS, Crouch K, Starns D, Warrenfeltz S, Aurrecoechea C, Stoeckert CJ, Jr., Kissinger JC, Roos DS, Hertz-Fowler C. 2018. FungiDB: An Integrated Bioinformatic Resource for Fungi and Oomycetes. J Fungi (Basel) 4.

139. Stajich JE, Harris T, Brunk BP, Brestelli J, Fischer S, Harb OS, Kissinger JC, Li W, Nayak V, Pinney DF, Stoeckert CJ, Jr., Roos DS. 2012. FungiDB: an integrated functional genomics database for fungi. Nucleic Acids Res 40:D675-81.

140. Pathirana RU, Friedman J, Norris HL, Salvatori O, McCall AD, Kay J, Edgerton M. 2018. Fluconazole-Resistant *Candida auris* Is Susceptible to Salivary Histatin 5 Killing and to Intrinsic Host Defenses. Antimicrob Agents Chemother 62.

141. Asner SA, Giulieri S, Diezi M, Marchetti O, Sanglard D. 2015. Acquired Multidrug Antifungal Resistance in Candida lusitaniae during Therapy. Antimicrob Agents Chemother 59:7715-22.

Chapter 4. Discussion, Future Directions, and Conclusion

4.1 Possible mechanisms for MG induction of Mrr1-regulated genes

The most straightforward hypothesis as to how MG activates transcription of Mrr1-regulated genes is that MG directly modifies one or more amino acids of the Mrr1 protein. As discussed in **Chapter 1**, MG preferentially reacts with arginine, lysine, and cysteine residues, and the reactivity of any residue is dependent upon its local environment (1-6). ClMrr1 contains 28 cysteine (2.2% of the protein), 62 arginine (4.9%), and 69 lysine (5.5%) residues. Of the cysteine residues, 6 are located within the conserved N-terminal Cys_6Zn_2 motif, but any of the remaining 22 cysteine residues could act as an MG-sensing switch. If MG does directly modify Mrr1, we favor cysteine as the target residue over arginine or lysine, because the gradual drop in *MDR1* expression after peaking at 15 - 30 min of MG exposure (**Appendix Fig. II.2**) implies a return to basal Mrr1 activity and thus, a reversible modification. Because we do not observe a change in the SDS-PAGE gel migration of HF-tagged Mrr1 from MG-treated cultures (data not shown), it is likely that only one to a few specific residues of Mrr1 would be modified by MG at the concentration used (5 mM). We could run a gel for a longer period of time to magnify and small size differences that may be present. Of course, the best way to definitively determine whether Mrr1 is directly modified by MG is to overexpress full-length, HF-tagged Mrr1 in *C. lusitaniae*, and either treat cultures with MG and then purify the tagged protein or purify HF-Mrr1 first and then treat it with MG *in vitro*. Samples could then be analyzed via mass spectrometry to determine which, if any, residues are MG-modified.

As glycation often leads to conformational changes of proteins, we can reasonably assume that glycated Mrr1 would be conformationally different from unmodified Mrr1,

and we can test this via Native PAGE against MG-treated or untreated strains expressing HF-tagged Mrr1. A conformational change could lead to increased Mrr1 activity in a few ways. One, glycated Mrr1 may have a stronger interaction with one or more of its binding partners, resulting in increased expression of shared target genes. This could be tested directly by performing a co-immunoprecipitation against full-length HF-tagged Mrr1 in cultures treated or not treated with MG. Due to the low intracellular quantities often observed for transcription factors, it may behoove us to create strain that overexpresses HF-tagged Mrr1 – conversely, overexpression of Mrr1 may result in increased interaction with binding partners and expression of target genes even in the absence of an inducer, which could make results difficult to interpret. Nonetheless, it would be interesting to investigate whether MG changes the propensity of Mrr1 to interact with any of its binding partners. This technique can also be employed to gain a better understanding of why *C. auris* Mrr1a can be induced by benomyl but not by MG when expressed in *C. lusitaniae* (**Fig. 3.4C-F**). That is, perhaps *C. auris* Mrr1a cannot bind as efficiently to some other factor in *C. lusitaniae* that is necessary for activation by MG but not by benomyl. If that is the case, it would also suggest that different factors are required for induction by benomyl versus MG, at least in *C. lusitaniae*.

Another possible way in which a conformational change in Mrr1 could increase transcriptional activation is by shielding specific serine, threonine, or tyrosine residues from phosphorylation by Ssn3. As Liu and Myers (7) have demonstrated, Ssn3 phosphorylates Mrr1 in *C. albicans* to negatively regulate its activity. Thus, if Ssn3 and Mrr1 have the same relationship in *C. lusitaniae*, MG might modify the structure of Mrr1 in such a way that Ssn3-phosphorylated residues become inaccessible. One way to test this

is to monitor the phosphorylation state of Mrr1 following treatment with MG in a strain expressing the full-length *MRR1*^{ancestral} allele (which is highly responsive to MG) and an isogenic strain from which *SSN3* (*CLUG_05119*) has been deleted. Additionally, it would be interesting to investigate whether Mrr1^{ancestral} becomes constitutively active in the absence of *SSN3* and, if so, whether MG is incapable of inducing a further increase of Mrr1 activity in this strain. Conversely, it is also possible that MG reacts with Ssn3 to cause a decrease in its kinase activity, thus relieving phosphorylation-dependent repression of Mrr1.

If MG does not directly modify Mrr1, an obvious candidate would be Cap1. It has already been demonstrated that Yap1, the *S. cerevisiae* homolog of Cap1, is reversibly modified by MG at any of its three C-terminal cysteine residues, resulting in its activation (8). Pap1 in *S. pombe* is similarly activated by MG (9). In addition to MG, other electrophilic compounds, such as N-ethylmaleimide (NEM) (10), acrolein (10), malondialdehyde (MDA) (11), 4-hydroxynonenal (12), and iodoacetamide (12), have also been shown to activate Yap1 via modification of its C-terminal cysteine residues. Yap1 displays at least two distinct mechanisms of activation by either reactive oxygen species or reactive electrophiles: hydrogen peroxide (H_2O_2) leads to intramolecular disulfide bond formation in Yap1 via the glutathione peroxidase Gpx3, and the N-terminal Cys residues 303 and 310 in addition to the C-terminal Cys residues 598 and 620 are required for stable activation by H_2O_2 (13, 14); whereas electrophilic activation of Yap1 occurs independently of Gpx3 or the N-terminal Cys residues (10, 12, 15). Notably, H_2O_2 and reactive electrophiles cause the Yap1-dependent differential expression of unique sets of genes (10). Likewise, H_2O_2 and reactive electrophiles do not confer cross-resistance to one

another, while electrophiles do confer Yap1-dependent cross-resistance to other electrophiles (10). Thus, Yap1 can be considered an independent sensor of both ROS and electrophilic stress.

Our work presented in **Chapter 2** paint an unclear picture of the possible role for Cap1 in the Mrr1-dependent response to MG. Deletion of either *MRR1* or *CAP1* in isolate S18 completely abolishes induction of *MGD1* and *MGD2* by MG, but not of *MDR1* (**Fig. 2.4D-F**). In fact, MG-induced *MDR1* expression in a *cap1*Δ single mutant does not differ significantly from that observed in the parental isolate S18, nor does the *mrr1*Δ/*cap1*Δ double mutant differ significantly in this regard from the *mrr1*Δ single mutant (**Fig. 2.4F**). Similarly, the *cap1*Δ single mutant does not exhibit a significant decrease in stimulation of growth in fluconazole by MG relative to the parental (**Fig. 2.5B**), nor is the *mrr1*Δ/*cap1*Δ double mutant significantly different from the mrr1Δ single mutant in this assay (**Fig. 2.5B**). Therefore, it appears that in *C. lusitaniae*, both Mrr1 and Cap1 are required for induction of *MGD1* and *MGD2* in response to MG, but there is not convincing evidence that Cap1 participates in MG-mediated *MDR1* induction, at least in this strain. In accordance with these observations, the *cap1*Δ mutant displays a substantial growth defect in MG (**Fig. S2.3B**) but its fluconazole MIC does not differ from the parental isolate S18 (**Table 2.1**). However, even if Cap1 is not required for induction of *MDR1* expression and stimulation of growth in fluconazole by MG, we cannot rule out the possibility that Cap1 can be activated by MG in a manner comparable to *S. cerevisiae* Yap1, particularly because induction of *MGD1* and *MGD2* does appear to be Cap1-dependent and expression of *MGD1* is regulated by Cap1 in *C. albicans* (16). To investigate whether MG activates Cap1 in *Candida* species, we can employ methodology similar to that of Maeta et al. (8). That

is, we can express a GFP-tagged ClCap1 in both *glo1*Δ and *GLO1*-intact *C. lusitaniae* strains and use fluorescence microscopy to examine whether exogenous and/or endogenous MG cause ClCap1-GFP to localize to the nucleus. The plasmid to express *ClCAP1-GFP* has already been created by Patricia Occipinti, a former member of the lab. Additionally, due to the genetic heterogeneity among our clinical isolates and the report of circuit diversification in *C. albicans* by Huang et al. (17), it is possible that Cap1 may participate in MG-induced *MDR1* expression in some strains or isolates but not others. Therefore, we could knock out *CAP1* from different isolates, including other clinical and environment isolates that are more distantly related to the isolates that have been the focus of this work, and examine their transcriptional and phenotypic response to exogenous MG.

Another transcription factor that may be involved in the Mrr1-dependent transcriptional response to MG is Mcm1, a binding partner of *C. albicans* Mrr1 that was described in **Chapter 1**. In *S. cerevisiae*, Mcm1 is a downstream, HOG pathway-independent target of the response regulator Sln1 (18, 19). This is noteworthy because activation of the HOG pathway by MG occurs through the Sln1 branch in *S. cerevisiae* (20, 21). Additionally, deletion of *ScFPS1*, which encodes a glycerol export protein, leads to elevated intracellular glycerol and phosphorylation of Sln1, resulting in increased Mcm1 activity (22). Because MG exposure also causes glycerol accumulation in *S. cerevisiae* (23), and the activity of Mcm1 and the HOG pathway are reciprocally regulated by Sln1 (18, 19, 22), we propose the following model: a) MG causes dephosphorylation of Sln1 by some unknown mechanism, resulting in activation of the HOG pathway; b) the activated HOG pathway upregulates expression of *GPD1*, leading to increased glycerol production; c) glycerol accumulation leads to phosphorylation of Sln1, thereby shutting off the HOG

pathway and activating Mcm1; and d) activated Mcm1 cooperates with Mrr1 to regulate expression of shared target genes including *MDR1* and *MGD1*. A visual representation of this model is depicted in **Fig. 4.1**. Of course, this model is contingent upon the observations reported in *S. cerevisiae* also holding true for *Candida* species. Several preliminary experiments we could perform to test our model are 1) generate repressible *MCM1* strains in *C. lusitaniae* to assess whether depletion of Mcm1 protein abolishes *MDR1* and *MGD1* induction by MG; 2) measure intracellular glycerol in *C. lusitaniae* cultures exposed to MG at different time points; and 3) use RT-qPCR to assess whether growth in glycerol induces expression of Mrr1-regulated genes.

Finally, it is possible that MG modulates the ability of Mrr1 to interact with its DNA targets, through modulation of SWI/SNF activity and/or direct glycation of histones. In *C. albicans*, Mrr1 and the SWI/SNF complex are mutually dependent on one another for binding to their shared target promoters, and thus the SWI/SNF complex is required for high MDR1 expression by gain-of-function Mrr1 as well as induction of *MDR1* in response to benomyl (7). The simplest preliminary experiment to investigate possible involvement of the SWI/SNF complex in the MG response is to assess whether genetic deletion of *SNF2* abolishes induction of *MDR1* and *MGD1* by MG. While we would not be able to conclude that the *SWI*/*SNF* complex itself is activated by MG based on this experiment alone, negative results (i.e., no difference in induction between $SNF2^{WT}$ strains and *snf2*Δ mutants) would likely rule out the SWI/SNF complex in the Mrr1-dependent MG response. Alternatively (or concurrently), it is possible that MG directly glycates basic residues on histones, decreasing nucleosome density and rendering the chromatin more accessible to transcriptional machinery. To investigate this hypothesis, we can evaluate the relative

nucleosome density around the promoters of *MDR1* and *MGD1* in MG-treated cultures via chromatin immunoprecipitation against histone H3 (7). If we find that MG treatment does lead to decreased histone binding at these promoters but that *SNF2* is not required for this process, histone glycation by MG would seem plausible. MG-mediated glycation of histone proteins has been observed *in vitro* (24-26) and *in vivo* (25, 27), and upregulation of salt stress responsive genes in *Arabidopsis thaliana* following salt exposure is associated with histone glycation by MG (27).

4.2 Investigating the functions of Mrr1b and Mrr1c in *C. auris*

As shown in **Fig. 3.1**, *MDR1* and *MGD1* appear to be the only genes whose expression is strongly regulated by Mrr1a in the *C. auris* isolate B11221. Because *MRR1a* contains a gain-of-function mutation in B11221, like other clade III isolates (28, 29), this isolate seemed like the ideal genetic background to assess the effects of *MRR1a* deletion. However, essentially nothing is yet known about the functions of Mrr1b and Mrr1c, other than that neither contributes to azole resistance *C. auris* (30). We hypothesize that the unexpectedly small number of genes (four in total) that are significantly differentially expressed between B11221 *mrr1a*Δ and its parent could be the result of compensation by Mrr1b and/or Mrr1c. We are currently in the process of generating plasmids to complement *MRR1b* and *MRR1c* into *C. lusitaniae* as we did with *MRR1a* to investigate whether expression of either gene can complement an *mrr1*Δ mutant. However, most zinc-cluster transcription factors are not active in the absence of either gain-of-function mutations or inducing signals (see reference (31) for review); there are currently no known gain-of-function mutations in *C. auris MRR1b* or *MRR1c*, and likewise it is not known what might

induce their activity. As a result, studying the functions of the genes may be difficult if they do not respond to any of the known activators of Mrr1. Regardless, we believe it Is worth the effort to investigate the roles of Mrr1b and Mrr1c and whether and how they contribute to *C. auris* pathogenesis or persistence.

4.3 Discussion on the possible clinical relevance of this work

It is noteworthy that many of the human diseases in which elevated levels of MG and AGEs have been observed are also associated with an increased risk of candidiasis and candidemia. We propose that the MG-detoxification capacity of yeast, which likely arose from a long evolutionary history of growth in high-sugar environments, contributes to the persistence of *Candida* in these patients, and that MG and other reactive aldehydes could reach significant signaling concentrations in the context of infection.

Methylglyoxal, glyoxalase I deficiency, and infection

The most likely sources of exogenous MG that a microbial pathogen would encounter in a mammalian host are production from immune cells and, in some cases, host-endogenous MG due to hyperglycemia, systemic GSH deficiency, and/or defects in glyoxalase expression or activity. As described in **Chapter 1**, phagocytes generate MG and other reactive aldehydes in response to stimulation by microbial antigens (32-38), suggesting that resistance against these compounds in vitro could also indicate resistance against phagocytic killing in the context of infection. In recent years, a few MG-specific fluorescent probes have been developed for use in living tissues. Dang et al. (39) have published on a near-infrared (NIR) fluorescent MG probe called DBTPP, which uses a

thiadiazole-fused o-phenylenediamine moiety to detect MG. DBTPP can noninvasively monitor MG levels in cell culture and in live mice (39). Gao et al. (40) have developed a two-photon fluorescent MG probe named NP, which relies on naphthalimide dye and o-phenylenediamine and has successfully been used in cells, tissues, and in live zebrafish. Another MG probe that may be useful for our purposes is NAP-DCP-4, which is cell-impermeable and designed for the purpose of monitoring MG in the supernatant of activated macrophages (41). We could utilize these probes to explore MG production in the context of microbial infection. Specifically, we would like to use the NIR probe DBTPP to visualize MG production in mice infected with different pathogens, such as *C. albicans* or *P. aeruginosa*. Because NIR fluorescent imaging is noninvasive, we would easily be able to monitor how the MG level changes during infection without having to sacrifice mice at each time point. We also think the NP probe would be interesting for use in a zebrafish model of infection to track MG production in relation to fluorescently tagged pathogens and immune cells. Finally, the cell-impermeable probe, NAP-DCP-4, would be useful for examining extracellular MG produced by macrophages or neutrophils *in vitro* following stimulation with microbial antigens.

Levels of MG are commonly elevated in many conditions associated with chronic inflammation, including Type 1 and Type 2 diabetes (**Chapter 1** and the references therein), psoriasis, multiple sclerosis, and cirrhosis. Chronic inflammation also contributes to the pathology of cystic fibrosis (CF) (see reference (42) for review), the disease afflicting the three patients in whom we have identified *C. lusitaniae* in the lungs. Although MG has not yet been directly measured in the context of cystic fibrosis (CF), levels of MDA are significantly elevated in the breath, plasma, and sputum of CF patients compared to healthy

controls (43), and MDA is correlated with a more severe decline in lung function among CF patients (43, 44). Carbonylated proteins are also significantly elevated in the plasma CF patients (45, 46). Additionally, Pariano et al. (47) have recently reported defective *GLO1* expression and Glo1 activity in *Cftr*$^{-/-}$ mice and in bronchial cells from human CF patients. Furthermore, higher expression of the receptor for advanced glycation endproducts (RAGE) is associated with more severe lung disease and inflammation in CF (48), and inhibition of RAGE signaling leads to significantly lower inflammation and fungal burdens in the lungs of *Cftr*$^{-/-}$ mice infected with *Aspergillus fumigatus* (49). Patients with CF also exhibit systemic deficiency in reduced glutathione (GSH) (50), which contributes to oxidative stress in the airways (51) and could plausibly exacerbate electrophilic stress, though the latter possibility has not yet been investigated.

Virulence

There is growing evidence that metabolism of MG and other reactive aldehydes plays a crucial role in the virulence of microbial pathogens. In the bacterium *Listeria monocytogenes*, mutants lacking the glyoxalase I gene *gloA* exhibit attenuated virulence in mice due to GSH depletion and inability to activate the master virulence regulator PrfA (52). Glyoxalase I is also critical for virulence in Group A *Streptococcus*; null mutants are hypersensitive to MPO-dependent neutrophil killing and display a dissemination defect *in vivo* (36). In *E. coli*, the MG reductase gene *ydjG* is one of nine genes upregulated upon colonization of the murine cecum, and deletion of *ydjG* leads to decreased cecal colonization (53). The genome of the murine malarial parasite *Plasmodium berghei* encodes two functional glyoxalase II genes; one is targeted to the cytosol and the other to

the apicoplast (54). Disruption of both genes in *P. berghei* inhibits liver-stage proliferation in mice by 90% (54). As for yeast, large-scale transcriptomics analyses have shown that expression of MG reductase genes is upregulated in *C. albicans* and *S. cerevisiae* during growth in physiologically relevant conditions. Specifically, *CaMGD1* (referred to as *GRP2* in the corresponding reference) is highly expressed during *C. albicans* colonization of the murine cecum (55), and *ScGRE2* is among the numerous stress-responsive genes induced after incubation in human blood *in vitro* for one hour (56). These examples illustrate the importance for MG detoxification for the capacity of microbes to colonize and persist in a mammalian host, due at least in part to MG production by host immune cells and possible endogenous MG generation under environmental stresses (see below). We are very interested in testing our *C. lusitaniae mrr1*Δ, *mgd1*Δ, *mgd2*Δ, and *glo1*Δ mutants in animal models of infection to investigate whether any of these mutants exhibit a defect in colonization and/or virulence.

Abiotic stress response

In addition to competition with other microbes, exposure to antimicrobial drugs, and onslaught by the immune system, microbial pathogens must cope with abiotic stresses such as osmotic stress, high temperatures, nutrient limitation, and a potentially wide range of pH. Due to its ability to activate stress-response pathways, as discussed in Chapter 1, MG is an intriguing potential stress signal. In fact, the involvement of MG metabolism in tolerance to a variety of abiotic stresses has been studied extensively in plants. In multiple plant species, intracellular MG increases significantly in response to drought (57, 58), salinity (57, 59-63), cold stress (57), heavy metals (59), or phosphorous deficiency (62).

Additionally, expression of genes involved in MG detoxification is upregulated in plants treated with NaCl (64-66), mannitol (64, 66), abscisic acid (64, 66), and heavy metals (65). Furthermore, overexpression of MG detoxification genes leads to increased tolerance to salinity (57, 63, 65, 67, 68), drought (68), heat (66, 68), and oxidative stress (66) in plants. Similar findings have been reported in microbes. For example, intracellular MG increases in *S. cerevisiae* exposed to H_2O_2 or a high concentration of NaCl (69). In the bacterium *Burkholderia pseudomallei*, expression of a particular NADPH-dependent dicarbonyl reductase is upregulated in response to salt stress, and overexpression protects *B. pseudomallei* from diacetyl, MG, and high salinity (70). To investigate the potential involvement of MG metabolism in stress tolerance of *Candida*, we would first assess our MG-sensitive mutants for defects in growth in high salinity, non-salt osmotic stress (i.e., sorbitol), heat, cold, and heavy metal stress. We are particularly interested in studying the potential for Mrr1-dependent (via *MGD1*) stress tolerance in *C. auris*, due to the organism's striking ability to persist on abiotic surfaces for comparatively long periods of time.

4.4 Speculation on a potential role for aldehyde metabolism in yeast quorum sensing

We note many similarities between the transcriptional response of *C. lusitaniae* (**Chapter 2**) and *C. auris* (**Chapter 3**) to MG and that of some *Candida* species to farnesol or tyrosol (71-74). In particular, farnesol induces expression of *MDR1* in *C. albicans* (73), *MGD1* (*GRP2*) in *C. parapsilosis* (74), and both in *C. auris* (72), while and tyrosol induces expression of both genes in *C. parapsilosis* (71). Farnesol and tyrosol, along with several other alcohols, are known as quorum sensing molecules in *Candida* species (see reference

(75) for review), but the mechanisms by which these alcohols modulate yeast transcription and physiology are unclear. Certain alcohol compounds can also act as signaling molecules in *S. cerevisiae*; for example, isoamyl alcohol is considered an inducer of filamentation in budding yeast (76). However, Hauser et al. (77) postulate that isovaleraldehyde, the cognate aldehyde of isoamyl alcohol, is the direct signal that promotes filamentation in *S. cerevisiae*, because Gre2 exhibits isovaleraldehyde reductase activity and *gre2*Δ mutants are hyperfilamentous. To clarify, the hypothesis is that isoamyl alcohol is converted via alcohol dehydrogenases to isovaleraldehyde, but Gre2 catabolizes isovaleraldehyde which dampens the signal. These factors led us to hypothesize that quorum-sensing alcohols such as farnesol are not the direct signals which modulate yeast behavior, but rather these alcohols are oxidized intracellularly by alcohol dehydrogenase enzymes to the corresponding aldehydes, which are the direct signals. Consequently, genes involved in aldehyde metabolism, such as Gre2 or Mgd1, would also play a pivotal role in this mode of quorum-sensing. Although alcohols like ethanol, isoamyl alcohol, and farnesol have been shown to promote filamentation in *S. cerevisiae* and inhibit it in *C. albicans* (see reference (75) for review), studies on the direct effects of aldehyde compounds on yeast morphology are lacking. To date, the only aldehydes with published morphological effects on yeast are acetaldehyde (78) and cinnamaldehyde (79), both of which inhibit the yeast-to-hyphae transition in *C. albicans*. There is also indirect evidence that MG inhibits filamentation in *C. albicans*, as a *glx3*Δ (glyoxalase III) mutant deficient in MG detoxification exhibits a filamentation defect (80).

There are several experiments we could perform to investigate our "aldehyde quorum sensing" hypothesis. First, we could directly test the morphological effects of

farnesal, tyrosal, isovaleraldehyde, and MG on *C. albicans* and *S. cerevisiae*. We would expect these aldehydes to have the same effects as their corresponding alcohols on each species – on that note, acetol, the cognate alcohol of MG, has not been assessed for morphological effects in yeast, so we would also test this compound. Likewise, we would test whether acetaldehyde promotes filamentation in S. cerevisiae since it represses filamentation in C. albicans. More interesting, however, would be to test whether loss of ADH activity results in these yeasts becoming "blind" to the alcohol signals. Due to the vast number of genes encoding ADH activity in the genomes of either organism, however, a genetic study might prove challenging. A more straightforward strategy would be to test whether pyrazole, a competitive inhibitor of ADH enzymes, renders yeast unable to respond to the alcohol signals in the ways they should (i.e., no change or diminished change in morphogenesis). Pyrazole has been utilized to examine toxicity of allyl alcohol and acrolein in *S. cerevisiae* (81). Specifically, it has been shown that inhibition of ADH activity by pyrazole alleviates the toxicity of allyl alcohol but not of acrolein (81), indicating allyl alcohol itself it not toxic, but that *S. cerevisiae* rapidly metabolizes it to the highly toxic acrolein via ADHs. Thus, it seems reasonable that a similar method would be useful in testing our signaling hypothesis.

4.5 Speculation on the importance of the co-regulation of *MDR1* and aldehyde-detoxification genes

It is noteworthy that in every *Candida* species with a published Mrr1 regulon, expression of *MDR1* is strongly co-regulated with expression of at least one gene encoding a protein with known or predicted MG reductase activity (82-87). Our finding that *MDR1*

and *MGD1* are not only the top two differentially expressed genes but are also among only a total of four genes differentially expressed between a wild-type *C. auris* clade III isolate (B11221) and its *mrr1a*Δ derivative (**Fig. 3.1C**) is particularly striking. What's more, in *C. albicans* (82, 83), *C. lusitaniae* (85, 86), and *C. parapsilosis* (84), Mrr1 appears to regulate expression of multiple known or predicted aldo-keto reductase and alcohol dehydrogenase genes. This trend continues even in the distantly related *S. cerevisiae*, in which the multidrug export gene *FLR1* is often co-expressed with *GRE2* (88-93), which encodes an aldehyde reductase that has demonstrated capability to detoxify and catabolize MG (94), isovaleraldehyde (77), and other reactive aldehyde compounds (95, 96).

Perhaps the simplest hypotheses to explain the conserved co-regulation of MFS efflux proteins with aldehyde reductase enzymes in yeast is that Mdr1 in *Candida* and Flr1 in *Saccharomyces* also participate in detoxification of reactive aldehydes, either by directly exporting aldehyde-derived adducts or indirectly by exporting some other substrate and/or importing protons. Direct export of AGEs by Mdr1 seems logical if one compares the structures of known Mdr1 substrates (**Fig. 1.2A**) with the structures of common MG-derived AGEs (**Fig. 1.4**); notably, many compounds in both categories contain an imidazole or pyrimidine group. If any of these efflux proteins do indeed confer protection against reactive aldehydes like MG or AA, we would reasonably expect increased susceptibility to these compounds in mutants lacking these efflux genes. However, as shown in **Appendix Fig. II-5**, *mdr1*Δ mutants are not significantly more sensitive to MG compared to their *MDR1*-intact parental strains, with the exception of the *mrr1*Δ/*mdr1*Δ double mutant.

Another hypothesis is that MFS efflux proteins like Mdr1 promote the production and/or accumulation of reactive aldehydes, and that co-expression of *MDR1* with *MGD1* and *FLR1* with *GRE2* evolved as a compensatory mechanism. If this were the case, we would expect deletion of *MDR1* to confer increased resistance to MG or other reactive aldehydes. However, it would then seem counterintuitive that MG induces expression of *MDR1* in *Candida* species (**Chapters 2 – 3**) and that AA induces expression of *FLR1* in *S. cerevisiae* (97).

The observation that expression of constitutively active Mrr1 renders *C. lusitaniae* more susceptible to H_2O_2 and that this sensitivity can be partially rescued by deletion of *MDR1* (86) supports a model in which Mdr1 alters the cellular redox balance. One mechanism that is theoretically possible is that Mdr1 activity promotes the depletion and/or oxidation of GSH. Although this function has not previously been reported for Mdr1 in any *Candida* species, other MFS transporters in yeast have demonstrated glutathione-proton antiporter activity, such as Gex1 and Gex2 in *S. cerevisiae* (98). Indeed, we have found that *C. lusitaniae* strains expressing *MRR1* with gain-of-function mutations are more susceptible to the glutathione-depleting agent diethyl maleate (DEM), and that this increased sensitivity is completely rescued upon deletion of *MDR1* (**Appendix Fig. II.6**), which adds support to the hypothesis that overexpression of *MDR1* negatively affects glutathione levels. However, if *MDR1* overexpression leads to GSH depletion via export in *C. lusitaniae*, we would expect to see lower levels of intracellular GSH in strains that overexpress *MDR1*, and this is not the case. Compared to two more isogenic strains complemented with low-activity *MRR1* alleles ($MRR1^{ancestral}$ and $MRR1^{L1191H+Q1197*}$), a *C. lusitaniae* strain complemented with the constitutively active Y813C allele exhibits higher

intracellular levels of both GSH and GSSG as measured by LC-MS (Demers et al., manuscript in preparation). That said, it is not out of the realm of possibility that other Mrr1-regulated genes highly expressed in this strain could compensate for Mdr1-mediated glutathione loss in the absence of oxidative stress or glutathione depletion. Thus, the only way to definitively rule out the glutathione hypothesis is to measure GSH and GSSG levels in strains with high Mrr1 activity and their isogenic *mdr1*Δ derivatives. If *mdr1*Δ mutants do exhibit higher levels of intracellular GSH and/or GSSG, extracellular glutathione should also be measured to determine whether differences between strains are the result of changes in efflux or biosynthesis.

If Mdr1 does export a molecule that would otherwise confer protection against ROS and/or reactive aldehydes, three more candidates are the polyamines putrescine, spermidine, and spermine. Putrescine has been implicated as an MG scavenger in the amoeba *Dictyostelium discoideum* (99, 100). In the mung bean plant, supplementation with exogenous spermine enhances tolerance to drought (101), heat stress (101), and cadmium (102) by increasing the activities of superoxide dismutase, catalase, glutathione peroxidase, glutathione reductase, and the glyoxalase system and decreasing accumulation and production of H_2O_2 and superoxide. Spermidine, the precursor of spermine, also protects against oxidative stress, lipid peroxidation, and MG in chickpea (103), rice (104), and lettuce (105). Therefore, it is conceivable that these polyamines have similar effects on antioxidant capacity and aldehyde defense in yeast, and that uncontrolled export of these compounds could render cells more susceptible to ROS and reactive aldehydes. The $MRR1^{Y813C}$ complement exhibits significantly lower intracellular levels of putrescine, spermidine, and spermine compared to the $MRR1^{ancestral}$ and $MRR1^{L1191H+Q1197*}$

complements (Demers et al., manuscript in preparation). This may contribute to the susceptibility of *Candida* strains with constitutively active Mrr1 to H_2O_2 and could explain the evolutionary pressure to co-express aldehyde detoxification genes like *MGD1* with the efflux gene *MDR1*. Of course, to support this hypothesis, we would need to first show that deletion of *MDR1* from the *MRR1*^{Y813C} complement restores polyamine levels to those of the complements expressing low-activity Mrr1 variants, and that putrescine, spermidine, and/or spermine can act as substrates of Mdr1.

Finally, because Mdr1 is a transmembrane protein, it is also possible that overexpression of *MDR1* causes alterations in plasma membrane characteristics such as fluidity, lipid or protein content, microdomain organization, or topography. Specifically, one hypothesis is that high levels of Mdr1 in the plasma membrane can cause changes that promote lipid peroxidation, a process which generates reactive carbonyls like acrolein or MDA as described in **Chapter 1**. A role for *MGD1* or other Mrr1-regulated genes in resistance against lipid peroxidation products has not yet been investigated in any *Candida* species, but MDA and acrolein have both been shown to induce Yap1 activity in *S. cerevisiae* (10, 11). It is also worth noting that in *S. cerevisiae*, a *GRE2*-null mutant exhibits increased sensitivity to chemicals which induce cell membrane stress (106). To address this hypothesis, we could analyze the plasma membrane composition in strains expressing gain-of-function *MRR1* alleles and their *mdr1*Δ derivatives. Polyunsaturated fatty acids are particularly susceptible to peroxidation (see reference (107) for review), so decreased levels of polyunsaturated fatty acids in the plasma membranes of *mdr1*Δ mutants compared to their parental strains would support the hypothesis that overexpression of *MDR1* leads to increased lipid peroxidation. We could also quantify acrolein and MDA in these strains.

Finally, it would also be interesting to assess the sensitivity of *mgd1*Δ, *mgd2*Δ, or *mdr1*Δ mutants in isogenic strains with different *MRR1* alleles to various membrane stressing agents.

4.6 Concluding Remarks

This work contributes to the knowledge regarding the function and activation of Mrr1, a central regulator of azole resistance in *Candida* species. Multidrug-resistant fungal infections remain a significant clinical problem with high healthcare costs and high rates of mortality, particularly for individuals with underlying medical conditions. Here, we have demonstrated that Mrr1 also contributes substantially to MG resistance in multiple *Candida* species, which may improve the ability of these organisms to persist and proliferate in the presence of MG derived from phagocytic attack or from dysregulated metabolism in the host due to underlying disease. A probable secondary effect of this phenomenon is that elevated physiological concentrations of MG or other reactive aldehydes systemically or at the site of infection may select for gain-of-function mutations in Mrr1, thus indirectly selecting for increased azole resistance. Furthermore, we have also shown that MG at subinhibitory concentrations induces expression of several Mrr1-regulated genes, including *MDR1*, and enhances growth in fluconazole in *C. lusitaniae*. This raises the possibility that MG or other reactive aldehydes encountered in the context of infection could induce expression of *MDR1* and other stress response genes, contributing to the failure of azole therapy. Unveiling the mechanism by which MG exerts its effects on azole resistance may open the door to the development of novel inhibitors of Mrr1 activation in addition to deepening our understanding of the undeniable relationship

between microbial stress response and drug resistance. Finally, if the observations reported here hold true *in vivo*, it is conceivable that minimizing local or even systemic MG levels, perhaps through proven MG scavengers or novel drugs based upon them, could reduce the incidence of antifungal failure, especially in patients predisposed to high levels of MG.

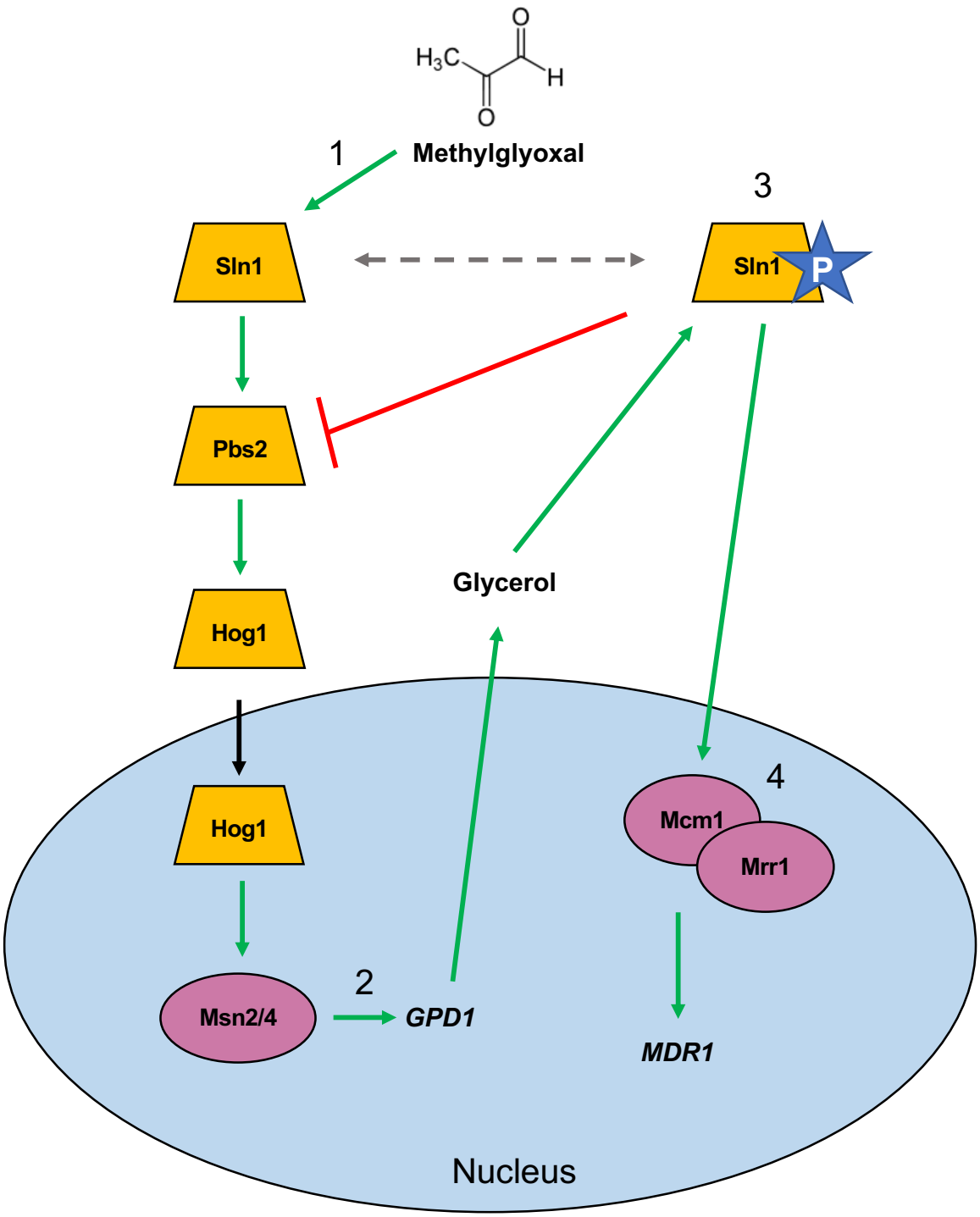

Figure 4.1. Proposed model for the mechanism of Mrr1-dependent transcriptional activation by MG through Sln1 and Mcm1 in *Candida* species. 1) MG triggers the dephosphorylation of Sln1, thereby activating the HOG pathway. 2) Upregulation of *GPD1* expression a result of HOG pathway activation leads to increased glycerol biosynthesis in

the cytosol. 3) Glycerol accumulation leads to dephosphorylation of Sln1, shutting off the HOG pathway and activating Mcm1. 4) Activated Mcm1 cooperates with Mrr1 to upregulate expression of shared target genes, such as *MDR1*.

References

1. Fica-Contreras SM, Shuster SO, Durfee ND, Bowe GJK, Henning NJ, Hill SA, Vrla GD, Stillman DR, Suralik KM, Sandwick RK, Choi S. 2017. Glycation of Lys-16 and Arg-5 in amyloid-β and the presence of Cu2+ play a major role in the oxidative stress mechanism of Alzheimer's disease. JBIC Journal of Biological Inorganic Chemistry 22:1211-1222.
2. Venkatraman J, Aggarwal K, Balaram P. 2001. Helical peptide models for protein glycation: proximity effects in catalysis of the Amadori rearrangement. Chemistry & Biology 8:611-625.
3. Ahmed N, Dobler D, Dean M, Thornalley PJ. 2005. Peptide Mapping Identifies Hotspot Site of Modification in Human Serum Albumin by Methylglyoxal Involved in Ligand Binding and Esterase Activity. Journal of Biological Chemistry 280:5724-5732.
4. Sjoblom NM, Kelsey MMG, Scheck RA. 2018. A Systematic Study of Selective Protein Glycation. Angewandte Chemie International Edition 57:16077-16082.
5. Acimovic JM, Stanimirovic BD, Todorovic N, Jovanovic VB, Mandic LM. 2010. Influence of the microenvironment of thiol groups in low molecular mass thiols and serum albumin on the reaction with methylglyoxal. Chem Biol Interact 188:21-30.
6. Pavićević ID, Jovanović VB, Takić MM, Penezić AZ, Aćimović JM, Mandić LM. 2014. Fatty acids binding to human serum albumin: Changes of reactivity and glycation level of Cysteine-34 free thiol group with methylglyoxal. Chemico-Biological Interactions 224:42-50.

7. Liu Z, Myers LC. 2017. *Candida albicans* Swi/Snf and Mediator Complexes Differentially Regulate Mrr1-Induced *MDR1* Expression and Fluconazole Resistance. Antimicrob Agents Chemother 61.

8. Maeta K, Izawa S, Okazaki S, Kuge S, Inoue Y. 2004. Activity of the Yap1 transcription factor in *Saccharomyces cerevisiae* is modulated by methylglyoxal, a metabolite derived from glycolysis. Mol Cell Biol 24:8753-64.

9. Zuin A, Vivancos AP, Sansó M, Takatsume Y, Ayté J, Inoue Y, Hidalgo E. 2005. The Glycolytic Metabolite Methylglyoxal Activates Pap1 and Sty1 Stress Responses in *Schizosaccharomyces pombe*. Journal of Biological Chemistry 280:36708-36713.

10. Ouyang X, Tran QT, Goodwin S, Wible RS, Sutter CH, Sutter TR. 2011. Yap1 activation by H_2O_2 or thiol-reactive chemicals elicits distinct adaptive gene responses. Free Radic Biol Med 50:1-13.

11. Turton HE, Dawes IW, Grant CM. 1997. Saccharomyces cerevisiae exhibits a yAP-1-mediated adaptive response to malondialdehyde. Journal of Bacteriology 179:1096-1101.

12. Azevedo D, Tacnet F, Delaunay A, Rodrigues-Pousada C, Toledano MB. 2003. Two redox centers within Yap1 for H2O2 and thiol-reactive chemicals signaling. Free Radic Biol Med 35:889-900.

13. Kuge S, Arita M, Murayama A, Maeta K, Izawa S, Inoue Y, Nomoto A. 2001. Regulation of the yeast Yap1p nuclear export signal is mediated by redox signal-induced reversible disulfide bond formation. Mol Cell Biol 21:6139-50.

14. Delaunay A, Isnard AD, Toledano MB. 2000. H_2O_2 sensing through oxidation of the Yap1 transcription factor. EMBO J 19:5157-66.

15. Kim D, Hahn JS. 2013. Roles of the Yap1 transcription factor and antioxidants in *Saccharomyces cerevisiae*'s tolerance to furfural and 5-hydroxymethylfurfural, which function as thiol-reactive electrophiles generating oxidative stress. Appl Environ Microbiol 79:5069-77.

16. Znaidi S, Barker KS, Weber S, Alarco AM, Liu TT, Boucher G, Rogers PD, Raymond M. 2009. Identification of the *Candida albicans* Cap1p regulon. Eukaryot Cell 8:806-20.

17. Lin X, Huang MY, Woolford CA, May G, McManus CJ, Mitchell AP. 2019. Circuit diversification in a biofilm regulatory network. PLOS Pathogens 15.

18. Fassler JS, Gray WM, Malone CL, Tao W, Lin H, Deschenes RJ. 1997. Activated alleles of yeast *SLN1* increase Mcm1-dependent reporter gene expression and diminish signaling through the Hog1 osmosensing pathway. J Biol Chem 272:13365-71.

19. Yu G, Deschenes RJ, Fassler JS. 1995. The essential transcription factor, Mcm1, is a downstream target of Sln1, a yeast "two-component" regulator. J Biol Chem 270:8739-43.

20. Aguilera J, Rodriguez-Vargas S, Prieto JA. 2005. The HOG MAP kinase pathway is required for the induction of methylglyoxal-responsive genes and determines methylglyoxal resistance in *Saccharomyces cerevisiae*. Mol Microbiol 56:228-39.

21. Maeta K, Izawa S, Inoue Y. 2005. Methylglyoxal, a metabolite derived from glycolysis, functions as a signal initiator of the high osmolarity glycerol-mitogen-

activated protein kinase cascade and calcineurin/Crz1-mediated pathway in *Saccharomyces cerevisiae*. J Biol Chem 280:253-60.

22. Tao W, Deschenes RJ, Fassler JS. 1999. Intracellular Glycerol Levels Modulate the Activity of Sln1p, a *Saccharomyces cerevisiae* Two-component Regulator. Journal of Biological Chemistry 274:360-367.

23. Aguilera J, Prieto JA. 2004. Yeast cells display a regulatory mechanism in response to methylglyoxal. FEMS Yeast Res 4:633-41.

24. Mir AR, uddin M, Alam K, Ali A. 2014. Methylglyoxal mediated conformational changes in histone H2A—generation of carboxyethylated advanced glycation end products. International Journal of Biological Macromolecules 69:260-266.

25. Zheng Q, Omans ND, Leicher R, Osunsade A, Agustinus AS, Finkin-Groner E, D'Ambrosio H, Liu B, Chandarlapaty S, Liu S, David Y. 2019. Reversible histone glycation is associated with disease-related changes in chromatin architecture. Nature Communications 10.

26. Galligan JJ, Wepy JA, Streeter MD, Kingsley PJ, Mitchener MM, Wauchope OR, Beavers WN, Rose KL, Wang T, Spiegel DA, Marnett LJ. 2018. Methylglyoxal-derived posttranslational arginine modifications are abundant histone marks. Proceedings of the National Academy of Sciences 115:9228-9233.

27. Fu Z-W, Li J-H, Feng Y-R, Yuan X, Lu Y-T. 2021. The metabolite methylglyoxal-mediated gene expression is associated with histone methylglyoxalation. Nucleic Acids Research 49:1886-1899.

28. Chow NA, Munoz JF, Gade L, Berkow EL, Li X, Welsh RM, Forsberg K, Lockhart SR, Adam R, Alanio A, Alastruey-Izquierdo A, Althawadi S, Arauz AB, Ben-Ami

R, Bharat A, Calvo B, Desnos-Ollivier M, Escandon P, Gardam D, Gunturu R, Heath CH, Kurzai O, Martin R, Litvintseva AP, Cuomo CA. 2020. Tracing the Evolutionary History and Global Expansion of Candida auris Using Population Genomic Analyses. mBio 11.

29. Iyer KR, Camara K, Daniel-Ivad M, Trilles R, Pimentel-Elardo SM, Fossen JL, Marchillo K, Liu Z, Singh S, Munoz JF, Kim SH, Porco JA, Jr., Cuomo CA, Williams NS, Ibrahim AS, Edwards JE, Jr., Andes DR, Nodwell JR, Brown LE, Whitesell L, Robbins N, Cowen LE. 2020. An oxindole efflux inhibitor potentiates azoles and impairs virulence in the fungal pathogen *Candida auris*. Nat Commun 11:6429.

30. Mayr EM, Ramirez-Zavala B, Kruger I, Morschhauser J. 2020. A Zinc Cluster Transcription Factor Contributes to the Intrinsic Fluconazole Resistance of *Candida auris*. mSphere 5.

31. MacPherson S, Larochelle M, Turcotte B. 2006. A fungal family of transcriptional regulators: the zinc cluster proteins. Microbiol Mol Biol Rev 70:583-604.

32. Hazen SL, Hsu FF, Heinecke JW. 1996. p-hydroxyphenylacetaldehyde is the major product of L-tyrosine oxidation by activated human phagocytes - A chloride-dependent mechanism for the conversion of free amino acids into reactive aldehydes by myeloperoxidase. Journal of Biological Chemistry 271:1861-1867.

33. Anderson MM, Hazen SL, Hsu FF, Heinecke JW. 1997. Human neutrophils employ the myeloperoxidase-hydrogen peroxide-chloride system to convert hydroxy-amino acids into glycolaldehyde, 2-hydroxypropanal, and acrolein. A mechanism for the generation of highly reactive alpha-hydroxy and alpha,beta-unsaturated

aldehydes by phagocytes at sites of inflammation. Journal of Clinical Investigation 99:424-432.

34. Hazen SL, Hsu FF, d'Avignon A, Heinecke JW. 1998. Human Neutrophils Employ Myeloperoxidase To Convert α-Amino Acids to a Battery of Reactive Aldehydes: A Pathway for Aldehyde Generation at Sites of Inflammation. Biochemistry 37:6864-6873.

35. Hazen SL, d'Avignon A, Anderson MM, Hsu FF, Heinecke JW. 1998. Human Neutrophils Employ the Myeloperoxidase-Hydrogen Peroxide-Chloride System to Oxidize α-Amino Acids to a Family of Reactive Aldehydes. Journal of Biological Chemistry 273:4997-5005.

36. Zhang MM, Ong CL, Walker MJ, McEwan AG. 2016. Defence against methylglyoxal in Group A Streptococcus: a role for Glyoxylase I in bacterial virulence and survival in neutrophils? Pathog Dis 74.

37. Gross NT, Hultenby K, Mengarelli S, Camner P, Jarstrand C. 2000. Lipid peroxidation by alveolar macrophages challenged with *Cryptococcus neoformans*, *Candida albicans* or *Aspergillus fumigatus*. Med Mycol 38:443-9.

38. Prantner D, Nallar S, Richard K, Spiegel D, Collins KD, Vogel SN. 2021. Classically activated mouse macrophages produce methylglyoxal that induces a TLR4-and RAGE-independent proinflammatory response. Journal of Leukocyte Biology 109:605-619.

39. Dang Y, Wang F, Li L, Lai Y, Xu Z, Xiong Z, Zhang A, Tian Y, Ding C, Zhang W. 2020. An activatable near-infrared fluorescent probe for methylglyoxal imaging in Alzheimer's disease mice. Chemical Communications 56:707-710.

40. Gao S, Tang Y, Lin W. 2018. Development of a Highly Selective Two-Photon Probe for Methylglyoxal and its Applications in Living Cells, Tissues, and Zebrafish. Journal of Fluorescence 29:155-163.

41. Wang W, Chen J, Ma H, Xing W, Lv N, Zhang B, Xu H, Wang W, Lou K. 2021. An "AND"-logic-gate-based fluorescent probe with dual reactive sites for monitoring extracellular methylglyoxal level changes of activated macrophages. Chemical Communications 57:8166-8169.

42. Trouvé P, Férec C, Génin E. 2021. The Interplay between the Unfolded Protein Response, Inflammation and Infection in Cystic Fibrosis. Cells 10.

43. Antus B, Drozdovszky O, Barta I, Kelemen K. 2015. Comparison of Airway and Systemic Malondialdehyde Levels for Assessment of Oxidative Stress in Cystic Fibrosis. Lung 193:597-604.

44. Brown RK, Wyatt H, Price JF, Kelly FJ. 1996. Pulmonary dysfunction in cystic fibrosis is associated with oxidative stress. European Respiratory Journal 9:334-339.

45. Causer AJ, Shute JK, Cummings MH, Shepherd AI, Gruet M, Costello JT, Bailey S, Lindley M, Pearson C, Connett G, Allenby MI, Carroll MP, Daniels T, Saynor ZL. 2020. Circulating biomarkers of antioxidant status and oxidative stress in people with cystic fibrosis: A systematic review and meta-analysis. Redox Biology 32.

46. Domínguez C, Gartner S, Liñán S, Cobos N, Moreno A. 1998. Enhanced oxidative damage in cystic fibrosis patients. BioFactors 8:149-153.

47. Pariano M, Costantini C, Santarelli I, Puccetti M, Giovagnoli S, Talesa VN, Romani L, Antognelli C. 2021. Defective Glyoxalase 1 Contributes to Pathogenic Inflammation in Cystic Fibrosis. Vaccines 9.

48. Lo AWI, Beucher J, Boëlle P-Y, Busson P-F, Muselet-Charlier C, Clement A, Corvol H. 2012. AGER -429T/C Is Associated with an Increased Lung Disease Severity in Cystic Fibrosis. PLoS ONE 7.

49. Iannitti RG, Casagrande A, De Luca A, Cunha C, Sorci G, Riuzzi F, Borghi M, Galosi C, Massi-Benedetti C, Oury TD, Cariani L, Russo M, Porcaro L, Colombo C, Majo F, Lucidi V, Fiscarelli E, Ricciotti G, Lass-Flörl C, Ratclif L, Esposito A, De Benedictis FM, Donato R, Carvalho A, Romani L. 2013. Hypoxia Promotes Danger-mediated Inflammation via Receptor for Advanced Glycation End Products in Cystic Fibrosis. American Journal of Respiratory and Critical Care Medicine 188:1338-1350.

50. Roum JH, Buhl R, McElvaney NG, Borok Z, Crystal RG. 1993. Systemic deficiency of glutathione in cystic fibrosis. Journal of Applied Physiology 75:2419-2424.

51. Dickerhof N, Pearson JF, Hoskin TS, Berry LJ, Turner R, Sly PD, Kettle AJ. 2017. Oxidative stress in early cystic fibrosis lung disease is exacerbated by airway glutathione deficiency. Free Radical Biology and Medicine 113:236-243.

52. Koehler TM, Anaya-Sanchez A, Feng Y, Berude JC, Portnoy DA. 2021. Detoxification of methylglyoxal by the glyoxalase system is required for glutathione availability and virulence activation in *Listeria monocytogenes*. PLOS Pathogens 17.

53. Vogel-Scheel J, Alpert C, Engst W, Loh G, Blaut M. 2010. Requirement of Purine and Pyrimidine Synthesis for Colonization of the Mouse Intestine by Escherichia coli. Applied and Environmental Microbiology 76:5181-5187.

54. Soga A, Shirozu T, Fukumoto S. 2021. Glyoxalase pathway is required for normal liver-stage proliferation of Plasmodium berghei. Biochemical and Biophysical Research Communications 549:61-66.

55. Rosenbach A, Dignard D, Pierce JV, Whiteway M, Kumamoto CA. 2010. Adaptations of *Candida albicans* for growth in the mammalian intestinal tract. Eukaryot Cell 9:1075-86.

56. Llopis S, Querol A, Heyken A, Hube B, Jespersen L, Fernandez-Espinar MT, Perez-Torrado R. 2012. Transcriptomics in human blood incubation reveals the importance of oxidative stress response in Saccharomyces cerevisiae clinical strains. BMC Genomics 13:419.

57. Yadav SK, Singla-Pareek SL, Ray M, Reddy MK, Sopory SK. 2005. Methylglyoxal levels in plants under salinity stress are dependent on glyoxalase I and glutathione. Biochem Biophys Res Commun 337:61-7.

58. Nahar K, Hasanuzzaman M, Alam MM, Fujita M. 2015. Glutathione-induced drought stress tolerance in mung bean: coordinated roles of the antioxidant defence and methylglyoxal detoxification systems. AoB Plants 7.

59. Melvin P, Bankapalli K, D'Silva P, Shivaprasad PV. 2017. Methylglyoxal detoxification by a DJ-1 family protein provides dual abiotic and biotic stress tolerance in transgenic plants. Plant Mol Biol 94:381-397.

60. Vemanna RS, Babitha KC, Solanki JK, Amarnatha Reddy V, Sarangi SK, Udayakumar M. 2017. Aldo-keto reductase-1 (AKR1) protect cellular enzymes from salt stress by detoxifying reactive cytotoxic compounds. Plant Physiol Biochem 113:177-186.

61. Mahmud JA, Hasanuzzaman M, Khan MIR, Nahar K, Fujita M. 2020. beta-Aminobutyric Acid Pretreatment Confers Salt Stress Tolerance in Brassica napus L. by Modulating Reactive Oxygen Species Metabolism and Methylglyoxal Detoxification. Plants (Basel) 9.

62. Rohman MM, Islam MR, Monsur MB, Amiruzzaman M, Fujita M, Hasanuzzaman M. 2019. Trehalose Protects Maize Plants from Salt Stress and Phosphorus Deficiency. Plants (Basel) 8.

63. Yadav SK, Singla-Pareek SL, Reddy MK, Sopory SK. 2005. Transgenic tobacco plants overexpressing glyoxalase enzymes resist an increase in methylglyoxal and maintain higher reduced glutathione levels under salinity stress. FEBS Letters 579:6265-6271.

64. Espartero J, Sanchez-Aguayo I, Pardo JM. 1995. Molecular characterization of glyoxalase-I from a higher plant; upregulation by stress. Plant Mol Biol 29:1223-33.

65. Veena, Reddy VS, Sopory SK. 1999. Glyoxalase I from Brassica juncea: molecular cloning, regulation and its over-expression confer tolerance in transgenic tobacco under stress. Plant J 17:385-95.

66. Turóczy Z, Kis P, Török K, Cserháti M, Lendvai Á, Dudits D, Horváth GV. 2011. Overproduction of a rice aldo–keto reductase increases oxidative and heat stress

tolerance by malondialdehyde and methylglyoxal detoxification. Plant Molecular Biology 75:399-412.

67. Ghosh A, Mustafiz A, Pareek A, Sopory SK, Singla-Pareek SL. 2022. Glyoxalase III enhances salinity tolerance through ROS scavenging and reduced glycation. Physiol Plant doi:10.1111/ppl.13693:e13693.

68. Gupta BK, Sahoo KK, Ghosh A, Tripathi AK, Anwar K, Das P, Singh AK, Pareek A, Sopory SK, Singla-Pareek SL. 2018. Manipulation of glyoxalase pathway confers tolerance to multiple stresses in rice. Plant, Cell & Environment 41:1186-1200.

69. Aguilera J, Prieto JA. 2001. The *Saccharomyces cerevisiae* aldose reductase is implied in the metabolism of methylglyoxal in response to stress conditions. Curr Genet 39:273-83.

70. Chamchoy K, Pumirat P, Reamtong O, Pakotiprapha D, Leartsakulpanich U, Boonyuen U. 2020. Functional analysis of BPSS2242 reveals its detoxification role in Burkholderia pseudomallei under salt stress. Sci Rep 10:10453.

71. Jakab Á, Tóth Z, Nagy F, Nemes D, Bácskay I, Kardos G, Emri T, Pócsi I, Majoros L, Kovács R, Druzhinina IS. 2019. Physiological and Transcriptional Responses of Candida parapsilosis to Exogenous Tyrosol. Applied and Environmental Microbiology 85.

72. Jakab Á, Balla N, Ragyák Á, Nagy F, Kovács F, Sajtos Z, Tóth Z, Borman AM, Pócsi I, Baranyai E, Majoros L, Kovács R, Mitchell AP. 2021. Transcriptional Profiling of the Candida auris Response to Exogenous Farnesol Exposure. mSphere 6.

73. Černáková L, Dižová S, Gášková D, Jančíková I, Bujdáková H. 2019. Impact of Farnesol as a Modulator of Efflux Pumps in a Fluconazole-Resistant Strain of Candida albicans. Microbial Drug Resistance 25:805-812.

74. Rossignol T, Logue ME, Reynolds K, Grenon M, Lowndes NF, Butler G. 2007. Transcriptional Response of *Candida parapsilosis* following Exposure to Farnesol. Antimicrobial Agents and Chemotherapy 51:2304-2312.

75. Chauhan NM, Mohan Karuppayil S. 2020. Dual identities for various alcohols in two different yeasts. Mycology 12:25-38.

76. Martínez-Anaya C, Dickinson JR, Sudbery PE. 2003. In yeast, the pseudohyphal phenotype induced by isoamyl alcohol results from the operation of the morphogenesis checkpoint. Journal of Cell Science 116:3423-3431.

77. Hauser M, Horn P, Tournu H, Hauser NC, Hoheisel JD, Brown AJ, Dickinson JR. 2007. A transcriptome analysis of isoamyl alcohol-induced filamentation in yeast reveals a novel role for Gre2p as isovaleraldehyde reductase. FEMS Yeast Res 7:84-92.

78. Chauhan NM, Raut JS, Mohan Karuppayil S. 2011. Acetaldehyde inhibits the yeast-to-hypha conversion and biofilm formation in *Candida albicans*. Mycoscience 52:356-360.

79. Taguchi Y, Hasumi Y, Abe S, Nishiyama Y. 2013. The effect of cinnamaldehyde on the growth and the morphology of *Candida albicans*. Medical Molecular Morphology 46:8-13.

80. Cabello L, Gómez-Herreros E, Fernández-Pereira J, Maicas S, Martínez-Esparza MC, de Groot PWJ, Valentín E. 2018. Deletion of *GLX3* in *Candida albicans*

affects temperature tolerance, biofilm formation and virulence. FEMS Yeast Research 19.

81. Kwolek-Mirek M, Bednarska S, Bartosz G, Bilinski T. 2009. Acrolein toxicity involves oxidative stress caused by glutathione depletion in the yeast *Saccharomyces cerevisiae*. Cell Biol Toxicol 25:363-78.

82. Morschhauser J, Barker KS, Liu TT, Bla BWJ, Homayouni R, Rogers PD. 2007. The transcription factor Mrr1p controls expression of the *MDR1* efflux pump and mediates multidrug resistance in *Candida albicans*. PLoS Pathog 3:e164.

83. Hoehamer CF, Cummings ED, Hilliard GM, Morschhauser J, Rogers PD. 2009. Proteomic analysis of Mrr1p- and Tac1p-associated differential protein expression in azole-resistant clinical isolates of *Candida albicans*. Proteomics Clin Appl 3:968-78.

84. Silva AP, Miranda IM, Guida A, Synnott J, Rocha R, Silva R, Amorim A, Pina-Vaz C, Butler G, Rodrigues AG. 2011. Transcriptional profiling of azole-resistant *Candida parapsilosis* strains. Antimicrob Agents Chemother 55:3546-56.

85. Demers EG, Biermann AR, Masonjones S, Crocker AW, Ashare A, Stajich JE, Hogan DA. 2018. Evolution of drug resistance in an antifungal-naive chronic *Candida lusitaniae* infection. Proc Natl Acad Sci U S A 115:12040-12045.

86. Demers EG, Stajich JE, Ashare A, Occhipinti P, Hogan DA. 2021. Balancing Positive and Negative Selection: *In Vivo* Evolution of *Candida lusitaniae MRR1*. mBio 12.

87. Kannan A, Asner SA, Trachsel E, Kelly S, Parker J, Sanglard D. 2019. Comparative Genomics for the Elucidation of Multidrug Resistance in *Candida lusitaniae*. mBio 10.

88. Hasunuma T, Ismail KSK, Nambu Y, Kondo A. 2014. Co-expression of *TAL1* and *ADH1* in recombinant xylose-fermenting *Saccharomyces cerevisiae* improves ethanol production from lignocellulosic hydrolysates in the presence of furfural. J Biosci Bioeng 117:165-169.

89. Shapira M, Segal E, Botstein D. 2004. Disruption of yeast forkhead-associated cell cycle transcription by oxidative stress. Mol Biol Cell 15:5659-69.

90. Berthelet S, Usher J, Shulist K, Hamza A, Maltez N, Johnston A, Fong Y, Harris LJ, Baetz K. 2010. Functional genomics analysis of the *Saccharomyces cerevisiae* iron responsive transcription factor Aft1 reveals iron-independent functions. Genetics 185:1111-28.

91. Suzuki T, Iwahashi Y. 2011. Gene expression profiles of yeast *Saccharomyces cerevisiae sod1* caused by patulin toxicity and evaluation of recovery potential of ascorbic acid. J Agric Food Chem 59:7145-54.

92. Shalem O, Dahan O, Levo M, Martinez MR, Furman I, Segal E, Pilpel Y. 2008. Transient transcriptional responses to stress are generated by opposing effects of mRNA production and degradation. Mol Syst Biol 4:223.

93. Kitagawa E, Akama K, Iwahashi H. 2005. Effects of iodine on global gene expression in *Saccharomyces cerevisiae*. Biosci Biotechnol Biochem 69:2285-93.

94. Chen CN, Porubleva L, Shearer G, Svrakic M, Holden LG, Dover JL, Johnston M, Chitnis PR, Kohl DH. 2003. Associating protein activities with their genes: rapid

identification of a gene encoding a methylglyoxal reductase in the yeast *Saccharomyces cerevisiae*. Yeast 20:545-54.

95. Moon J, Liu ZL. 2012. Engineered NADH-dependent *GRE2* from *Saccharomyces cerevisiae* by directed enzyme evolution enhances HMF reduction using additional cofactor NADPH. Enzyme Microb Technol 50:115-20.

96. Jayakody LN, Turner TL, Yun EJ, Kong, II, Liu JJ, Jin YS. 2018. Expression of Gre2p improves tolerance of engineered xylose-fermenting *Saccharomyces cerevisiae* to glycolaldehyde under xylose metabolism. Appl Microbiol Biotechnol 102:8121-8133.

97. Aranda A, del Olmo ML. 2004. Exposure of *Saccharomyces cerevisiae* to acetaldehyde induces sulfur amino acid metabolism and polyamine transporter genes, which depend on Met4p and Haa1p transcription factors, respectively. Appl Environ Microbiol 70:1913-22.

98. Dhaoui M, Auchère F, Blaiseau P-L, Lesuisse E, Landoulsi A, Camadro J-M, Haguenauer-Tsapis R, Belgareh-Touzé N, Brodsky JL. 2011. Gex1 is a yeast glutathione exchanger that interferes with pH and redox homeostasis. Molecular Biology of the Cell 22:2054-2067.

99. Park S-J, Kwak M-K, Kang S-O. 2017. Schiff bases of putrescine with methylglyoxal protect from cellular damage caused by accumulation of methylglyoxal and reactive oxygen species in Dictyostelium discoideum. The International Journal of Biochemistry & Cell Biology 86:54-66.

100. Kwak M-K, Lee M-H, Park S-J, Shin S-M, Liu R, Kang S-O. 2016. Polyamines regulate cell growth and cellular methylglyoxal in high-glucose medium independently of intracellular glutathione. FEBS Letters 590:739-749.

101. Nahar K, Hasanuzzaman M, Alam MM, Rahman A, Mahmud J-A, Suzuki T, Fujita M. 2016. Insights into spermine-induced combined high temperature and drought tolerance in mung bean: osmoregulation and roles of antioxidant and glyoxalase system. Protoplasma 254:445-460.

102. Nahar K, Rahman M, Hasanuzzaman M, Alam MM, Rahman A, Suzuki T, Fujita M. 2016. Physiological and biochemical mechanisms of spermine-induced cadmium stress tolerance in mung bean (Vigna radiata L.) seedlings. Environmental Science and Pollution Research 23:21206-21218.

103. Thapar Kapoor R, Ingo Hefft D, Ahmad A. 2021. Nitric oxide and spermidine alleviate arsenic-incited oxidative damage in Cicer arietinum by modulating glyoxalase and antioxidant defense system. Functional Plant Biology doi:10.1071/fp21196.

104. Banerjee A, Singh A, Roychoudhury A. 2019. Spermidine application reduces fluoride uptake and ameliorates physiological injuries in a susceptible rice cultivar by activating diverse regulators of the defense machinery. Environmental Science and Pollution Research 26:36598-36614.

105. Li C, Han Y, Hao J, Qin X, Liu C, Fan S. 2020. Effects of exogenous spermidine on antioxidants and glyoxalase system of lettuce seedlings under high temperature. Plant Signaling & Behavior 15.

106. Warringer J, Blomberg A. 2006. Involvement of yeast *YOL151W*/*GRE2* in ergosterol metabolism. Yeast 23:389-98.

107. Arai H. 2014. Oxidative Modification of Lipoproteins, p 103-114, Lipid Hydroperoxide-Derived Modification of Biomolecules doi:10.1007/978-94-007-7920-4_9.

Appendix I.

Acetaldehyde increased fluconazole tolerance in *Candida lusitaniae* in a partially Mrr1- and Mdr1- dependent manner

Results

Acetaldehyde induces *MDR1* expression in an Mrr1-dependent manner and stimulates FLZ resistance and in a partially Mrr1-dependent manner

We have previously demonstrated that the metabolically generated reactive carbonyl species (RCS) methylglyoxal (MG) induces *MDR1* expression in *C. lusitaniae* (1) and *C. auris* (2) and that MG stimulates fluconazole (FLZ) resistance in *C. lusitaniae* (1). Thus, we became interested in investigating whether other biologically relevant RCS would have similar effects on *Candida* species. Acetaldehyde (ACA), another small RCS, is an abundant component of air pollution (2-7) and cigarette smoke (8) and can be produced by *Candida* species and other commensal microbes in physiologically significant concentrations (9-18), so it is likely that *Candida* and other microbes would be exposed to this compound *in vivo*.

First, we tested whether ACA could induce expression of *MDR1* in *C. lusitaniae*, and if so, whether induction is dependent on Mrr1. For this purpose, we treated exponential-phase cultures of the strains U04 *mrr1*Δ and two of its derivatives complemented with either $MRR1^{ancestral}$, which encodes an Mrr1 variant with low basal activity and high inducibility by stimuli (19), or $MRR1^{Y813C}$, which encodes an Mrr1 variant with high basal activity and low inducibility (19), with 5 mM MG, 10 mM ACA, or dH_2O as a control for 15 minutes and measured *MDR1* expression via qRT-PCR. As expected, treatment with 5 mM MG led to a significant 12.5- and 1.5-fold change (relative to dH_2O

treatment) in *MDR1* expression in the *MRR1*^{ancestral} and *MRR1*^{Y813C} complements, respectively, while the 1.3-fold change in U04 *mrr1*Δ was not significant (**Fig. I.1**). On the other hand, treatment with 10 mM ACA resulted in a significant 19.3-fold change in *MDR1* expression in *MRR1*^{ancestral}, but *MDR1* expression was not significantly altered by ACA in either U04 *mrr1*Δ or the *MRR1*^{Y813C} complements (**Fig. I.1**). These data suggest that ACA induces *MRR1*-dependent induction of *MDR1* expression, but that ACA cannot increase the transcriptional activity of constitutively active Mrr1.

Consequently, we hypothesized that ACA could stimulate growth in FLZ and that this stimulation would be dependent on *MRR1*. To test this, we set up growth assays in 96-well plates with either YPD alone or YPD supplemented with 10 mM ACA and/or an inhibitory concentration of FLZ; 5 mM MG +/- FLZ was used as a control for growth stimulation. Because ACA is volatile, the ACA and FLZ + ACA conditions were set up in separate plates from the other conditions. Plates were incubated at 37˚C for 18 hours before we measured the OD_{600}. Neither 5 mM MG nor 10 mM ACA alone caused a significant change in growth relative to YPD alone for any of the strains tested (data not shown). In the presence of FLZ, MG caused a 1.6-, 10.4-, and 5.6-fold increase in OD_{600} for U04 *mrr1*Δ, the *MRR1*^{ancestral} complement, and the *MRR1*^{Y813C} complement, respectively (**Fig. I.2**). Meanwhile, ACA led to a 2.7-, 13.8-, and 3.0- fold increase in growth in FLZ for the three strains, respectively (**Fig. I.2**). The increased growth observed in the *MRR1*^{ancestral} complement for either MG or ACA was significantly higher than that observed in the other two strains, in concordance with the Mrr1 variant encoded by this allele being highly inducible. In contrast, the difference between U04 *mrr1*Δ and the *MRR1*^{Y813C} complement

were not statistically significant for either MG or ACA, which indicates that the induction of FLZ resistance in both strains is likely *MRR1*-independent.

To gain a more complete understanding of the involvement of *MRR1* and *MDR1* in the stimulation of FLZ resistance by ACA, we performed FLZ E-tests on solid YPD medium +/- 10 mM ACA for U04 *mrr1*Δ, the $MRR1^{ancestral}$ complement, the $MRR1^{Y813C}$ complement, and the *mdr1*Δ derivative of each strain. As shown in **Fig. I.3**, we observed a drastic decrease zone of inhibition for U04 *mrr1*Δ, the $MRR1^{ancestral}$ complement, and the $MRR1^{Y813C}$ complement; in fact, the $MRR1^{Y813C}$ complement, which was already FLZ-resistant, was able to grow robustly even at the maximum FLZ concentration of 256 µg/mL. The difference in induction of FLZ resistance, particularly for U04 *mrr1*Δ and the $MRR1^{Y813C}$ complement, between **Fig. I.3** and **Fig. I.2**, may be attributable to the use of solid versus liquid medium and/or the fact that we use a higher starting inoculum for E-tests than for liquid growth assays. Nonetheless, ACA can induce FLZ resistance in *C. lusitaniae* regardless of *MDR1* induction, as both U04 *mrr1*Δ and the $MRR1^{Y813C}$ complement exhibit increased FLZ resistance in the presence of ACA (**Fig. I.2** and **Fig. I.3**) despite neither strain displaying a change in *MDR1* expression upon ACA treatment (**Fig. I.1**). Likewise, ACA increased FLZ resistance in the three *mdr1*Δ mutants to varying degrees, although trailing growth in these strains make the results more difficult to interpret. The *mrr1*Δ/*mdr1*Δ double mutant and the $MRR1^{ancestral}$ *mdr1*Δ strain both exhibit a small change in FLZ MIC in the presence of ACA, increasing from about 0.5 to 1.0 µg/mL and from about 0.75 to 3.0 µg/mL respectively. However, ACA also appears to increase the rate of FLZ tolerance in these two strains, as evidenced by the increased number of small colonies growing within the zone of inhibition in the presence of ACA

(**Fig. I.3**). Meanwhile, the MIC of the *MRR1*^{Y813C} *mdr1*Δ strain increases from around 3.0 to 24 μg/mL in the presence of ACA (**Fig. I.3**). FLZ tolerance is less clear in this strain compared to the others, as although it demonstrates a substantial subpopulation of FLZ-tolerant colonies even in the absence of ACA, but its growth is noticeably more robust at high concentrations of FLZ in the presence of ACA (**Fig. I.3**). Together, the data shown in **Fig. I.1** through **Fig. I.3** suggest that ACA can increase FLZ resistance in *C. lusitaniae* via induction of *MDR1* expression in an *MRR1*-dependent manner, but it also induces other cellular changes that can enhance growth in FLZ independently of *MRR1* and/or *MRR1*.

ACA exhibits a dose-dependent effect on growth in FLZ

We wanted to investigate the effect of a range of ACA concentrations on FLZ resistance to determine the minimum concentration of ACA that can enhance growth in FLZ. Starting from 10 mM ACA in YPD with or without an inhibitory concentration of FLZ, we performed 2-fold serial dilutions of ACA down to 0.156 mM (156 μM) in culture tubes and inoculated each tube with an equal amount of either U04 *mrr1*Δ or the *MRR1*^{ancestral} complement. After 18 hours of growth on a rotary wheel at 37˚C, we measured the OD_{600} of each culture. **Fig I.4** shows the resulting plot of OD_{600} versus ACA concentration in the presence and absence of FLZ for both strains. In the absence of FLZ, ACA does not substantially affect growth at concentrations up to 5 mM and has a strong inhibitory effect at 10 mM (**Fig. I.4**). The severe inhibition of both strains by 10 mM ACA in this assay was surprising to us, as this concentration was not inhibitory in our 96-well plate growth assays. Therefore, ACA sensitivity could be affected by factors such as the volume, relative cell density, or surface area-to-volume ratio of the culture, or by

oxygenation; we do not have enough data to speculate in more detail at this time. In the presence of FLZ, the lowest concentration of ACA that led to a substantial increase in growth was 0.313 mM (313 μM) for the *MRR1*^{ancestral} complement, an increase of about 7.0-fold from an OD_{600} of around 0.4 to 2.5 (**Fig. I.4**). For U04 *mrr1*Δ, this concentration of ACA caused an approximate 2.9-fold increase in OD600, from an OD_{600} of about 0.17 to 0.49 (**Fig. I.4**). For both strains, the effect of ACA on growth in FLZ was dose-dependent, i.e., the endpoint OD_{600} in FLZ increased progressively with ACA concentration until 5 mM, at which point the inhibitory effects of ACA became apparent (**Fig. I.4**). Notably, the OD600 in FLZ was higher for the *MRR1*^{ancestral} complement compared to U04 *mrr1*Δ at each concentration of ACA (**Fig. I.4**). This suggests that although ACA can induce FLZ resistance without *MRR1*, as shown in **Fig. I.2** and **Fig. I.3**, expression of functional Mrr1 protein results in a greater benefit from ACA, particularly at lower concentrations (**Fig. I.4**).

The volatility of ACA allows for induction of FLZ resistance from adjacent wells

Finally, we investigated whether ACA could induce FLZ resistance in *C. lusitaniae* without being directly added to the growth medium and whether this effect would diminish with distance. To this end, we arranged clear 96-well plates with either dH_2O or 20 mM ACA in the four center wells, with the top half of each plate containing YPD medium as a control and the bottom half containing YPD + an inhibitory concentration of FLZ (**Fig. I.5A**), which varies by strain. We then added the same strain – either U04 *mrr1*Δ or the *MRR1*^{ancestral} complement – to the entire plate excluding the four wells in the center. After 18 hours of incubation at 37˚C, we measured the OD_{600} of each plate to compare growth in

the presence or absence of ACA. Relative to the plate which contained only dH_2O in the four center wells, the *MRR1*^{ancestral} complement exhibited a striking increase of growth in FLZ in the wells closest to those containing ACA, which tapered off with distance (**Fig. I.5B**). There was essentially no change in growth in the YPD control wells between the dH_2O plate and the ACA plate (**Fig. I.5B**), indicating that the increased growth in FLZ by ACA was due specifically to increased resistance rather than a general stimulation of growth in response to ACA. U04 *mrr1*Δ also displayed increased FLZ resistance in the wells closest to ACA, but the effect was much weaker than that observed for the *MRR1*^{ancestral} complement, with a maximum increase in OD_{600} of about 6-fold compared to the average 22-fold increase observed in the ACA-adjacent wells for the *MRR1*^{ancestral} complement (**Fig. I.5BC**). These results suggest that although *MRR1* is not an absolute requirement for stimulation of FLZ resistance by ACA, functional Mrr1 confers a stronger response to vaporized ACA.

Discussion and Next Steps:

The preliminary data presented in this Appendix build upon our previous work by showing that another RCS aside from MG can stimulate *MDR1* expression and FLZ resistance in *C. lusitaniae* in a manner that is at least partially dependent on *MRR1*. These data support our hypothesis that Mrr1 functions in an RCS- or reactive electrophilic species (RES)- sensing network which includes upregulation of *MDR1*, among other genes, in response to these toxic molecules. The importance of this work is that several RCS/RES are significantly elevated in individuals with a myriad of chronic diseases (see references (20-22) for review), and many patients with candidiasis or candidemia are afflicted by

underlying medical conditions. Additionally, it is also possible that pathogenic microbes would encounter RCS/RES produced during the innate cellular immune response (23-29). Our overarching hypothesis is that RCS/RES-mediated induction of azole resistance can occur in vivo and is one factor that contributes to failure of antifungal therapy.

The most obvious next step for the specific work presented here, in terms of publication, is to finish obtaining biological replicates for each experiment. Nonetheless, we feel that the data are robust enough to present them in this format at this time. Additionally, we want to investigate the volatile induction of FLZ resistance on the *MRR1*^{Y813C} complement for the sake of completion, and for the *mdr1*Δ derivatives of U04 *mrr1*Δ, the *MRR1*^{ancestral} complement, and the *MRR1*^{Y813C} complement. Although we do show in **Fig. I.3** that ACA can induce FLZ resistance to varying degrees in the *mdr1*Δ mutants, ACA is directly in the growth medium in this experiment. Because there is a clear difference in volatile stimulation between the *MRR1*^{ancestral} complement and U04 *mrr1*Δ (**Fig. I.5**), we think it is worthwhile to determine whether *MDR1* is required for volatile stimulation. Furthermore, we want to determine whether *MRR1* contributes to ACA resistance, as well as the Mrr1-regulated aldehyde reductase genes *MGD1* and *MGD2*, and the glyoxalase gene *GLO1*. Finally, we plan to investigate whether ACA has similar effects in other *Candida* species as in *C. lusitaniae*.

Materials and Methods

Strains, media, and growth conditions

The sources of all strains used in this study are listed in **Table I-S1**. All strains were stored long term in a final concentration of 25% glycerol at -80°C and freshly streaked onto

yeast extract peptone dextrose (YPD) agar (10 g/L yeast extract, 20 g/L peptone, 2% glucose, 1.5% agar) once every seven days and maintained at room temperature. All overnight cultures were grown in 5 mL YPD liquid medium (10 g/L yeast extract, 20 g/L peptone, 2% glucose) on a rotary wheel at 30°C. For experiments, medium was supplemented with FLZ (Sigma-Aldrich, stock 4 mg mL-1 in DMSO), 5 mM MG (Sigma-Aldrich, 5.55 M), or ACA at concentrations indicated in the text.

Quantitative Real-Time PCR

To exponential-phase cultures of *C. lusitaniae* (YPD, 37˚C) was added MG to a final concentration of 5 mM or ACA to a final concentration of 10 mM. Cultures were returned to the roller drum at 37˚C for 15 min, then centrifuged at 5000 rpm for 5 min. RNA isolation, gDNA removal, cDNA synthesis, and quantitative real-time PCR were performed as previously described (1). Transcripts were normalized to *C. lusitaniae ACT1* expression. Results were calculated in Microsoft Excel and plotted in GraphPad Prism 9.0.0 (GraphPad Software).

Induction of FLZ resistance by MG and ACA directly added to the medium

Exponential-phase cultures of *C. lusitaniae* were washed and diluted in dH_2O to an OD_{600} of 1; 60 µL of each diluted cell suspension was added to 5 mL fresh YPD. To each well of a clear 96-well flat-bottom plate (Falcon) was added 100 µL of YPD or YPD supplemented with FLZ, MG, FLZ and MG, ACA, or FLZ and ACA at twice the desired final concentration, and 100 µL of cell inoculum in YPD. The ACA and FLZ + ACA conditions were set up in plates separate from the other four conditions to prevent possible

interference due to the volatility of ACA. Plates were arranged in technical triplicate for each strain and condition and incubated at 37˚C for 18 hours before measuring OD_{600}. Results were calculated in Microsoft Excel and plotted in GraphPad Prism 9.0.0 (GraphPad Software).

E-tests

C. lusitaniae cultures were washed twice in dH_2O and resuspended in an OD_{600} of 10 in 1 mL. Washed, resuspended cells were swabbed across solid YPD or YPD supplemented with ACA at a final concentration of 10 mM using sterile cotton swabs. Flame-sterilized forceps were used to place a single FLZ E-test strip (Biomérieux) at the center of each plate. Plates were incubated at 37˚C for two days and then photographed.

Volatile induction of FLZ resistance by ACA

Each clear, flat-bottom 96-well plate (Falcon) was prepared as follows: 100 µL YPD were added to the top half of the plate, excluding wells D5 and D6; 100 µL supplemented with FLZ at twice the desired final concentration were added to the bottom half of the plate excluding wells E5 and E6; 200 µL of dH_2O or ACA diluted in dH_2O to a final concentration of 20 mM were added to wells D5, D6, E5, and E6. Exponential-phase cultures of *C. lusitaniae* were washed and diluted in dH_2O to an OD_{600} of 1; 60 µL of each diluted cell suspension was added to 5 mL fresh YPD. 100 µL of cell inoculum in YPD were added to each well of the plate excluding D5, D6, E5, and E6; only one strain was loaded per plate. Plates were incubated at 37˚C for 18 hours and OD_{600} across each plate was measured in a plate reader. Results were calculated in Microsoft Excel as follows:

subtract YPD blanks from each well; divide the OD_{600} in each well of the ACA plate by the OD_{600} in the corresponding well of the dH_2O plate. Results are reported as the fold change in OD_{600} in the ACA plate relative to the dH_2O plate.

Statistical Analysis and Figure Preparation

All graphs were prepared with GraphPad Prism 9.0.0 (GraphPad Software). One- and two-way ANOVA tests were performed in Prism; details on each test are described in the corresponding figure legends. All p-values were two-tailed and $p < 0.05$ were considered significant for all analyses performed and are indicated with asterisks or letters in the text: * $p < 0.05$; ** $p < 0.01$, *** $p < 0.001$, **** $p < 0.0001$, ns not significant.

Data availability

The data that support the findings of this study are available from the corresponding author upon request.

Acknowledgements

We thank Elora Demers for providing strains.

Author contributions. ARB and DAH conceived and designed the experiments and wrote the paper. ARB performed the experiments. ARB and DAH analyzed the data.

Funding. This study was supported by grant R01 5R01 AI127548 to DAH. Core services were provided by STANTO19R0 to CFF RDP, P30-DK117469 to DartCF, and P20-

GM113132 to BioMT. Sequencing services and specialized equipment were provided by the Genomics and Molecular Biology Shared Resource Core at Dartmouth, NCI Cancer Center Support Grant 5P30 CA023108-41. The content is solely the responsibility of the authors and does not necessarily represent the official views of the NIH.

Competing interests. The authors have declared that no competing interests exist.

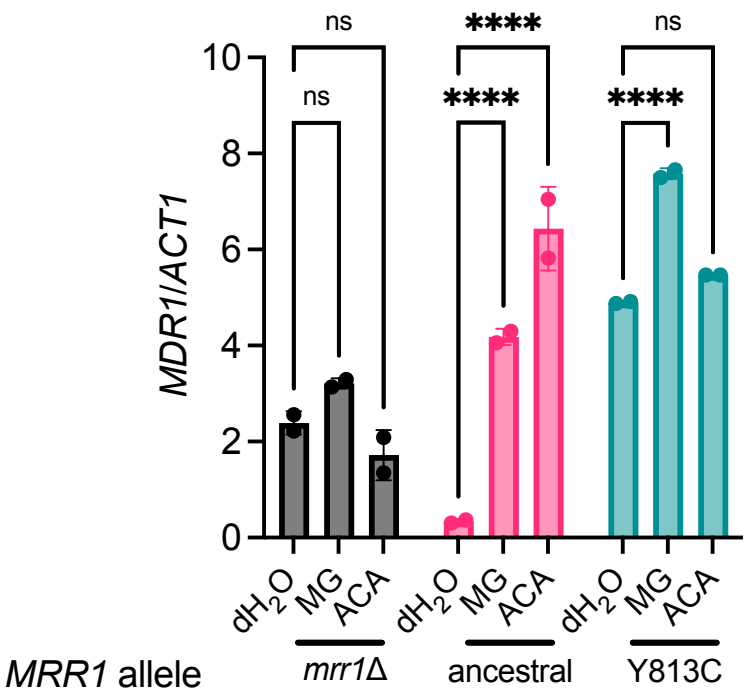

Figure I.1. Acetaldehyde induces *MDR1* expression in an Mrr1-dependent manner. *C. lusitaniae* strains U04 *mrr1*Δ ("*mrr1*Δ", black bars) U04 *mrr1*Δ + $MRR1^{ancestral}$ ("ancestral", magenta bars), and U04 *mrr1*Δ + $MRR1^{Y813C}$ ("Y813C", teal bars) were grown to exponential phase at 37°C and treated with 5 mM MG or 10 mM ACA for 15 min prior to analysis of *MDR1* transcript levels by qRT-PCR. Transcript levels are normalized to levels of *ACT1*. Data shown represent the mean ± SD from a single experiment performed in technical duplicate. Ordinary two-way ANOVA with Dunnett's multiple comparison test was used for statistical evaluation; **** $p < 0.0001$, ns not significant.

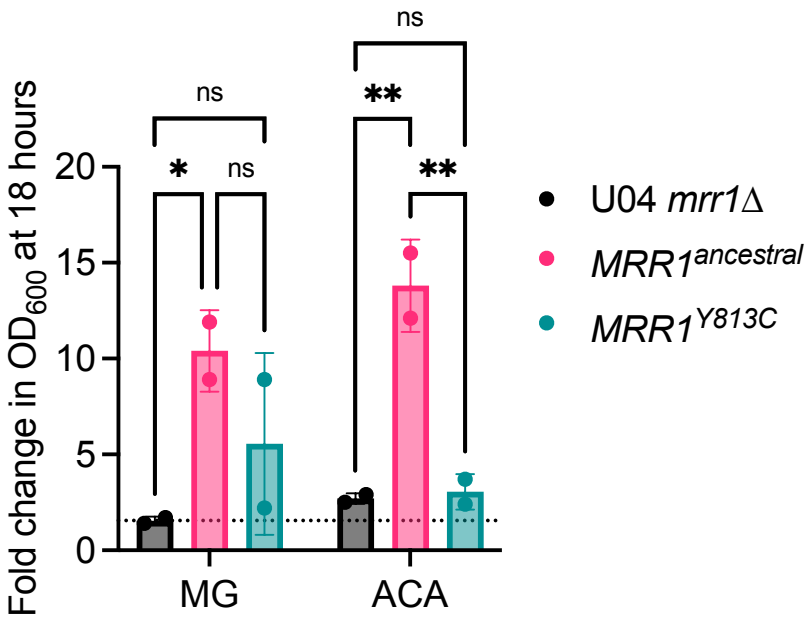

Figure I.2. Acetaldehyde stimulates growth in FLZ in an Mrr1-dependent manner.

C. lusitaniae strains U04 *mrr1*Δ ("*mrr1*Δ", black bars) U04 *mrr1*Δ + $MRR1^{ancestral}$ ("ancestral", magenta bars), and U04 *mrr1*Δ + $MRR1^{Y813C}$ ("Y813C", teal bars) were grown at 37°C in YPD supplemented with FLZ alone, FLZ + 5 mM MG, or FLZ + 10 mM ACA. Data are expressed as the fold change in OD_{600} for each strain in either FLZ + MG or FLZ + ACA relative to FLZ alone. The dotted line indicates a fold change of 1 (no change). Data shown represent the mean ± SD from two independent experiments. Ordinary two-way ANOVA with Tukey's multiple comparison test was used for statistical evaluation; * $p < 0.05$, ** $p < 0.01$, ns not significant.

YPD

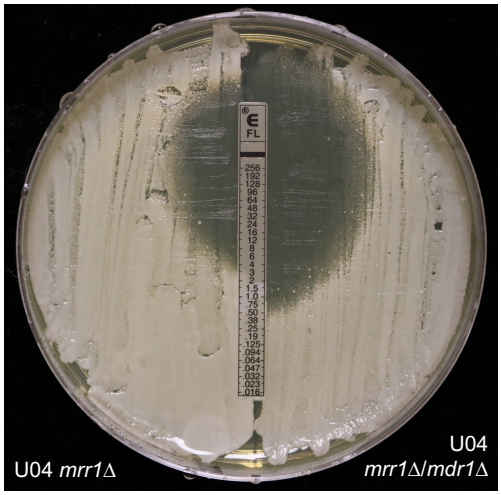

YPD + 10 mM ACA

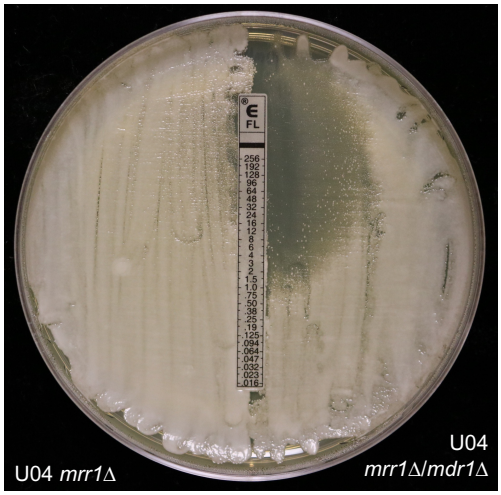

YPD

YPD + 10 mM ACA

YPD

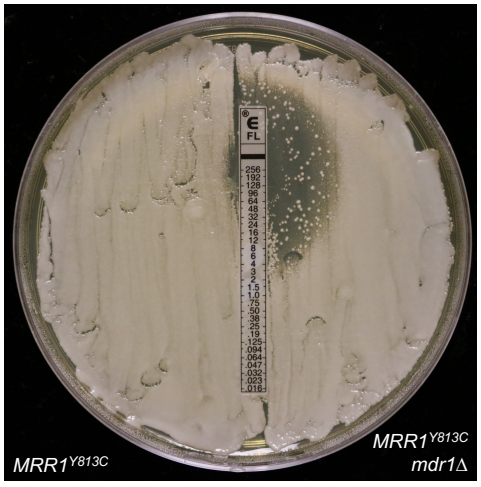

YPD + 10 mM ACA

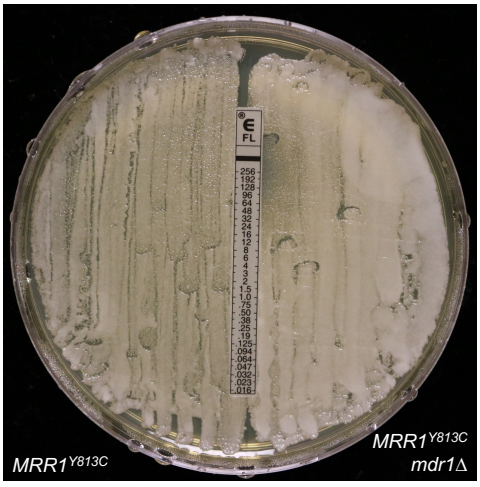

Figure I.3. Acetaldehyde can stimulate FLZ resistance and tolerance independently of *MRR1* or *MDR1*. *C. lusitaniae* strains U04 *mrr1*Δ, U04 *mrr1*Δ/*mdr1*Δ, U04 *mrr1*Δ + $MRR1^{ancestral}$, U04 *mrr1*Δ + $MRR1^{ancestral}$ *mdr1*Δ, U04 *mrr1*Δ + $MRR1^{Y813C}$, and U04 *mrr1*Δ + $MRR1^{Y813C}$ *mdr1*Δ were swabbed onto YPD agar with or without ACA at a final concentration of 10 mM and incubated with a FLZ E-test strip at 37˚C for two days. One representative experiment out of three independent experiments is shown.

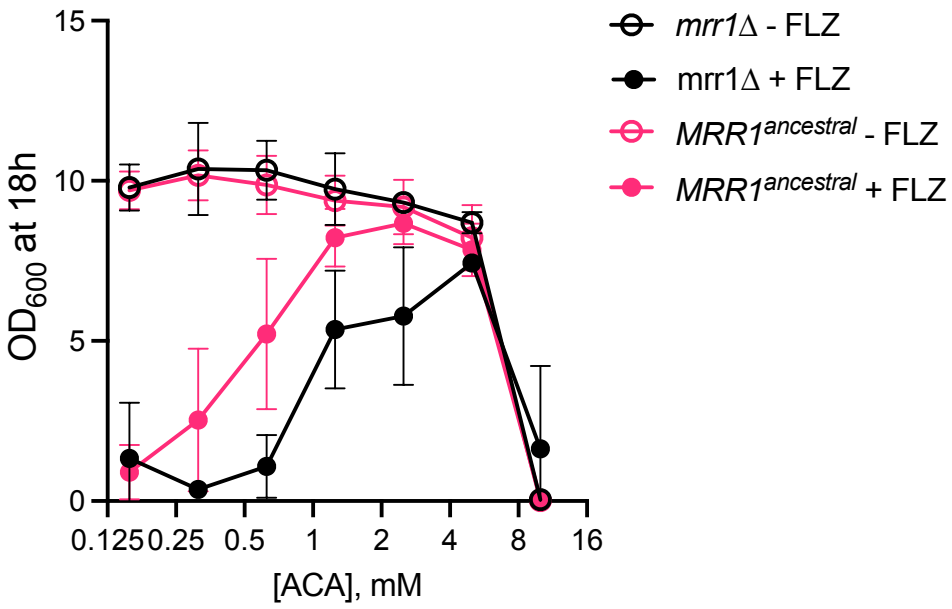

Figure I.4. The effect of acetaldehyde on FLZ resistance is dose dependent. *C. lusitaniae* strains U04 *mrr1*Δ ("*mrr1*Δ", black) and U04 *mrr1*Δ + *MRR1*^{ancestral} ("*MRR1*^{ancestral}", magenta) were grown for 18 hours at 37°C in serially diluted concentrations of ACA in YPD (open circles) or YPD + an inhibitory concentration of FLZ (closed circles). Data shown represent the mean ± SD from two independent experiments.

A

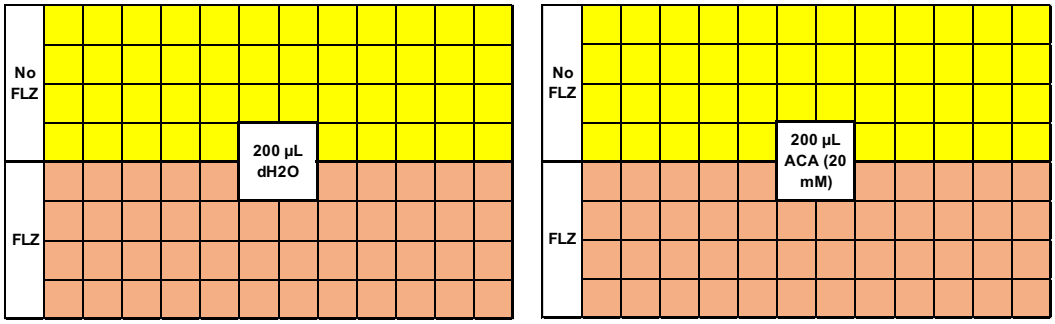

B

No FLZ	1.1	1.2	1.2	1.3	1.2	1.2	1.2	1.2	1.2	1.2	1.2	1.1
	1.1	1.0	1.1	1.0	1.1	1.1	1.2	1.2	1.2	1.2	1.1	1.1
	1.1	1.1	1.1	1.1	1.0	1.1	1.1	1.1	1.1	1.1	1.0	1.0
	1.1	1.1	1.1	1.1	1.1	dH2O or 20 mM ACA		1.1	1.1	1.1	1.1	1.0
1 µg/mL FLZ	1.1	1.6	1.8	3.9	23.4			23.0	6.1	3.3	2.2	2.3
	1.3	1.2	2.0	2.1	11.7	20.6	22.2	15.5	3.6	2.2	2.0	1.9
	1.8	2.0	1.6	2.7	3.9	5.9	5.2	4.6	3.2	2.2	1.9	2.9
	2.1	1.8	1.6	1.9	2.4	2.0	1.7	2.4	2.0	2.5	1.7	2.2

C

No FLZ	1.0	1.0	1.0	1.0	0.9	0.9	1.0	0.9	0.9	0.9	0.9	0.9
	1.0	1.0	1.0	1.0	1.0	1.0	1.0	1.0	1.1	1.1	1.0	1.1
	1.0	1.0	1.0	1.0	1.0	1.0	1.0	1.0	1.0	1.0	1.0	1.0
	1.0	1.0	1.0	1.2	1.0	dH2O or 20 mM ACA		1.1	1.1	1.1	1.0	1.1
3 µg/mL FLZ	1.7	1.1	2.0	3.9	4.0			5.3	2.1	1.6	1.5	1.7
	1.6	1.5	1.8	2.1	3.7	5.4	6.1	4.6	1.8	1.6	1.6	1.2
	1.7	3.0	2.0	2.6	3.0	2.6	2.9	2.2	1.7	1.5	1.3	1.0
	1.9	1.3	1.0	1.2	1.5	1.5	1.8	2.3	1.6	1.6	1.4	1.8

Figure I.5. Acetaldehyde induces FLZ resistance from proximal wells. *C. lusitaniae* strains were grown for 18 hours at 37˚C in YPD +/- FLZ in plates containing either dH_2O or 20 mM ACA in the four center wells. **(A)** Experimental setup. **(B-C)** Fold change in OD_{600} in each well of the ACA-containing plate compared to the dH_2O-containing plate for the *MRR1*^{ancestral} complement **(B)** and U04 *mrr1*Δ **(C)**. One representative experiment out of two independent experiments is shown.

References

1. Biermann AR, Demers EG, Hogan DA. 2021. Mrr1 regulation of methylglyoxal catabolism and methylglyoxal-induced fluconazole resistance in *Candida lusitaniae*. Mol Microbiol 115:116-130.
2. Biermann AR, Hogan DA. 2022. Transcriptional Response of *Candida auris* to the Mrr1 Inducers Methylglyoxal and Benomyl. mSphere doi:10.1128/msphere.00124-22:e0012422.
3. Altemose B, Gong J, Zhu T, Hu M, Zhang L, Cheng H, Zhang L, Tong J, Kipen HM, Ohman-Strickland P, Meng Q, Robson MG, Zhang J. 2015. Aldehydes in relation to air pollution sources: A case study around the Beijing Olympics. Atmospheric Environment 109:61-69.
4. Bao J, Li H, Wu Z, Zhang X, Zhang H, Li Y, Qian J, Chen J, Deng L. 2022. Atmospheric carbonyls in a heavy ozone pollution episode at a metropolis in Southwest China: Characteristics, health risk assessment, sources analysis. Journal of Environmental Sciences 113:40-54.
5. Zhou X, Li Z, Zhang T, Wang F, Tao Y, Zhang X. 2022. Multisize particulate matter and volatile organic compounds in arid and semiarid areas of Northwest China. Environmental Pollution 300.
6. Chai F, Li P, Li L, Qiu Z, Han Y, Yang K. 2022. Dispersion, olfactory effect, and health risks of VOCs and odors in a rural domestic waste transfer station. Environmental Research 209.

7. Zhang X, Wu Z, He Z, Zhong X, Bi F, Li Y, Gao R, Li H, Wang W. 2022. Spatiotemporal patterns and ozone sensitivity of gaseous carbonyls at eleven urban sites in southeastern China. Science of The Total Environment 824.

8. Seeman JI, Dixon M, Haussmann H-J. 2002. Acetaldehyde in Mainstream Tobacco Smoke: Formation and Occurrence in Smoke and Bioavailability in the Smoker. Chemical Research in Toxicology 15:1331-1350.

9. Tillonen J, Homann N, Rautio M, Jousimies-Somer H, Salaspuro M. 1999. Role of yeasts in the salivary acetaldehyde production from ethanol among risk groups for ethanol-associated oral cavity cancer. Alcohol Clin Exp Res 23:1409-15.

10. Nieminen MT, Uittamo J, Salaspuro M, Rautemaa R. 2009. Acetaldehyde production from ethanol and glucose by non-*Candida albicans* yeasts *in vitro*. Oral Oncol 45:e245-8.

11. Uittamo J, Siikala E, Kaihovaara P, Salaspuro M, Rautemaa R. 2009. Chronic candidosis and oral cancer in APECED-patients: production of carcinogenic acetaldehyde from glucose and ethanol by *Candida albicans*. Int J Cancer 124:754-6.

12. Gainza-Cirauqui ML, Nieminen MT, Novak Frazer L, Aguirre-Urizar JM, Moragues MD, Rautemaa R. 2013. Production of carcinogenic acetaldehyde by *Candida albicans* from patients with potentially malignant oral mucosal disorders. J Oral Pathol Med 42:243-9.

13. Jokelainen K, Roine RP, Vaananen H, Farkkila M, Salaspuro M. 1994. *In vitro* acetaldehyde formation by human colonic bacteria. Gut 35:1271-4.

14. Salaspuro M. 1997. Microbial metabolism of ethanol and acetaldehyde and clinical consequences. Addict Biol 2:35-46.

15. Vakevainen S, Tillonen J, Blom M, Jousimies-Somer H, Salaspuro M. 2001. Acetaldehyde production and other ADH-related characteristics of aerobic bacteria isolated from hypochlorhydric human stomach. Alcohol Clin Exp Res 25:421-6.

16. Homann N, Tillonen J, Rintamaki H, Salaspuro M, Lindqvist C, Meurman JH. 2001. Poor dental status increases acetaldehyde production from ethanol in saliva: a possible link to increased oral cancer risk among heavy drinkers. Oral Oncol 37:153-8.

17. Vakevainen S, Mentula S, Nuutinen H, Salmela KS, Jousimies-Somer H, Farkkila M, Salaspuro M. 2002. Ethanol-derived microbial production of carcinogenic acetaldehyde in achlorhydric atrophic gastritis. Scand J Gastroenterol 37:648-55.

18. Visapaa JP, Tillonen J, Salaspuro M. 2002. Microbes and mucosa in the regulation of intracolonic acetaldehyde concentration during ethanol challenge. Alcohol Alcohol 37:322-6.

19. Demers EG, Stajich JE, Ashare A, Occhipinti P, Hogan DA. 2021. Balancing Positive and Negative Selection: *In Vivo* Evolution of *Candida lusitaniae MRR1*. mBio 12.

20. O'Brien PJ, Siraki AG, Shangari N. 2005. Aldehyde sources, metabolism, molecular toxicity mechanisms, and possible effects on human health. Crit Rev Toxicol 35:609-62.

21. Schalkwijk CG, Stehouwer CDA. 2020. Methylglyoxal, a Highly Reactive Dicarbonyl Compound, in Diabetes, Its Vascular Complications, and Other Age-Related Diseases. Physiol Rev 100:407-461.

22. Ramasamy R, Vannucci SJ, Yan SS, Herold K, Yan SF, Schmidt AM. 2005. Advanced glycation end products and RAGE: a common thread in aging, diabetes, neurodegeneration, and inflammation. Glycobiology 15:16R-28R.

23. Hazen SL, Hsu FF, Heinecke JW. 1996. p-hydroxyphenylacetaldehyde is the major product of L-tyrosine oxidation by activated human phagocytes - A chloride-dependent mechanism for the conversion of free amino acids into reactive aldehydes by myeloperoxidase. Journal of Biological Chemistry 271:1861-1867.

24. Anderson MM, Hazen SL, Hsu FF, Heinecke JW. 1997. Human neutrophils employ the myeloperoxidase-hydrogen peroxide-chloride system to convert hydroxy-amino acids into glycolaldehyde, 2-hydroxypropanal, and acrolein. A mechanism for the generation of highly reactive alpha-hydroxy and alpha,beta-unsaturated aldehydes by phagocytes at sites of inflammation. Journal of Clinical Investigation 99:424-432.

25. Hazen SL, Hsu FF, d'Avignon A, Heinecke JW. 1998. Human Neutrophils Employ Myeloperoxidase To Convert α-Amino Acids to a Battery of Reactive Aldehydes: A Pathway for Aldehyde Generation at Sites of Inflammation. Biochemistry 37:6864-6873.

26. Hazen SL, d'Avignon A, Anderson MM, Hsu FF, Heinecke JW. 1998. Human Neutrophils Employ the Myeloperoxidase-Hydrogen Peroxide-Chloride System to

Oxidize α-Amino Acids to a Family of Reactive Aldehydes. Journal of Biological Chemistry 273:4997-5005.

27. Zhang MM, Ong CL, Walker MJ, McEwan AG. 2016. Defence against methylglyoxal in Group A *Streptococcus*: a role for Glyoxylase I in bacterial virulence and survival in neutrophils? Pathog Dis 74.

28. Gross NT, Hultenby K, Mengarelli S, Camner P, Jarstrand C. 2000. Lipid peroxidation by alveolar macrophages challenged with *Cryptococcus neoformans*, *Candida albicans* or *Aspergillus fumigatus*. Med Mycol 38:443-9.

29. Prantner D, Nallar S, Richard K, Spiegel D, Collins KD, Vogel SN. 2021. Classically activated mouse macrophages produce methylglyoxal that induces a TLR4-and RAGE-independent proinflammatory response. Journal of Leukocyte Biology 109:605-619.

Appendix II. Miscellaneous unpublished data pertaining to Mrr1 in *Candida* species

Results

Complementation with different *MRR1* alleles results in differential stimulation of growth in fluconazole (FLZ) by methylglyoxal (MG)

Given our previously published data showing that an mrr1Δ mutant exhibits significantly less stimulation of FLZ resistance by MG compared to its *MRR1*-intact parental isolate (1), we became interested in whether different *MRR1* alleles would confer varying degrees of FLZ resistance in response to MG. To explore this question, we assessed the growth of an *mrr1*Δ mutant in the U04 background and four isogenic complements each expressing a different *MRR1* allele in inhibitory concentrations of FLZ with or without 5 mM MG. The relative basal and benomyl-inducible activities of each Mrr1 variant have previously been characterized (2): $Mrr1^{ancestral}$, which expresses the *MRR1* allele that was predicted to have been encoded by the "founding strain" (or ancestral strain) of this clinical population, has low basal activity and is highly inducible by benomyl; $Mrr1^{L1191H + Q1197*}$ was present in several isolates at the time of initial identification, has low basal activity, and is also highly inducible by benomyl; $Mrr1^{Y813C}$ was also present in the initial identification, and has high basal activity and is weakly inducible by benomyl; and $Mrr1^{L1191H}$, an artificially generated variant to delineate the effects of the L1191H and Q1197* amino acid exchanges, also has high basal activity and is weakly inducible by benomyl.

In agreement with our published results in a different isolate background, growth of the U04 *mrr1*Δ in FLZ was not enhanced by 5 mM MG (**Fig. II.1A**), and the average

fold change in OD_{600} after 18 hours of growth in FLZ + MG compared to FLZ alone was only 1.5 (**Fig. II.1F**). Importantly, 5 mM MG was not inhibitory to any of the strains tested, confirming that the lack of an increase in FLZ resistance is not due to MG toxicity (**Fig. II.1A-E**). In contrast to U04 *mrr1*Δ, the $MRR1^{ancestral}$ complement displayed a striking stimulation of growth in FLZ in response to MG (**Fig. II.1B**), averaging an 8.7-fold increase in OD_{600} at 18 h (**Fig. II.1F**). The growth kinetics of the $MRR1^{L1191H + Q1197*}$ complement were comparable to those of U04 *mrr1*Δ (**Fig. II.1C**), and indeed the average 1.7-fold change in OD_{600} at 18 h observed for this strain was not significantly different from U04 *mrr1*Δ (**Fig. II.1F**). The $MRR1^{Y813C}$ complement displayed intermediate stimulation of growth in FLZ by MG (**Fig. II.1D**), with an average 4.9-fold change in OD_{600} at 18 h (**Fig. II.1F**). Like U04 *mrr1*Δ and the $MRR1^{L1191H + Q1197*}$ complement, the $MRR1^{L1191H}$ complement gained no significant growth benefit from 5 mM MG (**Fig. II.1E**), with an average fold change in endpoint OD_{600} of 2.3 (**Fig. II.1F**). Therefore, we can conclude that i) of the Mrr1 variants tested, $Mrr1^{ancestral}$ confers the most robust response to MG; ii) although the L1191H + Q1197* variant is inducible by benomyl (2), it is not inducible by MG under our conditions, and thus, it is likely that MG and benomyl activate Mrr1 through different mechanisms; and iii) constitutively active Mrr1 is overall less responsive to MG than $Mrr1^{ancestral}$, but some constitutively active variants are more inducible by MG than others.

Isogenic *C. lusitaniae* strains expressing different *MRR1* alleles display differences in the kinetics of *MDR1* induction by 5 mM MG

In prior work, we have shown that MG induces expression of several Mrr1-regulated genes in a time-dependent manner, i.e., expression of *MDR1* peaks at 15 minutes of exposure to 15 mM MG and begins to return to basal levels after 30 min in a clinical *C. lusitaniae* isolate with constitutively active Mrr1 (3). Due to the *MRR1*-dependent differences we observed in the stimulation of FLZ resistance by MG (**Fig. II.1**), we were interested in whether the kinetics of *MDR1* induction by MG would differ by *MRR1* allele. Therefore, we exposed exponential-phase cultures of three of the *MRR1* complement strains described above – expressing either $MRR1^{ancestral}$, $MRR1^{Y813C}$, or $MRR1^{L1191H}$ – to 5 mM MG for 15, 30, 60, or 120 minutes before harvesting cells for RNA isolation and quantitative real-time PCR. In accordance with the robust induction of growth in FLZ by MG that we observed for the $MRR1^{ancestral}$ complement (**Fig. II.1B**), this strain also displayed a significant, 7.5-fold increase in *MDR1* expression following 15 and 30 min of MG exposure (**Fig. II.2**). Similar to our previous observations, MG-induced *MDR1* expression in this strain began declining by 60 min of exposure, at which point it was 4.4-fold higher than the control (**Fig. II.2**). By 120 min, *MDR1* expression had fallen to a level 2.9-fold higher than the control, a difference which was not statistically significant (**Fig. II.2**). In the $MRR1^{Y813C}$ complement, *MDR1* expression increased 3.5-fold relative to the control at 15 min of MG exposure, but did not wane as in the $MRR1^{ancestral}$ complement, remaining at 3.3-, 3.1-, and 3.0-fold higher than the control at 30, 60, and 120 min respectively, although expression at 120 min was not significantly different from the control (**Fig. II.2**). Finally, *MDR1* expression was only induced by a maximum of 1.9-fold

in the *MRR1*^{L1191H} complement at 15 min of MG exposure, where it essentially remained for the duration of the experiment, with increases relative to the control averaging 1.8-, 1.7-, and 1.7-fold at 30, 60, and 120 min respectively (**Fig. II.2**). For this strain, the 60- and 120-min time points did not differ significantly from the control. The implications of these data are that activity of Mrr1^{ancestral} is strongly and rapidly responsive to MG but returns to basal levels once the cells have either acclimated to the MG or detoxified it; activity of Mrr1^{Y813C} is moderately inducible by MG but remains elevated even after prolonged exposure; and that activity of Mrr1^{L1191H} is only minimally inducible by MG.

Gain-of-function mutations in *MRR1* contribute to MG resistance in other, unrelated *C. lusitaniae* isolates

Since we have previously shown intraspecies heterogeneity in MG resistance across numerous isolates and strains of different *Candida* species, we wanted to determine whether *MRR1* contributes to MG resistance in *C. lusitaniae* isolates that are not closely related to those which we have already published. The P1 and P3 isolates and their *mrr1*Δ derivatives, isolated and generated respectively by Asner et al. (4) and Kannan et al. (5), were an ideal comparison, because the *MRR1* alleles of these isolates have already been characterized (4, 5). In brief, isolate P1 is FLZ-sensitive and is the earliest isolate of a temporal series from a single patient, while isolate P3 is FLZ-resistant with a gain-of-function *MRR1*^{V668G} allele and was isolated from the same patient as P1 at a later time point (4, 5). All four strains displayed comparable growth in YPD, indicating that none of them have inherent growth defects (**Fig. II.3A**). Interestingly, P3 grew markedly better in 15 mM MG compared to P1, and both *mrr1*Δ mutants were strikingly more sensitive to MG

than their *MRR1*-intact parental isolates (**Fig. II.3B**). These data support the hypothesis that the involvement of Mrr1 in MG resistance is broadly conserved, at least across isolates of *C. lusitaniae*.

Gain-of-function mutations in *MRR1* contribute to MG resistance in *C. albicans*

Because Mrr1 regulates several stress-responsive genes in *C. albicans* (6, 7), we hypothesized that hyperactive Mrr1 would confer increased resistance to MG in *C. albicans*. To test this, we performed growth kinetic assays on FLZ-sensitive isolates F2 and G2, FLZ-resistant isolates F5 and G5, and four isogenic *mrr1*Δ/Δ strains, three of which have been homozygously complemented with either $MRR1^{WT}$, $MRR1^{N803D}$, or $MRR1^{Q350L}$. We observed negligible growth differences between the four isogenic strains in the YPD control (**Fig. II.4A**), but the complements expressing either of the gain-of-function *MRR1* alleles, N803D or Q350L, grew strikingly better in YPD + 15 mM MG compared to the *mrr1*Δ/Δ mutant or the complement expressing wild-type *MRR1* (**Fig. II.4B**). Curiously, the $MRR1^{WT}$ complement was slightly but noticeably more sensitive to MG than the *mrr1*Δ/Δ mutant (**Fig. II.4B**). In the control condition, the FLZ-sensitive isolates F2 and G2 grew substantially better than the matched FLZ-resistant isolates F5 and G5, as evidenced by the faster growth rate of F2 compared to F5 (**Fig. II.4C**) and the higher final yield of both F2 and G2 compared to their counterparts (**Fig. II.4C** and **E**). However, F5 and G5 were markedly more resistant to 15 mM MG, as evidenced by their shorter lag period and faster growth rate (**Fig. II.4D** and **F**). Together, these data support a role for hyperactive Mrr1 in MG resistance in *C. albicans*.

MDR1 does not contribute to Mrr1-mediated MG resistance in *C. lusitaniae*

We have previously demonstrated that two genes, *MGD1* and *MGD2*, contribute to Mrr1-mediated MG resistance in *C. lusitaniae* (1). However, *mrr1*Δ mutants are more sensitive to MG than isogenic mutants lacking *MGD1* and/or *MGD2* (1), suggesting that other Mrr1-regulated genes are involved in *C. lusitaniae* MG resistance. Thus, we hypothesized that the major facilitator drug-proton antiporter encoded by *MDR1* could contribute to MG resistance by exporting MG-derived advanced glycation endproducts (AGEs) that may otherwise exert intracellular toxicity. We tested our hypothesis by evaluating growth in 15 mM MG of the Mrr1-hyperactive clinical isolate U04 (U04 WT), its *mrr1*Δ, *mdr1*Δ, and *mrr1*Δ/*mdr1*Δ derivatives, as well as isogenic strains complemented with either the native, constitutively active allele (Y813C) or the ancestral allele which we have previously demonstrated to have low basal activity (2) and the *mdr1*Δ derivatives of these two complements. There were no significant growth differences between any of these strains in our YPD control (data not shown). As expected, U04 WT and the $MRR1^{Y813C}$ complement were more resistant to MG compared to U04 *mrr1*Δ and the $MRR1^{ancestral}$ complement respectively (**Fig. II.5A-B**). In contrast, deletion of *MDR1* from U04 WT, the $MRR1^{Y813C}$ complement, or the $MRR1^{ancestral}$ complement did not significantly affect growth in 15 mM MG (**Fig. II.5A-B**). Notably, however, the U04 *mrr1*Δ/*mdr1*Δ mutant grew distinctively worse in MG compared to the U04 *mrr1*Δ single mutant (**Fig. II.5A**). These results suggest that in the presence of functional, constitutively active (Y813C) or inducible (ancestral) Mrr1, Mdr1 plays a negligible role in MG detoxification compared to other Mrr1-regulated genes but may confer minor protection against MG when other Mrr1-regulated genes are not meaningfully expressed.

MRR1-dependent overexpression of _MDR1_ increases susceptibility of _C. lusitaniae_ to glutathione depletion

Since the glyoxalase system, the major mechanism of MG detoxification in most organisms, is dependent on a catalytic amount of reduced glutathione (GSH), and we have previously demonstrated that gain-of-function mutations in *MRR1* confer increased MG resistance in *C. lusitaniae*, we hypothesized that constitutive Mrr1 activity would confer resistance to the GSH-depleting agent diethyl maleate (DEM). Therefore, we compared the growth in 1 mM DEM of U04 WT, U04 *mrr1*Δ, and the $MRR1^{Y813C}$ and $MRR1^{ancestral}$ complements in the U04 background. Surprisingly, the *mrr1*Δ mutant was more resistant to DEM than U04 WT (**Fig. II.6A**), and similarly, the complement expressing $MRR1^{ancestral}$ was more resistant to DEM than the complement expressing the gain-of-function $MRR1^{Y813C}$ (**Fig. II.6B**). Contrary to our hypothesis, constitutive Mrr1 activity renders *C. lusitaniae* more susceptible to GSH depletion via DEM.

Because *MDR1* is one of the genes most strongly regulated by Mrr1 in *C. lusitaniae* (2, 3), we investigated whether *MDR1* overexpression was a significant cause of the increased DEM susceptibility observed in strains expressing constitutively active Mrr1 by including isogenic *mdr1*Δ mutants in our growth assay. Deletion of *MDR1* increased the DEM resistance of U04 WT to that of the *mrr1*Δ mutant, and the *mrr1*Δ/*mdr1*Δ double mutant did not exhibit a further increase (**Fig. II.6A**), indicating that *MDR1* overexpression is likely the major cause of DEM sensitivity in U04 WT. Likewise, deletion of *MDR1* from both the $MRR1^{ancestral}$ and $MRR1^{Y813C}$ complements improved growth in DEM (**Fig. II.6B**). The improvement in the $MRR1^{ancestral}$ complement may be due to the fact that activity of

Mrr1^{ancestral} is highly inducible by stimuli (2) and DEM has been reported to induce Mrr1-dependent *MDR1* expression in *C. albicans* (8). Finally, we investigated whether *MDR1* deletion would influence the growth in DEM of the isolates L17 and U05, which contain a gain-of-function mutation (H467L) and a premature stop codon (L1191H + Q1197*) in *MRR1*, respectively (3). Deletion of *MDR1* from either isolate did not significantly affect growth in the YPD control (data not shown). As expected, deletion of *MDR1* from isolate L17 resulted in decreased lag time, increased growth rate, and higher yield in the presence of 1 mM DEM relative to L17 WT (**Fig. II.6C**). However, the U05 *mdr1*Δ mutant did not exhibit an observable difference in growth relative to U05 WT in the presence of 1 mM DEM (**Fig. II.6C**). We have previously reported that isolate U05 (3) and an *mrr1*Δ strain complemented with the *MRR1* allele from U05 (L1191H + Q1197*) (2) express *MDR1* at very low levels, and thus, our data here indicate that overexpression of *MDR1* leads to DEM sensitivity, but low-level *MDR1* expression does not.

Discussion and Next Steps:

The data presented in this Appendix contribute to our understanding of Mrr1-dependent induction of FLZ resistance by MG in *C. lusitaniae* and the importance of Mrr1 in MG resistance in multiple *Candida* species. Specifically, we have demonstrated that different Mrr1 variants in *C. lusitaniae* lead to differing stimulation of FLZ resistance and *MDR1* induction. Interestingly, full-length Mrr1 with low basal activity (Mrr1^{ancestral}) confers a strong and rapid "on-off" response to MG in terms of MDR1 expression, while full-length, constitutively active Mrr1 (Mrr1^{Y813C} and Mrr1^{L1191H}) exhibit a relatively low response that persists over time. These two different modes of activation may be beneficial

under different circumstances. Furthermore, we have demonstrated a role for Mrr1 in MG resistance in strains of *C. lusitaniae* that are unrelated to those from our group's cystic fibrosis (CF) study, and in *C. albicans*, suggesting that this phenomenon is broadly conserved throughout *Candida* species. Finally, we also shed more light on the oxidative stress sensitivity of *C. lusitaniae* strains expressing gain-of-function *MRR1* by demonstrating that constitutively active Mrr1 sensitizes *C. lusitaniae* to GSH depletion via DEM, and that this sensitivity can be completely mitigated by deletion of *MDR1*. This finding indicates that Mdr1 exports one or more molecules with antioxidant properties, and as a result, overexpression of *MDR1* leads to oxidative stress sensitivity. Alternatively, an overabundance of Mdr1 protein could be affecting the cell redox state through some other mechanism, perhaps by altering the plasma membrane composition in such a way that renders the membrane more susceptible to oxidation. Ultimately, our findings contribute toward a greater understanding of the evolutionary context of *MRR1* and *MDR1* in *Candida* species.

As stated in **Appendix I**, some of the experiments presented here are currently lacking a third biological replicate, and obtaining those replicates is a priority for these data. Otherwise, a clear next step is to continue our investigation of MG resistance across strains of different *Candida* species with known *MRR1* alleles, as we postulate that MG may be an important selective pressure for *MRR1*, particularly in the context of infection. Additionally, we have generated isogenic *C. lusitaniae* strains expressing His-FLAG-tagged versions of four of the Mrr1 variants described above ($Mrr1^{ancestral}$, $Mrr1^{L1191H + Q1197*}$, $Mrr1^{Y813C}$, and $Mrr1^{L1191H}$) and are in the process of performing ChIP experiments with these strains to determine i) whether these variants exhibit differential binding to their

target promoters under control conditions and ii) whether treatment with MG or benomyl changes the promoter occupancy of any of these Mrr1 variants. We are also interested in performing an RNAseq experiment with these strains +/- 5 mM MG as we did for *C. auris* (Chapter 3) to assess the Mrr1-dependent and independent MG response in *C. lusitaniae*. Finally, regarding GSH depletion and oxidative stress, we are interested in investigating the potential mechanisms for increased DEM sensitivity in MDR1-overexpressing strains of C. lusitaniae. Some hypotheses were outlined in Chapter 4, but we will reiterate here that our two leading hypotheses are that i) Mdr1 exports polyamines and thus, overexpression of *MDR1* leads to polyamine deficiency, and/or that when Mdr1 is present in large quantities, the plasma membrane becomes more susceptible to oxidative damage.

Materials and Methods

Strains, media, and growth conditions

All strains were stored long term in a final concentration of 25% glycerol at -80°C and freshly streaked onto yeast extract peptone dextrose (YPD) agar (10 g/L yeast extract, 20 g/L peptone, 2% glucose, 1.5% agar) once every seven days and maintained at room temperature. All overnight cultures were grown in 5 mL YPD liquid medium (10 g/L yeast extract, 20 g/L peptone, 2% glucose) on a rotary wheel at 30°C. For experiments, medium was supplemented with FLZ (Sigma-Aldrich, stock 4 mg mL-1 in DMSO), 5 mM or 15 mM MG (Sigma-Aldrich, 5.55 M), or 1 mM DEM as noted.

Growth Kinetics

Growth kinetic assays were performed as previously described in reference (1). In brief, exponential-phase cultures of *C. lusitaniae* or *C. albicans* were washed and diluted in dH_2O to an OD_{600} of 1; 60 µL of each diluted cell suspension was added to 5 mL fresh YPD. To each well of a clear 96-well flat-bottom plate (Falcon) was added 100 µL of YPD or YPD supplemented with FLZ, MG, FLZ and MG, or DEM at twice the desired final concentration, and 100 µL of cell inoculum in YPD. Plates were arranged in technical triplicate for each strain and condition and incubated in a Synergy Neo2 Microplate Reader (BioTek, USA) according to the following protocol: heat to 37°C, start kinetic, read OD_{600} once per hour for 36 hours, end kinetic. Results were calculated in Microsoft Excel and plotted in GraphPad Prism 9.0.0 (GraphPad Software).

Quantitative Real-Time PCR

To exponential-phase cultures of *C. lusitaniae* (YPD, 37˚C) was added MG to a final concentration of 5 mM. Cultures were returned to the roller drum at 37˚C for 15, 30, 60, or 120 min as indicated in the text, then centrifuged at 5000 rpm for 5 min. RNA isolation, gDNA removal, cDNA synthesis, and quantitative real-time PCR were performed as previously described (1). Transcripts were normalized to *C. lusitaniae ACT1* expression. Results were calculated in Microsoft Excel and plotted in GraphPad Prism 9.0.0 (GraphPad Software).

Statistical Analysis and Figure preparation

All graphs were prepared with GraphPad Prism 9.0.0 (GraphPad Software). Multiple t-tests and one-way ANOVA tests were performed in Prism; details on each test are described in the corresponding figure legends. All p-values were two-tailed and $p < 0.05$ were considered significant for all analyses performed and are indicated with asterisks or letters in the text: * $p < 0.05$; ** $p < 0.01$ and a-b, $p < 0.0001$; a-c, $p < 0.001$; b-c, $p < 0.01$.

Data availability

The data that support the findings of this study are available from the corresponding author upon request.

Acknowledgements

We thank Dominique Sanglard, Lawrence Myers, Joachim Morschhäuser, and Elora Demers for providing strains.

Author contributions. ARB and DAH conceived and designed the experiments and wrote the paper. ARB performed the experiments. ARB and DAH analyzed the data.

Funding. This study was supported by grant R01 5R01 AI127548 to DAH. Core services were provided by STANTO19R0 to CFF RDP, P30-DK117469 to DartCF, and P20-GM113132 to BioMT. Sequencing services and specialized equipment were provided by the Genomics and Molecular Biology Shared Resource Core at Dartmouth, NCI Cancer

Center Support Grant 5P30 CA023108-41. The content is solely the responsibility of the authors and does not necessarily represent the official views of the NIH.

Competing interests. The authors have declared that no competing interests exist.

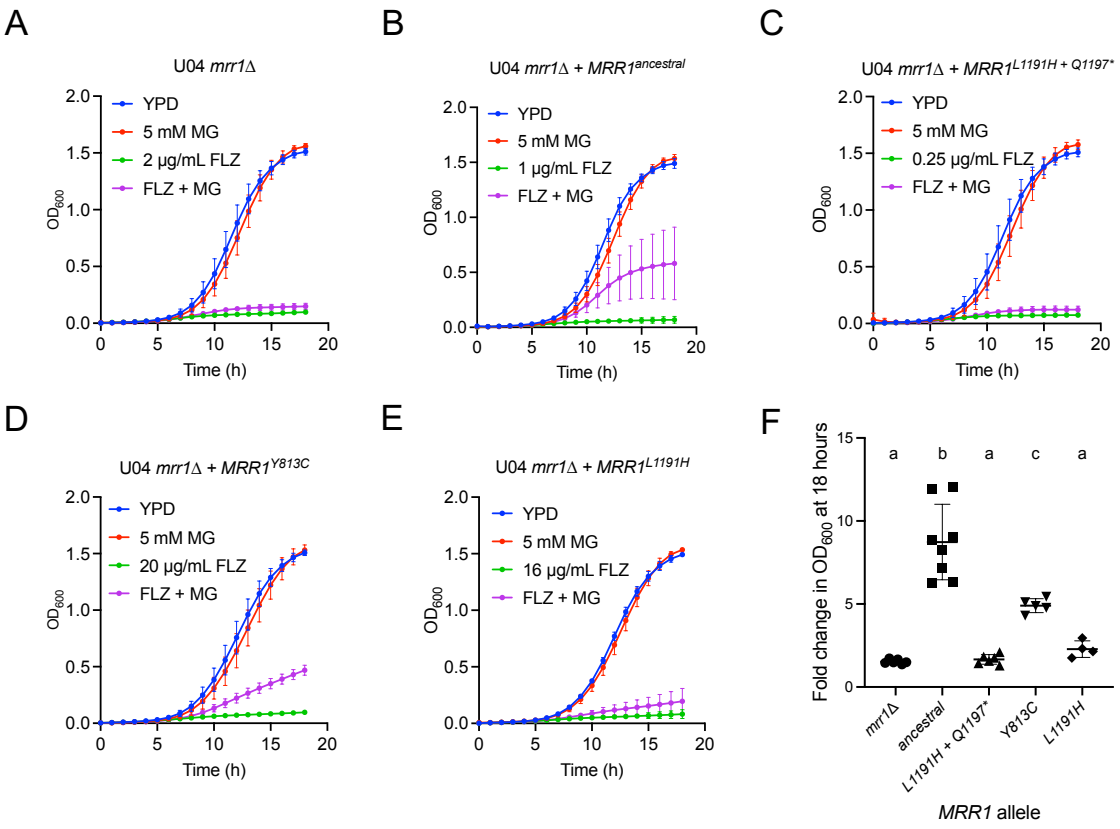

Figure II.1. The degree of MG-stimulated FLZ resistance is dependent on the *MRR1* allele in *C. lusitaniae*. **(A-E)** *C. lusitaniae* strains U04 *mrr1*Δ **(A)**, U04 *mrr1*Δ + $MRR1^{ancestral}$ **(B)**, U04 *mrr1*Δ + $MRR1^{L1191H + Q1197*}$ **(C)**, U04 *mrr1*Δ + $MRR1^{Y813C}$ **(D)**, or U04 *mrr1*Δ + $MRR1^{L1191H}$ **(E)** were grown at 37°C in YPD alone (blue), or with 5 mM MG (red), the indicated concentration of FLZ (green), or FLZ + 5 mM MG (purple). Data shown represent the mean ± SD from at least four independent experiments. (F) Fold change in OD_{600} after 18 hours of growth for each indicated strain at 37°C in FLZ versus FLZ + 5 mM MG. Data shown represent the mean ± SD from at least four independent experiments. Ordinary one-way ANOVA with Tukey's multiple comparison test was used for statistical evaluation; a-b, $p < 0.0001$; a-c, $p < 0.001$; b-c, $p < 0.01$.

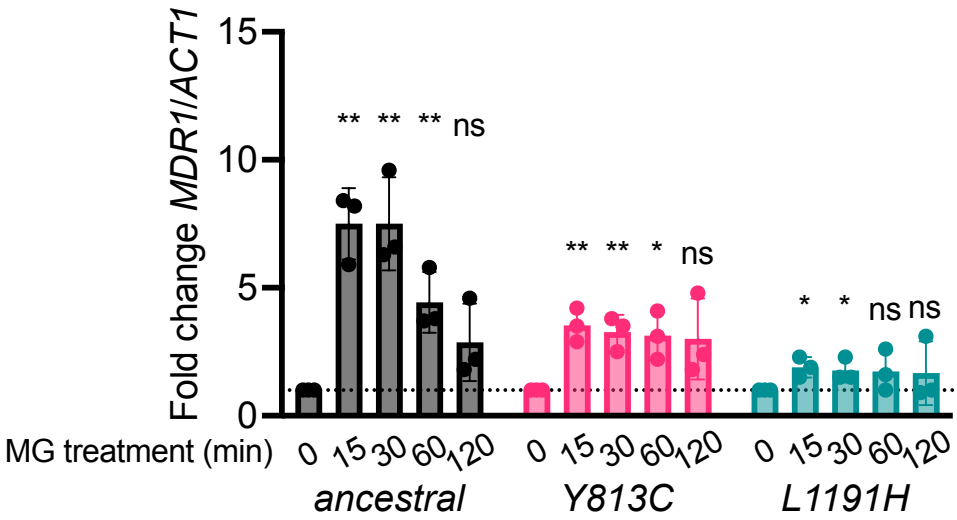

Figure II.2. Isogenic strains expressing different *MRR1* alleles display differences in the kinetics of *MDR1* induction by 5 mM MG. *C. lusitaniae* strains U04 *mrr1*Δ + $MRR1^{ancestral}$ ("ancestral", black bars), U04 *mrr1*Δ + $MRR1^{Y813C}$ ("Y813C", magenta bars), or U04 *mrr1*Δ + $MRR1^{L1191H}$ ("L1191H", teal bars) were grown to exponential phase at 37°C and treated with 5 mM MG for the time indicated prior to analysis of *MDR1* transcript levels by qRT-PCR. Transcript levels are normalized to levels of *ACT1* and presented as ratio at each time point relative to the control (0 min) for three independent experiments. Error bars represent the standard deviation across the three independent experiments. The dotted line represents a fold change of 1; i.e., no change in expression compared to the control. Multiple unpaired t-tests were used for statistical evaluation of each time point compared to 0 min for each strain; * $p < 0.05$, ** $p < 0.01$, ns not significant.

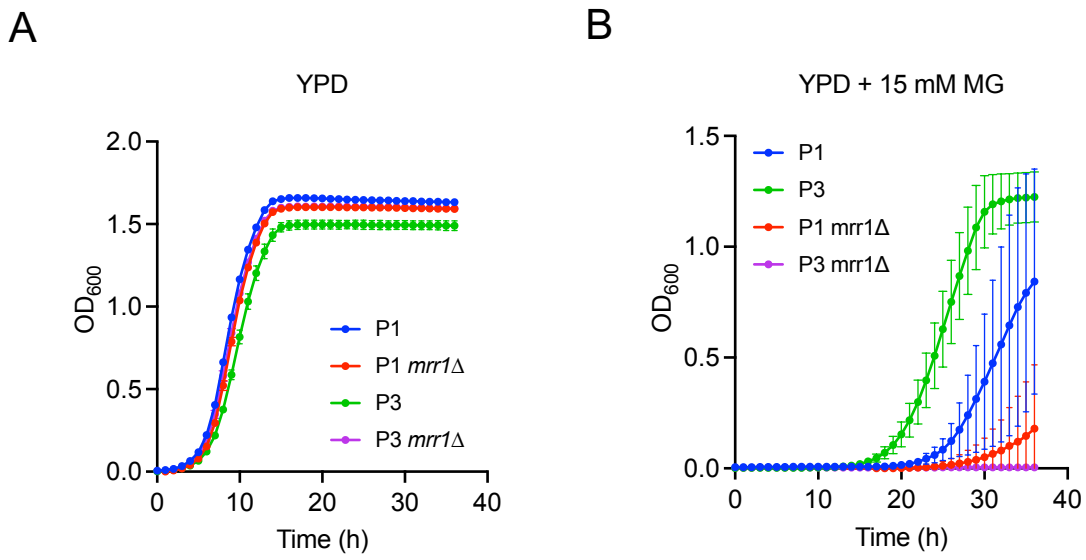

Figure II.3. Gain-of-function mutations in *MRR1* contribute to MG resistance in other *C. lusitaniae* clinical isolates. Growth curves of *C. lusitaniae* isolates P1 (blue), P3 (green), and their *mrr1*Δ (red and purple respectively) derivatives in YPD **(A)** or YPD supplemented with MG to a final concentration of 15 mM **(B)**. One representative experiment out of two independent experiments is shown due to day-to-day variability; error bars represent the standard deviation of technical replicates within the experiment.

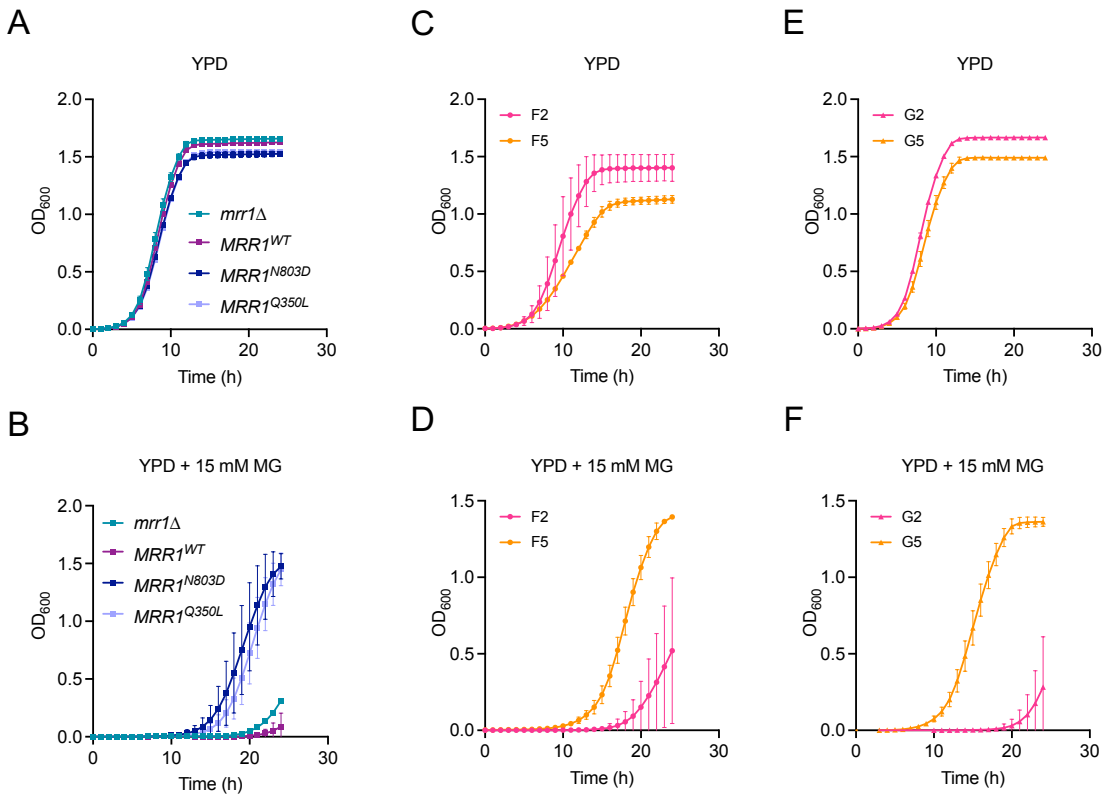

Figure II.4. Gain-of-function mutations in *MRR1* contribute to MG resistance in *C. albicans* clinical isolates and in isogenic strains complemented with different *MRR1* alleles. Growth curves of *C. albicans* mutants *mrr1*Δ (teal), complements expressing $MRR1^{WT}$ (purple), $MRR1^{N803D}$ (dark blue) or $MRR1^{Q350L}$ (light blue) **(A-B)**, and matched FLZ-sensitive (pink) and FLZ-resistant (orange) clinical isolates **(C-F)** in YPD **(A, C, E)** or YPD supplemented with MG to a final concentration of 15 mM **(B, D, F)**. Data shown represent the mean ± SD from two independent experiments.

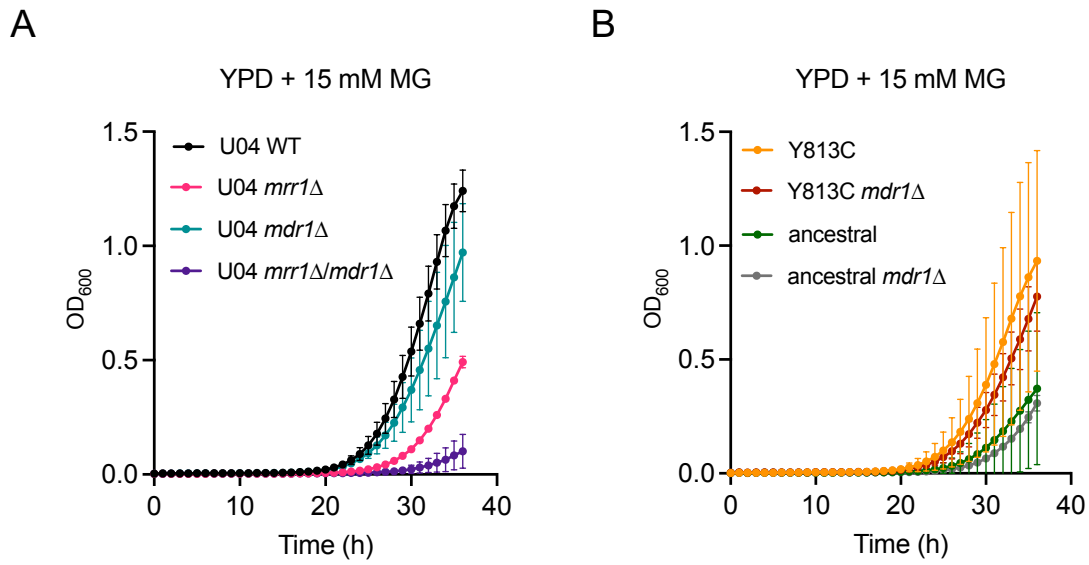

Figure II.5. *C. lusitaniae MDR1* does not contribute significantly to MG resistance in the presence of functional Mrr1. Growth curves of *C. lusitaniae* isolate U05 (WT, black) and its *mrr1*Δ (magenta), *mdr1*Δ (teal), and *mrr1*Δ/*mdr1*Δ (purple) derivatives **(A)**, or isogenic $MRR1^{ancestral}$ (dark green) and $MRR1^{Y813C}$ (orange) complements and their *mdr1*Δ derivatives (gray and dark red, respectively) in the U04 background **(B)** in YPD supplemented with MG to a final concentration of 15 mM. Data shown represent the mean ± SD from two independent experiments.

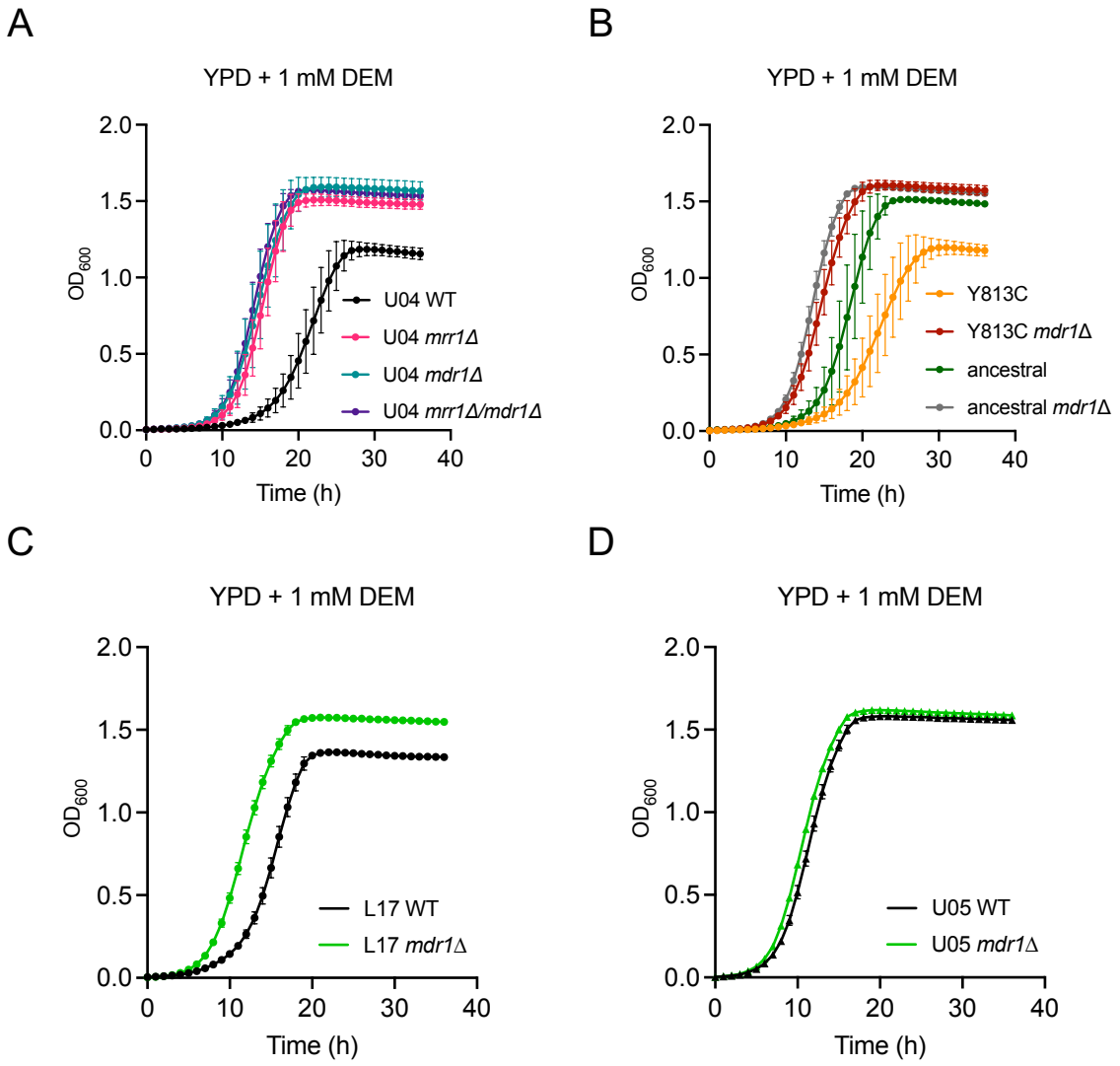

Figure II.6. *MRR1*-dependent *MDR1* overexpression increases susceptibility to GSH depletion by DEM in *C. lusitaniae*. Growth curves of *C. lusitaniae* isolate U05 (WT, black) and its *mrr1*Δ (magenta), *mdr1*Δ (teal), and *mrr1*Δ/*mdr1*Δ (purple) derivatives **(A)**, isogenic $MRR1^{ancestral}$ (dark green) and $MRR1^{Y813C}$ (orange) complements and their *mdr1*Δ derivatives (gray and dark red, respectively) in the U04 background **(B)**, or clinical isolates L17 and U05 (black) and their *mdr1*Δ derivatives (bright green) **(C-D)** in YPD supplemented with DEM to a final concentration of 1 mM. Data shown in **A-B** represent

the mean ± SD from two independent experiments. Data shown in **C-D** represent the mean +/- SD of technical triplicates from a single experiment.

References

1. Biermann AR, Demers EG, Hogan DA. 2021. Mrr1 regulation of methylglyoxal catabolism and methylglyoxal-induced fluconazole resistance in *Candida lusitaniae*. Mol Microbiol 115:116-130.
2. Demers EG, Stajich JE, Ashare A, Occhipinti P, Hogan DA. 2021. Balancing Positive and Negative Selection: *In Vivo* Evolution of *Candida lusitaniae MRR1*. mBio 12.
3. Demers EG, Biermann AR, Masonjones S, Crocker AW, Ashare A, Stajich JE, Hogan DA. 2018. Evolution of drug resistance in an antifungal-naive chronic *Candida lusitaniae* infection. Proc Natl Acad Sci U S A 115:12040-12045.
4. Asner SA, Giulieri S, Diezi M, Marchetti O, Sanglard D. 2015. Acquired Multidrug Antifungal Resistance in *Candida lusitaniae* during Therapy. Antimicrob Agents Chemother 59:7715-22.
5. Kannan A, Asner SA, Trachsel E, Kelly S, Parker J, Sanglard D. 2019. Comparative Genomics for the Elucidation of Multidrug Resistance in *Candida lusitaniae*. mBio 10.
6. Morschhauser J, Barker KS, Liu TT, Bla BWJ, Homayouni R, Rogers PD. 2007. The transcription factor Mrr1p controls expression of the *MDR1* efflux pump and mediates multidrug resistance in *Candida albicans*. PLoS Pathog 3:e164.
7. Hoehamer CF, Cummings ED, Hilliard GM, Morschhauser J, Rogers PD. 2009. Proteomic analysis of Mrr1p- and Tac1p-associated differential protein expression in azole-resistant clinical isolates of *Candida albicans*. Proteomics Clin Appl 3:968-78.

8. Harry JB, Oliver BG, Song JL, Silver PM, Little JT, Choiniere J, White TC. 2005. Drug-induced regulation of the *MDR1* promoter in *Candida albicans*. Antimicrob Agents Chemother 49:2785-92.